THE UNIVERSITY
of EDINBURGH

Scalar fields: fluctuating and dissipating in the early Universe

Sam Bartrum

A thesis submitted in fulfilment of the requirements
for the degree of Doctor of Philosophy
to the
University of Edinburgh
July 21, 2015

Lay summary

The most current, up-to-date observations seem to hint that the Universe underwent a period of rapid exponential growth in its earliest moments. This period of cosmic inflation can successfully explain the problems that the standard Hot Big Bang model of cosmology suffered from, including explaining why the Universe is so homogeneous, isotropic and flat. The evidence for inflation resides in the temperature fluctuations of the cosmic microwave background, which are generated from the quantum fluctuations of the inflaton, the scalar field responsible for driving this early rapid expansion. These temperature fluctuations, which are sourced by density fluctuations are then free to evolve under gravity and form the structure that we observe in the Universe today.

The first part of this thesis focuses on warm inflation, an alternative picture to the standard cold inflation paradigm. In the standard picture any pre existing matter or radiation is diluted to negligible amounts by this rapid expansion, leaving the Universe cold and empty once inflation has ended. This period is normally succeeded by a reheating period which repopulates the Universe with the necessary matter content to evolve into the one we observe today. Warm inflation on the other hand is a scenario where particle production occurs during this inflationary period and so the Universe stays warm for the duration. This alternative paradigm has interesting, distinct dynamics and predictions to the standard scenario. The particle production relevant for warm inflation arises from fluctuation-dissipation dynamics, a quantum effect arising at finite temperature. This dynamics is not only relevant to the inflationary period but also affects other scalar fields in cosmology, which arise frequently in particle physics models of the early Universe. The second part of this thesis considers the consequences of this dynamics on these scalar fields, in particular late time periods of inflation through dissipation can occur and this dynamics can also successfully explain the matter-antimatter asymmetry observed throughout the Universe.

Abstract

It is likely that the early Universe was pervaded by a whole host of scalar fields which are ubiquitous in particle physics models and are employed everywhere from driving periods of accelerated expansion to the spontaneous breaking of gauge symmetries. Just as these scalar fields are important from a particle physics point of view, they can also have serious implications for the evolution of the Universe. In particular in extreme cases their dynamical evolution can lead to the failure of the synthesis of light elements or to exceed the dark matter bound in contrast to observation. These scalar fields are not however isolated systems and interact with the degrees of freedom which comprise their environment. As such two interrelated effects may arise; fluctuations and dissipation. These effects, which are enhanced at finite temperature, give rise to energy transfer between the scalar field and its environment and as such should be taken into account for a complete description of their dynamical evolution. In this thesis we will look at these effects within the inflationary era in a scenario termed *warm inflation* where amongst other effects, thermal fluctuations can now act as a source of primordial density perturbations. In particular we will show how a model of warm inflation based on a simple quartic potential can be brought back into agreement with Planck data through renormalizable interactions, whilst it is strongly disfavoured in the absence of such effects. Moving beyond inflation, we will consider the effect of fluctuation-dissipation dynamics on other cosmological scalar fields, deriving dissipation coefficients within common particle physics models. We also investigate how dissipation can affect cosmological phase transitions, potentially leading to late time periods of accelerated expansion, as well as presenting a novel model of dissipative leptogenesis.

Declaration

This thesis is my own composition, and contains no material that has been accepted for the award of any other degree or professional qualification. Parts of this thesis are based on published research and where the work was done in collaboration with others, my role was as a primary contributor.

S. Bartrum
July 21, 2015

Acknowledgements

I would like to thank Arjun for supervising me throughout my PhD and for introducing me to the world of particle cosmology. I am grateful for the constant advice and support you have given.

I would also like to thank João for being so patient and for all the encouragement, guidance and knowledge which he has passed on to me. It has been great fun working with you.

To everyone else who has helped in some way, you should know who you are and that I am grateful.

Publications

The work in this thesis is based on the following publications completed during the course of my PhD:

Sam Bartrum, Arjun Berera, João G. Rosa . *Gravitino cosmology in supersymmetric warm inflation*. Phys. Rev. **D86** (2012) 123525.

Sam Bartrum, Arjun Berera, João G. Rosa . *Warming up for Planck*. JCAP **1306** (2013) 025.

Sam Bartrum, Mar Bastero-Gil, Arjun Berera, Rafael Cerezo, Rudnei O. Ramos, João G. Rosa . *The importance of being warm (during inflation)*. Phys. Lett. **B732** (2014) 116-121.

Sam Bartrum, Arjun Berera, João G. Rosa . *Fluctuation-dissipation dynamics of cosmological scalar fields*. Phys. Rev. **D91** (2015) 083540

Contents

Chapter 1

Introduction

The most up to date cosmological observations show that the Universe can be accurately described by a simple ΛCDM cosmology with an initial spectrum of density perturbations which are largely adiabatic, gaussian and almost but not exactly scale invariant.

It is remarkable that such a simple cosmology, based on the theory of general relativity for an isotropic and homogeneous spacetime, including a dark energy and cold dark matter component, can successfully describe the Universe from the era of decoupling all the way to the current accelerated expansion. However, it is not without its shortcomings. Indeed it cannot explain the initial spectrum of small, but extremely important density fluctuations present in the cosmic microwave background (CMB) and requires incredibly precise initial conditions to allow the Universe to evolve into the one we observe today. Extending the ΛCDM model to include a phase of accelerated expansion in the earliest moments of the Universe can successfully generate such a spectrum of density perturbations as well as potentially explaining the origin of these very precise initial conditions. In this inflationary scenario the density perturbations can be generated by the quantum vacuum fluctuations of an overdamped scalar field whilst it dominates the energy density of the Universe. This spectrum depends upon the scale of inflation and the slope of the scalar field's potential, thus constructing a model of inflation largely boils down to specifying a potential for this scalar field and attempting to motivate it from within a particle physics and gravitational framework. Due to the high energy density of the Universe during this inflationary phase where these perturbations are created, observations of the CMB allow us to probe particle physics at unprecedentedly high energies close to the Planck

scale, thus allowing one to test the ultraviolet completion of the Standard Model (SM).

Some of the first models of inflation, and perhaps some of the simplest, were based on a simple renormalizable potential for the inflaton field with a mass term and quartic self interaction. This is an attractive model as besides generating the correct amplitude and scaling of the adiabatic perturbations, it can also explain why, from general planckian initial conditions, a period of inflation can arise, a problem which may remain for other lower scale inflationary potentials. Unfortunately the most up-to-date Planck measurements of the temperature and polarisation anisotropies of the CMB have not detected primordial gravitational waves [1] and indeed foreground effects which mimic gravitational waves seem to be larger than expected, as BICEP unfortunately found out [2]. This seems to rule out these simple, attractive models of inflation which generically predict too large an amplitude of gravitational waves. This lack of detection has spawned an industry where increasingly complex inflationary potentials are proposed in an attempt to reconcile this single field picture of inflation with observations. Often these models are realised within string theory in an attempt to create an ultraviolet (UV) complete theory of inflation. String theory however tends to not be overly predictive and as such it is hard to generate concrete predictions, although it is crucial to point out that it is the only real framework on the market which gives a UV complete model of quantum gravity, which is no small feat. Inflationary models get significantly more complex as one includes additional couplings to gravity, modifies the kinetic terms of the inflaton or invokes many scalar fields to drive inflation. However as the complexity increases, generically the predictive power of a model decreases, in the sense that it can predict a much wider range of outcomes. This also has the knock on effect of leading to models with very degenerate predictions, making it hard to distinguish between them, potentially even if gravitational waves are detected. Therefore although the spectrum of density perturbations is about as simple as it gets, the failure of the simplest models seems to hint that more complicated physics is responsible for its generation.

The detection of the Higgs boson at the LHC in 2012 was not only the first observation of a fundamental scalar field in nature, but also the smoking gun of the electroweak phase transition, which seems to confirm our understanding of phase transitions in the role of breaking gauge symmetries. The detection of

one scalar field thus arguably makes it more likely that there should be more, a situation which naturally arises as one goes beyond the standard model (BSM). Indeed one must look to BSM physics if one is to explain neutrino masses, provide a dark matter candidate, unify the gauge couplings of the SM, solve the hierarchy problem, explain the absence of CP violation within the QCD sector and even to drive a period of inflation. It is thus likely that the early Universe contained a whole host of scalar fields arising from larger grand unification (GUT) groups, the compactification of extra dimensions or string theory and that it underwent a series of phase transitions as some larger symmetry group was broken down to the SM gauge group.

Scalar fields, although useful for particle physics, can be very dangerous for cosmology, in particular for Big Bang nucleosynthesis (BBN). Due to their Lorentz invariance, scalar fields are free to develop non-zero vacuum expectation values, a fact which leads them to dynamically evolve in their potential, either behaving as cold dark matter when oscillating or as an effective cosmological constant when overdamped. This makes it very easy for them to dominate the energy density of the Universe and decay at late times leading to a huge production of entropy and spoiling the abundance of light elements at the era of BBN or to exceed the dark matter bound. It is thus important, if not crucial, to understand the dynamical evolution of scalar fields, not only in an attempt to understand the inflationary era, but also to understand the late time evolution of the Universe.

Scalar fields however, are not isolated and necessarily have interactions with other degrees of freedom. In the context of inflation after the period of accelerated expansion has ended interactions must necessarily be present in order to convert the vacuum energy of the scalar field into radiation and repopulate the Universe with at least the SM degrees of freedom. It is often assumed that these interactions have a negligible affect on the evolution of the inflaton during inflation with them at most leading to radiative corrections to the inflaton's potential, however this need not necessarily be the case as we will shortly see. Scalar fields which are responsible for the spontaneous breaking of a gauge symmetry also necessarily have interactions. Indeed it is these interactions which lead to symmetry restoration at high temperatures in the early Universe. To date particle physics has mainly focussed on the equilibrium properties of such scalar fields in the broken and unbroken phases, however the interactions of the scalar field become important as one considers the dynamical evolution between these

phases.

If one wishes to fully describe the evolution of an interacting scalar field one should compute the effective action which takes into account the effects of the interactions with other degrees of freedom. Generically this leads to two interrelated effects which modify the scalar field's equation of motion; fluctuations and dissipation. These effects are significantly enhanced if the particles involved have non trivial statistical distributions, a scenario that arises naturally in the early Universe which is close to thermal equilibrium. Dissipation leads to energy exchange between the scalar field and the degrees of freedom to which it couples, generically acting as an additional friction term in its equation of motion. Fluctuations arise as a backreaction of these other degrees of freedom on the scalar field perturbing its motion. This is analogous to the scenario of an object in a rarefied gas where the object loses kinetic energy through collisions whilst at the same time experiencing fluctuations as these collisions perturb its motion. This fluctuation-dissipation dynamics can have interesting consequences on the dynamical evolution of cosmological scalar fields and are not effects which one should a priori neglect, indeed the same interactions which result in symmetry restoration can lead to significant dissipative effects so including one effect and not the other leads to an incomplete picture.

Fluctuation-dissipation dynamics may have played a role during the inflationary era. If the Universe was initially in thermal equilibrium before a period of inflation was triggered then it is possible that dissipation may have been able to sustain a thermal bath during inflation despite the quasi-exponential expansion. Such a scenario is referred to as *warm inflation* [3, 4, 5, 6, 7, 8, 9, 10] and can have interesting differences from the standard *cold inflation* picture. In particular dissipation leads to an extra source of friction which can help sustain inflation with steeper potentials thus alleviating the amount fine tuning needed. It can also allow for inflation to be realised at lower, possibly sub-planckian field values thus preventing the inflaton from developing large corrections to its potential from the effects of quantum gravity [11]. This is a scenario which commonly arises within supergravity (SUGRA) frameworks and is referred to as the *eta problem*. Note that this problem may also be avoided in other models, in particular those which have a shift symmetry forbidding these dangerous higher dimensional effective operators. In addition it can provide a graceful exit [12], such that while radiation is subdominant during inflation it smoothly

becomes dominant once inflation ends, without the need for a separate, largely unconstrained, reheating period. However potentially most importantly the primordial perturbations in this scenario can be sourced from classical, thermal fluctuations instead of quantum fluctuations thus changing the fundamental mechanism for the generation of structure in our Universe.

It is the goal of this thesis to consider the effects of fluctuation-dissipation dynamics both within the inflationary era and in the post-inflationary, radiation dominated Universe. Within the context of inflation we will show how a simple model based on a quartic potential and renormalisable interactions can agree remarkably well with the latest Planck data when these dissipative effects are taking into account. As we shall see this allows the Universe to stay warm during inflation and smoothly transition into the radiation era without a separate reheating period. In addition we will explore potential ways to observationally discriminate this alternative scenario, where classical thermal fluctuations source the primordial density perturbation, from the standard cold inflation models with quantum vacuum fluctuations. As mentioned previously, this dynamics is not exclusive to the inflationary era and other scalar fields in cosmology will also feel its effects. We consider how this can affect the evolution of the Universe when symmetries are broken during cosmological phase transitions as well as presenting a novel mechanism of dissipative leptogenesis.

We will begin this thesis with a brief review of some fundamental cosmology which will be necessary in order to set the scene for the remainder of the thesis. In Chapter 2 we will review the evolution of the Universe and how it evolves depending upon the energy densities which comprise it, before moving on to describe the ΛCDM model as well as some open questions associated with it. In Chapter 3 we will introduce inflation and describe how and to what degree it solves the problems associated with the standard cosmological model as well as summarising the current observational evidence. In Chapter 4 we will introduce warm inflation and fluctuation-dissipation dynamics, in particular we will show how these effects can help to bring the quartic potential back into agreement with observation whereas it seems to be ruled out in the standard scenario. In Chapter 5 we consider the thermal production of gravitinos during a period of warm inflation, demonstrating how an overabundance may be avoided which is a common problem within supergravity theories of the early Universe. In Chapter 6

we present additional consistency relations between the observables for the warm inflation scenario allowing for an easier way to test the warm inflation paradigm. In Chapter 7 we move on to discuss how fluctuation-dissipation dynamics arises within common particle physics models, focussing in particular on cosmological phase transitions and a dissipative model of leptogenesis. Chapter 8 is reserved for concluding remarks with discussion of future work and the prospects for the future field of inflationary cosmology.

Chapter 2

ΛCDM - The standard cosmological model

We are currently in the era of precision cosmology, where the properties of the CMB have been measured to an impressive degree of accuracy, which together with Large Scale Structure (LSS) surveys and supernovae observations have failed to observe any significant departure from a simple ΛCDM cosmology. ΛCDM is a particular parameterisation of the standard Hot Big Bang cosmological model based on the assumptions that the Universe is homogeneous and isotropic, with a cosmological constant and a cold dark matter component. The fact that almost the entirety of the $\sim$ 13.8 billion years of the Universe's life can be described by such a simple model is clearly impressive, however that is not to say that it is without issues and even with the accuracy of current observations there is still room for deviations from it. For example, we know that at the very least the earliest moments of the Universe must depart from ΛCDM if we are to explain the crucial deviations from homogeneity and isotropy observed in the CMB, which allow for structure formation, as well as providing explanations for the very precise initial conditions the present Universe requires. One possible extension to the ΛCDM model is the inclusion of an early period of accelerated expansion in the form of inflation which we will discuss in the next chapter.

In the following section we will introduce some key elements of the Big Bang cosmological model and introduce the ΛCDM model together with some open questions associated with it. This is not meant to be a comprehensive description, for reviews which are useful in learning this subject see [13, 14, 15] and references therein.

2.1 The expansion of the Universe

The starting point for our discussion will be the diffeomorphism invariant Einstein-Hilbert action:

$$S_{\mathrm{EH}} = \int d^4x\sqrt{-g}\left(\frac{m_{\mathrm{p}}^2}{2}(R-2\Lambda)+\mathcal{L}_{\mathrm{M}}\right) \ , \tag{2.1}$$

where $g = \det(g_{\mu\nu})$ is the determinant of the metric tensor, R is the Ricci scalar, $\mathcal{L}_{\mathrm{M}}$ is the matter Lagrangian and m_{p} is the reduced Planck mass. This action can be obtained from the leading order terms under the demand that the theory is invariant under general, differentiable coordinate transformations. Treating the metric tensor as a dynamical object and varying the action with respect to it leads, through the principle of least action, to Einstein's field equations (EFE):

$$R_{\mu\nu} - \frac{1}{2}g_{\mu\nu}R + \Lambda g_{\mu\nu} = \frac{1}{m_{\mathrm{p}}^2}T_{\mu\nu} \ . \tag{2.2}$$

This famous set of equations couples the curvature of space to the energy density within the Universe, in other words; "spacetime tells matter how to move; matter tells spacetime how to curve" [16]. It is interesting to note that the presence of an arbitrary constant, Λ which we identify as the cosmological constant, in the action can have serious implications within general relativity (GR), in particular it can act like a contribution to the stress-energy tensor and govern the dynamics of the Universe. We should note that this formulation of gravity is not unique in the sense that other diffeomorphism invariant terms may be present and many theories expand upon the Einstein-Hilbert action Eq. (2.1), in particular replacing the R term with a general function $f(R)$, however at least on Solar System scales the modified theory must not deviate too much from GR.

If one makes the reasonable assumption that the Universe is isotropic and homogeneous on sufficiently large scales, then the metric describing our Universe takes the form of the Friedmann-Robertson-Walker (FRW) metric:

$$ds^2 = -dt^2 + a(t)^2\left(\frac{dr^2}{1-kr^2} + r^2(d\theta^2+\sin^2\theta d\phi^2)\right) \ . \tag{2.3}$$

The scale factor, $a(t)$, allows for the time evolution of the spatial components which can lead to expansion or contraction and hence a dynamical Universe. k encodes the geometry of the Universe which takes discrete values $k = -1, 0, 1$

corresponding to a Universe which is open, flat and closed respectively. The assumption that the Universe is homogeneous and isotropic was initially a philosophically humble one; that we do not occupy some special place in the Universe. However, this cosmological principle has now been seen to agree with observations of the CMB which is incredibly close to homogeneous and isotropic on all scales [17]. Although it is worth pointing out that observations of super large scale structure questions whether this principle is truly valid today [18, 19].

The fact that observations imply that the Universe is largely isotropic with no preferred direction justifies describing its energy components as perfect fluids. Here by a perfect fluid we mean that it can be described completely by its rest frame energy density and pressure, with no energy flux or shear. The stress-energy tensor then takes a simple form $T^{\mu}_{\nu} = \mathrm{diag}(-\rho, p, p, p)$, where ρ and p are the energy density and pressure of the fluid. With a stress-energy tensor of this form and the FRW metric in Eq. (2.3), EFE give rise to the Friedmann equations:

$$\begin{aligned} H^2 = \left(\frac{\dot{a}}{a}\right)^2 &= \frac{\rho}{3m_{\mathrm{p}}^2} - \frac{k}{a^2} + \frac{\Lambda}{3} \,, \\ \dot{H} + H^2 = \frac{\ddot{a}}{a} &= -\frac{\rho + 3p}{6m_{\mathrm{p}}^2} + \frac{\Lambda}{3} \,. \end{aligned} \tag{2.4}$$

The Hubble parameter, $H = \dot{a}/a$ parametrises the expansion rate of the Universe and as we can see is intimately related to the fluid content. The first equation tells us the rate of change of the scale factor, where it is clear that a positive energy density, ρ and positive cosmological constant leads to an expanding Universe. For $k = 1$ and $\Lambda = 0$, as the Universe expands the curvature term comes to dominate over the energy density content eventually causing the scale factor to decrease and resulting in the collapse of the Universe. Observations show that the Universe is very close to flat today and so we will neglect the curvature term. In fact as we will see a period of accelerated expansion can make this term negligible and so it is typically neglected even during inflation. The second equation is of particular interest as it tells us whether the expansion rate is increasing or decreasing depending upon the dominant energy content. In particular if we ignore the cosmological constant, which as we will shortly discuss only becomes dominant at late times, it is clear that accelerated expansion requires a violation of the strong energy condition, requiring $\rho + 3p \leq 0$. This requires a peculiar equation of state, $\omega \leq -1/3$, since for common perfect fluids such as radiation

or pressureless matter (dust) $\omega = p/\rho = 1/3, 0$ respectively. Observations show that the Universe is currently undergoing a period of accelerated expansion and also that it is likely that it was as well in its earliest moments. The current phase seems to be well described by a Universe dominated by a cosmological constant, Λ, whilst the earlier period requires something a little more peculiar. We will discuss both of these in more detail later on.

The covariant conservation of the stress-energy tensor, $T^{\mu\nu}{}_{;\nu} = 0$, where the semi-colon indicates a covariant derivative, implies the conservation of momentum and energy in the expanding Universe. In particular one can find the conservation equation for perfect fluids:

$$\dot{\rho} + 3H(\rho + p) = 0 \ . \tag{2.5}$$

For a fluid with a constant equation of state, ω, one can show that $\rho \propto a(t)^{-3(1+\omega)}$ and so radiation and matter redshift differently as a function of the scale factor $\rho_{\rm R} \propto a(t)^{-4}$ and $\rho_{\rm m} \propto a(t)^{-3}$. Note that for $\omega = -1$ the energy density is constant, this will have important consequences for the late time accelerated expansion. One can also show that $a(t) \propto t^{2/3(1+\omega)}$ and so the behaviour of the scale factor for a radiation and matter dominated Universe is given by $a(t) \propto t^{1/2}, t^{2/3}$ respectively. Note that this expression does not hold for $\omega = -1$ in which case the scale factor grows exponentially. At first sight this seems to imply the presence of a singularity at $t = 0$ as the scale factor goes to zero and the energy densities become infinite. However this requires the assumption that GR is correct up to arbitrarily high energies, which isn't the case as we know that GR is non-renormalizable and quantum gravity effects need to be included. The scaling behaviour of these energy densities gives a natural evolution of the Universe where an initially radiation dominated Universe gives way to matter and eventually dark energy domination.

2.2 A brief history of time

To fully describe the evolution of the Universe one needs to study the Boltzmann equations for the individual particle species. Two important properties of the particles enter the Boltzmann equation and dictate to a large extent the history of the Universe, namely their mass and their interaction rate. As the

temperature cools particles which were initially relativistic, with $m \ll T$ become non relativistic and likewise particles which were in thermal equilibrium begin to decouple as their interaction rate, Γ, can no longer keep up with the expansion of the Universe. Indeed it is a good approximation to take this freeze out time as the moment when $H \simeq \Gamma$. As we will briefly describe below these two features will be responsible for key moments in the evolution of the Universe. In addition to these effects it is likely that the early Universe underwent a series of phase transitions, the nature of which depends upon the details of the particle physics model under consideration. At least one occurrence of spontaneous symmetry breaking occurred at around $T \simeq 1$ TeV, the process of electroweak symmetry breaking where the $SU(2)_L \times U(1)_Y$ sector of the standard model is spontaneously broken to $U(1)_Q$ through the finite vacuum expectation value of the Higgs scalar field. We will return to the issue of symmetry breaking in the early Universe later in this thesis, however we note that a large number of symmetries are thought to be broken as the Universe expands and cools, which can induce significant departures from the standard cosmological evolution.

We begin the story deep in the radiation era where temperatures were sufficiently high such that all the SM degrees of freedom where relativistic and in thermal equilibrium (we will ignore for now any BSM particle content). As the Universe expands in the radiation dominated era with $a(t) \propto t^{1/2}$, the temperature cools. When the temperature reaches $T \sim 1$ TeV the electroweak symmetry is broken and the $W^{\pm}$ and Z bosons acquire mass, the same happening to the SM fermion content. At around $T \sim 1$ MeV, weak interactions, such as $e^- + \nu_e \longleftrightarrow e^- + \nu_e$ or $e^- + e^+ \longleftrightarrow \nu_e + \bar{\nu}_e$ are too slow to keep the neutrinos in thermal equilibrium and thus they decouple from the radiation bath. Although these primordial neutrinos have not yet been directly observed (their existence is inferred from CMB and BBN measurements), detection of this Cosmic Neutrino Background (CνB) would provide an even earlier snapshot of the Universe than the CMB. A little later when $T \sim 0.1$ MeV the nuclear reactions fall out of equilibrium resulting in the freeze out of nuclear abundances. This is now the era of BBN where the first light elements, such as Li, He and H, are able to form. The nuclear processes involved in the production of these light elements are well known and the abundances predicted are in fantastic agreement with the observations of these abundances within metal poor stars. BBN thus acts as a stringent constraint on any exotic physics one wishes to add to the standard

picture. However, the observed abundance of Lithium is somewhat smaller than predicted, a situation which is often referred to as the *Lithium Problem*. A convincing resolution to this problem has not yet been found although the under-abundance could be due to unknown nuclear physics processes, new astrophysical depletion mechanisms taking place in these metal poor stars or indeed due to BSM physics. The temperature soon becomes too low for further synthesis of heavier elements and the era of BBN ends.

When $T \sim 1$ eV the matter and radiation energy densities become equal and this signals the end of the radiation era and the beginning of the matter dominated era. At around $T \sim 0.1$ eV a staggering $\sim 400,000$ years into the Universe's evolution, protons and electrons begin to combine to form neutral hydrogen atoms. This process makes the previously ionised primordial plasma neutral and allows photons, which where strongly coupled to the electrons, to freely propagate largely unimpeded through the Universe. This period is known as decoupling or recombination and the photons emitted from this moment gives rise to the CMB which has been measured to incredible accuracy by the recent Planck missions and acts as a second constraint on any new physics one wishes to consider. The temperature of the CMB is homogeneous and isotropic to a large degree however it does crucially exhibit small fluctuations which indicate fluctuations in the energy density at the era of decoupling. These density fluctuations evolve (oscillate) under the competition of radiation pressure and gravity until they collapse and begin to form structures on all scales from stars to superclusters of galaxies. At a redshift of $z \sim 20$, high energy photons from the first stars are able to reionize the hydrogen in the intergalactic medium, this occurs until $z \sim 6$ when the Universe becomes once more transparent. The first, more massive stars begin to run out of fuel as temperatures within the stars' cores are not high enough to fuse heavier elements and the resulting drop in radiation pressure leads to gravitational collapse. The core can then form a neutron star or black hole while the outer layers explode off dramatically forming the heavier elements such as Carbon or Oxygen which are crucial for planets and life to form as we know it. Finally at a redshift of $z \simeq 1$ or around 10 billion years, the mysterious dark energy comes to dominate the Universe causing the expansion to accelerate and effectively putting an end to structure formation.

2.3 Initial conditions of the ΛCDM model

Naively extrapolating the Hot Big Bang model back in time leads to some open questions about the initial conditions of the Universe which arguably have yet to have been met satisfactory explanation. The issues concern the very fine tuned initial conditions required from which the Universe can successful evolve into the one we observe today. These fine tuning issues are often referred to as the horizon problem, the flatness problem and the monopole problem. We will discuss each of these in turn and in the next chapter we will explain to what extent a period of inflation can solve these problems.

The *horizon problem* asks why the Universe is so homogeneous and isotropic on large scales. Measurement of the temperature anisotropies within the CMB show that the temperature at the time of decoupling was homogenous to within fluctuations of the order $\mathcal{O}(10^{-5})$ on all angular scales. Light takes a finite time to propagate through the Universe and so we can introduce the comoving particle horizon (or causal horizon) which is the maximum distance light could have travelled in a given interval of time. This is a measure of the scale on which things can be causally connected:

$$\tau \equiv \int_0^t \frac{dt'}{a(t')} = \int_0^a \left(\frac{1}{a'H(a')}\right) d\ln a' \ , \tag{2.6}$$

where we have used comoving coordinates, $d\tau = dt/a(t)$. For a Universe dominated by a fluid with an equation of state ω:

$$(aH)^{-1} \sim a^{\frac{1}{2}(1+3\omega)} \ . \tag{2.7}$$

The causal horizon thus evolves as:

$$\tau \sim a^{\frac{1}{2}(1+3\omega)} \ . \tag{2.8}$$

From this it is clear that the comoving horizon grows for a matter or radiation dominated era and interestingly decreases for scenarios where the dominant fluid has the equation of state $\omega \leq -1/3$. Note that a period of accelerated expansion thus causes the comoving horizon to decrease. Scales which are only just entering our horizon today must have been far outside the causal horizon at the era of decoupling. In fact it is not too hard to show that the current size of the

observable Universe must have been comprised of $\sim 10^5$ causally disconnected regions at the era of decoupling. So why do apparently causally disconnected regions of the CMB have almost exactly the same temperature?

Observations of the CMB and LSS show that the observable patch of the Universe is compatible with being flat. From Eq. (2.4) one can show that:

$$1 - \Omega(a) = -\frac{k}{(aH)^2} \ . \tag{2.9}$$

$\Omega = \rho/\rho_{\rm c}$ and $\rho_{\rm c} = 3H^2 m_{\rm p}^2$ is the critical density required for a flat Universe. As we just saw the comoving horizon $(aH)^{-1}$ grows during the matter and radiation dominated eras, therefore in order for the Universe to be very close to flat today, it must have been even closer to flat at early times. For example to ensure that the Universe is flat to within 1% today requires $|\Omega(a_{\rm p}) - 1| \lesssim 10^{-61}$ at the Planck era, even at the era of BBN we would require $|\Omega(a_{\rm BBN}) - 1| \lesssim 10^{-17}$. This is an extreme fine tuning of the initial conditions to ensure that the Universe can remain flat until the present. To understand this better we can differentiate Eq. (2.9) and we find:

$$\frac{d\Omega}{d\ln a} = (1+3\omega)(\Omega - 1) \ , \qquad \Omega(a) = 1 - a^{1+3\omega}(1 - \Omega_{\rm i}) \ . \tag{2.10}$$

It is thus clear that if the strong energy condition is satisfied then the Universe is naturally driven away from $\Omega = 1$, in fact $\Omega = 1$ is an unstable point. For $\Omega_{\rm i} > 1$ the Universe becomes overclosed and will collapse, whilst for $\Omega_{\rm i} < 1$ the Universe becomes open. Unless $\Omega_{\rm i}$ is very close to 1 initially then both scenarios are incompatible with observation. If, however, the strong energy condition is violated then the Universe is driven towards flatness.

The *monopole problem* asks the question as to why we have not observed any heavy relics which should have been abundantly produced in the early Universe. These relics, more generally, include any heavy stable particles (e.g. gravitinos) or topological defects such as cosmic strings or monopoles. Later chapters of the thesis will touch on topological defects and so it may be worthwhile to briefly describe the problem. The apparent unification of the three standard model gauge couplings at high energies around $\sim 10^{16}$ GeV hints at the possibility that the standard model may be embedded within a larger symmetry group. Commonly

considered examples include $SU(5)$, $SO(10)$ where in addition to the successful unification of the gauge couplings, relations between Yukawa couplings arising from the higher degree of symmetry allow for further explanation of the standard model structure. In the early universe this GUT symmetry is restored by thermal corrections arising from the coupling of the relativistic particle content to the GUT breaking field (see Appendix A). In the example of $SU(5)$ the symmetry is broken by a Higgs field in the adjoint representation acquiring a vacuum expectation value (see Chapter 7 for more details). At high temperatures the SM Higgs doublet, its triplet partner and the heavy GUT bosons are in thermal equilibrium and relativistic and thus induce a large thermal mass for the adjoint Higgs field. This restores the GUT symmetry as the origin, where the symmetry is unbroken, becomes a stable minimum. As the temperature cools these thermal corrections decrease and new minima occur with the adjoint Higgs field free to choose a direction within the vacuum manifold. The degeneracy of the vacuum manifold is then responsible for the formation of topological defects. These defects are classified by the homotopy classes of the vacuum manifold, which in general can be loosely thought of as the number of distinct ways the spatial dimensions at infinity can be mapped onto the vacuum manifold $\mathcal{M}$, $\pi_n(\mathcal{M})$. These mappings correspond to topologically distinct classical field configurations, which if non trivial (i.e. $\pi_n(\mathcal{M}) \neq 1$) , result in a stable configuration with a finite energy density. Depending upon the vacuum manifold and the symmetries associated with it different dimensional defects can form, these include domain walls, strings, monopoles and textures (for $n = 0, 1, 2, 3$ respectively). The monopole problem arises due to the presence of the $U(1)_Y$ symmetry group within the SM and as such the production of monopoles seems inevitable in the early Universe.

The Kibble mechanism [20] gives an estimate of how topological defects are formed in the early universe. The correlation length of the symmetry breaking field is finite and bounded by the horizon size due to causality. Thus one expects that within different causally disconnected domains of the universe the field configuration should be uncorrelated. At the boundaries joining these regions these topological defects would appear as the scalar field tries to minimise its energy density, thus Kibble argues that there should be $O(1)$ defects per Hubble volume. This gives an estimate of $n_{\mathrm{m}} \sim \xi^{-3} \sim H^3 \sim (T_{\mathrm{C}}^2/m_{\mathrm{p}})^3$, where T_C is the critical temperature at which the phase transition takes place. We should point out that this estimate is likely to be overly simple and neglects the effects of

quantum or thermal fluctuations on the formation process of these defects as well as perhaps severely overestimating the size of the correlation length. Despite this one can see that even with this estimate, which perhaps is on the small size, the abundance of these defects is much larger than observed. For GUT monopoles the contribution to the current density parameter is given by:

$$\Omega_{\rm m}h^2 \simeq 10^{11}\left(\frac{T_{\rm C}}{10^{15}\,{\rm GeV}}\right)^3\left(\frac{M_{\rm m}}{10^{15}\,{\rm GeV}}\right)\,, \tag{2.11}$$

where $M_{\rm m}$ is the monopole mass, which for GUT phase transitions is naturally close to the GUT scale. It is clear that GUT scale monopoles would very easily exceed the dark matter bound ($\Omega_{\rm m}h^2 \gtrsim 0.1$).

Perhaps one of the most compelling reasons to look beyond the standard Hot Big Bang model is the need to explain the spectrum of the temperature fluctuations observed in the CMB. These temperature fluctuations are the result of density fluctuations which after evolving under gravity give rise to structure on all the observable scales that we see today. These fluctuations are observed to be essentially adiabatic, nearly, but not quite, scale invariant and gaussian. As we will shortly see this distribution of fluctuations is very elegantly generated dynamically by inflation where quantum fluctuations are stretched by the de Sitter expansion and freeze out on causally disconnected scales, but we will return to this later.

2.4 The dark Universe

Although not strictly directly relevant for this thesis, it would be somewhat remiss to discuss the ΛCDM model without mentioning $\sim 95\%$ of its content. Two mysterious energy components are needed in order to obtain a satisfactory description of the Universe; namely dark matter, which makes up around 25% of the Universe and dark energy, which accounts for around 70%.

In the late 90s observations of Supernovae led to the conclusion that the Universe is currently undergoing a period of accelerated expansion. This has subsequently been supported through observations of the CMB, LSS and gravitational lensing. Observationally this dark energy is compatible with being an extra constant, positive energy density contributing to the expansion of the

Universe. From Eq. (2.4) it is clear that $\ddot{a} \geq 0$ for $\Lambda \geq 0$ in the absence of any other significant sources of pressure or energy density. In fact if Λ dominates then one finds the behaviour of the scale factor is $a(t) \sim \exp(\sqrt{\Lambda/3}t)$, i.e. a positive cosmological constant leads to a period of exponential accelerated expansion. As we shall see this has certain similarities to the early period of cosmic inflation. For excellent reviews on dark energy and the cosmological constant problem see [21, 22]. It is often remarked that it is curious that dark energy came to dominate so late in the cosmic evolution, at $z \simeq 1$, although this occurred around 5 billion years ago when the Universe was half way through its evolution. Had dark energy dominated much earlier then this could have prevented structure formation from taking place. This is the so called *cosmological coincidence problem* which can be rephrased as asking why is Ω_Λ comparable to Ω_m today [23].

The contribution of this component to the current density parameter is found to be $\Omega_\Lambda \sim 0.7$, corresponding to a tiny energy density $\rho_\Lambda \simeq 10^{-47}\ \mathrm{GeV}^4$ [21]. Any component which contributes to the stress energy tensor and is proportional to the metric tensor acts as a cosmological constant. This is precisely how the vacuum energy of a field theory contributes and so if the cosmological constant arises from the energy of the vacuum, then logically it should receive a contribution from the zero-point energies of quantum fields. Quantum mechanically we can describe this as follows by considering a massive free scalar field. This field will contribute to the stress-energy tensor in EFE Eq. (2.2) where the Hamiltonian density is given by the first component of the stress-energy tensor and thus the vacuum receives a contribution:

$$\langle 0|T^{00}|0\rangle = \frac{1}{2}\langle 0|\dot{\phi}^2 + \bigtriangledown\phi^2 + m^2\phi^2|0\rangle \ . \tag{2.12}$$

Upon quantisation the scalar field can be written in terms of raising and lowering operators for each momentum mode and the contribution from the mass term gives, for example:

$$\langle 0|\phi^2|0\rangle = \frac{1}{(2\pi)^3}\int \frac{d^3\mathbf{k}}{2\omega_k} \ , \tag{2.13}$$

where $\omega_k = \sqrt{k^2 + m^2}$. We can sum all the contributions to the Hamiltonian density and we find:

$$\langle \rho \rangle = \frac{1}{16\pi^3}\int d^3\mathbf{k}\,\omega_k \ . \tag{2.14}$$

This is clearly UV divergent and introducing a cut off $k_\mathrm{max} \gg m$ we find that the

leading contribution is:

$$\langle \rho \rangle \simeq \frac{k_{\max}^4}{16\pi^2} \ . \tag{2.15}$$

In the case where GR is assumed to be valid up to the Planck scale, this contribution gives $\rho \simeq 10^{71}\text{GeV}^4$ some 118 orders of magnitude larger than observed and even if we assume the cut off is the electroweak scale $k_{\max} \sim 1$ TeV then $\rho \simeq 10^9\text{GeV}^4$.

In order to give the correct vacuum energy the bare Λ parameter appearing in the action would have to cancel this contribution almost exactly, requiring a phenomenal degree of fine tuning in an analogous way to the Higgs hierarchy problem. One can include the contributions from other fields and include interactions formulating this calculation in terms of vacuum Feynman diagrams, however this basic fine tuning problem still persists. A possible resolution to this problem arises naturally in supersymmetry where the additional super-partners help to cancel the vacuum diagrams (as they contribute the opposite sign to loop integrals). Unfortunately supersymmetry is broken at present at an energy at least as large as 1 TeV and so the discrepancy remains. Even within a supergravity framework where SUSY can be broken and the vacuum energy tuned to be close to zero, this fine tuning remains.

The problem we have outlined here is referred to as the *cosmological constant problem* and is often quoted as being one of the most embarrassing predictions in physics, if not the whole of science. Clearly somewhere our approach is breaking down. There is a substantial amount of work in the field of dynamical dark energy, where the cosmological constant is replaced by a quintessence scalar field. Although there is no observational evidence to date of a time evolving equation of state of dark energy [24] it is hoped that the smallness of the observed vacuum energy can be explained dynamically. Typically in these approaches the contribution to the vacuum energy from zero-point energies is ignored or assumed to cancel with the bare parameter, or the vacuum itself is assumed to not gravitate.

The nature of dark matter is also not as yet understood, however it was first postulated in 1933 by Zwicky who observed that the gravitational mass of the Coma galaxy cluster was much greater than the luminous mass and thus concluded that the majority of the matter must be 'dark' [25]. Since then evidence has mounted from a variety of observations including the CMB, galaxy rotation

curves, baryon acoustic oscillations (BAO), structure formation and gravitational lensing. Despite the growing evidence for its existence to date there has been no conclusive direct detection of dark matter despite a few intriguing anomalies. Cold dark matter is the current favourite explanation for these observations, where the fact that it is cold refers to the fact that its free streaming length is sufficiently small such that it does not wash out density perturbations which give rise to structure formation observed today. Or in other words it was non relativistic at freeze out. Dark matter naturally has to be weakly interacting with the SM particle content to remain unobserved and so theoretical models consider dark matter which either interacts dominantly through the weak force or gravitationally, although it may interact strongly with any hidden sector content. In either case there are a multitude of models proposing various dark matter candidates all requiring BSM physics. Two important constraints on dark matter abundance come from CMB observations, where the acoustic peak structure is sensitive to the relative abundance of dark matter to baryonic matter, and BBN, where dark matter annihilations or decays can spoil the abundance of light elements. We will return in Chapter 5 to consider the thermal production of gravitinos, a potential dark matter candidate and see how these observational constraints can place bounds on their abundance and constrain cosmology.

2.5 Baryogenesis

One of the big open questions in cosmology is the presence of the cosmic baryon asymmetry i.e. why there is more matter than anti-matter. The Solar System is undeniably made up of matter, proved by planetary probes (and astronauts) not annihilating. Beyond the Solar System the observation of cosmic rays from local and distant galaxies show a deficit of antiprotons to protons of around 10^{-4}. In fact as we have failed to observe strong gamma ray emission from nucleon-antinucleon annihilation it is likely that the whole of the observable Universe is dominated by matter.

The annihilation of baryons and anti-baryons is not totally efficient in the early Universe. Starting from a baryon symmetric state baryons and anti-baryons are free to annihilate with one another, however as the Hubble parameter decreases the annihilation cross section begins to operate on too slow a time scale to keep up with the Hubble expansion and the annihilation effectively ceases. This occurs

at around $T \sim 22$ MeV and results in relative ratio of baryons to entropy of $n_{\rm B}/s \sim n_{\bar{\rm B}}/s \sim 10^{-20}$ [13], which is far too small to realise BBN successfully. This *annihilation catastrophe* would clearly be ameliorated by the presence of an initial baryon asymmetry.

The size of the baryon asymmetry can be constrained from a combination of CMB measurements, where the relative sizes of the acoustic peaks is sensitive to $\eta_s = (n_B - n_{\bar{B}})/s$ (where s is the entropy density) and from the abundance of light elements produced at BBN. The fact that these two measurements, which arise from different physical processes separated by almost $400,000$ years, agree is remarkable and they yield $\eta_s \sim 10^{-10}$. Although today matter far outweighs antimatter, at early times the abundance of quarks and antiquarks was comparable. In order to give rise to the observed asymmetry the initial relative baryon to anti-baryon abundance must have been of the order:

$$\frac{n_{\rm B} - n_{\bar{\rm B}}}{n_{\rm B}} \sim 10^{-8} \ . \tag{2.16}$$

So for every 100 million anti-baryons there was 100 million and 1 baryons! Either this tiny asymmetry was present at the beginning of the Universe as an initial condition or this asymmetry was generated dynamically at some point in the evolution. However, a period of inflation at early times dilutes any pre-existing matter or radiation energy densities to negligible amounts and so the observed asymmetry necessarily has to be produced after inflation ends and cannot simply arise from a certain specific initial condition. Despite this, in warm inflation there is the possibility of producing the baryon asymmetry through dissipative effects during inflation itself [26], we will return to this possibility later in the thesis. Although there have been a large number of different baryogenesis mechanisms proposed, it is clear that the asymmetry must be produced before BBN so that the production of light elements can proceed correctly. In addition to this if one wishes to dynamically produce a baryon asymmetry three conditions, pointed out by Sakharov [27], need to be satisfied. These are baryon number violation, C and CP violation and out of equilibrium dynamics. As this will be relevant for later work in this thesis, we will discuss these in turn. For an excellent review of baryogenesis see [28].

- *Out of equilibrium dynamics:*

If a process, say $A \to B + C$ is in thermal equilibrium then the forward and backward rates occur as fast as each other i.e. $\Gamma(A \to B+C) = \Gamma(B+C \to A)$. As long as this process is in equilibrium no net asymmetry can be produced, as any asymmetry produced through the decay is immediately destroyed through the inverse process. To study how the number density of a species evolves in the early Universe one should study its Boltzmann equation, however a good approximation can be made by comparing the different time scales of the processes involved. For example if a decay process $\Gamma > H$, then the decays (and inverse decays) are occuring on much shorter timescales than the expansion rate and as such this process will keep the decaying particle in thermal equilibrium. If on the other hand $\Gamma < H$ then the particle interactions can't keep up with the expansion and the particle will fall out of equilibrium. In particular if this happens before the particle becomes non relativisitic then the number density at freeze out can be large and not Boltzmann suppressed. Once frozen out the number density will dilute as $n(t) \propto a(t)^{-3}$ as the Universe expands.

This is just one way of generating out of equilibrium dynamics there are many others, in particular dissipation is naturally an out of equilibrium process through which the baryon asymmetry may be produced, we will discuss this in the following chapters.

- *C and CP violation:*

  In order to ensure an asymmetry is produced one requires that the production rate of particles and anti-particles is different. For a scalar field theory C violation is enough to ensure this. If one wishes to produce an asymmetry between fermions and anti-fermions then C violation is not enough, one must also ensure that CP is violated. This guarantees that the asymmetry is not just an asymmetry between left- and right-handed quarks (see [28] for more details). A CP violating phase naturally arises in complex Yukawa coupling matrices if there are at least three generations of fermions as this complex phase cannot then be absorbed by field redefinitions.

- *B violation:*

  The necessity for baryon number violation should be fairly obvious. Starting from a baryon symmetric Universe if all processes conserve baryon number

then no net baryon number can be produced. Although perturbative baryon number violation requires BSM physics a source of non-perturbative violation was found within the SM through electroweak sphaleron processes. These processes arise from the non trivial vacuum structure of the $SU(2) \times U(1)$ gauge group which admits degenerate minima. Instanton field configurations which tunnel between these minima give rise to the spontaneous production of quarks and leptons, violating B and L both by 3 units. Although at zero temperature the rate of this process is vanishingly small, at finite temperature this process becomes much more likely due to the thermal energy of the field configuration. At sufficiently high temperature these processes are in thermal equilibrium (from about 10^{13} GeV down to the electroweak scale) and so any initial baryon asymmetry will be efficiently washed out by the present. More specifically an initial $B + L$ will be damped away through these processes. However $B - L$ is conserved in this transition and so if a net $B - L$ asymmetry is produced this will remain until today. We note that this would require going beyond $SU(5)$ (e.g. to $SO(10)$) which has $B - L$ as an accidental global symmetry. Another alternative is to create an initial lepton asymmetry, $L_{\rm i} \neq 0$ which subsequently gets converted into a baryon asymmetry through these sphaleron transitions with $B_{\rm f} \simeq -L_{\rm i}/2$.

Early models of baryogenesis were based on GUT interaction structures, where B and CP violation can naturally arise. The canonical example is based on $SU(5)$ where the larger representations allow for quarks and leptons to transform in the same representation. Thus the heavy gauge bosons are free to mix baryonic and leptonic degrees of freedom and lead to baryon number violation. These heavy GUT bosons typically have a mass near the GUT scale $\sim 10^{16}$ GeV and so a large reheat temperature is required in order to create an initial thermal abundance. They can then decay out of equilibrium when the temperature of the Universe falls below their mass and generate a baryon asymmetry. However the discovery of electroweak sphalerons which wash out any produced baryon asymmetry led to an interesting alternative mechanism known as leptogenesis. By adding heavy right handed Majorana neutrinos to the SM particle content, then the out of equilibrium decays of these right handed neutrinos into the SM leptons and Higgs boson can lead to the production of a lepton asymmetry. This asymmetry can then be converted to a baryon asymmetry through the electroweak sphaleron

processes. A nice feature of this model is that these right handed neutrinos may also explain the lightness of the SM neutrinos through a see-saw mechanism and thus this model of baryogenesis is linked to low energy phenomenology. An alternative mechanism based on the naturally out of equilibrium nature of dissipation will be presented in Chapter 7 and so we will discuss leptogenesis in more detail there.

Chapter 3

Inflation

The theory of inflation was developed in the 1980s [29, 30, 31] as a solution to the horizon, flatness and monopole problems of the standard Hot Big Bang cosmology. The initial idea put forth by Guth considered a scalar field responsible for breaking some GUT group (e.g $SU(5)$) trapped at a metastable minimum with a large vacuum energy. As this vacuum energy comes to dominate the energy density of the Universe, the Universe expands at an exponential rate and subsequently supercools. This continues until the scalar field tunnels to the stable minimum releasing a huge amount of entropy and solving the problems of the standard Hot Big Bang model. This leads to bubble nucleation as different patches of the Universe tunnel into the stable state at different times and expand at the speed of light. Reheating in this model occurs when bubble walls collide, thermalising the latent energy stored in these walls. This scenario now known as the *old inflation* scenario had a number of problems associated with it, in particular it was inefficient at reheating the Universe due to the infrequent collisions of bubble walls which also tend to lead towards an overly inhomogeneous Universe in contradiction to observations.

Linde then put forth what is now known as the *new inflation* scenario [30] which is a small but crucial modification to the *old inflation* scenario. Again he considered a GUT phase transition, noting that when the field tunnels out of the metastable minimum it will find itself at some $\phi \lesssim \phi_{\min}$ and so the field within this bubble will still be evolving towards the stable minimum. If the effective potential is not too steep then the scalar field is overdamped and the potential energy of the scalar field is approximately constant inducing a period of exponential expansion. This means that the bubble itself is inflating and so the

entire observable Universe would be contained within a single bubble. Topological defects which form at the intersection of bubbles would not be present and the Universe would be homogeneous to a large degree. Reheating in this model occurs through the production of particles by the coherent oscillation of the scalar field about the stable minimum once it becomes underdamped.

The idea of *chaotic inflation* [32, 33] then got rid of the need for the inflaton field to initially begin its life trapped in some metastable state. It is perhaps likely that at the Planck scale the Universe had chaotic initial conditions, and from equipartition of energy the inflaton may have $(\nabla\phi)^2 \sim \dot{\phi}^2 \sim V(\phi) \simeq m_{\rm p}^4$. In such cases it is likely that there will be patches where $V(\phi)$ will dominate over the kinetic and gradient energies, if not initially then after a small amount of time and so inflation is likely to arise from these initial conditions. This got rid of the need to consider inflationary potentials of the symmetry breaking form and simpler monomial potentials where proposed. The recent bounds on the tensor to scalar ratio, r, seem to hint at the potential energy during inflation being $V(\phi) \ll m_{\rm p}^4$. This puts into question whether inflation is likely to occur from these chaotic initial conditions as gradient and kinetic energies can prevent it from occurring until the potential energy is too low to realise inflation successfully. However it is worth noting that once inflation occurs, quantum fluctuations can keep the inflaton field at sufficiently large field values such that inflation continues indefinitely in some patches. This eternal inflation picture generically results in bubbles of the Universe which are expanding at different (exponential) rates and so most of the volume of the Universe is inflating. This arguably, makes it likely that we find ourselves in a Universe which inflated.

In addition to potentially explaining the initial conditions problems, inflation can also dynamically generate the spectrum of density perturbations which we observe in the CMB. In the standard inflationary picture these perturbations arise from the quantum vacuum fluctuations of the inflaton field which get stretched and amplified during inflation, freezing out as classical perturbations on scales larger than the Hubble radius. Upon reentry they induce density perturbations which are then free to evolve under gravity giving rise to the structure we observe in the Universe today. This is the most popular picture of the generation of the initial density perturbations, however other scenarios are certainly viable. For example it is possible that thermal fluctuations are the source of the primordial perturbations, as considered in the warm inflation scenario or within string gas

cosmology (see [34] and references therein). One can even imagine scenarios where the perturbations are generated whilst the Universe is undergoing a slowly contracting phase before bouncing [35].

Inflation models are still largely based on the *chaotic inflation* scenario, however despite the fundamental idea being a relatively simple and elegant one, increasingly more complicated models have been developed with unfortunately relatively few observables to distinguish between them. As we shall see the high energy densities at which inflation is thought to occur offer a window into particle physics near the GUT and Planck scales. This has generated a huge industry in model building, the goal being to come up with a UV complete model of inflation, with string theory providing a natural setting for this endeavour. Other models try to be more economical and use the already discovered Higgs boson to drive the inflationary period, however this typically requires modifying how matter couples to gravity [36]. It is not the intention of this thesis to review these models, however one key result which we wish to present is that if a finite temperature is sustained during inflation then one of the simplest models based on a chaotic potential can become compatible with Planck data. In this chapter we will introduce inflation, discussing the dynamics and generation of perturbations before applying this to a simple quartic potential in anticipation of the following chapter.

3.1 Motivation

As we showed in the last section, the ΛCDM model extrapolated back to the earliest times requires an incredible degree of fine tuning of the initial conditions to explain the flatness, homogeneity and isotropy of the Universe we observe. It is hoped that a period of accelerated expansion can dynamically explain these features and may remove the need for such precise initial conditions.

As we noted previously, if the Universe is dominated by a fluid with an equation of state $\omega \leq -1/3$, then the (comoving) causal horizon decreases as the Universe undergoes accelerated expansion. If this fluid dominates for a sufficiently long period then the entirety of the CMB we observe may have been in causal contact at early times. This would explain the incredible degree of homogeneity and isotropy of the temperature. One can equivalently view a period of accelerated expansion as stretching scales to sizes larger than the

particle horizon, so that our Universe today is expanding in a much larger bubble which was previously causally connected. A period of accelerated expansion also dynamically drives the Universe towards $\Omega = 1$, as the energy density stored in the curvature dilutes away much faster than the energy density of the fluid driving the expansion. The Kibble mechanism suggests that topological defects are formed with a number density of roughly one per Hubble volume. A period of accelerated expansion where the scale factor grows exponentially inflates each Hubble volume by a huge amount and the number density dilutes by approximately $\exp(3N_{\rm e}) \simeq 10^{70}$, where $N_{\rm e}$ is a measure of the duration of this accelerated expansion. Clearly this is more than enough to explain the absence of such defects today. All of these features occur in the inflationary scenario that we will outline below.

3.2 Scalar field dynamics

The equation of motion for a scalar field in expanding spacetime can be derived from the Einstein-Hilbert action Eq. (2.1) with the matter lagrangian $\mathcal{L}_{\rm m} = \frac{1}{2}g^{\mu\nu}\partial_\mu\phi\partial_\nu\phi - V(\phi)$ and is given by:

$$\ddot{\phi} + 3H\dot{\phi} - \frac{1}{a^2}\nabla^2\phi + V_\phi = 0 \ . \tag{3.1}$$

V_ϕ is the derivative of the potential energy with respect to the field. The equation of state for a scalar field can be obtained from the stress energy tensor:

$$\omega = \frac{p_\phi}{\rho_\phi} = \frac{\frac{1}{2}\dot{\phi}^2 - \frac{1}{6}\frac{(\nabla\phi)^2}{a^2} - V}{\frac{1}{2}\dot{\phi}^2 + \frac{1}{2}\frac{(\nabla\phi)^2}{a^2} + V} \ . \tag{3.2}$$

If we consider the case of a homogeneous scalar field ($\nabla^2\phi \simeq 0$), then it is curious to note that in the regime where $\dot{\phi}^2 \ll V$ the equation of state, $\omega \simeq -1$, is exactly what is required to drive a period of accelerated expansion and solve the problems of the Hot Big Bang model. Indeed for $\omega = -1$ the energy density stays constant despite the expansion and thus acts like a cosmological constant. This in fact is the motivation behind attributing the early period of accelerated expansion to the dynamics of a scalar field.

Now in order to solve the horizon and flatness problems mentioned earlier it is necessary to sustain such a period of accelerated expansion for a finite period

of time. To do this it is convenient to introduce two 'slow roll' conditions [37]:

$$\epsilon_\phi = \frac{m_{\rm p}^2}{2}\left(\frac{V_\phi}{V}\right)^2 \ll 1, \qquad \eta_\phi = m_{\rm p}^2\left(\frac{V_{\phi\phi}}{V}\right) \ll 1 \ . \tag{3.3}$$

These conditions assume that the Universe is already inflating with the first condition ensuring that $V \gg \dot{\phi}^2/2$ (or equivalently that ω does not deviate too much from -1) and the second that the evolution of this parameter is sufficiently slow. When these two conditions are satisfied the scalar field is overdamped and the equation of motion reduces to:

$$3H\dot{\phi} + V_\phi \simeq 0 \ . \tag{3.4}$$

In this regime the Hubble parameter is approximately constant and the Friedmann equations Eq. (2.4) shows that the scale factor is growing exponentially, $a(t) \sim \exp(Ht)$. Due to the large amount of expansion required it is convenient to parametrise the amount of expansion by the number of e-foldings:

$$N_{\rm e} \equiv \ln\frac{a_{\rm e}}{a_{\rm i}} = \int_{t_{\rm i}}^{t_{\rm e}} H dt = \int_{\phi_{\rm e}}^{\phi_{\rm i}} \frac{V}{V_\phi m_{\rm p}^2} d\phi \ . \tag{3.5}$$

The subscripts i and e label the value at the beginning and end of inflation. Inflation ends when the slow roll parameters become $\mathcal{O}(1)$ at which point the field ceases to slow roll, becomes underdamped and the equation of state of the fluid can no longer generate the accelerated expansion. We will return, after discussing the cosmological perturbations, to the subject of the number of e-folds of inflation which are required.

3.3 Cosmological perturbations and observables

The inflaton, being a quantum field, inevitably has quantum fluctuations. Due to the quasi-de Sitter spacetime during inflation these quantum fluctuations will grow as they are stretched by the quasi exponential expansion and thus crucially can become large enough to account for the large scale structure we observe in the Universe today (for good reviews see e.g.[38, 39, 40]).

EFE relate matter to spacetime curvature and so it is evident that fluctuations in the scalar field, which lead to fluctuations in the stress-energy tensor, will

induce fluctuations in the space-time metric. We can split the inflaton field into a homogeneous part, which satisfies the classical equation of motion and a small perturbation, $\delta\phi$. The evolution of the perturbation can be obtained from Eq. (3.1) and is given by:

$$\delta\ddot{\phi} + 3H\delta\dot{\phi} + V_{\phi\phi}\delta\phi - \frac{\nabla^2}{a^2}\delta\phi = 0 \ . \tag{3.6}$$

When the scalar field is overdamped and slow rolling, $V_{\phi\phi}^{1/2} \simeq m_\phi \ll H$, which can be seen from the η slow roll parameter, we can neglect the mass term and in Fourier space the modes evolve independently. We quantise the fluctuations using the usual raising and lowering operators and by introducing $\chi_k(\tau) = a(t)\delta\phi_k(\tau)$, where we are now working in conformal time, τ the evolution of the Fourier modes reduces to:

$$\chi_k'' + k^2\left(1 - \frac{2}{k^2\tau^2}\right)\chi_k = 0 \ . \tag{3.7}$$

Thus the modes obey a harmonic oscillator-like equation with a growing and decaying mode. We note that due to the growth of the scale factor the physical wavelength of the perturbations, $\lambda_{\rm phys} = 2\pi a/k$, grows until they become larger than the Hubble radius, $a/k \gg H^{-1}$. At this point two points on the wave separated by a distance greater than this are no longer in causal contact. Deep inside the horizon, when $|k\tau| \gg 1$, the modes behave like they are in Minkowski space and thus we can chose the vacuum state of the fluctuations to be the Bunch-Davies vaccum. This is defined as the minimal energy state which is annihilated by the lowering operators for all the Fourier $\mathbf{k}$ modes:

$$\hat{a}_{\mathbf{k}}|0\rangle = 0 \ . \tag{3.8}$$

This places the constraint on the initial amplitude of the mode functions:

$$\lim_{\tau\to-\infty}\chi_k(\tau) = \frac{e^{-ik\tau}}{\sqrt{2k}} \ . \tag{3.9}$$

We note that this is not a unique choice and many non trivial vacuum configurations could be possible, including the possibility that the perturbations have statistical distributions which will be relevant for the warm inflation scenario. Upon specification of the vacuum state the mode functions are uniquely

determined:

$$\chi_k = \frac{e^{-ik\tau}}{\sqrt{2k}}\left(1 - \frac{i}{k\tau}\right) \ . \tag{3.10}$$

The two point fluctuation correlation can then be computed:

$$\langle \delta\phi_{\mathbf{k}} \delta\phi_{\mathbf{k}'} \rangle = (2\pi)^3 \delta(\mathbf{k} - \mathbf{k}') \frac{H^2}{2k^3}(1 + k^2\tau^2) \ . \tag{3.11}$$

We can define the power spectrum for this distribution, $\langle \delta\phi^2 \rangle = \int \Delta^2_\phi(k) d\ln k$, which on superhorizon scales approaches a constant (remember τ decreases during inflation):

$$\Delta^2_\phi = \left(\frac{H}{2\pi}\right)^2 \ . \tag{3.12}$$

Although the power spectrum is a constant, the variance of the inflaton fluctuations grows linearly with the number of e-folds as scales continue exiting the horizon and freezing out. Crucially the Hubble parameter in practice is not constant but slowly decreases with the evolution of the inflaton, which gives rise to a slight deviation from scale-invariance.

As we mentioned previously these fluctuations induce fluctuations in the metric, which can be decomposed as follows:

$$ds^2 = -(1 + 2\Phi)dt^2 + 2aB_i dx^i dt + a^2[(1 - 2\Psi)\delta_{ij} + E_{ij}]dx^i dx^j \ . \tag{3.13}$$

A general perturbation thus has 10 components. However, there is some subtlety, when we decomposed our scalar field into a homogeneous part and a fluctuation we essentially fixed a surface to define the perturbation relative to. Thus not all the 10 components of the perturbed metric are actually physical, we have a gauge redundancy as the two sources of perturbations are not unrelated. It is thus convenient to define gauge invariant quantities which by definition are independent of the way in which we decompose the field. The two most commonly used are the *comoving curvature perturbation*, $\mathcal{R}$, and the *uniform-density hypersurface perturbation*, ζ:

$$-\zeta \equiv \Psi + \frac{H}{\dot{\rho}}\delta\rho \ , \qquad \mathcal{R} \equiv \Psi - \frac{H}{\rho + p}\delta q \ , \tag{3.14}$$

where δq is the scalar part of the three momentum density $T^0_{\ i} = \partial_i(\delta q)$. On superhorizon scales and also during slow roll these two gauge invariant quantities

are equivalent. In addition they are conserved on superhorizon scales in the absence of entropy perturbations. In the spatially-flat gauge, $\Psi = 0$ the curvature perturbation becomes:

$$\mathcal{R} = \frac{H}{\dot{\phi}}\delta\phi \ . \tag{3.15}$$

The two point correlation of $\mathcal{R}$ is then given by:

$$\langle \mathcal{R}_{\mathbf{k}}\mathcal{R}_{\mathbf{k}'}\rangle = \left(\frac{H}{\dot{\phi}}\right)^2 \langle \delta\phi_{\mathbf{k}}\delta\phi_{\mathbf{k}'}\rangle \ . \tag{3.16}$$

And so we can define the power spectrum for this curvature perturbation:

$$\Delta^2_{\mathcal{R}}(k) = \frac{H_*^2}{(2\pi)^2}\frac{H_*^2}{\dot{\phi}_*^2} \ . \tag{3.17}$$

$\mathcal{R}$ approaches a constant on super-horizon scales and as such we can evaluate it at horizon crossing (the moment when $k = aH$ indicated by the $*$ subscript) and it will remain constant until re-entry. The power spectrum of the adiabatic perturbations is measured from CMB observations and is found to be $\simeq 2 \times 10^{-9}$ [41]. The power spectrum for the tensor modes can be analysed analogously (note that the vector modes are not sourced by perfect fluids during inflation) by again expanding the action and quantising the perturbations. The gravitational waves in this case (with two polarisations) behave as a massless field and the power spectrum is given by:

$$\Delta^2_{\mathrm{t}}(k) = \frac{2}{\pi^2}\frac{H_*^2}{m_{\mathrm{p}}^2} \ . \tag{3.18}$$

The crucial differences here are the m_{p} suppression, arising from the expansion of the Einstein-Hilbert action, and the absence of the $(H_*/\dot{\phi}_*)^2$ prefactor due to the fact that tensor perturbations are already gauge invariant objects.

These adiabatic perturbations freeze out on super-horizon scales and remain conserved until horizon reentry. Once inflation ends and the Universe begins to reheat the comoving horizon begins to increase. Perturbations which were super horizon now reenter and begin to evolve once more under the influence of causal processes.

These power spectra exhibit a slight scale dependence due to the slowly

evolving Hubble parameter and one can parametrise such a dependence by:

$$\Delta^2_{\mathcal{R}}(k) = A_{\rm s}(k_*)\left(\frac{k}{k_*}\right)^{n_{\rm s}-1} , \qquad \Delta^2_{\rm t}(k) = A_{\rm t}(k_*)\left(\frac{k}{k_*}\right)^{n_{\rm t}} . \tag{3.19}$$

$A_{\rm s}$, $A_{\rm t}$ are the scalar and tensor amplitudes measured at some pivot scale and the spectral indices, $n_{\rm s}, n_{\rm t}$ contain the scale dependence:

$$n_{\rm s} - 1 \equiv \frac{d\ln\Delta^2_{\mathcal{R}}(k)}{d\ln k} = -6\epsilon_* + 2\eta_* , \tag{3.20}$$

$$n_{\rm t} \equiv \frac{d\ln\Delta^2_{\rm t}(k)}{d\ln k} = -2\epsilon_* . \tag{3.21}$$

It is interesting to note that the standard slow roll inflation model makes the generic prediction that the tensor index is negative within the range $0 \gtrsim n_{\rm t} \gtrsim -2$ and so the tensor spectrum is red. This is due to the fact that the Hubble parameter sets the scale of the tensor perturbations whilst also necessarily decreasing as modes leave the horizon, assuming that the null-energy condition is not violated. If primordial gravitational waves are detected at some point in the future a blue measurement for the tilt of the tensor power spectrum would seem to rule out most inflation models and a measurement of $n_{\rm t} \lesssim -2$ would disfavour this simple slow roll picture. One can also look at the running of the spectral indices, which parametrises the dependence of $n_{\rm s}$ on the scale. These are typically $\mathcal{O}(\epsilon,\eta)^2$:

$$n'_{\rm s} \simeq -2\epsilon(12\epsilon - 8\eta + \xi) , \qquad n'_{\rm t} \simeq -4\epsilon(\epsilon - \eta) , \tag{3.22}$$

where $\xi = 2m^2_{\rm p}(V_{\phi\phi\phi}/V_\phi)$. Thus for slow roll models of inflation where $n_{\rm s} - 1 \sim \mathcal{O}(\epsilon,\eta)$ the running of the spectral indices are extremely small $\sim \mathcal{O}(10^{-3})$ and to date there is no significant evidence for running [1].

One can also define the tensor-to-scalar ratio which measures the relative power in the gravitational wave spectrum compared to the adiabatic scalar perturbations:

$$r \equiv \frac{\Delta^2_{\rm t}}{\Delta^2_{\mathcal{R}}} = 16\epsilon_* . \tag{3.23}$$

We can immediately see that there is a consistency relation [42] for the cold inflation paradigm where:

$$r = -8n_{\rm t} . \tag{3.24}$$

More specifically this is a test for models of inflation based on a single slowly rolling scalar field generating the entirety of the adiabatic perturbation. Deviations from this relation arise for multi field models, the curvaton scenario and for warm inflation, amongst others. This is a powerful testable relation for a whole class of inflationary models and is clearly an important goal for future observations. It is also interesting to note that the value of r provides a direct measurement of the scale of inflation:

$$V^{1/4} \simeq 10^{16} \left(\frac{r}{0.1}\right)^{1/4} \text{GeV} \ . \tag{3.25}$$

Thus an observable measurement of r corresponds to inflation taking place near the GUT scale and thus inflationary physics may act as a probe for particle physics at these high energies. Inflation may however have occurred at much lower energies, this is compatible with observation as long as the reheat temperature is sufficiently high to allow for BBN to take place. However such low scale models predict a vanishingly small r and as such are less interesting from an observational point of view.

For single field models of cold inflation, as long as $r(N_\text{e})$ is approximately constant during inflation, which is compatible with a close-to-flat tensor power spectrum, we obtain the Lyth bound [43]:

$$\frac{\Delta\phi}{m_\text{p}} \simeq \sqrt{\frac{r}{8}} N_\text{e} \ . \tag{3.26}$$

For observable, larger values of $r \gtrsim 0.01$ this requires inflation to take place at trans-planckian field values $\Delta\phi \gtrsim m_\text{p}$, models which do this are referred to as large field models. There are ways to evade this bound for example the field need not be single valued in its evolution. This occurs in axion monodromy models of inflation where the inflaton (which is protected by a shift symmetry) has a periodic potential and as such the inflaton can wind itself around this potential many times during its evolution, effectively allowing for the field to travel planckian distances at sub planckian field values. This bound is also modified in the warm inflation scenario as we will show in the following chapter.

The exact number of e-folds of accelerated expansion is not known but at least around $N_\text{e} \gtrsim 60$ are needed to address the horizon problem. Cosmologically observable scales, from the size of the observable Universe down to the size of

galaxies, were generated in a window of about ~ 10 e-folds during inflation, thus our observations can only constrain the inflationary dynamics in this limited small window. Although the total number of e-folds may never be known, we can estimate to some extent the number of e-folds before the end of inflation when a certain cosmological scale left the horizon. A given comoving scale leaves the horizon during inflation when $k = aH$, due to the decreasing comoving Hubble radius this scale is driven far outside the horizon. Once inflation ends and the comoving Hubble radius begins to increase, in the radiation and matter dominated eras, this scale will eventually reenter once more when $k = aH$. If we consider a scale corresponding to the size of our observable Universe then if this was generated $N_{\rm e}$ e-folds before the end of inflation, then it will reenter $N_{\rm e}$ e-folds after inflation has ended. Thus one can use the knowledge of the post inflationary evolution to constrain the inflationary duration somewhat (see [44] for more details). Unfortunately due to the largely unconstrained era of reheating there is significant uncertainty in the number of e-folds of the post inflationary evolution and any late time periods of entropy production can add to this uncertainty. There may be more hope within the warm inflation scenario where the inflationary period undergoes a smooth transition into the radiation era, without the need for a separate reheating period. Canonical values considered are typically in the range $N_{\rm e} \sim 50-60$, although this is a fairly relaxed constraint. We once again note that inflation itself may last considerably longer than this such that the horizon, flatness and monopole problems are all easily solved.

3.3.1 Monomial potentials

One of the simplest classes of models of inflation is based on monomial potentials of the form $V = \lambda(\phi/m_{\rm p})^n m_{\rm p}^4$. For $n = 2, 4$ this potential can arise as either a mass term or a self interaction in a renormalisable quantum field theory. Other values, including non integer values, are possible for example $n = 4/3, 1, 2/3$ arise within axion monodromy models. These monomial potentials give rise to slow roll parameters $\epsilon = (n^2/2)(m_{\rm p}/\phi_*)^2$, $\eta = n(n-1)(m_{\rm p}/\phi_*)^2$. Inflation thus occurs for super planckian field values, $\phi_* \gtrsim m_{\rm p}$, with the following observational predictions:

$$n_{\rm s} - 1 \simeq -\frac{2+n}{2N_{\rm e}} \ , \qquad r \simeq \frac{4n}{N_{\rm e}} \ . \tag{3.27}$$

The current bound on $r \lesssim 0.1$ already restricts $n \lesssim 3/2$ for $50 \lesssim N_{\rm e} \lesssim 60$. Thus the quartic potential ($r \sim 0.3$) is strongly ruled out and the quadratic potential ($r \sim 0.14$) is disfavoured in comparison with other models predicting lower values.

In the next chapter we will return to the quartic potential and show how it can be brought back into agreement with Planck data through finite temperature effects.

3.4 Isocurvature

If inflation is driven by a single field then upon decay its fluctuations are transferred democratically to all the degrees of freedom it decays into with $\delta(n_{\rm m}/n_{\rm R}) = 0$. The perturbations in each component of the fluid are then equal:

$$\frac{\delta\rho_{\rm R}}{\rho_{\rm R}} = \frac{4}{3}\frac{\delta\rho_{\rm m}}{\rho_{\rm m}} \ . \tag{3.28}$$

There is a relative factor of 4/3 between the perturbations due to the different scaling behaviours of relativistic and non-relativistic matter. Observations of the CMB find that the dominant perturbations are adiabatic, however there is room for deviations from this. In principle there are two distinct types of isocurvature perturbations which are detectable; matter isocurvature perturbations and neutrino isocurvature perturbations. One can define such perturbations as follows:

$$\mathcal{S}_{\rm m} = \frac{\delta\rho_\gamma}{\rho_\gamma} - \frac{4}{3}\frac{\delta\rho_{\rm m}}{\rho_{\rm m}} \ , \tag{3.29}$$

$$\mathcal{S}_\nu = \frac{4}{3}\frac{\delta\rho_\gamma}{\rho_\gamma} - \frac{4}{3}\frac{\delta\rho_\nu}{\rho_\nu} \ . \tag{3.30}$$

In general the matter isocurvature modes can be made from the fractional contributions of cold dark matter and baryonic components, although these are presently indistinguishable (note that the 21cm observations might alleviate this degeneracy [45]):

$$\mathcal{S}_{\rm m} = \frac{\Omega_{\rm cdm}}{\Omega_{\rm m}}\mathcal{S}_{\rm cdm} + \frac{\Omega_{\rm B}}{\Omega_{\rm m}}\mathcal{S}_{\rm B} \ . \tag{3.31}$$

The neutrino isocurvature perturbation includes the effects of any other relativistic species present at the era decoupling with these degrees of freedom usually parametrised by an effective number of neutrino degrees of freedom,

$N_{\rm eff}$. It is also important to note that if all the degrees of freedom thermalise after inflation, then the isocurvature perturbations are washed out as then the temperature uniquely determines the number density of the species present. However thermalisation cannot occur on superhorizon scales and so any relative superhorizon perturbations remain until they re-enter the horizon. It is often convenient to parameterise the isocurvature perturbations by their relative power in comparison to the adiabatic modes. In this thesis we will mainly be concerned with baryon isocurvature perturbations and thus with the ratio $B_{\rm B} = S_{\rm B}/\zeta$. The bounds on this parameter are sensitive to the scale dependence of the isocurvature power spectrum, $n_{\rm iso} = d\ln S_{\rm B}/d\ln k$ and whether the perturbation is (anti) correlated or uncorrelated with the adiabatic spectrum. We will introduce these bounds as they become relevant in the following chapters noting how baryon isocurvature perturbations produced during warm inflation can be observationally distinct from those produced from axion or curvaton models.

Models of inflation involving more than one field driving the expansion easily give rise to isocurvature perturbations as can curvaton scenarios, where the decay products experience fluctuations from two independent field perturbations. More importantly for this thesis isocurvature perturbations can arise within the warm inflation scenario. In this case the inflaton dissipates its vacuum energy into light degrees of freedom and if the interactions violate C, CP and some global quantum number then it will also produce an asymmetry in these light degrees of freedom e.g. between squarks and anti-squarks. This asymmetry then inherits the field fluctuations and is generically fully (anti) correlated with the adiabatic perturbations. We will discuss this further in later chapters.

3.5 Non-gaussianity

Although not strictly relevant for this thesis, non-gaussianity is a powerful observational constraint that may be able to help distinguish between the multitude of inflation models on the market. As we previously saw, the inflaton perturbations (in the massless limit) have a gaussian distribution defined by:

$$\langle \delta\phi_k \rangle = 0 \ , \qquad \langle \delta\phi_k \delta\phi_{k'} \rangle = (2\pi)^3 \delta(\mathbf{k}-\mathbf{k}') \frac{H^2}{2k^3} \tag{3.32}$$

However the presence of a mass term (or interactions with itself or other degrees of freedom) for the inflaton leads to higher order odd-n point correlations (higher order even-n correlators can be expressed in terms of combinations of 2-point correlators), in particular the three point correlator or bi-spectrum of the curvature perturbation:

$$\langle \mathcal{R}_{k_1} \mathcal{R}_{k_2} \mathcal{R}_{k_3} \rangle = (2\pi)^3 \delta(k_1 + k_2 + k_3) B_{\mathcal{R}}(k_1, k_2, k_3) \ . \tag{3.33}$$

The delta function arises out of translational invariance of the background. The dependence upon the three momenta, the shape of $B(k_1, k_2, k_3)$ depends upon the inflationary model in consideration which gives rise to peaks of the bispectrum in different regions. Maldacena derived a powerful result for single field models of inflation [46]:

$$\langle \mathcal{R}_{k_1} \mathcal{R}_{k_2} \mathcal{R}_{k_3} \rangle_{k_3 \to 0} = (2\pi)^3 \delta(k_1 + k_2 + k_3)(1 - n_{\rm s}) \mathcal{P}_{\mathcal{R}_1} \mathcal{P}_{\mathcal{R}_2} \tag{3.34}$$

In this so called squeezed limit the bispectrum is suppressed by $(1-n_{\rm s}) \sim 0.04$ and vanishes for a scale invariant spectrum. Therefore any significant measurement of primordial non gaussianity would rule out single field models of slow roll inflation. On the other hand models of inflation involving multiple fields interacting with the inflaton can lead to significant levels of non-gaussianity at levels which may be detectable in the future.

3.6 Reheating

In the cold inflation picture any pre existing matter or radiation distributions are diluted to negligible amounts by the quasi-exponential expansion of the Universe. Thus once inflation ends the Universe needs to reheat and be repopulated with at least the Standard Model degrees of freedom so that BBN can take place. In order for this to happen some mechanism needs to take place so that the vacuum energy of the inflaton can be converted into the SM degrees of freedom. This requires the inflaton to have couplings with other degrees of freedom, thus the decay of the inflaton condensate can act as the reheating mechanism.

Typically once inflation ends the inflaton field becomes underdamped with $m_\phi \gg H$ and begins to oscillate about the minimum of its potential with a frequency $\omega^2 = V_{\phi\phi}$. Perturbative reheating is often modelled through an extra

phenomenological reheating term, $\Gamma\dot{\phi}$ in the scalar field's equation of motion:

$$\ddot{\phi} + 3H\dot{\phi} + \Gamma\dot{\phi} + V_\phi = 0 \ . \tag{3.35}$$

The presence of this decay width in the equation of motion comes from the replacement of the mass $m^2 \to m^2 + \Pi(\omega)$, where $\Pi(\omega)$ is the result of summing all the 1PI corrections to the two point propagator. If kinematic decay is possible then $Im(\Pi) = m\Gamma$ which we can interpret as a decay width and this term can then be described as a friction term $\Gamma\dot{\phi}$ in the case where the field is oscillating (see [47, 13, 48]). This decay width can be calculated perturbatively once the relevant interactions are known. We emphasise that in this approach this term was not derived from some fundamental lagrangian, if one wishes to treat the effects of the interactions on the background scalar field one should look at the quantum effective action, which is precisely what warm inflation does, but we will discuss this in more detail later. In this picture the energy density of the field obeys:

$$\dot{\rho_\phi} + 3H\dot{\phi}^2 + \Gamma\dot{\phi}^2 = 0 \ . \tag{3.36}$$

If the field is oscillating one can average this equation over a cycle where $\langle V \rangle = \langle \dot{\phi}^2/2 \rangle = \rho_\phi$. It is also easy to see that $p_\phi = 0$ and so an oscillating scalar field (in a quadratic potential) behaves as pressureless dust, as non-relativistic matter and its energy density will redshift as $\rho_{\rm m} \propto a(t)^{-3}$. Assuming that the decay products are relativistic and thermalised, in this regime we thus have two coupled equations describing the radiation, $\rho_{\rm R}$, and scalar field energy densities:

$$\begin{aligned} \dot{\rho_\phi} + 3H\rho_\phi + \Gamma\rho_\phi = 0 \ , \\ \dot{\rho_{\rm R}} + 4H\rho_{\rm R} = \Gamma\rho_\phi \ . \end{aligned} \tag{3.37}$$

Thus the decays transfer energy from the scalar field to the radiation. We can estimate the reheat temperature in this model by noting that as soon as the decay is possible i.e. $\Gamma \simeq H$ then the vacuum energy of the scalar field will be quickly transferred into radiation. The reheat temperature in this instantaneous picture is thus given by:

$$T_{\rm RH} \simeq \left(\frac{90}{g_* \pi^4}\right)^{1/4} \sqrt{\Gamma m_{\rm p}} \ . \tag{3.38}$$

The picture we outlined above is termed *perturbative reheating* in the sense that reheating can be treated as the decay of the oscillating scalar field as a single particle with a decay width calculated perturbatively through QFT. One can go beyond this simple perturbative picture to consider *preheating* which takes into account the time dependent mass of the decay products and can result in a very rapid particle production within the first few oscillations of the inflaton field [49, 50, 51].

The reheating temperature is largely unconstrained apart from the bound from BBN, $T_{\rm RH} \gtrsim 1$ MeV. There are some theoretical upper bounds on the reheat temperature coming from not wanting to restore GUT symmetries which may cause topological defects such as monopoles to be reborn - one of the reasons inflation was initially proposed. Another constraint comes from the thermal production of gravitinos, which can be over produced or spoil the abundances of light elements at BBN, however this is a very model dependent problem and we will discuss this further in a later chapter.

As an aside we will mention briefly the justification for treating the inflaton as being a largely non interacting system, at least until reheating starts. In the vacuum the decay width for the inflaton into other, lighter degrees of freedom goes as the mass of the inflaton $\Gamma \sim m_\phi$. However in order to sustain the exponential expansion, one requires $m_\phi \ll H$ and so $\Gamma \ll H$. Thus the inflaton is effectively stable on Hubble time scales and the interactions should have a negligible effect on the dynamics. As we will later show if the inflaton is interacting with particles in non trivial distributions then the interactions can indeed have a significant effect on the dynamics, beyond the quantum corrections to the effective potential. In a somewhat simple argument if the inflaton is interacting with a thermal bath at a temperature, T, with all particles including the inflaton in thermal equilibrium and relativistic, then the decay width of the inflaton $\Gamma \sim T$. If $T > H$ then the timescale for this decay is shorter than the timescale characterising the expansion and thus the inflaton can decay. Note this is still compatible with maintaining slow roll if $m_\phi \ll H < T$. Although this is a somewhat overly simple picture as we shall see the presence of this new scale, T, during inflation can allow for significant energy transfer between the inflaton and a radiation bath similar to Eq. (3.37) through interactions without violating slow roll.

Chapter 4

Warm inflation

More than three decades since its original proposal [52, 30, 31], inflation has passed one of its most stringent tests with the recent measurements of the temperature anisotropies of the CMB made by the Planck satellite [1]. In particular, simple models of inflation based on the dynamics of a slowly rolling scalar field generate a primordial spectrum of density perturbations that is essentially adiabatic, gaussian and nearly but not exactly scale-invariant, in agreement with observations.

While Planck has been able to strongly constrain and in some cases even rule out certain inflationary models, the fundamental mechanism driving inflation has yet to be discovered. The standard cold inflation picture assumes that the accelerated expansion quickly erases all traces of any pre-inflationary matter or radiation distributions, so that slow-roll inflation occurs in an almost perfect vacuum state. However, the inflaton field is necessarily coupled to other degrees of freedom in order to dissipate its vacuum energy and reheat the universe, so one may envisage scenarios where dissipative effects become important during and not only after the slow-roll phase. These are generically known as warm inflation scenarios [3, 4, 5, 6, 7] (see also [8, 9, 10]), and raise the interesting possibility that the inflationary universe is not in a perfect vacuum, even though vacuum energy is the dominant component for accelerated expansion to take place.

Warm inflation arises as a consequence of fluctuation-dissipation dynamics which in turn arises through the interactions of the inflaton field with other degrees of freedom, in particular this is enhanced if they have non-trivial statistical distributions. Dissipation through these interactions leads to energy exchange between the inflaton and the degrees of freedom to which it couples,

inducing particle production concurrent with the accelerated expansion and in certain parametric regimes can sustain a radiation bath during inflation. Dissipation therefore acts as a source term in the Boltzmann equation for the radiation and if it is large enough then it can counter the effects of Hubble dilution, with the temperature slowly varying as opposed to exponentially decreasing. Thus dissipation acts as an additional source of damping that can allow for longer periods of accelerated expansion, which is particularly important in supergravity/string theories, where F-term supersymmetry breaking typically induces large inflaton masses, thus alleviating the associated eta-problem [53, 54, 55, 56, 57]. Whilst radiation is a subdominant component of the energy balance in the universe when accelerated expansion is occurring, in several scenarios it may actually come to dominate at a later stage, providing a smooth transition into a radiation-dominated era, in alternative to the standard reheating picture. Dissipation comes with its own associated noise, which encompasses the effect of the light degrees of freedom back-reacting on the inflaton perturbing its motion. These thermal fluctuations may then act as a classical source for the primordial density perturbations, challenging the widely held view that it is quantum fluctuations which are responsible for the structure in the Universe. The spectrum of the primordial density fluctuations may thus be significantly modified [4, 11, 58, 59, 60, 61], in particular the amplitude of tensor perturbations is suppressed and potentially observable deviations from a gaussian spectrum are induced [62, 63, 64, 65, 66].

In this chapter, before describing warm inflation, we will begin by introducing fluctuation-dissipation dynamics. This dynamics is not exclusive to the inflaton field and in a later section we will see that it can have serious consequences for other cosmological scalars [67]. We will then move on to show how it can affect the dynamics and observables of the inflationary period, giving rise to the warm inflation paradigm. Finally, we will consider a simple model of inflation with a quartic potential and renormalizable interactions and show how fluctuation-dissipation dynamics can bring this model back into remarkable agreement with the latest Planck data.

4.1 Fluctuation-dissipation dynamics

Scalar fields employed in particle physics and their associated cosmological models are not isolated systems and generically interact with other degrees of freedom. Their dynamics is therefore described by a quantum effective action that encodes the effects of all interactions with other fields and from which one can determine their equation of motion. In the cosmological context, this effective action must take into account the non-trivial statistical states of both the dynamical field and the degrees of freedom with which it interacts. The black-body spectrum of the Cosmic Microwave Background and the successful predictions of BBN show that the universe was in a state very close to local thermal equilibrium for a great part of its early history, and we will henceforth assume that all relevant particle states always remain near this configuration.

For static fields the effective action reduces to a local effective potential, which takes the well-known Coleman-Weinberg form at leading order in a perturbative expansion [68]. From the finite temperature effective potential one can derive the thermodynamic properties of the cosmological fields, such as their energy density, entropy and pressure, as well as thermal mass corrections. Static fields are, however, generically of little interest in cosmology, and for dynamical fields the effective action includes non-local effects beyond the leading effective potential approximation.

Time non-local effects may take different forms depending on the regime considered. The simplest case is the *adiabatic* regime, where the field varies on time scales that largely exceed the typical time scales of the relevant microphysical processes. This is for example the case of the inflaton field, which in the simplest scenarios is slowly rolling in order to produce a quasi-de Sitter phase. Local thermal equilibrium in the ambient heat bath can be maintained if scattering and/or decay processes within it are sufficiently fast, namely faster than Hubble expansion, such that an adiabatic approximation will be valid for large classes of cosmological scalar fields.

In the adiabatic limit, a system has sufficient time to relax to an equilibrium configuration in response to the perturbing effect of the time non-local terms in the effective action, and linear response theory can be used to study the system's evolution. The leading time non-local effect is dissipation of the scalar field's energy into the degrees of freedom in the heat bath, which manifests itself through

an effective friction term in the field's equation of motion.

The simplest example of this is the creation and subsequent annihilation of particle-antiparticle pairs coupled to the background field, where this coupling makes the amplitude of creation and annihilation field-dependent. Suppose then that pairs are created at a time t where the scalar field takes a value $\phi(t)$. They will then annihilate at time $t + \delta t$ where the field has shifted by an amount $\delta\phi = \dot{\phi}\delta t + \dots$ in the adiabatic regime, and to leading order there will be a net particle production proportional to $\dot{\phi}$, resulting in a transfer of energy from the scalar field into the produced degrees of freedom. This will perturb the local thermal equilibrium in the ambient heat bath but the system can relax into a new equilibrium configuration if adiabatic dissipation is slower than other microphysical processes.

Dissipation corresponds to the systematic effect of the particles in the heat bath on the evolution of the field and the resulting friction opposes the latter's evolution through the creation and annihilation of particles in the heat bath in a field-dependent fashion, as outlined above. This is entirely analogous, for example, to the systematic friction force produced on a moving mirror by a rarefied gas of molecules that randomly hit the the mirror in a brownian motion [69]. Much like this random brownian motion also results in an irregular motion of the mirror, fluctuations in the cosmological heat bath will also backreact on the evolution of the scalar field and introduce a degree of randomness. The two effects, fluctuations and dissipation, result from the same interactions between the scalar field and the heat bath and are thus interconnected. This is a general result that applies to large classes of dissipative systems in nature and is known as the *fluctuation-dissipation theorem*, the details of which depend on the statistical state of the system and its microscopic properties.

4.1.1 A simple derivation

The calculation of dissipation and its associated noise within a quantum field theory framework is an involved process requiring a detailed non-equilibrium statistical calculation. This has been performed and outlined in various papers (in particular see [7] for an overview) and we outline the calculation briefly in Appendix A. In this section we will give a brief heuristic derivation of dissipation, largely following the discussion within [70, 71] which will give a nice physical

description of the dynamics, hopefully allowing for an easier understanding of the remainder of this thesis without becoming too involved in the field theory behind these calculations.

Consider a massive scalar field, ϕ, interacting with a light scalar, χ with an interaction given by $\mathcal{L}_{\rm int} = g^2\phi^2\chi^2/2$. Performing an averaging procedure over the fields, the equation of motion generically has the form:

$$\ddot{\phi} + 3H\dot{\phi} + m^2\phi + g^2\phi\langle\chi^2\rangle = 0 \ , \tag{4.1}$$

where $\langle\phi\rangle = \phi$ represents the classical, statistically averaged field value. Although this is not a rigorously derived expression, it is qualitatively similar to the expression obtained from the field theory approach. The statistical average of the $\langle\chi^2\rangle$ term can be determined by inspecting the quantised scalar field in momentum space:

$$\langle\chi^2\rangle = \frac{1}{(2\pi)^3}\int\frac{d^3k}{\omega_\chi}\langle a^\dagger_{\mathbf{k}}a_{\mathbf{k}}\rangle \ . \tag{4.2}$$

In a state of thermal equilibrium the number density operator $\langle a^\dagger_{\mathbf{k}}a_{\mathbf{k}}\rangle^{\rm eq} = n^{\rm eq}_\chi(k) = (e^{\omega_\chi/T}-1)^{-1}$ can be identified with the Bose-Einstein distribution with $\omega_\chi = \sqrt{k^2+g^2\phi^2}$ where $k = |\mathbf{k}|$. Note that the χ field's mass depends upon the background field value and, as such, if the field value varies in time so does the mass of the χ field. This affects the number density of the χ particles which will try to readjust to maintain thermal equilibrium.

Suppose the system is initially in thermal equilibrium, then the field ϕ evolves by an amount $\Delta\phi$. The mass of the χ fields changes in this time, however their number density takes a certain time, related to the interaction rates to relax back to equilibrium. Thus the number density departs from its equilibrium value and remains equal to its equilibrium value when the field was at $\phi - \Delta\phi \simeq \phi - \dot{\phi}\Delta t$. The number density changes by $\Delta n_\chi \simeq n_\chi - n^{eq}_\chi \simeq -(dn^{\rm eq}_\chi/d\phi)\dot{\phi}\delta t$ which in turn induces a change in $\langle\chi^2\rangle$:

$$\langle\chi^2\rangle \simeq \langle\chi^2\rangle_{\rm eq} - \frac{\dot{\phi}}{(2\pi)^3}\int\frac{d^3k}{\omega_\chi}\frac{dn^{\rm eq}_\chi}{d\phi}\delta t \ . \tag{4.3}$$

For $m_\chi = g\phi \ll T$, then the first term gives rise to a thermal mass for the ϕ field of the form $\langle\chi^2\rangle_{\rm th} \sim T^2$, whilst in the opposite, non-relativistic limit where $m_\chi \gg T$ the thermal effects are Boltzmann (exponentially) suppressed. It takes a finite amount of time for the χ fields to reobtain thermal equilibrium after

this perturbation, a timescale, Γ_χ^{-1}, which is characterised by the decays, inverse-decays and scattering process which thermalise the light degrees of freedom. If we take $\delta t \sim \Gamma_\chi^{-1}$ then the χ fields can maintain thermal equilibrium throughout the evolution of the ϕ field. The equation of motion for the scalar field thus takes the form:

$$\ddot{\phi} + 3H\dot{\phi} + m_{\rm T}^2\phi + \Upsilon\dot{\phi} = 0 \ , \tag{4.4}$$

where $m_{\rm T}$ includes the thermal mass corrections. We identify Υ as the dissipative coefficient:

$$\Upsilon = \frac{g^4\phi^2}{T}\int \frac{d^3k}{(2\pi)^3}\frac{n_\chi(1+n_\chi)}{\Gamma_\chi\omega_\chi^2} \ . \tag{4.5}$$

As the fields involved are relativistic they all have thermal masses $\lesssim T$. The dominant contribution to this integral comes from momenta of order $k \sim m \sim T$ and so the dissipation coefficient has the form $\Upsilon \simeq C\phi^2/T$ where C contains the numerical factors. Note in particular that it does not depend upon the coupling with the light χ fields due to the cancellation with the decay width.

Although this is not a rigorous derivation of dissipative effects, and in particular does not include the fluctuations arising from the back-reaction of the light fields, several important features are illuminated. Firstly if the masses of the fields coupled to the dissipating scalar field are non-relativistic then thermal effects are exponentially suppressed and effectively switch off. There are two time scales involved; the time scale on which the dissipating field is moving and the timescale on which the light fields return to equilibrium. In the *adiabatic regime* the field is moving slowly on the time scale of the particle physics processes which act to restore the equilibrium, $\Gamma \gg |\dot{\phi}/\phi|$, thus the system can maintain thermal equilibrium despite this out-of-equilibrium dynamics. An important point of the above derivation is to notice that the dissipative term arises as a higher order term in the expansion compared to the thermal mass term and as such should always be suppressed with respect to it. This was pointed out in [71] where the authors realised that it would be hard to realise warm inflation where the light fields coupled directly to the inflaton as it would be hard to sustain slow roll, even with the aid of dissipation, against these thermal corrections. This problem can however be avoided if the light fields are sequestered from the inflaton field as we will shortly discuss.

4.1.2 Dissipation coefficients

The combined effect of fluctuations and dissipation leads to an effective Langevin-like equation (see Appendix A) for a cosmological scalar field interacting with the ambient heat bath of the form (see e.g. [72, 73, 5, 6, 74, 75] and references therein):

$$\ddot{\phi} + (3H + \Upsilon)\dot{\phi} - \frac{1}{a^2}\nabla^2\phi + V'(\phi) = \zeta \ , \tag{4.6}$$

where Υ denotes the dissipation coefficient and ζ the related random noise term, with the remaining terms yielding the usual Klein-Gordon equation in a flat FRW universe. Note that the potential includes thermal corrections from the particles the scalar field couples to. In the adiabatic regime, the noise term is gaussian to leading order and its correlator satisfies the following fluctuation-dissipation relation in momentum-space [7, 61, 76]:

$$\begin{aligned}\langle\zeta(\mathbf{k},t)\zeta(\mathbf{k}',t')\rangle = &\left[(1+2n(k))\frac{3H^2\sqrt{1+4\pi Q/3}}{\pi} + 2\Upsilon T\right] \\ &\times a^{-3}(2\pi)^3\delta^3(\mathbf{k}+\mathbf{k}')\delta(t-t') \ ,\end{aligned} \tag{4.7}$$

where we have also included a "quantum noise" contribution, given by the first term within brackets and $Q = \Upsilon/3H$. This results from a coarse-graining of the scalar field as employed in the stochastic approach to inflation [77], with short-wavelength (sub-horizon) field modes inducing an effective noise in the dynamics of the long-wavelength "classical" modes. While the form in Eq. (4.7) is obtained for a sharp mode splitting, a smooth filtering function generically results in a coloured noise distribution [78]. We have also included the effect of a generic phase-space mode distribution $n(k)$ [76], which vanishes in the standard stochastic inflation approach, but becomes significant, in particular, when the scalar field is itself thermalized and $n(k)$ is the Bose-Einstein distribution. For example, for $T \gg H, |V''(\phi)|$ and $Q \ll 1$, the first term within brackets becomes proportional to HT for modes crossing the horizon.

As discussed above, the dissipative friction term is associated with a net particle creation in the ambient heat bath. One can then integrate Eq. (4.6) and average over the noise term to obtain the evolution of the scalar field's energy density, and use energy conservation to derive the associated equation for the

heat bath:

$$\dot{\rho_\phi} + 3H\dot{\phi}^2 = -\Upsilon\dot{\phi}^2, \qquad \dot{\rho_\alpha} + 3H(\rho_\alpha + p_\alpha) = \Upsilon\dot{\phi}^2, \tag{4.8}$$

where we take the heat bath to be described, to leading order, by a perfect fluid of density ρ_α and pressure p_α. If it is composed of relativistic particles that thermalize sufficiently fast, the latter corresponds to a radiation fluid with equation of state $p_{\rm R} = \rho_{\rm R}/3$.

As we discuss below in more detail, we will be mainly interested in interactions between cosmological scalar fields and other (complex) scalar and fermionic degrees of freedom. Gauge interactions may also be of relevance for early universe cosmology, but since the main features of vector boson interactions are well described by scalar degrees of freedom we will not consider this case explicitly to simplify our discussion. We will thus consider a generic (renormalizable) Lagrangian of the form:

$$\mathcal{L} = f(\phi)|\chi|^2 + g\phi\bar{\psi}\psi \ , \tag{4.9}$$

where χ and ψ denote complex scalar and fermion fields in the heat bath and $f(\phi)$ is a generic function of the dynamical scalar field we are interested in.

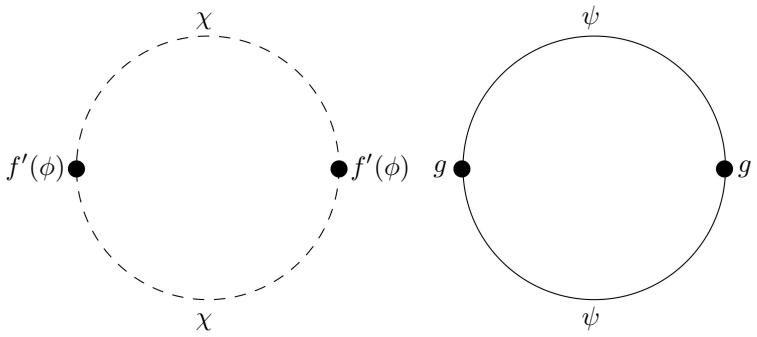

Figure 4.1: Leading 1-loop contributions of scalar and fermion degrees of freedom to the dissipation coefficient. The thick dashed and solid lines indicate dressed propagators for scalars and fermions, respectively.

The leading 1-loop contributions of these interactions to the effective action are illustrated in Fig. 4.1 and, for a nearly-thermal heat bath at temperature

$T = 1/\beta$, these yield an adiabatic dissipation coefficient of the form:

$$\Upsilon = \frac{f'(\phi)^2}{T}\int \frac{d^4p}{(2\pi)^4}\rho_\chi(p_0,\mathbf{p})^2 n_{\rm B}(p_0)(1+n_{\rm B}(p_0)) + \frac{g^2}{2T}\int \frac{d^4p}{(2\pi)^4}{\rm Tr}\left[\rho_\psi(p_0,\mathbf{p})^2\right] n_{\rm F}(p_0)(1-n_{\rm F}(p_0)) \ , \tag{4.10}$$

where $n_{\rm B}(\omega) = (e^{\beta\omega}-1)^{-1}$ is the Bose-Einstein and $n_{\rm F}(\omega) = (e^{\beta\omega}+1)^{-1}$ is the Fermi-Dirac distribution for particle modes of energy ω. The functions ρ_χ and ρ_ψ represent the spectral functions of the scalar and fermion fields in the heat bath and can be computed from the corresponding (dressed) propagators at finite temperature, using e.g. the real-time formalism [79, 7, 80, 81]. For example, in the scalar field case one obtains:

$$\rho_\chi = \frac{4\omega_p\Gamma_\chi}{(p_0^2-\omega_p^2)^2+4\omega_p^2\Gamma_\chi^2} \ , \tag{4.11}$$

where $\omega_p = \sqrt{|\mathbf{p}|^2+m_\chi^2}$, with the field mass corresponding to its renormalized value including thermal corrections, and Γ_χ is the (finite temperature) decay width of the field. A similar, albeit more complicated expression, can be obtained in the fermionic case [80].

From Eq. (4.10) one can deduce a few generic aspects of dissipation coefficients in the adiabatic regime. Firstly, we see that if the fields χ and ψ were in a trivial (vacuum) state, the dissipation coefficient would vanish. Dissipation is thus an effect intrinsic to the motion of the scalar field in the presence of a heat bath with non-trivial occupation numbers, corresponding as argued above to the systematic effect of the heat bath degrees of freedom on the field's motion. Secondly, the spectral functions correspond to the imaginary part of the field propagators and are consequently proportional to their decay width, as shown above. Hence, if the field's χ and ψ were stable there would be no dissipation. However, at finite temperature interacting fields have always a non-zero decay width, arising from a combination of decays, inverse decays and Landau damping processes. Finally, the dissipation coefficient will in general be both field- and temperature-dependent. The temperature dependence is explicit in the distribution functions but will also arise in general in the masses and decay width of the fields. The field dependence can be explicit in the scalar case, for a generic function $f(\phi)$, but will also arise from the masses (and consequently the decay width of the fields),

noting that from Eq. (4.9) one obtains at tree-level $m_\chi^2 = f(\phi)$ and $m_\psi^2 = g^2\phi^2$.

The integrals in Eq. (4.10) can be computed numerically in general. There exists, however, two approximate regimes where the computation can be performed analytically. In the *low temperature regime*, $m_\chi, m_{\psi_\chi} \gg T$, the distribution functions $n_{\rm B}, n_{\rm F}$ become exponentially (Boltzmann) suppressed for on-shell field modes, $p_0^2 = \omega_p^2$, so that their contribution can be neglected. The main contribution in this case comes from off-shell or virtual modes with $|\mathbf{p}|, p_0 \ll m_\chi, m_\psi$, for which the spectral functions take a simple form, e.g. $\rho_\chi \simeq 4\Gamma_\chi/m_\chi^3$ in the scalar case. One can see that the dominant contribution comes from modes with $|\mathbf{p}| \ll m_\chi, m_\psi$ from studying the spectral functions in the integrand. The *low-momentum* dissipation coefficient (LM) is thus approximately given by:

$$\Upsilon^{\rm LM} \simeq \frac{16 f'(\phi)^2}{T} \int \frac{d^4p}{(2\pi)^4} \frac{\Gamma_\chi^2}{m_\chi^6} n_{\rm B}(1+n_{\rm B}) + \frac{2g^2}{T} \int \frac{d^4p}{(2\pi)^4} \frac{{\rm Tr}({\rm Im}\Sigma^2)}{m_\psi^2} n_{\rm F}(1-n_{\rm F}) \tag{4.12}$$

where ${\rm Im}\Sigma$ is the imaginary part of the fermion self energy, from which their decay width can be extracted in the conventional way. This approximation is valid in the narrow width limit where $m_i \gg \Gamma_i$ for $i = \chi, \psi$ (see [81] for more details). The integrals involving the distribution functions and the decay widths can then be performed numerically [80, 81]. A simple example that we will consider below is the case where $f(\phi) \propto \phi^2$, with $m_\chi \propto \phi$ and $\Gamma_\chi \propto m_\chi$. In this case, it is not difficult to see that $\Upsilon^{\rm LM} \propto T^3/\phi^2$ for the scalar contribution, while the corresponding fermionic contribution is suppressed by further powers of $T/m_\psi \ll 1$ as shown in [80].

In the opposite *high-temperature regime*, $m_\chi, m_\psi \ll T$, it is energetically possible to excite on-shell modes in the thermal bath and their occupation numbers are not Boltzmann-suppressed. These will then give the dominant contribution to the dissipation coefficient, and one can expand the spectral functions about their poles at $p_0 = \omega_p$ to yield:

$$\Upsilon^{\rm P} \simeq \frac{f'(\phi)^2}{T} \int \frac{d^3p}{(2\pi)^3} \frac{1}{\Gamma_\chi \omega_p^2} n_{\rm B}(1+n_{\rm B}) + \frac{2g^2}{T} \int \frac{d^3p}{(2\pi)^3} \frac{m_\psi^2}{\Gamma_\psi \omega_p^2} n_{\rm F}(1-n_{\rm F}) \tag{4.13}$$

The 3-momentum integrals can then be easily computed analytically in different regimes (see e.g. [81]). In particular, for light on-shell modes one typically obtains

$\Gamma_i \propto m_i \propto T$, for $i = \chi,\ \psi$, yielding $\Upsilon^{\rm P} \propto \phi^2/T$ for scalar modes and $\Upsilon^{\rm P} \propto T$ for fermionic modes [80, 81].

In the general case, the dissipation coefficient receives contributions from both on-shell and off-shell modes, and numerical calculations show that adding both contributions yields a very good approximation to the full result. In particular, it has been observed that the on-shell contribution can be dominant for masses $m_i \gtrsim T$ despite the associated Boltzmann-suppression, particularly for small decay widths [81].

These two regimes will be relevant for different types of particle physics and cosmological scenarios. On the one hand, in a typical phase transition the relevant Higgs field is stabilized at the origin at high temperatures and starts rolling towards the minimum of its potential below a critical temperature (potentially after tunneling in a first order phase transition). In this case, the fields it couples to are initially light, and on-shell dissipation dominates. As T decreases and the field value approaches the true minimum, these fields become heavier and the contribution of low-momentum modes will grow until it potentially dominates. On the other hand, a light scalar ϕ can attain very large values during inflation, after which it will eventually roll towards the minimum of its potential. In this case, off-shell modes will typically dominate initially, while on-shell modes will become increasingly more significant if ϕ evolves towards smaller values and χ, ψ become lighter.

In Chapter 7 we give a series of examples, by no means exhaustive, of dissipation coefficients for dynamical scalar fields in the SM and its typically considered extensions, within different dynamical regimes that may be relevant for the cosmic history.

4.2 Warm inflation dynamics

We will now discuss the consequence of FD dynamics within the context of warm inflation. We consider the scenario where the inflaton is interacting with other degrees of freedom which are in a thermalised state and in the adiabatic regime dissipation leads to a friction term in the inflaton's equation of motion:

$$\ddot{\phi} + 3H(1+Q)\dot{\phi} + V_\phi = 0\ , \tag{4.14}$$

where $Q = \Upsilon/3H$ and V_ϕ denotes the derivative of the potential (including thermal corrections) with respect to the inflaton field and the potential. Noting that the effective density and pressure of the inflaton condensate are given by $\rho_\phi = \dot{\phi}^2/2 + V(\phi)$ and $p_\phi = \dot{\phi}^2/2 - V(\phi)$, respectively, this can be rewritten as:

$$\dot{\rho_\phi} + 3H(p_\phi + \rho_\phi) = -\Upsilon\dot{\phi}^2 \ . \tag{4.15}$$

The inflaton dissipates its energy through particle production and, if the resulting particles are relativistic and relax to an equilibrium configuration sufficiently fast, a nearly-thermal radiation bath is sourced all through inflation. For g_* relativistic degrees of freedom this yields the following evolution equation for the radiation density, $\rho_{\rm R} = \pi^2 g_* T^4/30$:

$$\dot{\rho_{\rm R}} + 4H\rho_{\rm R} = \Upsilon\dot{\phi}^2 \ , \tag{4.16}$$

with inflation occurring for $\rho_\phi \gg \rho_{\rm R}$. Accelerated expansion occurs in warm inflation analogously to cold inflation, i.e. when the dominant energy component has an equation of state $\omega \leq -1/3$. This occurs in the slow-roll regime, where $V(\phi) \gg \dot{\phi}^2, \ddot{\phi} \ll H\dot{\phi}$. In the presence of dissipative effects, this can be translated into the modified slow-roll conditions:

$$\epsilon_\phi = \frac{m_{\rm p}^2}{2}\left(\frac{V_\phi}{V}\right)^2 < 1+Q \ , \qquad \eta_\phi = m_{\rm p}^2\left(\frac{V_{\phi\phi}}{V}\right) < 1+Q \ ,$$
$$\sigma_\phi = m_{\rm p}^2\left(\frac{V_\phi}{\phi V}\right) < 1+Q \ . \tag{4.17}$$

The first two are similar, up to the additional friction term, as the cold inflation slow roll conditions and the last slow roll parameter, σ_ϕ, arises due to the field dependence of the dissipation coefficient. In particular this allows for $\epsilon, |\eta| \gtrsim 1$ in the strong dissipation regime, $Q \gtrsim 1$, therefore alleviating the need for very flat potentials [6]. In the slow-roll regime the equations of motion reduce to:

$$\begin{aligned} 3H(1+Q)\dot{\phi} &\approx -V_\phi \ , \\ 4\rho_{\rm R} &\approx 3Q\dot{\phi}^2 \ . \end{aligned} \tag{4.18}$$

When the field is slow rolling the radiation quickly reaches a steady state solution with the dissipative source term balancing the effect of Hubble dilution.

Earlier attempts to construct models of warm inflation considered a direct

coupling between the inflaton and the light fields that form the radiation bath, but in this case a sufficiently large dissipation coefficient also induces a large thermal mass to the inflaton field, which makes it difficult to achieve a sufficiently long period of accelerated expansion [82, 71] with typically only a few e-folds of accelerated expansion being possible before the adiabatic condition is violated.

However if inflation is occurring at sufficiently large field values then the fields which couple to it are typically much heavier than the temperature of the thermal bath. In this case the thermal corrections to the potential are Boltzmann suppressed, but so is dissipation. It is likely however that there are other degrees of freedom which do not couple directly to the inflaton but do couple to these heavy fields allowing for the decay into radiation. A generic renormalisable superpotential demonstrating this mechanism is given by [83, 84]:

$$W = f(\Phi) + g\Phi X^2 + hXY^2 \ . \tag{4.19}$$

where the inflaton corresponds to the scalar component of the chiral multiplet Φ, $\phi = \sqrt{2}\langle\Phi\rangle$, with a scalar potential $V(\phi) = |f'(\phi)|^2$ that spontaneously breaks supersymmetry (SUSY) during inflation. Both the bosonic and fermionic components of the superfield X then acquire masses proportional to φ and can decay into the Y scalars and fermions, which remain light and form the radiation bath. For $T \ll m_X$ and a broad range of couplings and field multiplicities, the leading contribution to the time non-local effective action corresponds to 1-loop diagrams involving virtual X-scalars, and has been discussed in [83, 80, 85], yielding a dissipation coefficient of the form:

$$\Upsilon = C_\phi \frac{T^3}{\phi^2} \ , \qquad C_\phi \simeq \frac{1}{4}\alpha_h N_X \ , \tag{4.20}$$

for $\alpha_h = h^2 N_Y/4\pi \lesssim 1$ and $N_{X,Y}$ chiral multiplets. Supersymmetry suppresses radiative and thermal corrections to the scalar potential, yielding at 1-loop order:

$$\Delta V^{(1)}/V \simeq (\alpha_g/8\pi)\log(m_X^2/\mu^2) \ , \tag{4.21}$$

where $\alpha_g = g^2 N_X/4\pi \lesssim 1$ and μ is the renormalization scale. It is important to note here that the radiative corrections to the potential are suppressed for perturbative values of the effective coupling $g^2 N_X$, whilst dissipation can be large as C_ϕ depends upon N_X and not the coupling, g. This is due to the

supersymmetric interaction structure in Eq. (4.19) and thus avoids the problems with thermal corrections dominating over dissipation as described in [71].

We note that there is also a contribution to dissipation from the excitation of on-shell X scalars, where a sufficiently small coupling h can counter the effects of Boltzmann suppression. This contribution can be significant in some regimes but it is a complicated expression which is not amenable to analytical computation. In the inflationary part of this thesis we will constrain ourselves to considering only the contribution from the low momentum modes, which is naturally the dominant process for $\mathcal{O}(1)$ couplings.

With this form of dissipative coefficient the following relation can be derived from the slow-roll equations Eq. (4.18):

$$Q^{1/3}(1+Q)^2 = 2\epsilon_\phi \left(\frac{C_\phi}{3}\right)^{1/3} \left(\frac{C_\phi}{4C_{\rm R}}\right) \left(\frac{H}{\phi}\right)^{8/3} \left(\frac{m_{\rm p}}{H}\right)^2 \ . \tag{4.22}$$

With this relation the evolution of the dynamical quantities can be written in terms of the slow-roll parameters:

$$\frac{\phi'}{\phi} = -\frac{\sigma_\phi}{(1+Q)} \ , \tag{4.23}$$

$$Q' = \frac{Q}{(1+7Q)}(10\epsilon_\phi - 6\eta_\phi + 8\sigma_\phi) \ , \tag{4.24}$$

$$\left(\frac{T}{H}\right)' = \frac{2}{(1+7Q)} \left(\frac{2+4Q}{1+Q}\epsilon_\phi - \eta_\phi + \frac{1-Q}{1+Q}\sigma_\phi\right) \left(\frac{T}{H}\right) \ . \tag{4.25}$$

The prime indicates a derivative with respect to the number of e-folds, $dN_{\rm e} = Hdt$ and $C_{\rm R} = g_*\pi^2/30$. Note that Eq. (4.23) is independent of the form of the dissipative coefficient. When the slow roll parameters are satisfied the variation of these quantitites is slow on the time scale of the Hubble expansion and thus slow roll is maintained. We note that these expressions only hold for the dissipation coefficient in Eq. (4.20) however a more general stability analysis was performed in [60] for a general dissipation coefficient. One can then integrate these equations to calculate the number of e-folds of inflationary expansion, which we will show explicitly for the quartic potential later in this chapter.

In the slow-roll regime, radiation quickly reaches a quasi-stationary configuration and we obtain $\rho_{\rm R}/\rho_\phi \simeq (\epsilon/2)Q/(1+Q)^2 \ll 1$. Radiation is then a subdominant component, allowing for accelerated expansion. At the end of inflation,

however, for $\epsilon \sim 1+Q$ we have $\rho_{\rm R}/\rho_\phi \sim (1/2)Q/(1+Q)$, and radiation may become a relevant component if $Q \gtrsim 1$ at this stage. In fact, in models where dissipation becomes stronger as inflation proceeds, radiation will typically come to dominate once the slow-roll regime has ended, yielding a smooth 'graceful exit' into a radiation-dominated universe.

4.3 Primordial power spectrum

Fluctuation-dissipation dynamics modifies the evolution of inflaton perturbations, which are sourced by a gaussian white noise term, ξ_k [6, 11, 59]:

$$\delta\ddot{\phi}_k + 3H(1+Q)\delta\dot{\phi}_k + \frac{k^2}{a^2}\delta\phi_k \simeq \sqrt{2\Upsilon T}a^{-3/2}\xi_k \ , \tag{4.26}$$

in the slow-roll regime. Note that we have the only included the thermal noise on the right hand side. In the stochastic approach the short wavelength (sub-Hubble) modes act as a noise for the large "classical" wavelength modes, in which case the noise correlator takes the form Eq. (4.7). We recall that the intensity of the noise is related to the dissipation coefficient through the fluctuation-dissipation theorem and, as shown in the first article in [81], dissipation from scalar modes dominates over the fermionic one in the low temperature regime that we are considering here. Spatial correlation properties may, however, be different for fermionic modes [86]. Also, as mentioned above, dissipative processes may maintain a non-trivial distribution of inflaton particles, $n(k)$, which for sufficiently fast interactions should approach the Bose-Einstein distribution at the ambient temperature, $n_{\rm BE}(k) = (e^{k/aT}-1)^{-1}$. In this case the associated creation and annihilation operators have correlation functions $\langle \hat{a}_{-\mathbf{k}}\hat{a}^\dagger_{\mathbf{k}'}\rangle = [n+1](2\pi)^3\delta^3(\mathbf{k}+\mathbf{k}')$ and $\langle \hat{a}^\dagger_{\mathbf{k}'}\hat{a}_{-\mathbf{k}}\rangle = n(2\pi)^3\delta^3(\mathbf{k}+\mathbf{k}')$. For a generic inflaton phase-space distribution at the time when observable CMB scales leave the horizon during inflation, t_*, one then obtains the dimensionless power spectrum [6, 9, 11, 59, 61]:

$$\Delta^2_{\mathcal{R}} = \left(\frac{H_*}{\dot{\phi}_*}\right)^2\left(\frac{H_*}{2\pi}\right)^2\left[1+2n_*+\left(\frac{T_*}{H_*}\right)\frac{2\sqrt{3}\pi Q_*}{\sqrt{3+4\pi Q_*}}\right] \ , \tag{4.27}$$

which yields the standard cold inflation result in the limit $n_*, Q_*, T_* \to 0$. The full calculation of this expression is a little involved, but we can gain some understanding by making a comparison to the cold inflation scenario. Imagine

that dissipation has a negligible effect on the dynamics of the scalar field, however it can maintain a non trivial distribution of inflation particles. The calculation of the power spectrum largely follows the vacuum scenario except that one identifies the number density operator of the fluctuations with a statistical distribution. We find:

$$\langle \delta\phi^2 \rangle \simeq \int \frac{d^3k}{(2\pi)^3} \frac{|\delta\phi_k|^2}{2k} (2n_* + 1) \ . \tag{4.28}$$

On superhorizon scales $|\delta\phi_k|^2 \simeq H/k$ and so we can identify the power spectrum as $\Delta^2_\phi = (H/2\pi)^2(2n+1)$. Thus the primordial curvature power spectrum takes the form:

$$\triangle^2_{\mathcal{R}} \simeq \left(\frac{H_*}{\dot{\phi}_*}\right)^2 \left(\frac{H_*}{2\pi}\right)^2 (1+2n_*) \overset{T_* \gg H_*}{\simeq} 2 \left(\frac{T_*}{H_*}\right) \left(\frac{H_*}{\dot{\phi}_*}\right)^2 \left(\frac{H_*}{2\pi}\right)^2 \ . \tag{4.29}$$

In the last equality we assume the inflaton has a thermal distribution and that $T_* \gg H_*$. We can compare this to the first two terms in Eq. (4.27) finding that it gives the same result. The final term in Eq. (4.27) arises as the leading order correction from the fluctuation-dissipation dynamics.

The full expression in Eq. (4.27) neglects, however, the coupling between inflaton and radiation fluctuations associated with the temperature dependence of the dissipation coefficient in Eq. (4.20), an effect that may significantly enhance the perturbation growth for strong dissipation, $Q \gtrsim 1$ [87]. Since this coupling is negligible if the relevant scales become super-horizon when dissipation is weak, we can obtain an accurate description of the spectrum by taking the limit $Q_* \ll 1$ in the expression above, which yields:

$$\Delta^2_{\mathcal{R}} \simeq \left(\frac{H_*}{\dot{\phi}_*}\right)^2 \left(\frac{H_*}{2\pi}\right)^2 \left[1 + 2n_* + 2\pi Q_* \frac{T_*}{H_*}\right] \ . \tag{4.30}$$

This assumption is justified in models where Q grows during inflation, such that dissipation has a negligible effect 50-60 e-folds before the end of inflation but becomes stronger towards the end, thus helping to prolong the period of accelerated expansion. We will show that this is indeed the case for the example of chaotic inflation and will discuss the potential effects of strong dissipation at horizon-crossing at the conclusion of this chapter.

Note that both the second and third terms within the brackets in Eq. (4.30) are positive-definite, the former corresponding to non-trivial inflaton occupation

numbers and the latter to the leading effect of fluctuation-dissipation dynamics. Hence, the amplitude of the scalar power spectrum always exceeds the vacuum result in warm inflation scenarios. On the other hand, gravity waves are weakly coupled to the thermal bath and the spectrum of tensor modes retains its vacuum form, $\Delta_{\rm t}^2 = (2/\pi^2)(H_*^2/m_{\rm p}^2)$. This therefore suppresses the tensor-to-scalar ratio, yielding a modified consistency relation for warm inflation:

$$r \simeq \frac{8|n_{\rm t}|}{1 + 2n_* + 2\pi Q_* T_*/H_*} \ , \tag{4.31}$$

where $n_{\rm t} = -2\epsilon_*$ is the tensor index. The primordial tensor spectrum can thus be used to distinguish warm from cold inflation scenarios, the former consequently modifying the Lyth bound [43, 56] (see also [88] for other scenarios where the Lyth bound does not apply). Whereas previous studies have focused more on the strong dissipation regime, this result explicitly shows that warm inflation can have a significant observational impact for weak dissipation, where temperatures well above the Hubble rate can be sustained. Most importantly, non-trivial inflaton occupation numbers may also generically lower the tensor-to-scalar ratio, which as we illustrate below may have a significant effect on inflationary predictions.

In the limit where inflaton particle production is inefficient and n_* gives a negligible contribution to the power spectrum, the scalar spectral index is nevertheless modified by the third term in Eq. (4.30), yielding:

$$n_{\rm s} - 1 \simeq 2\eta_* - 6\epsilon_* + \frac{2\kappa_*}{1+\kappa_*}\left(7\epsilon_* - 4\eta_* + 5\sigma_*\right) \ , \tag{4.32}$$

where $\kappa \equiv 2\pi QT/H$. Modifications are, however, more prominent in the opposite limit of nearly-thermal inflaton fluctuations, with $n_* \simeq n_{\rm BE*}$. For $T_* \gtrsim H_*$ and $Q_* \ll 1$ we then obtain:

$$n_{\rm s} - 1 \simeq 2\sigma_* - 2\epsilon_* \ , \tag{4.33}$$

which is, in particular, independent of the curvature of the potential, which only determines its running:

$$n_{\rm s}' \simeq 2\sigma_*(\sigma_* + 2\epsilon_* - \eta_*) - 4\epsilon_*(2\epsilon_* - \eta_*) \ . \tag{4.34}$$

In this case, a red-tilted spectrum, $n_{\rm s} < 1$, corresponds to either potentials with a negative slope, such as hill-top models, or large field models where

$\epsilon_* > 2(m_{\rm p}/\phi_*)^2$.

4.4 Warm inflation with a quartic potential

To illustrate the effects of both dissipation and occupation numbers on observational predictions, let us consider the quartic model, $V(\phi) = \lambda\phi^4$, which corresponds to a superpotential $f(\Phi) = \sqrt{\lambda}\Phi^3/3$ and is the canonical model of chaotic inflation [32]. In this case, we have $\epsilon_\phi = 2\sigma_\phi = 2\eta_\phi/3 = 8(m_{\rm p}/\phi)^2$, which yields $n_{\rm s} - 1 \simeq -8(m_{\rm p}/\phi_*)^2$ for a thermalized inflaton distribution from Eq. (4.33). This gives a red-tilted spectrum with $n_{\rm s} \simeq 0.97$ for $\phi_* \simeq 16m_{\rm p}$, which is super-planckian but smaller than the corresponding field value in the vacuum case, $\phi_* \simeq 25m_{\rm p}$. This also gives $r \simeq 8(1-n_{\rm s})(H_*/T_*)$, within the upper bound obtained by Planck, $r < 0.1$ (95% CL), for $T_* > 2.4H_*$, as well as a small negative running $n_{\rm s}' = -(n_{\rm s}-1)^2 \simeq -9\times10^{-4}$ and a tensor index $n_{\rm t} = 2(n_{\rm s}-1) \simeq -0.06$.

The number of e-folds of inflation can be computed by integrating the slow-roll equations, which may be done analytically for the quartic model [89]. In particular, one can use the form of the dissipation coefficient in Eq. (4.20) to express the coupled inflaton and radiation equations in the slow-roll regime as a single equation for the dissipative ratio Q:

$$\frac{dQ}{dN_{\rm e}} = C_*\frac{Q^{6/5}(1+Q)^{6/5}}{1+7Q} \ , \tag{4.35}$$

where $C_* \simeq 5\epsilon_{\phi*}Q_*^{-1/5}$ for $Q_* \ll 1$. This shows explicitly that Q grows during inflation, justifying our assumption that the system may evolve from the weak to the strong dissipation regime. Inflation ends in this case when $|\eta| = 1+Q$, which yields $Q_{\rm e} \simeq (2/3(1-n_{\rm s}))^{5/2}Q_*^{1/2}$ for a thermal spectrum and hence $Q_{\rm e} \gtrsim 1$ for $Q_* \gtrsim 10^{-6}$. As discussed earlier, the relative abundance of radiation will then also grow towards the end of inflation, with $\rho_{\rm R}/V(\phi) \propto Q^{7/5}$ in this case, until it smoothly takes over after slow-roll has ended. Integrating Eq. (4.35) from horizon-crossing to the end of the slow-roll regime, we obtain:

$$N_{\rm e} \simeq \epsilon_{\phi*}^{-1}\left(1 + bQ_*^{1/5}\right) \ , \tag{4.36}$$

where $b \simeq 2.81$. This yields the required $50-60$ e-folds of inflation with $n_{\rm s} \simeq 0.96-0.97$ for $Q_* \simeq 0.001-0.01$. For comparison, in the standard cold inflation

regime, one finds $n_{\rm s} = 1 - 3/N_{\rm e}$, giving $n_{\rm s} = 0.94 - 0.95$ for $N_{\rm e} = 50 - 60$. This clearly shows that even for weak dissipation at horizon-crossing one may obtain substantially different observational results.

For both limits of nearly-thermal and negligible inflaton occupation numbers, one can use the observed amplitude of curvature perturbations, $\Delta^2_{\mathcal{R}} \simeq 2.2 \times 10^{-9}$ [90] and the form of the dissipation coefficient in Eq. (4.20) to relate the different quantities at horizon-crossing, with e.g. $Q_* \simeq 2 \times 10^{-8} g_*(T_*/H_*)^3$ in the nearly-thermalized regime. This allows one to express both $n_{\rm s}$ and r in terms of the dissipative ratio or temperature at horizon-crossing for a given number of e-folds of inflation and relativistic degrees of freedom, which is illustrated in Figures 4.2 and 4.3.

As one can see, observational predictions for the quartic model depend on the distribution of inflaton fluctuations, n_*. For $n_*, \kappa_* \ll 1$, the spectrum has the same form as in cold inflation, but from Eq. (4.36) one obtains $N_{\rm e} = 50 - 60$ for smaller field values than in cold inflation, yielding a larger tensor fraction and a more red-tilted spectrum. When $\kappa_* \gtrsim 1$, however, the spectrum becomes more blue-tilted and r is suppressed, although for weak dissipation it remains too large.

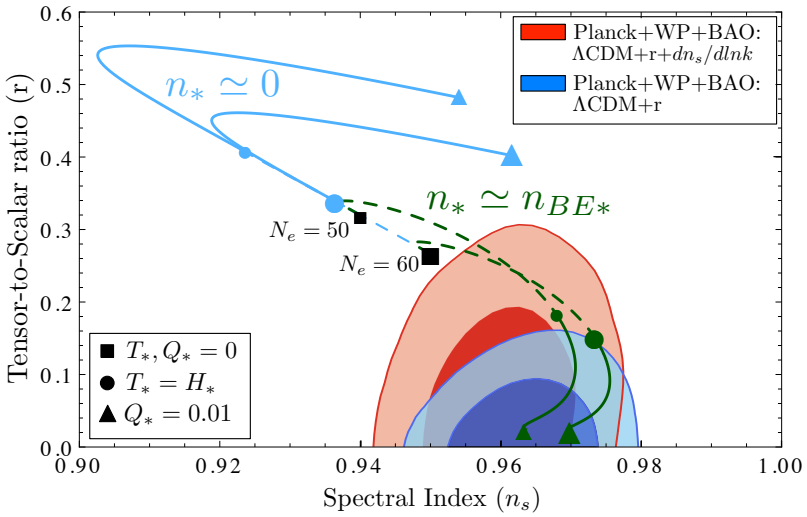

Figure 4.2: Trajectories in the $(n_{\rm s}, r)$ plane for $V(\phi) = \lambda\phi^4$ as a function of the dissipative ratio, $Q_* < 0.01$, 50-60 e-folds before the end of inflation, compared with the Planck 2013 results [90], for $g_* = 228.75$ relativistic degrees of freedom. The dark green (light blue) curves correspond to nearly-thermal (negligible) inflaton occupation numbers n_*, with dashed branches for $T_* \lesssim H_*$. Note that corresponding curves converge in the cold inflation limit, $T_*, Q_* \to 0$.

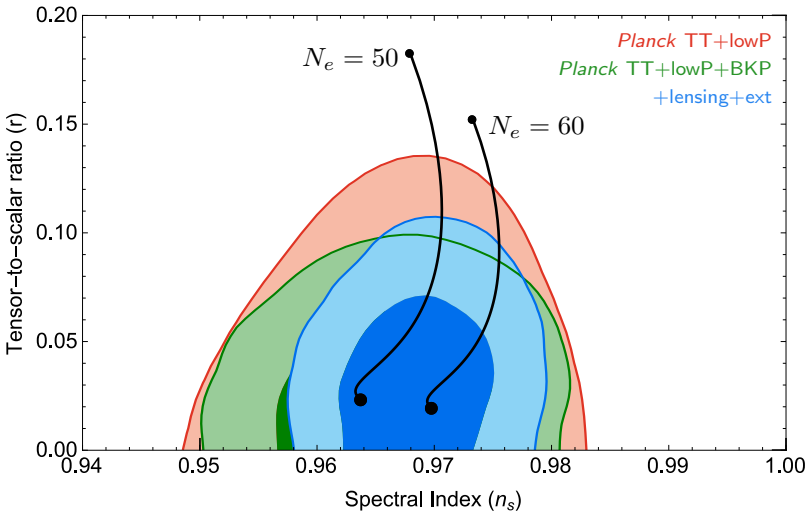

Figure 4.3: Updated comparison against the recent 2015 Planck data [1] of the quartic potential predictions with nearly thermal inflaton occupation numbers. The upper dots on the trajectories indicate $T_* = H_*$ whilst the lower dots indicate $Q_* \simeq 0.01$. $g_* = 228.75$.

On the other hand, for nearly-thermal inflaton occupation numbers tensor modes are more strongly suppressed and one obtains a remarkable agreement with the Planck results for $T_* \gtrsim H_*$. Note that for $T_* \lesssim H_*$ the concept of thermal equilibrium is ill-defined, since the average particle modes have super-horizon wavelengths, so in Figure 4.2 we represent this regime with dashed curves to nevertheless illustrate the transition from a cold to a warm spectrum. Also, we take the MSSM value $g_* = 228.75$ only as a reference, with fewer light species further lowering the tensor-to-scalar ratio, since T_*/H_* is larger. In Figure 4.3 we show the predictions for a thermal distribution of inflaton particles with the most recent Planck constraints [1].

This agreement is particularly significant, since the quartic potential is the simplest renormalizable model of chaotic inflation, involving no other scales other than the inflaton field value. As originally argued by Linde [32], in large-field models inflation is naturally triggered from a chaotic field distribution following the pre-planckian era, in domains where $V(\phi) \sim m_{\rm p}^4$ quickly dominates over gradient and kinetic energy densities. On the other hand, when inflation only occurs for a $V(\phi) \ll m_{\rm p}^4$ plateau, the post-planckian universe must be unnaturally smooth, requiring a fine-tuning of initial conditions that the inflationary paradigm

is supposed to solve [91].

While other modifications such as a non-minimal coupling to gravity may also bring the quartic model into agreement with observations [92], the renormalizable nature of the interactions leading to dissipation is an attractive feature of warm inflation, with only a few controllable parameters. Note, in particular, that interactions with other bosonic and/or fermionic fields are always required since the vacuum energy of the inflaton field must be transferred into light degrees of freedom at the end of inflation to 'reheat' the universe. In this sense, warm inflation scenarios do not introduce any non-standard modifications to the basic inflationary models but simply correspond to parametric regimes where the universe is kept warm throughout inflation, $T \gtrsim H$. For the dissipation coefficient in Eq. (4.20), one obtains in particular $T_*/H_* \sim (C_\phi/g_*)N_{\rm e}^{-2} \gtrsim 1$, which may be achieved for $N_X \gg N_Y \gtrsim 1$ and $g, h \ll 1$, while keeping radiative corrections under control, $\alpha_{g,h} \lesssim 1$. We may express the number of heavy species as:

$$N_X \simeq \frac{8\times 10^5}{\alpha_h}\left(\frac{0.04}{1-n_{\rm s}}\right)^4\left(\frac{r}{0.01}\right)^2\left(\frac{Q_*}{10^{-3}}\right) \ , \tag{4.37}$$

where we have assumed a thermal distribution of inflaton perturbations. This large multiplicity of X species is typical of the form of the dissipation coefficient in Eq. (4.20) [84, 93], but is expected to be significantly reduced in other regimes, such as for on-shell X modes [81]. Large multiplicities may be obtained in D-brane constructions [57], where the X fields correspond to strings stretched between brane and antibrane stacks and their number thus grows with the square of the brane multiplicity. Due to brane-antibrane annihilation at the end of inflation, these modes will not, however, play a role in the post-inflationary universe. Field multiplicities are also enhanced by the Kaluza-Klein tower in extra-dimensional scenarios [94].

An interesting possibility arises when we consider B- and CP-violating interactions for the X fields in Eq. (4.19), with complex couplings and distinct decay channels. In this case, the out-of-equilibrium nature of dissipation can generate a cosmological baryon asymmetry during inflation [26]. The resulting baryon-to-entropy ratio depends on the inflaton field, so that inflaton fluctuations yield both adiabatic and baryon isocurvature (BI) perturbations with a nearly-scale invariant spectrum. For the quartic model with $n_* \simeq n_{\rm BE*}$, BI and adiabatic modes are anti-correlated with relative amplitude $B_{\rm B} \simeq 3(n_{\rm s}-1) \simeq -0.12$ and a

blue-tilted spectrum $n_{\rm iso} \simeq (3-n_{\rm s})/2 \simeq 1.02$ [95]. This then yields for the relative matter isocurvature spectrum $\beta_{\rm iso} \simeq (\Omega_b/\Omega_c)^2 B_{\rm B}^2 \simeq 4.8 \times 10^{-4}$, well within the bound $\beta_{\rm iso} < 0.0087$ obtained by Planck for anti-correlated isocurvature modes with $n_{\rm s} \simeq n_{\rm iso}$, which is in fact the case that best improves the fit to the data [90]. On the other hand the baryon asymmetry may be produced through the dissipation of a field distinct from the inflaton. In Chapter 7 we will present a model of dissipative leptogenesis where the field responsible for generating right handed neutrinos masses creates a lepton asymmetry through dissipation as it evolves in the radiation era. In this scenario the isocurvature perturbations may be in fact be uncorrelated with the adiabatic perturbations.

The interactions required to produce a baryon asymmetry through dissipation are analogous to those considered in conventional thermal GUT baryogenesis or leptogenesis models, with the scalar X fields corresponding to e.g. heavy GUT bosons or right-handed neutrinos [26]. However, since only virtual X modes are involved in the dissipative processes, baryogenesis may occur below the GUT scale, as opposed to thermal GUT baryogenesis models, avoiding the production of dangerous relics such as monopoles. In particular, we obtain for the temperature at the end of inflation in the quartic model:

$$T_{\rm e} \simeq 10^{14} \left(\frac{1-n_{\rm s}}{0.04}\right)^{\frac{5}{2}} \left(\frac{0.01}{r}\right)^{\frac{1}{2}} \left(\frac{10^{-3}}{Q_*}\right)^{\frac{3}{10}} \ {\rm GeV} \ . \tag{4.38}$$

We note that the effective reheating temperature is roughly an order of magnitude lower since radiation typically takes a few e-folds to take over after the end of slow-roll [89]. While gravitinos may still be ubiquitously produced at these temperatures, the inflaton may not decay completely right after inflation if $Q_{\rm e} \lesssim 10$ [96], as is the case of the quartic model for $Q_* < 0.01$. The inflaton may then come to dominate over the radiation bath at a later stage and the entropy produced by its eventual decay may dilute the excess of gravitinos, thus avoiding the potentially associated cosmological problems [96].

Our results motivate a closer look at thermalization processes and, in particular, we can estimate the total production rate of inflaton particles from the 3-body decay rate of the N_X heavy species in the plasma given above. At horizon-crossing, the inflaton is a relativistic degree of freedom, since $m_{\phi_*} =$

$\sqrt{3}\eta_* H_* \ll T_*$, and we obtain:

$$\frac{\Gamma_{\phi_*}}{H_*} \simeq 9\,(\alpha_g \alpha_h)^{\frac{3}{2}} \left(\frac{1-n_{\rm s}}{0.04}\right)^{\frac{3}{2}} \left(\frac{0.01}{r}\right)^{\frac{3}{2}} \left(\frac{0.005}{Q_*}\right)^{\frac{1}{2}}, \tag{4.39}$$

where we assumed $n_* = n_{\rm BE*}$. Moreover, finite temperature Bose factors may considerably enhance this for small couplings [97], with e.g. the two-body decay width increasing up to a factor $T/m_Y \sim \sqrt{12}/h$ [81]. Also, Γ_ϕ/H increases during inflation, so that deviations from thermal equilibrium should become less significant. We then expect inflaton particles to be produced sufficiently fast and remain close to thermal equilibrium with the ambient plasma if the effective couplings $\alpha_{g,h}$ are not too small. Both the inflaton and other light fields could actually be in a pre-inflationary thermal state with $T \gtrsim H$, with dissipation and the above mentioned processes maintaining a slowly-varying temperature. Without dissipation, however, thermal effects would be quickly redshifted away, yielding quite different observational features [98].

4.5 Discussion

In this chapter, we have shown that the presence of even small dissipative effects at the time when observable scales leave the horizon during inflation may have a significant effect on the spectrum of primordial fluctuations in the warm regime, for $T \gtrsim H$. This generically lowers the tensor-to-scalar ratio and yields a modified consistency relation for warm inflation that may be used to distinguish it in a model-independent way from the standard supercooled scenarios if a tensor component is found and accurately measured. The main modifications to the scalar spectrum arise from the presence of dissipative noise that sources inflaton fluctuations and from the changes in the phase space distribution of inflaton modes as a consequence of inflaton particle production in the plasma. We have shown, in particular, that the latter effect may bring the simplest chaotic inflation scenario with a quartic potential into agreement with the Planck results for a nearly-thermal distribution. Inflation may thus be triggered from chaotic initial conditions at the Planck scale in an observationally consistent way, through simple renormalizable interactions with matter fields that must be present in any inflationary model, as opposed to e.g. a non-minimal coupling to the gravitational sector. The cosmic baryon asymmetry may also be produced

during warm inflation, inducing baryon isocurvature perturbations that are within the current Planck bounds for a quartic potential and which may be probed in the near future.

Although for the quartic model a nearly-thermal spectrum is observationally preferred, as is the case for $V(\phi) \propto \phi^6$, this is not necessarily true in general. For example, models such as SUSY hybrid inflation driven by small radiative corrections [99], which follows from Eq. (4.19), are consistent with the Planck data when n_* is negligible and only the fluctuation-dissipation term modifies the spectrum. In particular, dissipation increases the number of e-folds in this case, whereas in the cold regime only $N_{\rm e} < 50$ is observationally allowed [90]. Other low-scale models such as hill-top scenarios are consistent for both the thermal regime [100] and when the fluctuation-dissipation term in Eq. (4.30) is dominant, the same holding for exponential [10] or inverse power-law potentials, although an alternative reheating mechanism is needed for $Q_* \ll 1$ since dissipation never becomes sufficiently strong in this case. A detailed analysis of these and other potentials is something which we will investigate in the future.

We have focused on the regime where dissipation is still sub-leading at horizon-crossing, which is simpler to realize since it requires smaller values of T_*/H_* and lower field multiplicities. Non-gaussian effects should also be suppressed in this case, with $f_{\rm NL} \sim \mathcal{O}(1)$ by extrapolating the results in [63] to weak dissipation, within the bounds obtained by Planck [90]. The Planck collaboration has searched for signals of non-gaussianity in warm inflation models in the strong dissipation regime [101], but a dedicated analysis of the bispectrum for $Q_* \ll 1$ is required and further motivated by our results, although some progress has been made in [66].

For strong dissipation the coupling between inflaton and radiation perturbations enhances the growth of fluctuations, making the spectrum more blue-tilted for increasing Q. To check the validity of our results for the quartic potential, we have evolved the fluctuations numerically extending the analysis in [102] to weak dissipation, the details of which will be presented in the future. We find that the primordial spectrum is modified if $Q_* \gtrsim 0.01$ when the largest scales become super-horizon, since in this case the smallest observable scales leave the horizon 8-10 e-folds later when $Q \gtrsim 1$. Shear viscous effects have been shown to suppress the enhanced growth [102], but since these imply departures from thermal equilibrium a more detailed analysis is required. The results presented

in Figure 4.2 and Figure 4.3 for $Q_* < 0.01$ are nevertheless in good agreement with the numerical spectrum. Note that even weak dissipative effects can lower the tensor-to-scalar ratio below the reach of Planck, $r \gtrsim 0.05$, or other CMB polarization experiments such as the Atacama B-mode Search or the South Pole Telescope, with $r \gtrsim 0.03$.

The significant changes to the primordial spectrum from dissipative and thermal effects may also extend beyond the SUSY realization of warm inflation considered in this chapter. In non-SUSY models, for example, while couplings between the inflaton and other fields must be smaller to prevent large radiative corrections, there may exist parametric regimes where thermalization occurs sufficiently fast to yield near-equilibrium occupation numbers. One could also envisage alternative models, e.g. the decay of multiple scalar fields that become underdamped at different stages during inflation and produce inflaton particles during the first few oscillations about the minima of their potential.

Warm inflation may thus provide a first principles dynamical mechanism to sustain non-trivial occupation numbers for the inflaton and other light particles, based on renormalizable interactions, and it would be interesting to investigate whether phenomenological excited states [103, 104] could find concrete realizations in this context. The most important effect of dissipation and/or a non-trivial inflaton particle distribution is the lowering of the tensor-to-scalar ratio in the modified consistency relation in Eq. (4.31), so we expect future CMB B-mode polarization searches to shed new light on the nature of inflaton fluctuations.

Chapter 5

Gravitino production in supersymmetric warm inflation

In the early Universe, gravitinos may be abundantly produced, potentially leading to an overproduction in contradiction to observation or the spoiling of the abundances of light elements predicted by BBN. In cold inflation thermal production of gravitinos occurs only during the reheating phase and thus constraints are placed on the reheat temperature (the maximum temperature after inflation when the Universe becomes radiation dominated) to avoid such disastrous outcomes. There is, however, a certain amount of tension in this case between having a large enough reheat temperature to allow for a thermal mechanism of baryogenesis/leptogenesis, whilst keeping it low enough to avoid overproducing gravitinos. In warm inflation due to the presence of a thermal bath, the production of gravitinos is concurrent with the accelerated expansion, however this tension can be relieved, as a baryon asymmetry may in fact be produced at low temperatures through dissipative effects [105], potentially avoiding overproduction of gravitinos (see also [106] for an alternative low temperature model of baryogenesis).

Gravitino production in warm inflation has been considered previously in [107, 108], where it was assumed that the effective 'reheat temperature' occurs when the radiation energy density becomes equal to the inflaton energy density, $\rho_\phi = \rho_{\rm R}$, and that standard reheating constraints on gravitino production can be applied. This may, however, overestimate the temperature at which the gravitino yield freezes out, as radiation does not yet fully dominate the energy density at this stage. Moreover, standard reheating constraints may not *a priori* be applied

in warm inflation scenarios due to the non-negligible abundance of gravitinos produced during inflation, which may potentially lead to a larger yield. This may, in fact, be the case also in conventional models, since the reheating phase is not necessarily instantaneous and thermal production of gravitinos may potentially occur for the duration of reheating and not freeze out until the Universe is fully radiation dominated, resulting in a cumulative effect similar to that of warm inflation. Finally, we note that supersymmetry is broken during inflation, leading to gravitino masses parametrically close to the Hubble parameter and potentially to massive gauginos, which may also modify the production rate during warm inflation. Similarly, this may change the standard reheating constraints, as the gravitino mass also varies during the oscillating phase.

With these new insights in mind, we revisit the production of gravitinos in supersymmetric warm inflation, numerically evolving the Boltzmann equation for gravitinos into the radiation era. In Section 5.1 we give a brief review of the standard gravitino cosmology in cold inflation and in Section 5.2 we focus on the dynamics of warm inflation with monomial potentials in the sub-planckian regime. We discuss thermal gravitino production in warm inflation in Section 5.3 and present results for stable and unstable gravitinos, considering the effects of inflaton-dependent gaugino masses in both cases. In Section 5.4 we summarise our main results and discuss possible directions of future research in this topic.

5.1 Standard gravitino cosmology

Supersymmetry is an attractive theory for inflationary dynamics due to the presence of a whole host of scalar fields, for example the superpartners of Standard Model quarks and leptons, automatically protecting the scalar potential from quadratic loop corrections that may spoil its required flatness. However, several single field models typically require inflaton expectation values close to the planck scale, where supergravity effects start playing an important role. The gauge particle of supergravity is the massless spin-3/2 gravitino and, when supersymmetry is broken, the gravitino becomes massive and absorbs the spin-1/2 goldstino through the super-Higgs mechanism. Due to its indiscriminate coupling, the neutral gravitino couples to all fields universally, whether in Standard Model/visible sector or other hidden/sequestered sectors, with planck-suppressed interactions, making it a potential candidate for dark matter. This

suppressed coupling makes it, however, unlikely to be detected at man-made colliders. Gravitinos may nevertheless be abundantly produced in the early Universe through a variety of thermal and non-thermal processes due to the large energies involved. Unfortunately, due to our ignorance of the mechanism behind supersymmetry breaking, its mass is unknown and can only be constrained by cosmological considerations.

Without a period of inflation the constraints on the gravitino mass are quite severe. In the standard cosmological model, the early Universe is radiation-dominated and, at early enough times, the temperature will be high enough for gravitinos to be in thermal equilibrium with the radiation bath. For stable gravitinos, the early freeze-out associated with planck-suppressed interactions can thus result in overproduction incompatible with observations unless $m_{\tilde{G}} \lesssim 1\,\mathrm{keV}$ [109]. For an unstable gravitino, its mass needs to be larger than $\sim 10\,\mathrm{TeV}$, otherwise it will decay during or after BBN and spoil the predictions for the light element abundances [110]. With a period of inflation, any initial population of gravitinos is diluted away and, in cold inflation models, no gravitinos are thermally produced until reheating. These strict bounds on the gravitino mass are thus somewhat relaxed and replaced by upper limits on the reheat temperature [111].

Gravitinos are primarily produced by the scattering of particles in a thermal bath. Due to the stronger coupling, the dominant production comes from inelastic $2 \to 2$ QCD processes involving left handed quarks (q), squarks ($\tilde{q}$), gluons (g), gluinos ($\tilde{g}$) and gravitinos ($\tilde{G}$) such as $g + g \to \tilde{g} + \tilde{G}$, $q + \bar{q} \to \tilde{g} + \tilde{G}$ and $\tilde{q} + g \to \tilde{q} + \tilde{G}$. While this contribution to the thermal gravitino production rate in supersymmetric QCD has been calculated in [112], in this thesis we will adopt the complete $SU(3)_c \times SU(2)_L \times U(1)_Y$ thermal production rate computed in [113]. Gravitinos can also be produced from the decay of the inflaton during its oscillating phase after inflation (see [114, 115, 116, 117, 118, 119, 120]). However, as we discuss below, this only becomes significant during the radiation era and, due to the suppression of inflaton oscillations for strong dissipation, it is subdominant for the monomial models we consider. They can also be produced through the decay of other particles in the thermal bath, assuming this is kinematically allowed. However, during inflation the Hubble parameter is in general much larger than the relevant planck-suppressed decay widths, $H \gg \Gamma_{\mathrm{decay}}$, so that these decays will also not occur until the Hubble parameter

drops significantly in the radiation era. As it is our aim to highlight the differences between the gravitino production in warm and cold inflation, we will thus focus on thermal production processes.

If gravitinos are abundantly produced in the early Universe, this can pose a problem for inflationary model building. There are two situations to consider in gravitino cosmology, depending on whether the gravitino is the lightest supersymmetric partner (LSP) and stable by virtue of R-Parity conservation, or otherwise the gravitino is unstable and will decay at some stage in the cosmological evolution. Constraints on primordial abundances come in either case from two sources. Firstly, the abundance of the LSP must not exceed the observed dark matter abundance (5.1) [121]:

$$\Omega_{\rm DM}h^2 = 0.105^{+0.007}_{-0.010} \ . \tag{5.1}$$

Secondly, the decay products of the next to LSP (NLSP) must not spoil BBN predictions for light element abundances. Radiative decay of the NLSP where photons and charged particles are emitted can induce electromagnetic showers, disintegrating the light elements. The NLSP can also decay into quarks or gluons, which subsequently hadronise. These hadrons can then induce interconversions between the background protons and neutrons, enhancing the neutron to proton ratio and thus resulting in an overproduction of ^{4}He. The energetic nucleons can also destroy the background ^{4}He and non-thermally produce D, T, ^{3}He, ^{6}Li and ^{7}Be. There is also the possibility that if the LSP is charged then it could bind with background nuclei and change the nuclear reaction rates, in particlar that of ^{6}Li.

If the gravitino is not the LSP then it is unstable and can decay through planck-suppressed interactions. The decay width is then given approximately by:

$$\Gamma_{\tilde{G}} \simeq \frac{m^3_{\tilde{G}}}{m^2_{\rm p}} \ . \tag{5.2}$$

If $m_{\tilde{G}} \lesssim 20\,\text{TeV}$, its lifetime is longer than 1 s [122] and so it will be subject to the BBN constraints mentioned above. It will also decay into the LSP which needs to satisfy the dark matter constraint in Eq. (5.1). If the gravitino is stable then it must satisfy the dark matter constraint (5.1) and the decay of the NLSP into the gravitino must avoid upsetting BBN predictions. For more details on BBN

constraints on LSP and non-LSP gravitino primordial abundances see [123, 122, 124, 125, 126, 127, 128, 129, 130]. The problems mentioned above constitute the so called "gravitino problem".

The number density of gravitinos is described by the Boltzmann equation:

$$\dot{n}_{\tilde{G}} + 3Hn_{\tilde{G}} = C_{\tilde{G}} \ , \tag{5.3}$$

where we neglect gravitino decay and gravitinos produced from decays of other fields. The collision term, $C_{\tilde{G}}$, describes gravitino production in a thermal bath and is given by [113]:

$$C_{\tilde{G}} = \frac{3\zeta(3)T^6}{16\pi^3 m_{\rm p}^2} \sum_{i=1}^{3} \left(1 + \frac{m_{\tilde{g}_i}^2}{3m_{\tilde{G}}^2}\right) c_i g_i^2 \log\left(\frac{k_i}{g_i}\right) \ . \tag{5.4}$$

The index i runs over the gauge groups $(U(1)_Y, SU(2)_L, SU(3)_c)$ where $m_{\tilde{g}_i}$ are the gaugino masses, g_i are the gauge couplings and $c_i = (11, 27, 72)$, $k_i = (1.266, 1.312, 1.271)$. The reheating phase is assumed to be instantaneous, immediately entering the radiation era.

Defining the gravitino-to-photon yield, $Y_{\tilde{G}} = n_{\tilde{G}}/n_\gamma$, with $n_\gamma = 2\zeta(3)T^3/\pi^2$, and assuming that $Ta =$ constant, where a is the scale factor, we obtain from Eq. (5.3):

$$\frac{dY_{\tilde{G}}}{dT} = -\frac{C_{\tilde{G}}}{H(T)Tn_\gamma(T)} \ . \tag{5.5}$$

As $C_{\tilde{G}} \sim T^6$, with only a mild temperature dependence from the couplings and gaugino masses, Eq. (5.5) can be approximately integrated. Assuming that any initial population of gravitinos before the reheating phase is diluted away, $Y_{\tilde{G}}(T_{\rm R}) = 0$ and that we are interested in the yield of gravitinos at temperatures $T \ll T_{\rm R}$, e.g. at BBN, then:

$$Y_{\tilde{G}}(T) \approx \frac{C_{\tilde{G}}(T_{\rm R})}{H(T_{\rm R})n_\gamma(T_{\rm R})} \ . \tag{5.6}$$

However, TR only remains constant away from particle mass thresholds, as it is instead the entropy density that is conserved, $sR^3 =$constant. We can take this into account by diluting the yield:

$$Y_{\tilde{G}}(T_1) = \frac{s(T_1)/n_\gamma(T_1)}{s(T_2)/n_\gamma(T_2)} Y_{\tilde{G}}(T_2) = \frac{g_*(T_1)}{g_*(T_2)} Y_{\tilde{G}}(T_2) \ , \tag{5.7}$$

where $g_*(T)$ is the number of relativistic degrees of freedom in thermal equilibrium at temperature T. Note that this is generically well below the gravitino yield in thermal equilibrium. We then obtain the following expression for the present abundance of gravitinos:

$$\begin{aligned}\Omega^{\rm th}_{\tilde{G}}h^2 &= m_{\tilde{G}}n_{\tilde{G}_0}\rho_c^{-1}h^2 \\ &= \sum_{i=1}^{3}\omega_i g_i^2\left(1+\frac{m^2_{\tilde{g}_i}}{3m^2_{\tilde{G}}}\right)\ln\left(\frac{k_i}{g_i}\right)\left(\frac{m_{\tilde{G}}}{100\,\text{GeV}}\right)\left(\frac{T_{\rm R}}{10^{10}\,\text{GeV}}\right)\ . \quad (5.8)\end{aligned}$$

The subscript '0' indicates the present day value, with $T_0 = 2.73\,\text{K}$ and $g_*(T_0) = 3.91$. We use the MSSM value for $g_*(T_{\rm R}) = 228.75$ and the critical density $\rho_c = 8.1\times10^{-47}h^2\,\text{GeV}^4$ with the constants $\omega_i = (0.018, 0.044, 0.117)$. It is understood that the couplings and masses should be evolved with the temperature. This provides the standard cold inflation constraints on the reheat temperature and gravitino mass to avoid overproduction for an LSP gravitino. It is evident that for $m_{\tilde{G}} \approx 100\,\text{GeV}$, to avoid $\Omega^{\rm th}_{\tilde{G}} \gtrsim 1$, the reheat temperature $T_{\rm R} \lesssim 10^{10}\,\text{GeV}$. If the gravitino is the NLSP, then each gravitino will decay into one LSP and the primordial gravitino yield in Eq. (5.6) can be converted into the LSP yield through:

$$\Omega_{\rm LSP}h^2 = \frac{m_{\rm LSP}}{m_{\tilde{G}}}\Omega^{\rm th}_{\tilde{G}}h^2\ . \quad (5.9)$$

We can see that $\Omega^{\rm th}_{\tilde{G}}h^2 > 0.105$ is allowed as long as $m_{\rm LSP}/m_{\tilde{G}}$ is sufficiently small. For unstable gravitinos with $m_{\tilde{G}} \lesssim 20$ TeV the strongest constraints come from BBN abundances, whilst above this the dark matter constraint for the LSP dominates [122]. These constraints are often defined in the literature in terms of the gravitino-to-entropy yield, $Y^s_{\tilde{G}} = n_{\tilde{G}}/s$, which can be easily related to the more convenient definition in terms of the photon energy density used in Eq. (5.5). We will take the conservative bounds of $Y^s_{\tilde{G}} \lesssim 10^{-16}$ for $100\,\text{GeV} \lesssim m_{\tilde{G}} \lesssim 1\,\text{TeV}$ and $Y^s_{\tilde{G}} \lesssim 10^{-14}$, $Y^s_{\tilde{G}} \lesssim 10^{-17}$ for $1\,\text{TeV} \lesssim m_{\tilde{G}} \lesssim 3\,\text{TeV}$ for branching ratios into hadrons of $B_{\rm h} = 10^{-3}$, $B_{\rm h} = 1$ respectively [127]. For stable gravitinos the BBN constraints on the primordial yield from NLSP decays are quite model dependent, varying upon which particle is the NLSP, as well as its thermal abundance and mass. For more details on scenarios with sneutrino, slepton and neutralino NLSPs, see e.g. [124, 125].

5.2 Monomial potentials

As a working example we will use the superpotential in Eq. (4.19) and will take the inflaton superpotential to be of the form:

$$W(\Phi) = \frac{\lambda}{r+1}\frac{\Phi^{r+1}}{m_{\rm p}^{r-2}} \ . \tag{5.10}$$

For $r = 0$, $\lambda < 0$ we recover supersymmetric hybrid inflation, with the X scalars corresponding to the waterfall field(s), and for $r > 1$ we recover chaotic inflation models. Assuming a canonical Kähler potential for the inflaton field, $K(\Phi, \Phi^\dagger) = \Phi^\dagger\Phi$, this results in the following scalar potential:

$$\begin{aligned} V = \lambda^2 m_{\rm p}^4 \left(\frac{|\phi|}{m_{\rm p}}\right)^{2r} \exp\left(\frac{|\phi|^2}{m_{\rm p}^2}\right) \\ \times \left[1 + \frac{1}{r+1}\left(\frac{|\phi|}{m_{\rm p}}\right)^2 \left(2 - \frac{3}{r+1}\right) + \frac{1}{(r+1)^2}\left(\frac{|\phi|}{m_{\rm p}}\right)^4\right] \ . \end{aligned} \tag{5.11}$$

Given our ignorance of fundamental quantum gravity effects, we will restrict our analysis to the sub-planckian regime $|\phi| \ll m_{\rm p}$, where supergravity effects may also be ignored and the potential takes the simpler monomial form:

$$V \approx \lambda^2 \left(\frac{|\phi|}{m_{\rm p}}\right)^{2r} m_{\rm p}^4 \ . \tag{5.12}$$

Note for non-minimal Kähler potentials super-planckian field values may be considered without supergravity corrections inducing large mass corrections, particularly if some symmetry forbids the inflaton field from appearing in the Kähler potential. The slow-roll parameters are given by:

$$\begin{aligned} \eta_\phi = 2r(2r-1)\left(\frac{\phi}{m_{\rm p}}\right)^{-2} \ , \qquad \epsilon_\phi = \frac{r}{2r-1}\eta \ , \\ \sigma_\phi = m_{\rm p}^2\left(\frac{V_\phi}{\phi V}\right) = \frac{\eta}{2r-1} \ . \end{aligned} \tag{5.13}$$

Inverting Eq. (4.22) we obtain a relation between ϕ and Q:

$$\left(\frac{\phi}{m_{\rm p}}\right) = \left(\frac{r^6 C_\phi^4 \lambda^2}{9 C_{\rm R}^3}\frac{1}{Q(1+Q)^6}\right)^s \ , \tag{5.14}$$

where $s = 1/(14-2r)$ and $C_{\rm R} = g_*\pi^2/30$. The evolution of Q during inflation is found by differentiating Eq. (4.22) with respect to the number of e-folds.

$$\begin{aligned}\frac{dQ}{dN_{\rm e}} &= \frac{Q}{1+7Q}(10\epsilon_\phi - 6\eta_\phi + 8\sigma_\phi) \\ &= \frac{Q^{1+2s}(1+Q)^{12s}}{1+7Q}\left[\frac{2r}{s}\left(\frac{9C_{\rm R}^3}{r^6 C_\phi^4 \lambda^2}\right)^{2s}\right] . \end{aligned} \tag{5.15}$$

It is clear from Eq. (5.15) that for $0 < r < 7$, Q increases during inflation. The number of e-folds of inflation can then be obtained by integrating Eq. (5.15), giving:

$$N_{\rm e} = \int_{Q*}^{Q_{\rm e}} \frac{dN_{\rm e}}{dQ} dQ = C_Q \int_{Q_*}^{Q_{\rm e}} \frac{1+7Q}{Q^{1+2s}(1+Q)^{12s}} dQ \ , \tag{5.16}$$

with

$$C_Q = \frac{s}{2r}\left(\frac{r^6 C_\phi^4 \lambda^2}{9C_{\rm R}^3}\right)^{2s} . \tag{5.17}$$

The 'e' subscript denotes the number of e-folds at which the slow-roll conditions are violated, while the '$*$' subscript indicates the value when cosmological scales leave the horizon during inflation. Performing the integral, this yields:

$$N_{\rm e} = C_Q[F_r(Q_{\rm e}) - F_r(Q_*)] \ , \tag{5.18}$$

where

$$\begin{aligned} F_r(x) = \frac{1}{2}x^{-2r}\Bigg(&\frac{14x}{1-2r}{}_2F_1(1-2x, 12x, 2-2x, -x) \\ &-\frac{1}{2}{}_2F_1(-2x, 12x, 1-2x, -x)\Bigg) , \end{aligned} \tag{5.19}$$

and ${}_2F_1(a,b,c,z)$ is the hypergeometric function. As $Q \to \infty$, the number of e-folds approaches a constant and so it is not always possible to achieve the desired number of e-folds of inflation in areas of parameter space where Q diverges too early, corresponding to the breakdown of the slow-roll approximation.

It is important to ensure that $T > H$, so that the dissipative coefficient can be calculated neglecting expansion effects. If we set $T_*/H_* > 1$ at horizon crossing,

then this will hold for the duration of inflation, for $0 < r < 7$, as we can see from Eqs. (5.14) and the following:

$$\frac{T}{H} = \left(\frac{9Q}{C_\phi \lambda^2}\right)^{1/3} \left(\frac{\phi}{m_\mathrm{p}}\right)^{2(1-r)/3} . \tag{5.20}$$

Choosing C_ϕ as our other free parameter, the slow-roll dynamics are fully determined. We can use the amplitude of the primordial power spectrum, $\Delta_\mathcal{R} \approx 5 \times 10^{-5}$ [131], to fix Q_*:

$$\Delta_\mathcal{R} \approx \left(\frac{H_*}{2\pi}\right) \left(\frac{3H_*^2}{V_\phi}\right) (1+Q_*)^{5/4} \left(\frac{T_*}{H_*}\right)^{1/2} . \tag{5.21}$$

Combining Eq. (5.21) with the dissipation coefficient, $C_\phi T^3/\phi^2$, and the relation between Q and ϕ in Eq. (4.22), we arrive at:

$$(1+Q_*)^{1/2} Q_* = \frac{16\pi^2}{3} P_\mathcal{R} C_\mathrm{R} \left(\frac{T_*}{H_*}\right)^3 . \tag{5.22}$$

Note that Q_* only depends on (T_*/H_*) and not on C_ϕ or the form of the potential. Once we have Q_*, we can integrate Eq. (5.16) to obtain the total number of e-folds. The regime where $|\phi| \ll m_\mathrm{p}$ corresponds to the strong dissipation limit, $Q_* \gg 1$. Making this approximation, we have:

$$N_\mathrm{e} = \frac{7}{2rs} \left(\frac{1}{Q_*^{2rs}} - \frac{1}{Q_\mathrm{e}^{2rs}}\right) C_Q . \tag{5.23}$$

In Figure 5.1, we show the region of parameter space for the quartic ($r = 2$) and quadratic ($r = 1$) potentials where we can ignore supergravity corrections with a reasonable number of e-folds of inflation. We note that the quadratic potential, being flatter, requires lower values of C_ϕ than the quartic model to achieve the same number of e-folds of inflation in the sub-planckian regime. Notice that, although we need somewhat large values of C_ϕ to obtain 40-60 e-folds of inflation, this allows inflation to occur at sub-planckian field values, which is not possible in standard inflation and is therefore a very attractive feature of warm inflation.

For monomial potentials, we can also derive the following relation:

$$\frac{\eta_\phi}{1+Q} = \left(\frac{2(2r-1)}{r}\right) \left(\frac{\rho_\mathrm{R}}{V}\right) \left(\frac{1+Q}{Q}\right) . \tag{5.24}$$

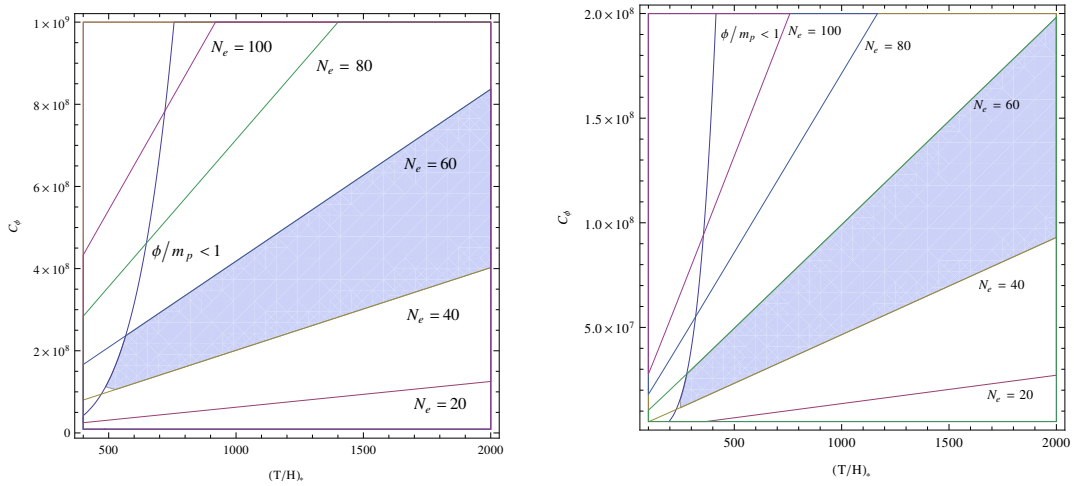

Figure 5.1: Total number of e-folds for the quartic ($r = 2$, left) and quadratic ($r = 1$, right) potentials. The region where $|\phi| < m_{\rm p}$ is to the right of the labelled line. The shaded region corresponds to between 40 and 60 e-folds of sub-planckian inflation.

We can thus see that, when the radiation energy density becomes equal to the inflaton energy density, $\rho_{\rm R} = \rho_\phi \approx V$, the slow-roll condition $\eta_\phi < 1 + Q$ has already been violated. This means, in particular, the breakdown of the slow-roll equation for the radiation energy density, as $\dot{\rho_{\rm R}}$ becomes significant and radiation soon takes over. We wish to ultimately calculate the gravitino yield after inflation and this means that we need to evolve the full set of equations into the radiation era. To do this we must numerically solve the equations of motion (4.14) and (4.16), which we will discuss in the next section.

5.3 Gravitino production in warm inflation

5.3.1 Particle masses

In the presence of supersymmetry breaking, the gravitino gains a mass:

$$m_{\tilde{G}} = m_{\rm p} \exp(G/2) \ , \tag{5.25}$$

where $G = K + \ln|W|^2$ is the Kähler function which is a combination of the Kähler potential, K, and the superpotential, W (see for example [132, 133, 134]). For the monomial superpotential in Eq. (5.10) and a canonical Kähler potential,

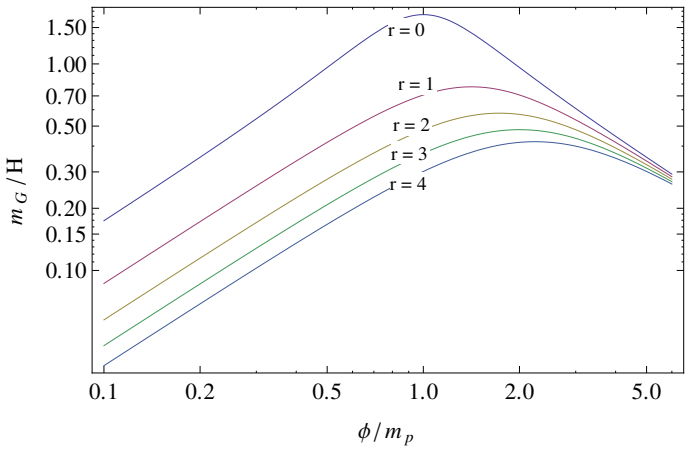

Figure 5.2: $m_{\tilde{G}}/H$ for various monomial potentials.

the gravitino mass is then given by:

$$m_{\tilde{G}} = \frac{\lambda m_{\rm p}}{r+1}\left(\frac{|\phi|}{m_{\rm p}}\right)^{r+1}\exp\left(\frac{|\phi|^2}{2m_{\rm p}^2}\right) \ . \tag{5.26}$$

Comparing this to the Hubble parameter during inflation $H^2 \approx (V/3m_{\rm p}^2)$, we get

$$\frac{m_{\tilde{G}}}{H} = \frac{\sqrt{3}}{r+1}\left(\frac{|\phi|}{m_{\rm p}}\right)\left[1+\frac{1}{r+1}\left(\frac{|\phi|}{m_{\rm p}}\right)^2\left(2-\frac{3}{r+1}\right)+\frac{1}{(r+1)^2}\left(\frac{|\phi|}{m_{\rm p}}\right)^4\right]^{-1/2} . \tag{5.27}$$

As discussed, we are interested in the sub-planckian regime, for which:

$$\frac{m_{\tilde{G}}}{H} \approx \frac{\sqrt{3}}{r+1}\left(\frac{|\phi|}{m_{\rm p}}\right) \ . \tag{5.28}$$

In Figure 5.2, we can see that even if inflation is sub-planckian the gravitino mass can be a non-negligible fraction of the Hubble parameter during inflation, resulting in the gravitino mass being typically well above the TeV scale, in contrast with what was assumed in earlier works [108]. For example, with a quartic potential, where $\lambda \sim 10^{-7}$ yields the observed amplitude of density perturbations, if $\phi/m_{\rm p} \approx 1/2$ then $m_{\tilde{G}} \sim 10^{10}\,\text{GeV}$.

As discussed earlier, thermal production of gravitinos proceeds through the scattering of gauge bosons, gauginos, quark and squarks. It is, in particular, strongly dependent on the ratio of gaugino to gravitino masses, $m_{\tilde{g}}/m_{\tilde{G}}$. Having

seen that supersymmetry breaking during inflation results in massive gravitinos, it is interesting to also consider its effect on the gaugino masses, which are given by the quadratic term in the Lagrangian [132]:

$$\mathcal{L}_{\text{gaugino}} = \frac{m_{\text{p}}}{4} \exp(G/2) G^l (G^{-1})^k_l \frac{\partial f^*_{\alpha\beta}}{\partial \phi^{*k}} \lambda^\alpha \lambda^\beta \ , \tag{5.29}$$

where $f_{\alpha\beta}$ is the gauge kinetic function, which is a holomorphic function of the chiral superfields in the model. It is dimensionless and symmetric with respect to its two adjoint indices and, in renormalisable theories, it is proportional to $\delta_{\alpha\beta}/g^2_\alpha$. Whether this function depends or not on the inflaton field is a model-dependent question and for completeness we will consider both cases separately. Interesting examples of inflaton-dependent gauge kinetic functions may arise in extra-dimensional theories such as superstring/M-theory, where the inflaton is identified with a modulus field (see e.g. [135]). Considering the case where the inflaton's supersymmetry breaking effect is communicated to the visible sector through gravitational interactions, we can expand the gauge kinetic function in powers of ϕ/m_{p}, yielding:

$$f_{\alpha\beta} \approx \delta_{\alpha\beta} \left(\frac{1}{g^2_\alpha} + f_\alpha \frac{\phi}{m_{\text{p}}} + ... \right) \ , \tag{5.30}$$

where f_α is a dimensionless coupling, which for simplicity we will assume is universal to all the gauginos and will take to be $\mathcal{O}(1)$. Although the inflaton field modifies the gauge couplings, this will not change the running of the couplings significantly since we are considering sub-planckian field values. With the above expansion for the gauge kinetic function, the gaugino mass is given by:

$$m_{\tilde{g}} = \frac{m_{\text{p}}}{4} \frac{\lambda}{r+1} \left(\frac{|\phi|}{m_{\text{p}}} \right)^{r+2} \left(1 + (r+1) \left(\frac{\phi}{m_{\text{p}}} \right)^{-2} \right) f \exp\left(\frac{|\phi|^2}{2m^2_{\text{p}}} \right) \ , \tag{5.31}$$

and for sub-planckian field values this reduces to:

$$m_{\tilde{g}} \approx \frac{\lambda m_{\text{p}}}{4} \left(\frac{|\phi|}{m_{\text{p}}} \right)^r f = \frac{\sqrt{V}}{4m_{\text{p}}} f = \frac{\sqrt{3}}{4} H f \ . \tag{5.32}$$

The gaugino masses are thus proportional to the Hubble parameter. We then

find that:

$$\frac{m_{\tilde{g}}}{m_{\tilde{G}}} \approx \frac{(r+1)f}{4}\left(\frac{\phi}{m_{\rm p}}\right)^{-1} , \tag{5.33}$$

so that gauginos are generically heavier than gravitinos during inflation, which will have important consequences on gravitino production.

If the only source of supersymmetry breaking were the inflaton superpotential, then it is evident that as the inflaton rolls to its minimum supersymmetry would be restored. This is obviously not the case in nature, and so we will consider a supersymmetry breaking contribution from a hidden sector that gives rise to TeV-scale supersymmetric partners. The details of this hidden sector will not be important to the thermal production mechanism and so we can take the following phenomenological approximation for the masses:

$$m_{\tilde{G}} = m_{\tilde{G}_\phi} + m_{\tilde{G}_0} , \tag{5.34}$$

$$m_{\tilde{g}_i} = m_{\tilde{g}_{i\phi}} + m_{1/2}\frac{g_i(T)^2}{g(T_{\rm GUT})^2} , \tag{5.35}$$

where the subscript 'ϕ' denotes the inflaton contribution and '0' indicates the low-energy hidden sector contribution.

5.3.2 Gravitino yield evolution

We numerically solve the warm inflation equations (4.14) and (4.16) along with the Boltzmann equation for the gravitino number density, Eq. (5.3), with the collision term given by Eq. (5.4). We run the couplings and gaugino masses with temperature at one-loop assuming they unify at the GUT scale, $T_{\rm GUT} = 2\times10^{16}\,{\rm GeV}$, with universal gaugino mass $m_{1/2} = 400\,{\rm GeV}$ [1]. For convenience, we evolve the equations in terms of number of e-folds, $Hdt = dN_{\rm e}$, which we will use both during and after inflation. We find that the thermally produced gravitino yield freezes out and approaches a constant value after inflation ends when the following three conditions are met:

- The gravitino has settled to its low-energy mass, given by the hidden sector contribution $m_{\tilde{G}_0}$;

[1] The current bounds on gluino masses seem to hint that $m_{\tilde{g}} \gtrsim 800$ GeV [136] and so the value of $m_{1/2}$ used in this analysis is likely to be a little light, despite this we do not expect our results to change significantly.

- The Universe is in the radiation-dominated regime, where $\rho_{\rm R} \sim \exp(-4N_{\rm e})$, i.e. radiation must have ceased being significantly produced by dissipation;
- Thermal production of gravitinos must have stopped, so that the collision term in the Boltzmann equation is negligible and thus the number density evolves as $n_{\tilde{G}} \sim \exp(-3N_{\rm e})$.

A helpful consequence of being in the sub-planckian regime is that the large value of C_ϕ makes the primordial yield independent of (T_*/H_*) in both quadratic and quartic models.

Having focused on the end of inflation, previous analyses have neglected the contribution from the non-vanishing inflaton value to the gravitino mass. To estimate the significance of this effect, we also consider the evolution of the gravitino yield for the unrealistic case where $m_{\tilde{G}} = m_{\tilde{G}_0}$ throughout inflation, and in Figure 5.3 we show an example of our results for a quartic potential in both cases, with inflaton-independent gaugino masses. During inflation the true yield is suppressed compared to the inflaton-independent gravitino yield due to the large gravitino mass suppressing the collision term in Eq. (5.4). We then observe a sudden increase in the true yield as the gravitino mass rapidly decreases and settles to its low-energy value, causing the $m_{\tilde{g}}^2/m_{\tilde{G}}^2$ term to dominate. The yield increases until the gravitino mass reaches $m_{\tilde{G}_0}$ and it is then just a matter of a few e-folds until the collision term becomes negligible and radiation fully dominates, at which point the yield freezes out.

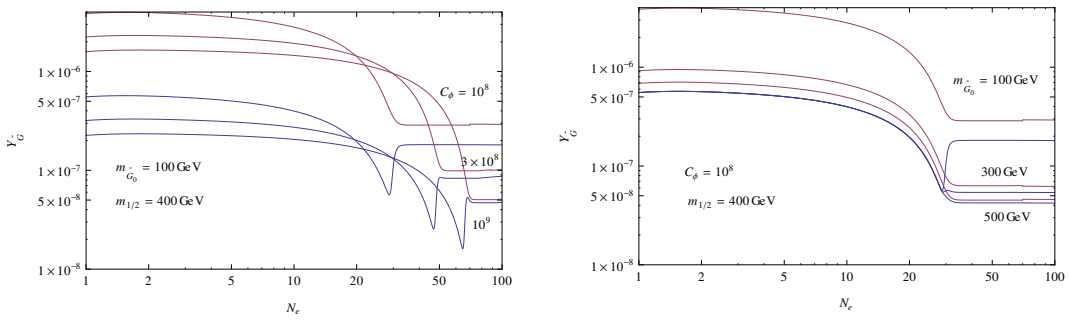

Figure 5.3: The gravitino yield as a function of the number of e-folds for the quartic potential with inflaton-dependent (blue) and independent (red) gravitino mass, with inflaton-independent gaugino masses in both cases. In the left plot we vary C_ϕ and in the right plot we vary $m_{\tilde{G}_0}$

In Figure 5.4, we show the difference in the thermal gravitino yield after freeze-out between inflaton-dependent and inflaton-independent gravitino masses. For large C_ϕ there is a negligible difference between the two cases. Increasing $m_{\tilde{G}_0}$ reduces this difference, due to the $m_{\tilde{g}}^2/m_{\tilde{G}}^2$ term never dominating, and in the large $m_{\tilde{G}_0}$ limit $C_{\tilde{G}} \sim T^6$.

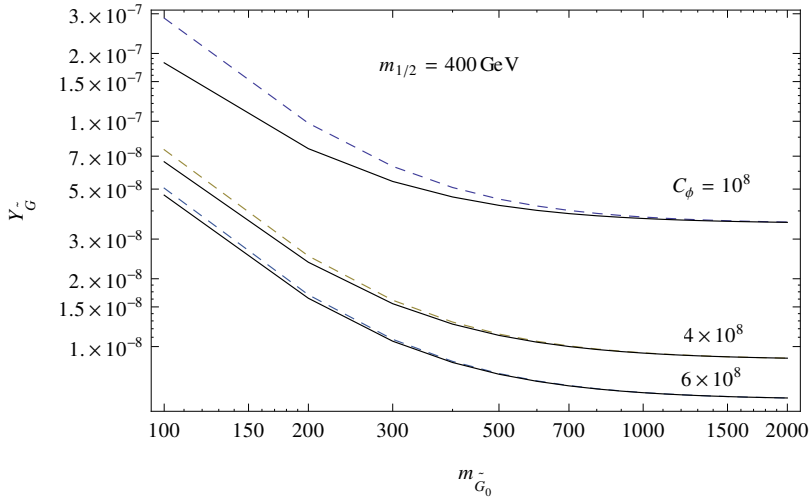

Figure 5.4: Comparison between the thermally produced yield after freeze-out for inflaton-dependent (solid) and inflaton-independent (dashed) gravitino masses with a quartic potential and inflaton-independent gaugino masses.

In Figure 5.5, we plot the gravitino yield as a function of the number of e-folds, indicating where the above conditions are met. It is clear from this figure that the yield is not yet constant when $\rho_{\rm R} = \rho_\phi$ and that it changes quite drastically over a short number of e-folds until it becomes constant. Moreover, for the same parameters as in Figure 5.5, applying the standard reheating constraints using the temperature at which $\rho_{\rm R} = \rho_\phi$ or the temperature at which the yield freezes out results in $Y_{\tilde{G}} \sim 10^{-9}$ and $Y_{\tilde{G}} \sim 10^{-10}$, respectively, which are a few orders of magnitude lower than the true yield. This is due to the cumulative effect of gravitino production throughout warm inflation and that has been neglected in earlier analyses of this problem.

Figure 5.6 shows the gravitino yield as a function of the number of e-folds for inflaton-dependent gaugino masses. We observe that, during inflation, gauginos are heavier than the gravitino and so the yield is larger than in the case where the gaugino masses do not depend on the inflaton field, once again due to the $m_{\tilde{g}}^2/m_{\tilde{G}}^2$ term in Eq. (5.4). The rise in $Y_{\tilde{G}}$ is due to $m_{\tilde{g}}/m_{\tilde{G}} \sim (\phi/m_{\rm p})^{-1}$, so that as

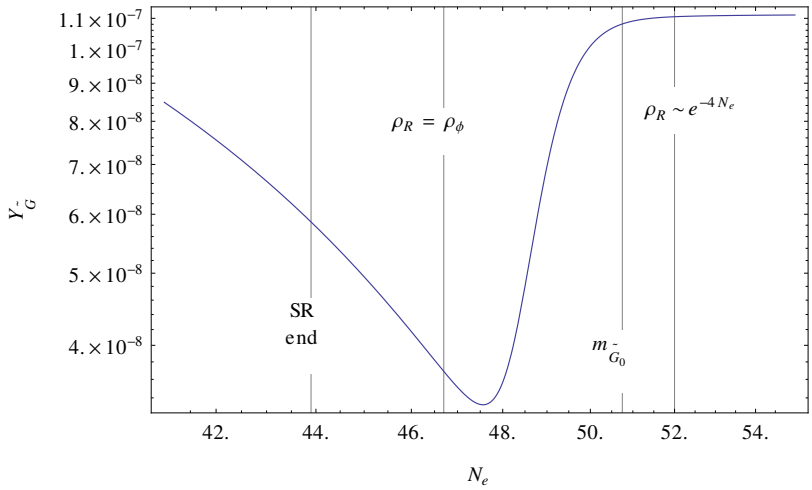

Figure 5.5: The gravitino yield as a function of the number of e-folds for a quartic potential, indicating the number of e-folds at which slow-roll ends, $\rho_{\rm R} \approx \rho_\phi$, $m_{\tilde{G}} \approx m_{\tilde{G}_0}$ and $\rho_{\rm R} \sim \exp(-4N_{\rm e})$. These results correspond to $C_\phi = 2 \times 10^8$, $(T_*/H_*) = 1000$ and $m_{\tilde{G}_0} = 100\,\text{GeV}$.

the inflaton field decreases this term enhances the yield until the gravitino mass settles at its low-energy value, $m_{\tilde{G}_0}$. As before, it is only a matter of a few e-folds until the collision term becomes negligible and the Universe is in the radiation era. During this short number of e-folds the collision term evolves as $C_{\tilde{G}} \sim T^6$ and so the yield decreases until it freezes out. We also find that, as expected, the lower the value of $m_{\tilde{G}_0}$, the larger the final yield is.

5.3.3 Stable gravitinos

Figure 5.7 shows the contribution of stable gravitinos to the current density parameter, $\Omega_{\tilde{G}}h^2$, for the quartic and quadratic potentials for inflaton-independent gaugino masses. Similarly, in Figure 5.8 we plot this contribution for inflaton-dependent gaugino masses.

We can see that for sufficiently large C_ϕ, it is possible to avoid an over production, $\Omega_{\tilde{G}}h^2 \leq 1$, for a broad range of gravitino masses. This is related to the fact that increasing C_ϕ reduces the temperature of the radiation bath during inflation and hence reduces the thermal production. This can be achieved with lower values of C_ϕ in the quadratic model than the quartic, due to the former being flatter. If the gaugino masses depend on the inflaton, the overproduction problem

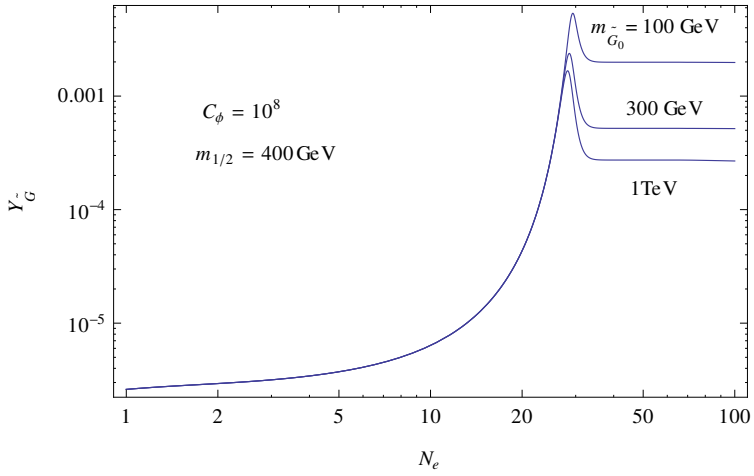

Figure 5.6: The gravitino yield for inflaton-dependent gaugino masses as a function of the number of e-folds, for a quartic potential with $C_\phi = 10^8$ and different values of $m_{\tilde{G}_0}$.

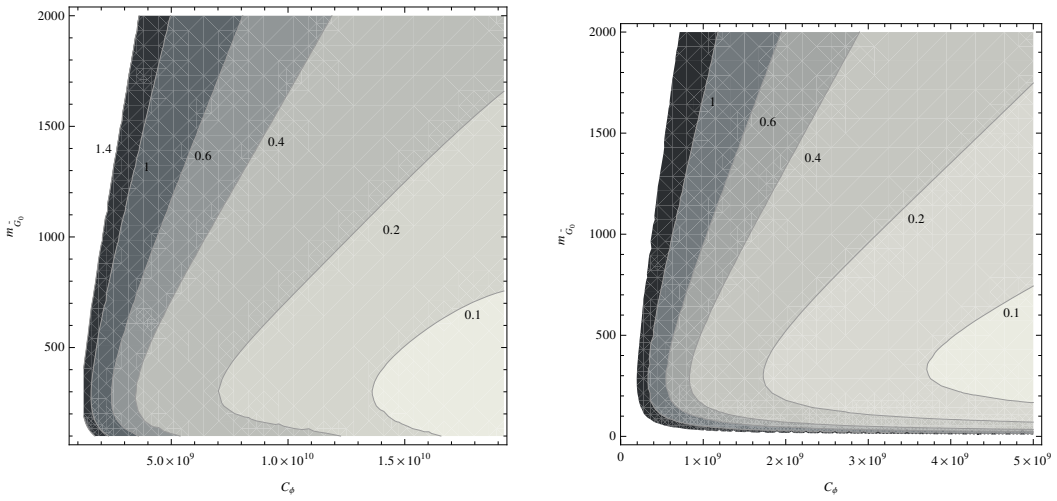

Figure 5.7: Contribution to the density parameter $\Omega_{\tilde{G}}h^2$ from an LSP gravitino for the quartic (left) and the quadratic (right) potentials, with inflaton-independent gaugino masses. Masses are given in GeV.

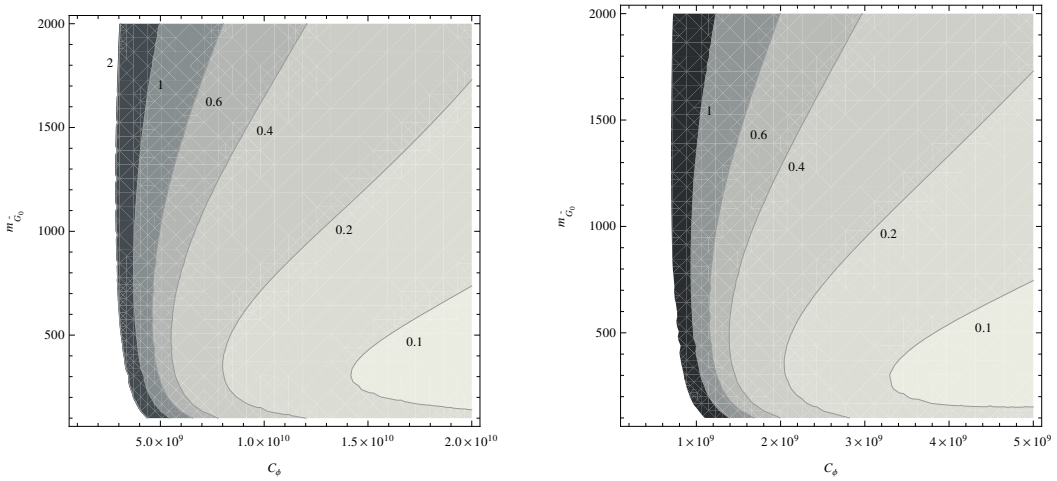

Figure 5.8: Contribution to the density parameter $\Omega_{\tilde{G}}h^2$ from an LSP gravitino for the quartic (left) and the quadratic (right) potentials, with inflaton-dependent gaugino masses. Masses are given in GeV.

becomes more severe. We can nevertheless satisfy the dark matter constraint for LSP gravitinos, $\Omega_{\tilde{G}}h^2 \lesssim 0.1$, if $C_\phi \gtrsim 1.5 \times 10^{10}$ for the quartic and $C_\phi \gtrsim 4 \times 10^9$ for the quadratic potentials. At these large values of C_ϕ, there is little difference between inflaton-dependent and independent gaugino masses scenarios.

For comparison with standard reheating predictions, we may define an effective reheat temperature as the temperature at which the gravitino yield becomes constant. In Figure 5.9, we illustrate the difference between the results predicted by Eq. (5.8) at this effective temperature with those obtained with the full numerical simulation for a quartic potential.

We can conclude that, if the gaugino masses depend on the inflaton field, the standard reheating prediction is drastically different from the true warm inflation result, where the gravitino problem is more severe. If the gaugino masses are inflaton-independent then the standard prediction also leads to an underestimation of $\Omega_{\tilde{G}}h^2$. This implies that in warm inflation the effective reheat temperature needs to be somewhat lower than in standard reheating in order to avoid $\Omega_{\tilde{G}}h^2 \gtrsim 1$. For example, for a 1 TeV gravitino, standard constraints require $T_{\rm R} \lesssim 2 \times 10^{10}\,{\rm GeV}$ for $\Omega_{\tilde{G}}h^2 \lesssim 1$, whereas in warm inflation we require $T_{\rm R} \lesssim 5 \times 10^9\,{\rm GeV}$.

As discussed earlier, in the cold inflation picture it is assumed that the yield of gravitinos at the reheat temperature is zero, $Y_{\tilde{G}}(T_{\rm R}) = 0$ (see Section 5.1). This is

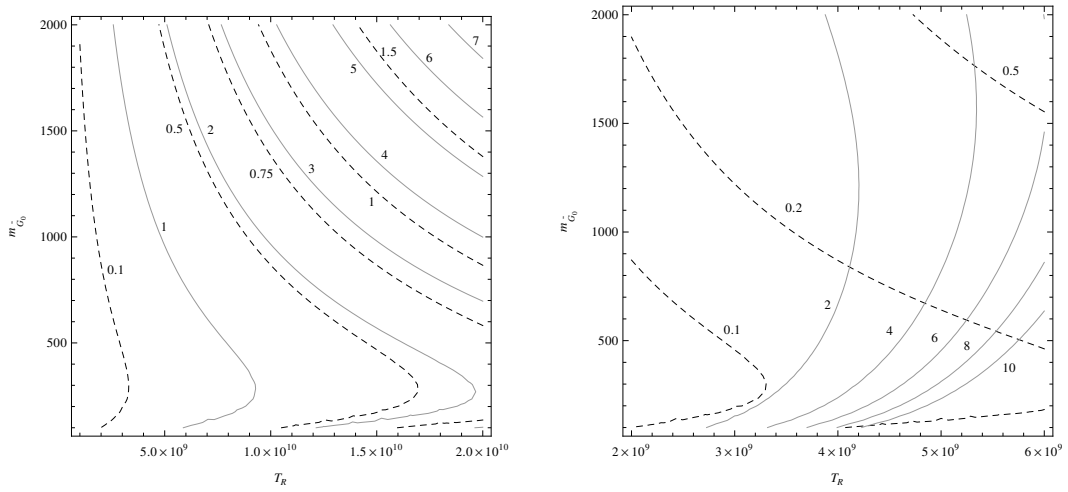

Figure 5.9: Comparison between the predictions for $\Omega_{\tilde{G}}h^2$ using Eq. (5.8) at the effective reheat temperature (dashed) and the full numerical simulation (solid) for inflaton-independent gaugino masses (left) and inflaton-dependent gaugino masses (right), with a quartic potential. All quantities are given in GeV.

perfectly valid in cold inflation, where due to the absence of a thermal bath during inflation, gravitinos are not produced. However, in warm inflation gravitinos are produced for the duration of inflation and so there is a non-negligible yield at the effective reheat temperature. Referring to Eq.(5.5) and ignoring the temperature dependence of the masses and couplings, we see that in a Hubble time the gravitino yield behaves as $\Delta Y_{\tilde{G}} \sim T(\rho_{\rm R}/\rho_\phi)^{1/2}$. Even though $\rho_{\rm R}/\rho_\phi$ is increasing during inflation, the temperature is decreasing and so, for monomial potentials in the strong dissipative regime, $\Delta Y_{\tilde{G}} \sim \phi^{r/7}$, which decreases. The gravitino yield is thus non-negligible during warm inflation and in fact larger than the final value. Moreover, previous analyses of gravitino production during warm inflation assumed not only that the standard analysis at the end of inflation was applicable, but also that the gravitino yield froze out when $\rho_\phi = \rho_{\rm R}$. We have seen that both these assumptions do not yield a good estimate for the gravitino abundance, both due to the cumulative effect of gravitino production during inflation and the fact that freeze-out does not occur until the Universe is fully radiation-dominated, which occurs a few e-folds after inflaton-radiation equality. In particular, this results in an effective reheat temperature lower than previously estimated by more than one order of magnitude, as illustrated in Figure 5.10.

Constraints on the LSP gravitino also come from decays of the NLSP spoiling

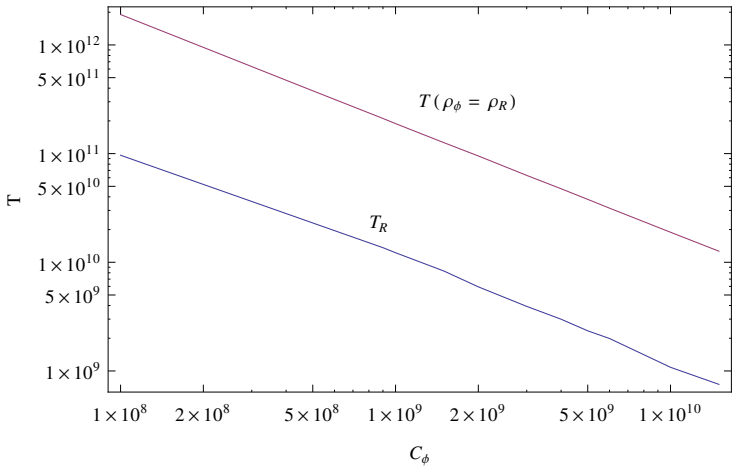

Figure 5.10: The temperature, in GeV, at which $\rho_\phi = \rho_{\rm R}$ and the effective reheat temperature, $T_{\rm R}$, at which the gravitino yield freezes out, as a function of C_ϕ for quartic potential.

BBN predictions for light-element abundances. It is typical to assume that the NLSP is the MSSM-LSP and that it will only decay into the gravitino and Standard Model particles. The NLSP lifetime typically depends upon the gravitino mass and their mass difference, $m_{\rm NLSP} - m_{\tilde{G}}$, and so unless the gravitino is light and/or the NLSP is very heavy, it will be subject to BBN constraints. As the NLSP does not have planck-suppressed interactions with the other particles in the thermal bath, it may be in thermal equilibrium during inflation and freeze out in the radiation era. Its thermally produced yield will then be given by the freeze-out temperature, which places constraints on the NLSP and low scale gravitino masses but not on the warm inflation dynamics. In this respect the situation is the same as in cold inflation and, given that this is a model-dependent issue, we will not explore it any further, pointing the interested reader to the reviews in [125, 124].

5.3.4 Unstable gravitino

If the gravitino is the NLSP then we have the constraints from BBN on the primordial yield given in Section 5.1, and in order to obtain such low yields we must consider large values of C_ϕ. For $m_{\tilde{G}} \approx 100\,{\rm GeV}$ the bound on the gravitino-to-entropy yield is $Y^s_{\tilde{G}} \lesssim 10^{-16}$, which translates into $C_\phi \gtrsim 10^{15}$. Similarly, for $m_{\tilde{G}} = 1\,{\rm TeV}$ the bounds are $Y^s_{\tilde{G}} \lesssim 10^{-14}$ and $Y^s_{\tilde{G}} \lesssim 10^{-17}$ for branching ratios

into hadrons of $B_{\rm h} = 10^{-3}$ and $B_{\rm h} = 1$, respectively. This requires $C_\phi \gtrsim 10^{12}$ and $C_\phi \gtrsim 10^{15}$, which are approximately the same for both the quartic and the quadratic potentials.

Also, in the case of a gravitino NLSP, each gravitino will then decay into one LSP. We can convert the primordial gravitino yield into the LSP yield using Eq. (5.9). In Figure 5.11, we show the lines at which $\Omega_{\rm LSP}h^2 = 0.1$ for a range of values of C_ϕ in the quartic and quadratic potentials.

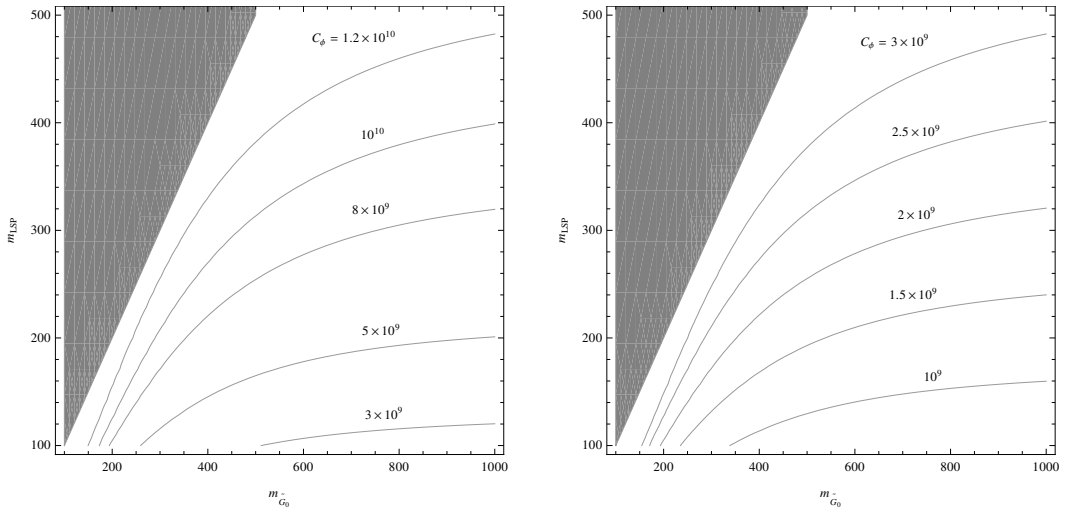

Figure 5.11: Lines of $\Omega_{\rm LSP}h^2 = 0.1$ for various values of C_ϕ in the quartic (left) and quadratic (right) potentials, with NLSP gravitinos. The shaded region indicates where the LSP is heavier than the gravitino. Masses are given in GeV.

We can see that the dark matter constraint can be satisfied for more reasonable values of C_ϕ than for the LSP gravitino. In particular, if $m_{\rm LSP} = 100\,{\rm GeV}$ and $m_{\tilde{G}_0} = 1\,{\rm TeV}$, the dark matter constraint is satisfied for $C_\phi \gtrsim 2.5\times10^9$ (quartic) and $C_\phi \gtrsim 6\times10^8$ (quadratic). If the NLSP gravitino mass, $m_{\tilde{G}} \gtrsim 20\,{\rm TeV}$, then it decays before BBN and the strongest constraint is given by the dark matter bound on the LSP. For $m_{\tilde{G}_0} = 20\,{\rm TeV}$ the dark matter constraint is satisfied for $m_{\rm LSP} = 100\,{\rm GeV}$ with $C_\phi \gtrsim 2.2\times10^9$ ($C_\phi \gtrsim 6\times10^8$) and for $m_{\rm LSP} = 1\,{\rm TeV}$ with $C_\phi \gtrsim 2.5\times10^{10}$ ($C_\phi \gtrsim 6\times10^9$) in the quartic (quadratic) potential.

5.4 Discussion

In this chapter, we have revisited the gravitino problem in warm inflation, focusing on thermal production which, providing the main difference from

standard or cold inflation, places the strongest constraints on warm inflation dynamics. By performing a full numerical evolution of the gravitino yield into the radiation era we improve upon previous analyses. Firstly, in the context of thermal gravitino production, the effective reheat temperature is the temperature at which the gravitino yield freezes out and not the temperature at which the inflaton energy density equals the radiation energy density. This allows the temperature to drop by approximately an order of magnitude, which lowers the final temperature at which gravitinos are produced compared to previous estimates. Secondly, we found that an analysis similar to standard reheating is in fact inadequate in describing gravitino production, due to the non-negligible yield produced throughout the whole duration of warm inflation. Finally, we have also taken into account the enhanced particle masses during inflation due to supersymmetry breaking, in particular the gravitino and potentially the Standard Model gauginos.

Taking all of these issues into account, our work shows, in particular, that the final gravitino yield is substantially lowered for stronger dissipative effects, as in practice this lowers the temperature of the radiation bath during warm inflation significantly. One can see this from the slow roll equations where $T \sim Q^{-1/4}$ for strong dissipation and can be understood as the effect of dissipation slowing the fields motion and thus suppressing the source term in the radiation equation. We have presented regions of parameter space where the LSP gravitino can satisfy the dark matter bound and, for an NLSP gravitino, we determined the regions where the LSP abundance does not exceed the amount of dark matter present in our Universe and have given values of the dissipation parameter C_ϕ for which late decays do not spoil the predictions of BBN.

Although thermal production is the dominant source of gravitinos during warm inflation, other non-thermal mechanisms may play a role at a later stage. Gravitinos can, in particular, also be produced from particle decays, but due to the large Hubble parameter during warm inflation these decays will not take place until the radiation era, at which point the standard cosmological results can be used. They can also be produced from the direct decay of the inflaton field, although we have found that, in the sub-planckian regime, the dissipative ratio Q is necessarily large, which prevents the inflaton field from entering an oscillating phase. Figure 5.12 shows the inflaton field evolution as we artificially switch off dissipation at $\rho_{\rm R} = \rho_\phi$, at which point oscillations immediately begin.

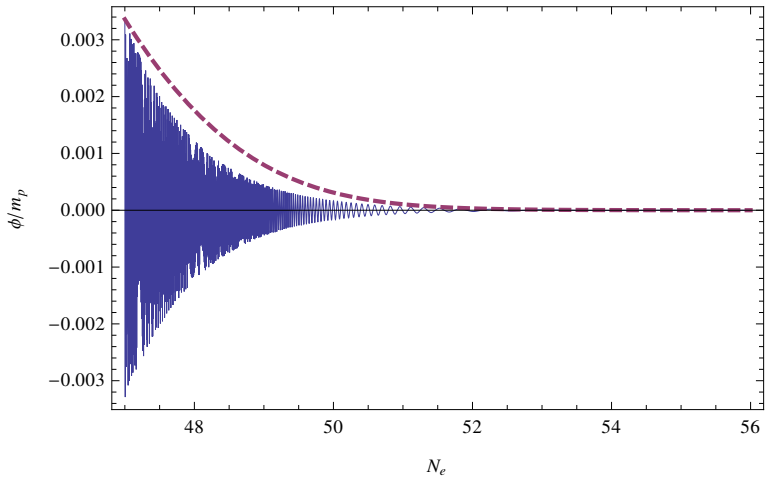

Figure 5.12: Switching off dissipation at $\rho_{\mathrm{R}} = \rho_\phi$, showing that the large dissipation keeps the inflaton field from oscillating in the radiation era. The dashed (solid) line corresponds to the case with (without) dissipation.

Dissipation will actually switch off when the heavy fields are no longer kinematically allowed to decay into the light degrees of freedom, which depends on their low scale mass hierarchy. For example, if supersymmetry is indeed a solution to the gauge hierarchy problem, we may expect light scalar masses to lie close to the TeV scale and dissipation to switch off at temperatures of this order. Apart from these kinematical constraints, the form of the dissipation coefficient in Eq. (4.20) may actually hold down to very low temperatures. For example, to avoid exceeding the dark matter bound for the LSP gravitino, we require $C_\phi \sim 1.5 \times 10^{10}$ and for 40 e-folds of inflation, if the coupling $g \sim 1$, the system remains in the low-temperature regime down to $T \sim 10\,\mathrm{MeV}$, at which point $\rho_{\mathrm{R}}/\rho_\phi \sim 10^{12}$. It is therefore unlikely in this case that any oscillations of the inflaton field may come to play a significant role in gravitino or, in fact, any entropy production. In particular, a significant dilution of the gravitino yield through a late inflaton decay along the lines proposed in [108] may be difficult to attain, although this may depend on the form of the inflaton potential, which goes beyond the scope of this work.

Our analysis revealed that it is possible to satisfy the dark matter constraint for LSP gravitinos and LSPs produced from NLSP gravitinos at large values of the dissipation parameter C_ϕ, which requires large couplings and field multiplicites, pointing towards beyond the Standard Model scenarios. The gravitino problem is more severe for unstable gravitinos potentially spoiling the predictions of BBN,

and in this case much larger values of C_ϕ are required.

One should note that such large values of the dissipation coefficient are nevertheless required in order to overcome the severe eta-problem affecting monomial potentials for sub-planckian values. Above the Planck scale, the potential gets exponentially steeper with increasing field values, requiring larger values of C_ϕ to obtain 40-60 e-folds of inflation and also to suppress the resulting gravitino abundance. Using the full supergravity potential in Eq. (5.2) places a lower bound of $C_\phi \gtrsim 10^8$ and $C_\phi \gtrsim 2\times 10^7$ for 40 e-folds of inflation in the quartic and quadratic potentials, corresponding to $\phi_* \sim m_{\rm p}$. Of course a non-canonical choice for the Kähler potential may alleviate this eta-problem, but supergravity is in any case unlikely to be the complete theory near the Planck scale and so any analysis along these lines must be taken with a pinch of salt. It should nevertheless be emphasized that simple monomial potentials cannot yield the required number of e-folds for sub-planckian values without dissipation, which is an attractive feature of warm inflation despite the large field multiplicities and/or couplings required.

To realise inflation in these models at sub-planckian field values requires strong dissipation at horizon crossing. However, as we mentioned previously, for strong dissipation the coupling between the inflaton and radiation perturbations enhances the growth of fluctuations. This enhances the power spectrum and makes the spectrum more blue-tilted for increasing Q. This work was completed before this issue was realised, however, if the radiation fluid departs from thermal equilibrium then shear viscous effects may act to suppress the growing mode [102] potentially leaving our analysis unchanged.

In this work, we have considered a general scenario where all the MSSM degrees of freedom are in thermal equilibrium during inflation. However, it has been pointed out in [85] that, in the low-temperature regime, $m_X \ll T$, fermionic degrees of freedom may actually not thermalize, as both their contribution to the dissipation coefficient and their thermal scattering cross section are suppressed compared to scalar fields. This is related to the structure of the superpotential (4.19) and the broken supersymmetry during inflation, which imply that the light fermions in the Y multiplets only interact via the heavy X bosons and fermions, whereas the light scalars have unsuppressed interactions. Moreover, although the effects of gauge fields and their superpartners on the dissipation coefficient have yet to be analyzed in detail, their contributions to the dissipation

coefficient may also be suppressed for sufficiently small gauge couplings. This would imply a thermal bath concurrent with inflation essentially composed of scalar particles, which would prevent gravitino production during inflation and eliminate the cumulative effect observed in our numerical simulations, at the same time requiring somewhat lower values of C_ϕ for sub-planckian inflation. Both fermionic and gauge degrees of freedom will nevertheless be 'reheaten' after inflation with either the exit from the low-temperature regime or the Hubble parameter dropping sufficiently in the radiation era. Although it requires further investigation, this may occur only at very low temperatures, as discussed above, in which case thermal gravitino production will be negligible.

In cold inflation there is a tension between having a large enough reheat temperature for thermal baryogenesis/leptogenesis to occur and it being low enough to avoid overproduction of gravitinos and other unwanted relics (see e.g. [28]). As discussed previously, in warm inflation this can be alleviated, as a baryon asymmetry can be produced through dissipation itself [105]. This can lead to distinctive baryon isocurvature perturbations in the CMB anisotropies spectrum that may be observable in the near future, we will discuss this in more detail in the next chapter. Indeed the baryon asymmetry may be produced through dissipative effects after inflation ends within the radiation era, we will present a simple mechanism for this dissipative leptogenesis scenario in Chapter 7. Warm inflation and fluctuation-dissipation dynamics thus exhibit several attractive features that address not only the problems of inflationary dynamics itself but also many of the associated cosmological puzzles.

We would like to point out that the results from our analysis have a certain amount of crossover with cold inflation. Standard reheating is unlikely to be instantaneous and so the production of gravitinos will occur for the duration of the reheating phase. This will lead to an accumulated abundance similar to the one we have observed in warm inflation and so may change the standard reheating temperature constraints. The gravitino gets a mass from inflation and so, when the inflaton is oscillating about its minimum, the gravitino mass will also change at the same rate. If the oscillations are adiabatic, $\dot{m}_{\tilde{G}}/m_{\tilde{G}} \lesssim \Gamma_{\text{scattering}}$, then this effect can be analysed for various potentials in a similar way to the analysis performed in this work. It may then result in significant differences in the thermal production of gravitinos during the standard reheating picture.

With this work, we hope to have shed some light on gravitino production

in warm inflation, with the way now paved for other potentials and dissipative coefficients to be analysed. In particular, the fact that inflation gives a mass to the gravitino may have a more significant impact on the thermal production in other potentials. Our analysis also brought to light some issues that may be significant to standard reheating and we hope that this motivates further exploration of this topic.

Chapter 6

Warm inflation consistency relations

Although the CMB data can be described by a single scalar field slowly rolling down a nearly-flat potential dominating the early stages of an otherwise empty universe, one may wonder whether this is the only simple or even the most likely description of the early universe in the spirit of Occam's razor. In particular, the Planck data strongly disfavors the simplest monomial potentials in chaotic inflation, which have historically been considered as the simplest renormalizable inflationary scenarios, pointing instead towards plateau-like models. In several cases, the latter require a severe parameter fine-tuning unless a special symmetry is present or, alternatively, include modifications of Einstein's gravity, which are not yet fully understood despite the remarkable agreement with the data. Is Planck really validating the inflationary paradigm or, as suggested by some authors [91], does this create more problems than it solves? One may also wonder whether a completely isolated inflaton field is the most natural scenario, or if the inclusion of (renormalizable) interactions with other fields may also be in agreement with the Planck results.

A fundamental question to address is whether the data really establishes an inflationary universe in a true vacuum state or if more general statistical distributions may yield equally good or even better descriptions of the observational results. A particularly simple and natural possibility is the presence of a thermal state during inflation, which despite the accelerated expansion rate may be sustained if for example the inflaton itself can act as source of particles that quickly thermalize. Warm inflation thus provides a natural background to

test alternatives to the standard inflationary paradigm and address the general question of whether primordial density perturbations have a quantum or thermal origin.

As proposed in [85], if the heavy mediators, appearing in Eq. (4.19), decay through B- and CP-violating interactions, the production rates of baryons and anti-baryons will be different and a baryon asymmetry may be produced during inflation, a mechanism known as warm baryogenesis. Dissipation is naturally an out-of-equilibrium process, with annihilations of the light degrees of freedom being inefficient in repopulating the classical background condensate, thus satisfying the Sakharov conditions. The structure of the interactions closely resembles that of GUT baryogenesis models, similarly requiring at least two heavy mediators with different masses and complex Yukawa couplings, and in fact the two-stage superpotential is a natural feature of GUT-like gauge theories and associated D-brane constructions [57].

The asymmetry approaches a steady state solution during inflation, due to the slowly varying temperature of the thermal bath and will freeze out once inflation ends and the Hubble parameter drops sufficiently to make the dissipative mechanism inefficient. The produced asymmetry is suppressed in the low-temperature regime, allowing for $\mathcal{O}(1)$ couplings with CP violating phases and mass differences at the few percent level whilst producing an asymmetry within the observed window. This is in contrast to standard thermal GUT scenarios where heavily suppressed couplings are required to generate the observed asymmetry. Furthermore, standard thermal GUT baryogenesis models require a reheating temperature above the GUT threshold in order to generate a baryon asymmetry from an initial population of heavy fields in thermal equilibrium, which may lead to an overproduction of dangerous GUT relics or gravitinos. On the other hand, the temperature during warm inflation must be below the heavy mass threshold, preventing the production of GUT monopoles and potentially solving the gravitino problem for sufficiently strong dissipation [89].

As the baryon asymmetry produced through dissipation depends on the inflaton vev and the temperature of the thermal bath, the resulting baryon-to-entropy ratio will exhibit fluctuations that are fully correlated or anti-correlated with the adiabatic inflaton fluctuations and induce baryon isocurvature perturbations that are subsequently imprinted on the CMB. Warm baryogenesis thus avoids

the problems that plague standard models of thermal GUT baryogenesis whilst simultaneously being a testable model of baryogenesis.

In warm inflation, the observables that characterize the density and tensor perturbations spectrum depend not only on the slow-roll parameters, as in cold inflation, but also on the value of the dissipative coefficient when the relevant scales exit the horizon during inflation, $Q = \Upsilon/3H$, and on the number of relativistic degrees of freedom, g_*. In general, this yields too many parameters to allow one to fully relate the observable quantities. On the other hand, the generation of baryon isocurvature perturbations provides an additional observable and, furthermore, canonical potentials used in inflationary model building are characterized by only two or three parameters. As we will show, this will allow us to derive several consistency relations that can be directly tested against observational results.

In this work, we focus on consistency relations between observables based on the two-stage supersymmetric warm inflation model given in Eq. (4.19), in the low-temperature regime, assuming the observed baryon asymmetry is produced during inflation and that adiabatic perturbations originate solely from thermal fluctuations of the inflaton field. Here, we anticipate the main results of this work, which are the consistency relations for weak and strong dissipation, $Q \ll 1$ and $Q \gg 1$, respectively, that hold for any generic inflationary potential. These relate the scalar and tensor spectral indices, $n_{\rm s}$ and $n_{\rm t}$, the associated running parameters, $n'_{\rm s}$ and $n'_{\rm t}$ as well as the running-of-the-running of the scalar index $n''_{\rm s}$, the tensor-to-scalar ratio, r, the fraction of baryon isocurvature perturbations, $B_{\rm B}$ and its spectral index, $n_{\rm iso}$. For $Q \ll 1$:

$$
\begin{aligned}
B_{\rm B} &= 4n_{\rm t} - 9(n_{\rm s}-1) + \frac{8(n_{\rm s}-1)^2 - 4n'_{\rm s}}{n_{\rm s}-1+n_{\rm t}} \ , \\
n_{\rm iso} &= \frac{1}{4}\Bigg(5(n_{\rm s}-1) - 4n_{\rm t} + \frac{8(n_{\rm s}-1)(n'_{\rm s} - 2(n_{\rm s}-1)^2)}{(n_{\rm s}-1+n_{\rm t})^2} + \frac{6((n_{\rm s}-1)^2 - 2n'_{\rm s})}{n_{\rm s}-1+n_{\rm t}} + \\
&\frac{-7 + 7n_{\rm s}^3 + 16n''_{\rm s} - 3n_{\rm t} - 12n'_{\rm s}(3+n_{\rm t}) - 3n_{\rm s}^2(7+n_{\rm t}) + 3n_{\rm s}(7+12n'_{\rm s}+2n_{\rm t})}{1 + n_{\rm s}^2 + 4n'_{\rm s} - n_{\rm t}(5+4n_{\rm t}) + n_{\rm s}(5n_{\rm t}-2)} \Bigg) \ .
\end{aligned}
\tag{6.1}
$$

And for $Q \gg 1$:

$$n_{\rm iso} = \left(8n_{\rm t}\left[8n_{\rm t}(1-n_{\rm s})+3n_{\rm t}^2-3n_{\rm t}'\right]\right)^{-1}\Big(2n_{\rm t}(2(1-n_{\rm s})+45n_{\rm t})n_{\rm t}' \\ +n_{\rm t}^2\left[-32((n_{\rm s}-1)^2+4n_{\rm s}')+4(n_{\rm s}-1)n_{\rm t}+9n_{\rm t}^2\right]-3n_{\rm t}'^2\Big)\ . \tag{6.2}$$

We will place these relations in context below and apply them to some canonical potentials. These relations correspond to the dissipation coefficient obtained in the low-temperature regime through the excitation of heavy virtual modes coupled directly to the inflaton, which is the most well-studied case in the literature (see e.g. [84, 89, 93] for recent studies of warm inflation dynamics in this scenario). In this sense, these results cannot be used to probe the full warm inflation paradigm. One should note that, in the low-temperature regime, the excitation of on-shell models may give the dominant contribution to the dissipation coefficient for sufficiently small Yukawa couplings [85], a scenario that is, however, outside the scope of this work.

On the other hand, as we show below, in warm inflation models we find:

$$r < 8|n_{\rm t}|\ , \tag{6.3}$$

independently of the form of the dissipation coefficient, with $r = 8|n_{\rm t}|$ corresponding to cold single-field models. This is also a generic feature of multiple-field inflationary models [137], so that the consistency relations in Eq. (6.1) and Eq. (6.2) may be crucial in distinguishing these from warm inflation models if $r < 8|n_{\rm t}|$ is observed.

We begin by introducing the relevant observables in Section 6.1. We then analyze in more detail a few canonical examples, namely monomial, hybrid and hilltop models, in Section 6.2 before concluding in Section 6.3.

6.1 Observables

For $T > H$, the dominant contribution to the primordial perturbation spectrum are thermal fluctuations of the inflaton field, as opposed to the conventional quantum fluctuations in cold inflation models. Upon exiting the horizon these thermal fluctuations freeze out as classical perturbations and during slow-roll the

amplitude of the curvature perturbation power spectrum is given by [6, 59] [1]

$$\Delta_{\mathcal{R}} \approx \left(\frac{H}{2\pi}\right)\left(\frac{3H^2}{V_\phi}\right)(1+Q)^{5/4}\left(\frac{T}{H}\right)^{1/2} , \tag{6.4}$$

where all quantities are evaluated at horizon-crossing. Note that the cold inflation limit is obtained when $T/H \to 1$ and $Q \to 0$, i.e. in the absence of dissipation the temperature corresponds to that of the cosmological de Sitter horizon. Eq. (6.4) is strictly valid for a dissipation coefficient that is independent of the temperature of the radiation bath, whereas here we consider the T-dependent coefficient obtained in the supersymmetric two-stage model described above. In this case the inflaton and radiation perturbations can become strongly coupled in the regime $Q \gg 1$, which leads to an additional growth of the fluctuations before freeze out [87]. Although this has a negligible effect for weak dissipation, where Eq. (6.4) holds, this enhances the amplitude of the scalar power spectrum for strong dissipation and may also modify the associated spectral index depending on the variation of the dissipative ratio Q at horizon crossing. However, although we expect the radiation bath to remain close to thermal equilibrium, the dissipative nature of the particle production process may induce non-negligible departures from a perfect fluid description. In particular, shear viscous effects have been shown to damp the growth of the coupled inflaton-radiation perturbations, while preserving the background dynamics, such that for sufficiently large shear viscosity one recovers the form of the scalar power spectrum for a T-independent dissipation coefficient [102]. Since significant shear viscosities are expected for not too large values of the coupling h determining the self-interactions in the light sector Y [102], in the remainder of this work we will thus assume that Eq. (6.4) yields a sufficiently good approximation to the form of the scalar power spectrum.

The dependence of the curvature power spectrum, Eq. (6.4), on the scale of the perturbations is given by the scalar spectral index [84]:

$$n_{\rm s} - 1 \equiv \frac{d\ln\Delta_{\mathcal{R}}}{d\ln k} = \frac{1}{(1+Q)(1+7Q)}(-(2+9Q)\epsilon_\phi - 3Q\eta_\phi + (2+18Q)\sigma_\phi) \ . \tag{6.5}$$

[1] Note that due to the earlier undertaking of this work, this form of the power spectrum differs from that which is presented in Chapter 4 which takes into account the distribution of inflaton fluctuations. However the power spectrum used in this chapter gives the same behaviour in the limits where $Q \gg 1$ and $Q \ll 1$ (with a thermal distribution of inflaton particles $n_* \simeq T/H$) as that of Eq. (4.27) and so the observables computed here in these limits and thus the main results of this chapter remain largely unchanged.

The running of the scalar spectral index is given by:

$$n_{\rm s}' \equiv \frac{dn_{\rm s}}{dN_{\rm e}} = (1-n_{\rm s})\frac{Q'}{1+Q} + \frac{1}{1+Q}(-(2-5A_Q)\epsilon_\phi' - 3A_Q\eta_\phi' + (2+4A_Q)\sigma_\phi') + \frac{Q'}{(1+Q)(1+7Q)^2}(5\epsilon_\phi - 3\eta_\phi + 4\sigma_\phi) \ , \tag{6.6}$$

where $A_Q = Q/(1+7Q)$ and primes denotes derivatives with respect to the number of e-folds, in particular:

$$\epsilon_\phi' = \frac{2\epsilon_\phi}{(1+Q)}(2\epsilon_\phi - \eta_\phi) \ , \qquad \eta_\phi' = \frac{\epsilon_\phi}{(1+Q)}(2\eta_\phi - \xi_\phi) \ ,$$
$$\sigma_\phi' = \frac{\sigma_\phi}{(1+Q)}(\sigma_\phi + 2\epsilon_\phi - \eta_\phi) \ , \tag{6.7}$$

with $\xi_\phi = 2m_{\rm p}^2(V_{\phi\phi\phi}/V_\phi)$.

Tensor modes are not affected by dissipation due to the weak coupling of the graviton to the thermal bath and so the tensor perturbation spectrum is governed by quantum vacuum fluctuations. The tensor-to-scalar ratio is then modified with respect to cold inflation by an additional thermal factor:

$$r = \left(\frac{H}{T}\right)\frac{16\epsilon_\phi}{(1+Q)^{5/2}} \ . \tag{6.8}$$

We note that as long as the inflaton is solely responsible for the generation of adiabatic perturbations, which are thermally produced, we may use the slow-roll equations to show that:

$$r = \frac{2}{\pi^2\Delta_{\mathcal{R}}}\left(\frac{H}{m_{\rm p}}\right)^2 \ , \tag{6.9}$$

which is analogous to the cold inflaton result. However, one should note that thermal fluctuations are generically larger than quantum fluctuations, yielding the same amplitude for different field values. In particular, in large field models, one may obtain the observed amplitude for $\phi < m_{\rm p}$ [84].

The scale dependence of the tensor power spectrum is given by the tensor spectral index, which due to the decreasing Hubble parameter is always negative:

$$n_{\rm t} \equiv \frac{d\ln\Delta_{\rm t}}{d\ln k} = -\frac{2\epsilon_\phi}{1+Q} \leq 0 \ , \tag{6.10}$$

where $|n_{\rm t}| \ll 2$ in order to satisfy the slow-roll conditions. In cold inflation with

a single slowly rolling scalar field we thus find $r = 8|n_{\rm t}|$, which is a well-known consistency relation. In warm inflation, the relation between the tensor-to-scalar ratio and the tensor spectral index is, on the other hand, given by:

$$r = -\left(\frac{H}{T}\right)\frac{8n_{\rm t}}{(1+Q)^{3/2}} < 8|n_{\rm t}| \ , \tag{6.11}$$

for $T > H$, while one recovers the equality for $T/H \to 1$ and $Q \to 0$. Thus, if a future experiment measures r and $n_{\rm t}$ and finds $r < 8|n_{\rm t}|$, this could be a hint for a thermal origin of the adiabatic perturbations, although this is also the case for generic multiple field models as mentioned earlier and other observables must be used in order to break this degeneracy.

There is also the possibility that the observed baryon asymmetry is produced during warm inflation through dissipative effects as described earlier. In this scenario the baryon asymmetry $\eta_s \propto (T/m_\chi)^2 \propto (T/\phi)^2$ and so fluctuations in the temperature and inflaton field are directly transferred to the baryon-to-entropy ratio which yields baryon isocurvature perturbations that freeze out during inflation and are imprinted on the CMB [105]. However, the temperature fluctuations are generated themselves by fluctuations in the inflaton field and so these isocurvature perturbations, given by $S_{\rm B} = \delta\eta_s/\eta_s$, are thus fully correlated or anti-correlated with the adiabatic perturbations. It is convenient to express this in terms of the ratio between the baryon isocurvature perturbations and the curvature perturbation ζ, which for the dissipative coefficient in Eq. (4.20) is given by [85]:

$$B_{\rm B} \equiv \frac{S_{\rm B}}{\zeta} = \frac{2}{(1+Q)^2(1+7Q)}(2\eta_\phi(1+Q) - \epsilon_\phi(3+Q) - \sigma_\phi(3+5Q)) \ . \tag{6.12}$$

Whether isocurvature perturbations are correlated or anti-correlated with adiabatic perturbations depends upon the sign of $B_{\rm B}$. Note that if the field generating the asymmetry is distinct from the one that generates the adiabatic perturbations then the isocurvature perturbations will be completely uncorrelated with the adiabatic perturbations, an example of this scenario will be presented in Chapter 7.

The spectral index of the isocurvature perturbations is in principle another observable that can be used to test the warm baryogenesis scenario. For the

dissipative coefficient in Eq. (4.20) the isocurvature spectral index is given by:

$$\begin{aligned} n_{\rm iso} &= \frac{d\ln S_{\rm B}}{d\ln k} = -\frac{7Q}{(1+7Q)^2}(10\epsilon_\phi - 6\eta_\phi + 8\sigma_\phi) \\ &+ \frac{2\epsilon_\phi(2\eta_\phi - \xi_\phi)(1+Q) - 2\epsilon_\phi(2\epsilon_\phi - \eta_\phi)(3+Q) - \sigma_\phi(\sigma_\phi + 2\epsilon_\phi - \eta_\phi)(3+5Q)}{(1+Q)(2\eta_\phi(1+Q) - \epsilon_\phi(3+Q) - \sigma_\phi(3+5Q))} \\ &+ \frac{(2\eta_\phi - \epsilon_\phi - 5\sigma_\phi)(10\epsilon_\phi - 6\eta_\phi + 8\sigma_\phi)Q}{(1+7Q)(2\eta_\phi(1+Q) - \epsilon_\phi(3+Q) - \sigma_\phi(3+5Q))} - \frac{2\epsilon_\phi - \eta_\phi}{(1+Q)} \\ &+ \frac{\epsilon_\phi(2-Q) - \eta_\phi(2+5Q) + 2\sigma_\phi(1+Q)}{2(1+7Q)(1+Q)} \,. \end{aligned} \tag{6.13}$$

This implies that the baryon isocurvature spectral index will typically be proportional to a combination of slow-roll parameters for weak dissipation, which is further suppressed by the dissipative ratio Q for strong dissipation (see below). Hence, we expect this to be small in general, although formally it can take any positive or negative value depending on the form of the inflaton potential. For comparison, in the curvaton scenario the spectral index of the (cold dark matter) isocurvature spectrum is the same as for the adiabatic spectrum (see e.g. [138]), whereas isocurvature modes produced from the quantum fluctuations of axion fields correspond to an almost scale invariant spectrum [139].

The bounds on anti-correlated cold dark matter isocurvature modes from the 9-year WMAP data analysis (WMAP 9), using the combined WMAP + eCMB + BAO + H_0 data and taking into account that $\Omega_{\rm CDM}/\Omega_{\rm B} \approx 5$, yield an upper bound $|B_{\rm B}| \leq 0.33$ for $B_{\rm B} < 0$ [140]. Fully correlated modes have not been analyzed with WMAP 9 data, with an earlier analysis yielding $B_{\rm B} < 0.43$ [138].

In the Planck 2013 data release, new bounds were placed on the presence of a combination of cold dark matter and baryon isocurvature modes (CDI), which are indistinguishable from the CMB point of view. For a general admixture of adiabatic and isocurvature perturbations, independently of their correlation or the latter's spectral index, the Planck 2013 results yield $\beta_{\rm iso} < 0.075$ for the CDI fraction at the comoving wavenumber $k_{\rm low} = 0.002$ Mpc^{-1} [141]. This translates into a bound $|B_{\rm B}| \lesssim 1.5$, which is surprisingly less constraining than the WMAP results. According to the Planck collaboration, this is related to the fact that the data actually prefers models with a significant contribution of CDI (or neutrino density isocurvature modes), driven mainly by the amplitude deficit observed at low multipoles. Although no definite evidence for isocurvature modes was found in the data, it nevertheless allows for a substantially large fraction of isocurvature

modes. [2]

Given the model-dependence of the sign of $B_{\rm B}$ and the value of $n_{\rm iso}$ discussed above, in our analysis below we will include the general bound from Planck 2013 and the earlier WMAP bounds to illustrate our results. One should nevertheless keep in mind that, for particular potentials, $n_{\rm iso}$ will be related to $n_{\rm s}-1$ and more stringent bounds should apply as for the axion and curvaton cases. For example, for monomial potentials, $V(\phi)\propto\phi^n$, and a dissipative coefficient of the form Eq. (4.20), we find:

$$\begin{aligned} \frac{n_{\rm iso}}{n_{\rm s}-1} &= \frac{1}{2}-\frac{2}{n-2}\ , & Q &\ll 1\ , \\ \frac{n_{\rm iso}}{n_{\rm s}-1} &= \frac{42-11n}{84-30n}\ , & Q &\gg 1\ . \end{aligned} \tag{6.14}$$

We would like to emphasize that the warm baryogenesis scenario may generate isocurvature perturbations which are either correlated or anti-correlated with adiabatic perturbations, depending on the inflaton potential, whereas the recent literature has focused mostly on anti-correlated and uncorrelated modes, motivated by curvaton and axion models. We hope that this work motivates the need to look for fully correlated isocurvature modes in future data.

In general, for the low-temperature dissipative coefficient in Eq. (4.20), the expressions for the observables are too complicated to yield simple relations amongst them. If, however, we look at the strong ($Q\gg 1$) and weak ($Q\ll 1$) dissipative regimes separately, these expressions simplify considerably and such consistency relations can be obtained. To illustrate these relations, we will use the 68% and 95% C.L. contours in the $(n_{\rm s}, n_{\rm s}')$ plane obtained from the Planck 2013 data for a ΛCDM cosmology with a running scalar spectral index with and without tensor perturbations [141].

[2]The updated constraints on CDM isocurvature modes from the Planck 2015 data release [1] yield somewhat tighter constraints with $B_{\rm B}\lesssim 0.19$ (0.15) for correlated (anti-correlated) isocurvature modes. These bounds are however weakened slightly with the addition of Planck lensing data resulting in $B_{\rm B}\lesssim 0.25$ (0.39) again for correlated (anti-correlated) isocurvature modes.

Weak dissipation

In the weak dissipative limit the observables reduce to:

$$n_{\rm s}-1\approx-2\epsilon_\phi+2\sigma_\phi\ ,\qquad n_{\rm s}'\approx-2\epsilon_\phi'+2\sigma_\phi'\ ,\qquad n_{\rm s}''\approx-2\epsilon_\phi''+2\sigma_\phi''\ ,$$
$$r\approx\frac{16\epsilon_\phi}{Q^{1/3}}\left(\frac{16\pi^2\Delta_{\mathcal{R}}C_{\rm R}}{3}\right)^{1/3}\ ,\qquad n_{\rm t}\approx-2\epsilon_\phi\ ,\qquad B_{\rm B}\approx2(2\eta_\phi-3\epsilon_\phi-3\sigma_\phi)\ ,$$
$$n_{\rm iso}\approx\frac{9\epsilon_\phi^2+2\epsilon_\phi(\xi_\phi-4\eta_\phi+3\sigma_\phi)+\sigma_\phi(6\sigma_\phi-5\eta_\phi)}{3\epsilon_\phi-2\eta_\phi+3\sigma_\phi}\ . \tag{6.15}$$

From these expressions we can derive two consistency relations for an arbitrary inflationary potential with the low-temperature dissipative coefficient in the weak dissipative regime, $Q\ll1$:

$$B_{\rm B}=4n_{\rm t}-9(n_{\rm s}-1)+\frac{8(n_{\rm s}-1)^2-4n_{\rm s}'}{(n_{\rm s}-1)+n_{\rm t}}\ , \tag{6.16}$$

$$n_{\rm iso}=\frac{1}{4}\Bigg(5(n_{\rm s}-1)-4n_{\rm t}+\frac{8(n_{\rm s}-1)(n_{\rm s}'-2(n_{\rm s}-1)^2)}{(n_{\rm s}-1+n_{\rm t})^2}+\frac{6((n_{\rm s}-1)^2-2n_{\rm s}')}{n_{\rm s}-1+n_{\rm t}}$$
$$+\frac{7(n_{\rm s}-1)^3+36(n_{\rm s}-1)n_{\rm s}'+16n_{\rm s}''-3(n_{\rm s}-1)^2n_{\rm t}-12n_{\rm s}'n_{\rm t}}{(n_{\rm s}-1)^2+4n_{\rm s}'+5(n_{\rm s}-1)n_{\rm t}-4n_{\rm t}^2}\Bigg)\ . \tag{6.17}$$

Figure 6.1 shows the contours of $B_{\rm B}$ from Eq. (6.16) in the ($n_{\rm s}$,$n_{\rm s}'$) plane for $n_{\rm t}=-0.01$. For $|n_{\rm t}|\leq0.01$ the effect of the tensor index becomes negligible in Eq. (6.16) and the parameter space plot tends to this limiting form. For $n_{\rm t}\lesssim-0.4$ we do not find any solutions within the 95% C.L., so that this places an upper bound on $|n_{\rm t}|$ in the weak dissipative regime in the warm baryogenesis scenario.

Strong dissipation

In the strong dissipative regime there is no consistency relation involving only $n_{\rm s}, n_{\rm s}', r, n_{\rm t}, B_{\rm B}$, as there are 5 parameters (ϵ_ϕ, η_ϕ, σ_ϕ, ξ_ϕ, Q) for a given value of

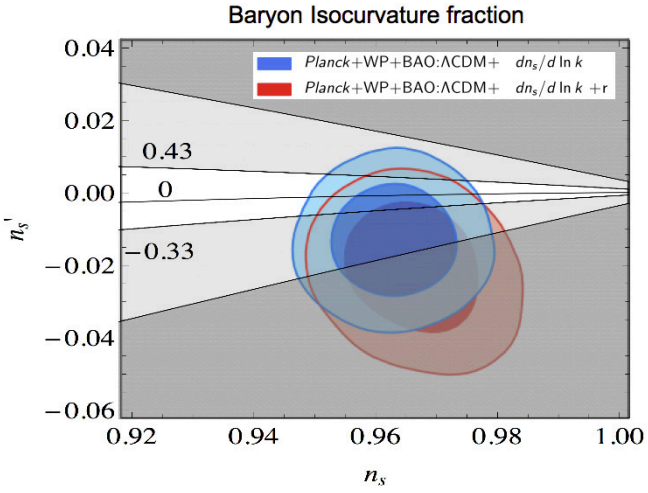

Figure 6.1: Contours of $B_{\rm B}$ in the $(n_{\rm s},n'_{\rm s})$ plane for $Q \ll 1$, with $n_{\rm t} = -0.01$. The dark grey excluded region represents the bounds on $B_{\rm B}$ from Planck 2013, while the lighter gray indicates previous limits from WMAP.

g_* and only 5 observables. In the strong dissipative limit these are given by:

$$
\begin{aligned}
&n_{\rm s} - 1 \approx \frac{3}{7Q}(6\sigma_\phi - 3\epsilon_\phi - \eta_\phi) \ , \quad r \approx \frac{16\epsilon_\phi}{Q^3}\left(\frac{16\pi^2\Delta_{\mathcal{R}}C_{\rm R}}{3}\right)^{1/3} \ , \quad n_{\rm t} \approx -2\frac{\epsilon_\phi}{Q} \ , \\
&n'_{\rm s} \approx -\frac{3}{49Q^2}(54\epsilon_\phi^2 + 6\eta_\phi^2 - 2\eta_\phi\sigma_\phi + 6\sigma_\phi^2 - \epsilon_\phi(7\xi_\phi + 20\eta_\phi + 48\sigma_\phi) \ , \\
&B_{\rm B} \approx \frac{2}{7Q^2}(2\eta_\phi - \epsilon_\phi - 5\sigma_\phi) \ .
\end{aligned} \tag{6.18}
$$

However, if we somewhat forward-thinkingly include the running of the tensor spectral index:

$$
n'_{\rm t} = -2\frac{\epsilon'_\phi}{1+Q} + 2\frac{Q'\epsilon_\phi}{(1+Q)^2} = \frac{4\epsilon_\phi}{(1+Q)^2(1+7Q)}(-(2+9Q)\epsilon_\phi + \eta_\phi + 4Q(\eta_\phi + \sigma_\phi)) \ , \tag{6.19}
$$

we obtain the following consistency relation:

$$
r = -\frac{1152B_{\rm B}^2 n_{\rm t}^3}{(n_{\rm t}(8(1-n_{\rm s}) + 3n_{\rm t}) - 3n'_{\rm t})^2}\left(\frac{16\pi^2\Delta_{\mathcal{R}}C_{\rm R}}{3}\right)^{1/3} \ . \tag{6.20}
$$

We note that the dependence of this relation on the number of relativistic degrees of freedom, g_*, is rather mild. For example, for $g_* = \mathcal{O}(10-100)$, the tensor-to-scalar ratio varies only by a factor of ~ 2.

If in addition, we may consider the isocurvature spectral index, which in the strong dissipative regime is given by:

$$n_{\rm iso} = \frac{27\epsilon_\phi^2 + 28\epsilon_\phi\xi_\phi - 17\epsilon_\phi\eta_\phi - 18\eta_\phi^2 - 3\epsilon_\phi\sigma_\phi - 29\eta_\phi\sigma_\phi + 80\sigma_\phi^2}{14Q(\epsilon_\phi - 2\eta_\phi + 5\sigma_\phi)} \ , \tag{6.21}$$

so that we can derive the following consistency relation relating $n_{\rm iso},\ n_{\rm s},\ n'_{\rm s}, n_{\rm t}$ and $n'_{\rm t}$:

$$\begin{aligned} n_{\rm iso} = \left(8n_{\rm t}\left[8n_{\rm t}(1-n_{\rm s}) + 3n_{\rm t}^2 - 3n'_{\rm t}\right]\right)^{-1}\Big(n_{\rm t}^2\Big[- 32((n_{\rm s}-1)^2 + 4n'_{\rm s}) \\ +4(n_{\rm s}-1)n_{\rm t} + 9n_{\rm t}^2\Big] + 2n_{\rm t}(2(1-n_{\rm s}) + 45n_{\rm t})n'_{\rm t} - 3n_{\rm t}'^2\Big) \ . \end{aligned} \tag{6.22}$$

However, since we do not expect the running of the tensor spectral index nor the baryon isocurvature spectral index to be accurately measured in the near future, we will not include the consistency relations in Eq. (6.17), Eq. (6.20) and Eq. (6.22) in the remainder of our analysis.

6.2 Inflationary models

In the previous section we have derived general consistency relations between observables that are independent of the form of the inflationary potential in both the weak and the strong dissipative regimes. If we consider specific potentials, the slow-roll parameters are typically no longer independent and we may find stronger consistency relations. In particular, we obtain, in some cases, consistency relations that are independent of the baryon isocurvature perturbations, so that these relations hold even if the baryon asymmetry is not produced during warm inflation. In this section, we thus consider a few canonical models, in particular monomial, hybrid and hilltop potentials.

6.2.1 Monomial potentials

Monomial potentials have the generic form $V = V_0(\phi/m_{\rm p})^n$. In cold inflation, one typically requires super-planckian field values in order to achieve $\sim 40-60$ e-folds of accelerated expansion. For warm inflation, on the other hand, this can be achieved in the sub-planckian regime due to the additional friction.

The slow-roll parameters for the monomial models are given by:

$$\epsilon_\phi = \frac{n^2}{2}\left(\frac{m_{\rm p}}{\phi}\right)^2, \qquad \eta_\phi = n(n-1)\left(\frac{m_{\rm p}}{\phi}\right)^2, \qquad \sigma_\phi = \frac{\eta_\phi}{(n-1)}\,,$$
$$\xi_\phi = 2(n-1)(n-2)\left(\frac{m_{\rm p}}{\phi}\right)^2\,. \tag{6.23}$$

This yields a blue spectral index, $n_{\rm s} > 1$, for the quadratic potential (in contrast to cold inflation), which is disfavoured by the latest Planck data. On the other hand, as we have seen in Chapter 4, for the quartic potential one finds a spectral index in excellent agreement with the Planck measurement, even in the weak dissipative regime [84, 142].

Weak dissipative regime

In the weak dissipative regime, we derive the following consistency relations:

$$B_{\rm B} = (1-n_{\rm s}) - \frac{4n_{\rm s}'}{(n_{\rm s}-1)}\,, \qquad n_{\rm t} = (n_{\rm s}-1) - \frac{n_{\rm s}'}{(n_{\rm s}-1)}\,. \tag{6.24}$$

Note that the tensor spectral index is always negative, so that these consistency relations only hold in the regions of the ($n_{\rm s}$,$n_{\rm s}'$) plane where $n_{\rm t} < 0$, i.e. the model can only yield values of the scalar spectral index and running in this region. Also, $n_{\rm t} \gtrsim -2$ in order to satisfy the slow-roll conditions when the observable scales leave the horizon during inflation.

As we illustrate in Figure 6.2, for $n_{\rm s} \leq 1$ the allowed regions where $B_{\rm B}$ is within the observational bounds and $-2 < n_{\rm t} < 0$ overlap with the 95% C.L. region, with $n_{\rm t}$ falling within the 68% C.L. contour for $n_{\rm t} \sim -0.1$. Also, a positive running would indicate a positive correlation between the isocurvature and adiabatic perturbations with $B_{\rm B} \gtrsim 0.1$ and a tensor spectral index $n_{\rm t} \gtrsim -0.1$. A negative running may, on the other hand, give anti-correlated isocurvature modes.

Strong dissipative regime

In the strong dissipative regime the value of Q at horizon-crossing becomes an additional parameter determining the relevant observables compared to the weak

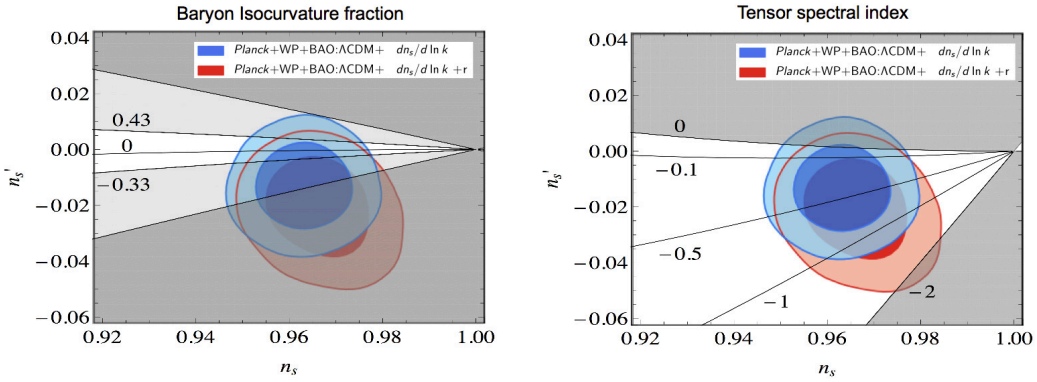

Figure 6.2: Contours of $B_{\rm B}$ (left) and $n_{\rm t}$ (right) in the ($n_{\rm s}$,$n_{\rm s}'$) plane for monomial potentials in the weak dissipative regime. We exclude the grey (light grey) regions where $B_{\rm B}$ is outside the observational bounds for Planck 2013 (WMAP) (left) and where the consistency relation yields $n_{\rm t} > 0$ or $n_{\rm t} \leq -2$ (right).

dissipative regime. Thus, we may only obtain a single consistency relation:

$$n_{\rm t} = -7\frac{n_{\rm s}'}{n_{\rm s}-1} \ . \tag{6.25}$$

In the strong dissipative regime, $n_{\rm t}$ is consistent with the 95% C.L. limit and only for larger values, $n_{\rm t} \sim -0.5$, does $n_{\rm t}$ fall within the 68% C.L. contour, as shown in Figure 6.3. For $n_{\rm s} \leq 1$ (≥ 1) the running is necessarily negative (positive), which gives a strong constraint independent of whether the observed baryon asymmetry is produced during warm inflation. In this regime, there is no consistency relation involving $B_{\rm B}$, but since Eq. (6.25) only holds for $Q \gg 1$ this effectively limits the value of $B_{\rm B}$ at each point in the ($n_{\rm s}$,$n_{\rm s}'$) plane.

6.2.2 Hybrid potentials

We will now consider an example of small field models, hybrid models, where the inflaton couples to one or more 'waterfall fields' with a Higgs-like potential. These fields couple to the inflaton in an analogous fashion to the mediator fields in the supersymmetric model given by Eq. (4.19), so this provides a natural framework for warm inflation. During inflation, these fields are heavy and overdamped at the origin, yielding a constant cosmological constant that drives the accelerated expansion. This flat potential may be lifted by radiative corrections, soft SUSY breaking mass terms, non-renormalisable interactions or supergravity corrections,

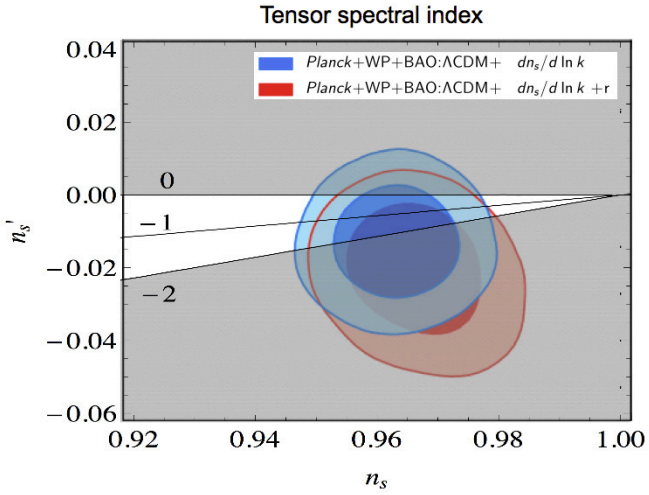

Figure 6.3: Contous of $n_{\rm t}$ in the $(n_{\rm s},n_{\rm s}')$ plane for monomial potentials in the strong dissipative regime. We exclude the grey region where the consistency relation yields $n_{\rm t} > 0$ or $n_{\rm t} \leq -2$.

typically yielding a leading correction of the form:

$$V = V_0 \left(1 + \frac{\gamma}{n}\left(\frac{\phi}{m_{\rm p}}\right)^n\right) \ , \tag{6.26}$$

for $n > 0$, while for $n = 0$ the dominant contribution comes from logarithmic radiative terms:

$$V = V_0 \left(1 + \gamma \ln\left(\frac{\phi}{m_{\rm p}}\right)\right) \ . \tag{6.27}$$

Here, we will focus on the most common scenarios where either the $n = 0$ or the $n = 2$ term dominates, both in the strong and weak dissipative regimes. The slow-roll parameters for the hybrid models are given by:

$$\epsilon_\phi = \frac{\gamma^2}{2}\left(\frac{m_{\rm p}}{\phi}\right)^{2-2n} \ , \qquad \eta_\phi = (n-1)\gamma\left(\frac{m_{\rm p}}{\phi}\right)^{2-n} \ , \qquad \sigma_\phi = \frac{\eta_\phi}{(n-1)} \ ,$$
$$\xi_\phi = 2(n-1)(n-2)\left(\frac{m_{\rm p}}{\phi}\right)^2 \ , \tag{6.28}$$

where we assumed that, at horizon-crossing, the potential is dominated by the constant term, V_0. This limits the values of γ and ϕ and hence the validity of consistency relations between observables. Note that when the corrections dominate, the potential behaves effectively as a monomial and the relations

derived earlier apply.

For the $n = 2$ hybrid model, $n_{\rm s} > 1$ as for the quadratic monomial potential, in both the weak and the strong dissipation regimes at horizon crossing. Since this is disfavoured by the Planck data, we will not consider the consistency conditions in this case, focusing only on the logarithmic hybrid potential.

$n = 0$; Weak dissipative regime

For the logarithmic hybrid model in Eq.(6.27), we obtain the following consistency relations:

$$B_{\rm B} = 13(1 - n_{\rm s}) \pm 8\sqrt{2(n_{\rm s} - 1)^2 - n_{\rm s}'}\,, \qquad n_{\rm t} = (1 - n_{\rm s}) \pm \sqrt{2(n_{\rm s} - 1)^2 - n_{\rm s}'}\,. \tag{6.29}$$

Note that the '+' solutions correspond to $\gamma < 1$, while the '−' solutions hold for $\gamma > 1$. We find that only the '−' solution has a region of parameter space in which the corrections are small and the consistency relation predictions are compatible with the Planck 2013 results.

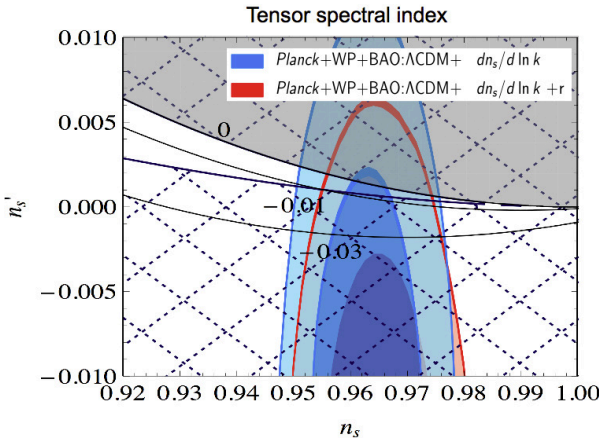

Figure 6.4: Contours of $n_{\rm t}$ in the $(n_{\rm s}, n_{\rm s}')$ plane for the $n = 0$ hybrid model in the weak dissipative regime, using the '−' solution. We exclude the grey regions where the consistency relation predicts a positive or imaginary $n_{\rm t}$. In the blue cross-hatched region the radiative corrections dominate, $\gamma|\ln(\phi/m_{\rm p})| \geq 1$.

As illustrated in Figures 6.4 and 6.5, the logarithmic corrections dominate in a large fraction of the parameter space, where the potential behaves effectively as a single monomial. The constant part only dominates in a narrow region of

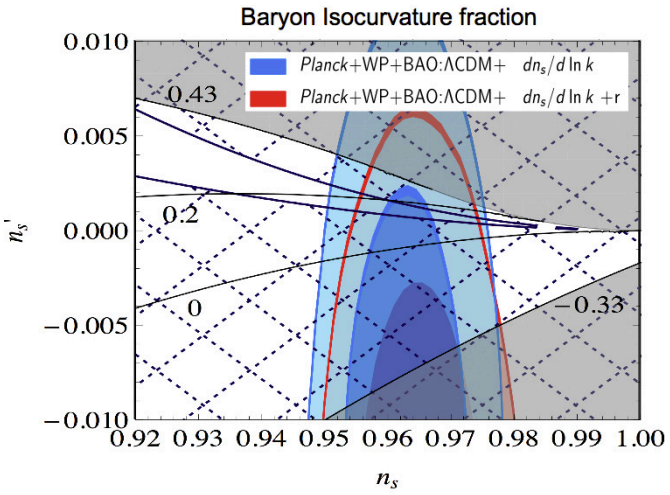

Figure 6.5: Contours of $B_{\rm B}$ in the $(n_{\rm s},n'_{\rm s})$ plane for the $n = 0$ hybrid model in the weak dissipative regime, using the '$-$' solution. The light grey region indicates where $B_{\rm B}$ exceeds WMAP bounds. In the blue cross-hatched region the radiative corrections dominate, $\gamma|\ln(\phi/m_{\rm p})| \geq 1$.

parameter space, where $n'_{\rm s} \sim 0.005$, $n_{\rm t} \sim -0.01$ and we find relatively large, positive values of $B_{\rm B} \sim 0.2 - 0.4$.

$n = 0$; Strong dissipative regime

For the logarithmic hybrid model, $n = 0$, in the strong dissipative regime we find the following relation:

$$n_{\rm t} = \frac{1}{9}\left(2(1-n_{\rm s}) \pm \sqrt{4(n_{\rm s}-1)^2 - 126n'_{\rm s}}\right) \ . \tag{6.30}$$

Note that the '+' and '$-$' solutions correspond to $\gamma < 7/12$ and $\gamma > 7/12$, respectively. However, the '+' solution only yields $n_{\rm t} < 0$ for $n_{\rm s} \gtrsim 2$ and hence is not consistent within the observationally allowed region. In Figure 6.6 we illustrate the contours of $n_{\rm t}$ for the '$-$' solution.

For this relation, we find that $Q \gg 1$ is satisfied and the logarithmic corrections are subdominant within the region where $n_{\rm t} < 0$ for $n_{\rm s} \geq 1$. For $n_{\rm s} \leq 1$ keeping the logarithmic corrections subdominant gives an upper bound on $n'_{\rm s}$, for example for the central value of $n_{\rm s} \sim 0.96$ we find $|n'_{\rm s}| \geq 0.005$ with $n'_{\rm s} \leq 0$.

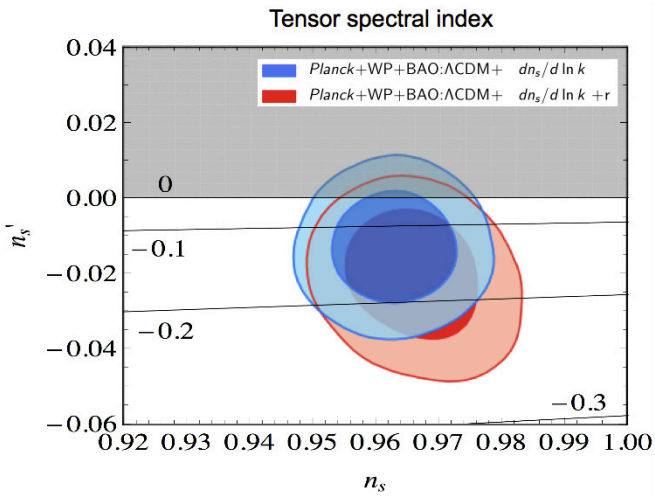

Figure 6.6: Contours of n_t in the $(n_\mathrm{s},n_\mathrm{s}')$ plane for the hybrid model with $n = 0$ in the strong dissipative regime. We exclude the grey region where the consistency relation yields $n_\mathrm{t} > 0$ or imaginary.

6.2.3 Hilltop potentials

Hilltop scenarios are small field models where inflation occurs near a maximum of the potential, being parametrized by:

$$V = V_0 \left(1 - \frac{M}{2}\left(\frac{\phi}{m_\mathrm{p}}\right)^2\right) \ . \tag{6.31}$$

Hence, this is equivalent to the $n = 2$ hybrid model with a negative mass squared, $\gamma \to -M$. The consistency relations are thus the same for the hilltop model as for the $n = 2$ hybrid model, although the requirement $M(\phi/m_\mathrm{p})^2/2 \leq 1$ or ≥ 0 yields distinct constraints on the parameters.

Weak dissipative regime

In the weak dissipative regime we derive the following consistency relation for the hilltop potential:

$$B_\mathrm{B} = (1 - n_\mathrm{s}) - \frac{2n_\mathrm{s}'}{n_\mathrm{s} - 1}, \qquad n_\mathrm{t} = \frac{n_\mathrm{s}'}{2(1 - n_\mathrm{s})}. \tag{6.32}$$

The only simultaneously allowed regions of parameter space for B_B and n_t correspond to $n_\mathrm{s} \leq 1$ with negative running, $n_\mathrm{s}' \sim -0.001$, as shown in Figure

6.7. Within this region we find $n_t \sim -0.01$ and $-0.05 \lesssim B_B \lesssim 0.1$.

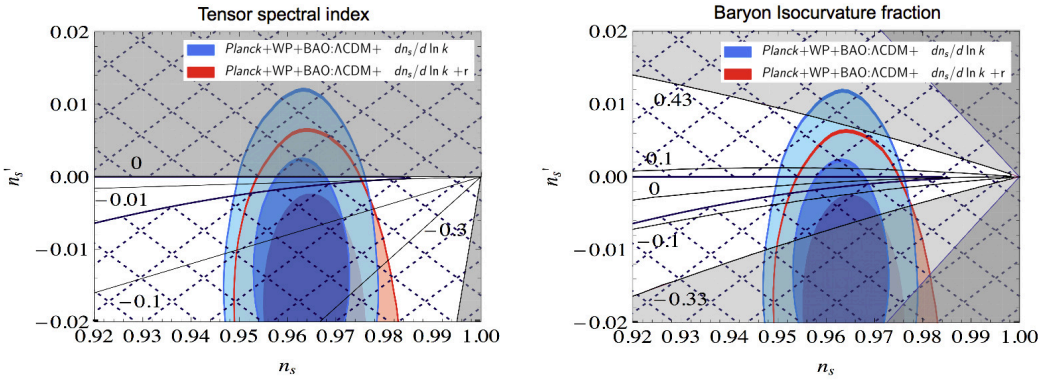

Figure 6.7: Contours of n_t (left) and B_B (right) in the (n_s,n_s') plane for the hilltop model in the weak dissipative regime. The consistency relations and exclusions are the same as for the $n = 2$ hybrid model, although the region in which the calculation is valid is distinct.

Strong dissipative regime

In the strong dissipative regime we derive the following consistency relation:

$$n_t = \frac{1}{9}\left(14(1-n_s) \pm \sqrt{154(n_s-1)^2 - 315 n_s'}\right) . \tag{6.33}$$

However, only the '−' solution yields regions of parameter space where the constant term dominates and the consistency relation is compatible with the observational results.

Although the region where the consistency relation is valid is rather small in this case, it is in an observationally relevant range. In particular, it predicts $n_t \sim -0.02$ with a small but non-vanishing spectral running, $n_s' \sim -0.002$.

6.3 Discussion

The work in this chapter was done prior to and just after the 2013 Planck release and so in terms of comparison to data it is somewhat outdated. However the main ideology and methodology behind this work is still relevant today. It is our intent at some point in the future to use our improved understanding of the

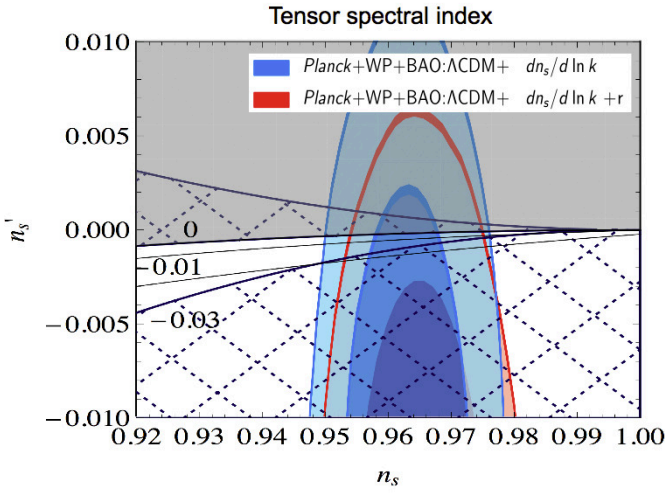

Figure 6.8: Contours of $n_{\rm t}$ in the $(n_{\rm s},n_{\rm s}')$ plane for the hilltop model in the strong dissipative regime. We exclude the grey region where the consistency relation yields $n_{\rm t} > 0$. The blue cross-hatched region indicates where $M(\phi/m_{\rm p})^2/2 \geq 1$ or < 0.

power spectrum presented in Chapter 4 to reanalyse the models considered in this chapter and present updated consistency relations.

In this chapter, we have derived consistency relations between observables for warm inflation models based on supersymmetric two-stage interactions in the low-temperature regime. We have focused on the most well-studied case where dissipation is dominantly generated by the excitation and decay of heavy virtual modes coupled directly to the inflaton. We have obtained relations amongst the parameters characterizing the spectrum of adiabatic perturbations in the scalar and tensor sectors, as well as the fraction of baryon isocurvature perturbations and its spectral index associated to the generation of the observed baryon asymmetry during warm inflation through the dissipative interactions.

The relations between the different observables are, in general, rather intricate and it is not always possible to express them in a simple analytical form. However, we have shown that in the weak and strong dissipative regimes one may obtain generic relations that are independent of the inflationary potential and which constitute the main result of this work, in Eqs. (6.16), (6.17), (6.20) and (6.22).

In addition we have noted that the thermal origin of the adiabatic perturbations modifies the relation between the tensor-to-scalar ratio and the tensor spectral index, giving $r < 8|n_{\rm t}|$, which is always smaller than the corresponding

cold inflation prediction. Although this is also a feature of supercooled models with multiple scalar fields, this inequality may be used along with the consistency relations derived in this work to probe the thermal nature of the inflationary state of the Universe.

In the warm baryogenesis scenario, the correlation between the produced baryon isocurvature perturbations and the main adiabatic fluctuations, as well as the isocurvature spectral index, depend on the form of the inflationary potential, yielding in general less stringent bounds on the isocurvature fraction than for example in the axion or curvaton scenarios. However, when considering specific inflationary potentials the model predicts a spectral index that can be used to derive stronger bounds on the isocurvature contribution. Even if an isocurvature component is unambiguously found, Planck cannot distinguish between cold dark matter and baryon isocurvature perturbations, with a promising observational avenue being future 21 cm fluctuation surveys [45].

Many of the consistency relations derived in this work require a knowledge of the properties of the tensor power spectrum, in particular its (running) scale dependence. In this sense, some of our results may only be tested with the next generation of CMB polarization and gravitational wave detection experiments. However, current forecasts seem to suggest that unless r is sufficiently large, then any primordial gravitational waves will be obscured by foreground effects, making it extremely challenging to test these consistency relations [143]. It is clear that a better understanding of the dust and lensing which gives rise to the foreground, as well as combining analyses from the various current and future experiments will be necessary in the hunt for primordial gravitational waves.

Although our analysis has focused on a particular realization of warm inflation that has been well established in the context of quantum field theory, our results should be put in a wider perspective of an alternative paradigm where thermal or even non-thermal statistical states describe the evolution of the inflationary universe. In particular, we expect other related models to yield relations between CMB observables that can be directly tested against observational data, such as those presented in this work. Hence, we hope that our work motivates further research in this direction from both the observational and theoretical perspectives.

Chapter 7

Fluctuation-dissipation dynamics of cosmological scalar fields

Scalar fields play a major role in modern cosmological theories. Depending on the balance between the kinetic, potential and gradient energy stored in these fields, they can mimic fluids with distinct equations of state and so have been proposed as leading candidates to describe the early phase of inflationary expansion, as well as dark matter and dark energy.

Scalar fields are also a key ingredient in modern particle physics theories and the recent discovery of what is now widely accepted to be the electroweak Higgs boson at the LHC puts the existence of fundamental scalar degrees of freedom on firm experimental ground. Indeed, these are ubiquitous in extensions of the Standard Model (SM) of particle physics, such as grand unified theories, supersymmetric theories or extra-dimensional scenarios, namely within the context of string/M-theory compactifications. The study of the cosmological dynamics of scalar fields, both at the classical and quantum levels, is thus of crucial importance to understand the early history of our Universe.

One of the most prominent roles of scalar fields is the phenomenon of spontaneous symmetry breaking in fundamental gauge theories, where vector bosons and fermions acquire mass through the Bose-condensation of a scalar field. This process of spontaneous symmetry breaking sees an initial symmetric state go to a state of broken symmetry, all due to the change of a single parameter, the vacuum expectation value (vev) of a scalar field $\langle\phi\rangle$. The electroweak Higgs mechanism is the best known example of this simple idea, which is also expected to apply to the spontaneous breaking of higher-rank gauge symmetry groups that

extend the SM at high energy scales.

The significance of spontaneous symmetry breaking for cosmology was pointed out several decades ago by Kirzhnits and Linde [144]. They observed that this behavior would be a feature of quantum field theories at finite temperature, whereby at very high temperatures the vev of the scalar field would be a single value that restores symmetry and then, at some specific critical temperature, this vev would change and lead to a phase of broken symmetry. The description of this process fits well within the Landau theory of phase transitions. These two simple ideas of spontaneous symmetry breaking and its realization in finite temperature quantum field theory as a phase transition have been the foundation for cosmological phase transitions [145, 146]. Such behavior has since been applied to numerous areas in cosmology including inflation, defects, baryogenesis [147], and cosmic magnetic fields [148].

The study of cosmological phase transitions has so far been centered primarily on their equilibrium properties. In particular, most of the interest has gone into studying the particle physics features in the symmetric and broken phases. The dynamics that induces the change from one phase to the other is, however, also a necessary component of this entire process. This change will involve the motion of the order parameter $\langle\phi\rangle$ from the symmetry-restored to broken phase. Since this scalar order parameter is the expectation value of a quantum field, which in general interacts with other fields that comprise the radiation bath, its evolution between the different phases will generically involve energy exchange. Due to the tendency for the equipartion of energy in dynamical systems, this appears primarily as energy exchange between the single dynamical scalar degree of freedom and the many degrees of freedom comprising the heat bath. This thus results in dissipation of the scalar field's energy into the ambient radiation fluid.

The order parameter experiences another effect when immersed in the radiation bath. All the random interactions of the bath constituents with the single order parameter will slightly push the scalar field around in all different directions, thus inducing fluctuations. These two processes of dissipation and fluctuations of the order parameter are intrinsically related to each other by the underlying dynamical quantum mechanical equations [149]. This is the basis of fluctuation-dissipation theorems and it is applicable to the dynamics of cosmological phase transitions just as it is to any phase transitions or out-of-equlibrium situation in condensed matter systems [150, 151, 152, 153].

As such, wherever a cosmological phase transition is present, fluctuation-dissipation dynamics will be present hand- in-hand during the out-of-equilibrium transition period between the two equilibrium phases. This phase transition dynamics will add three new features to the equilibrium description. First, the background evolution of the scalar order parameter will affect the expansion behaviour of the Universe. Second, there will be particle production. Third, there will be fluctuations created in the Universe in the wake of this transition. The first feature has been examined in great detail in the cosmology literature. For the last two features, there are many quantum field theory calculations of fluctuation and/or dissipation dynamics [82, 154, 155, 156, 73, 157, 158, 159, 160, 70, 72, 73] but very little has been explicitly applied to particle physics models during cosmological phase transitions. One exception is in the case of inflation, where warm inflation, which was introduced in Chapter 4, captures all three of these features [142, 95, 89, 161, 162, 5, 11, 59, 60, 84, 163, 7]. However, cosmological phase transitions can and generically do occur with no inflation and, in these cases also, all three of these features will be present. They are an intrinsic part of the evolution history of the early Universe and the dynamics emerging from whatever is the underlying particle physics model.

Fluctuation-dissipation effects will, more generally, be present in the dynamics of any cosmological scalar field, regardless of the occurrence of phase transitions. For example, several completions of the SM predict the existence of very light scalars, such as extra-dimensional moduli or axion-like fields. These fields will be underdamped during the early inflationary phase and driven to potentially very large values by random quantum fluctuations. After inflation, once the expansion rate has decreased sufficiently, they will be able to dynamically relax to their minimum energy configuration. This may in several cases lead to large-amplitude oscillations that overclose the Universe or spoil the successful predictions of Big Bang Nucleosynthesis (BBN) for light element abundances, which poses a considerable challenge for cosmological models in beyond the SM scenarios. Interactions with other degrees of freedom in the ambient heat bath may, however, induce energy dissipation and fluctuations in these scalar fields, modifying their dynamical evolution and potentially their role in the subsequent cosmic history.

Another case where fluctuation-dissipation dynamics may be of relevance is the cosmological variation of fundamental constants driven by scalar fields.

These could include e.g. unknown scalars driving variations of the fine-structure constant, α, or even the cosmological evolution of the SM Higgs field, which determines all fermion masses and in particular the electron-proton mass ratio $m_{\rm e}/m_{\rm P}$ (see e.g. [164]). In the latter case dissipation could delay the electroweak phase transition, as we will discuss in this work for generic phase transitions, and potentially yield temporal variations of the electron-proton mass ratio $m_{\rm e}/m_{\rm P}$. Additionally, the associated fluctuations will also induce spatial variations of this ratio, which depending on their size and scale could in principle lead to observable effects.

This fluctuation-dissipation dynamics is not specific to near thermal equilibrium conditions. Whatever the statistical state is, a relation exists between the dissipation produced by the system and the fluctuations induced by the radiation bath. The near thermal equilibrium regime is, however, amenable to explicit calculations using well developed thermal field theory methods and will be the focus of this chapter. The early Universe is generally believed to be in a near thermal equilibrium state and so these calculations based on thermal field theory have significant relevance to it. Nevertheless, there could be processes in the early cosmic stages where a scalar field moves too quickly or the underlying microphysical processes are too slow to justify a near thermal equilibrium approximation. Thus it should be kept in mind that the calculations done in this chapter could also be extended to these regimes; it would be a technical, albeit complicated, step further, but the underlying concept is the same as developed in this chapter.

It is the goal of this work to set the stage for the study of cosmological fluctuation-dissipation dynamics within concrete particle physics models. We will discuss different examples of dissipation (and related noise) coefficients within the SM and beyond, exploring their distinct parametric regimes and domains of applicability. We will then outline some of the generic consequences of dissipation, particle production and induced fluctuations in the dynamics of cosmological scalar fields, both with and without the occurrence of phase transitions. We will focus on the post-inflationary dynamics, where the effects of fluctuation-dissipation dynamics remain largely unexplored, there existing already a considerable literature devoted to this topic in inflationary cosmology in the context of warm inflation dynamics.

To better illustrate the cosmological impact of these processes, we will analyze

in detail two concrete scenarios. Firstly, we will consider a high-temperature phase transition in the early Universe, where the associated Higgs field can dissipate its energy into fermionic modes through standard Yukawa interactions. In particular, we will show that, by slowing down the field's motion, dissipation will delay the phase transition, leading to additional entropy production and Hubble expansion that can dilute the abundance of dangerous relics such as topological defects. Furthermore, if the transition is sufficiently delayed, the Higgs field may come to dominate the energy balance and yield an additional (short) period of inflationary expansion. This results in a more efficient dilution of thermal relics, similarly to thermal inflation models, although dissipative friction can sustain accelerated expansion below the temperatures at which thermal effects can hold the Higgs field in the symmetric phase. Both thermal and dissipative (warm) inflation are, in fact, due to the same interactions between the Higgs field and the thermal bath degrees of freedom and may occur within the same cosmological phase transition, as we show in this work.

Secondly, we will consider the relaxation of a scalar field from a large post-inflationary value to its minimum energy configuration. We will show that its coupling to a B- or L-violating sector can lead to the dissipative production of a baryon or lepton asymmetry, respectively, in the spirit of the *warm baryogenesis* scenario proposed in [26] in the inflationary context. To illustrate this generic mechanism, we develop a concrete model of *dissipative leptogenesis*, where dissipation results from the excitation and decay of heavy right-handed neutrinos, which gain a large Majorana mass from the coupling to a dynamical scalar field. As opposed to standard leptogenesis and other thermal baryogenesis scenarios, these are mainly produced off-shell, which allows for baryogenesis at parametrically low temperatures and therefore avoids the troublesome overproduction of thermal relics.

These two examples show that dissipative effects can have an important role in the cosmic history, particularly in addressing some of the most important puzzles in modern cosmology. We therefore hope that they motivate a more thorough exploration of this topic and of more general non-equilibrium processes in cosmology.

This work is organized as follows. In Section 7.1 and 7.2 we show examples of how dissipation arises within common particle physics models, focusing in particular on the electroweak phase transition and Grand Unified Theories. In

Section 7.3 we describe the effects of fluctuation-dissipation dynamics in high-temperature phase transitions. In Section 7.4 we describe the post-inflationary production of a baryon asymmetry through dissipative effects, describing in detail the *dissipative leptogenesis* scenario and its observational signatures. We summarize our main results and conclusions in Section 7.5, also discussing prospects for future research in this area.

7.1 Dissipation in the SM and supersymmetric extensions

The SM gauge group, $SU(3)_c \times SU(2)_L \times U(1)_Y$, is broken spontaneously to $SU(3)_c \times U(1)_Q$ by the non-vanishing vacuum expectation value of the electroweak Higgs boson. In typical cosmological scenarios, the reheating temperature after inflation largely exceeds the critical temperature of the electroweak phase transition. Quarks, leptons and electroweak gauge bosons are relativistic and in thermal equilibrium, and their backreaction on the Higgs effective potential at high temperatures stabilizes the Higgs field at the symmetric minimum. As the Universe cools down, the effective potential approaches its zero temperature form and the Higgs field will roll towards the finite vev that spontaneously breaks the electroweak symmetry. As the field rolls from the origin towards the broken minimum, we then expect dissipative processes to be mainly mediated by on-shell quarks and leptons, as well as the weak gauge bosons. The former, in particular, have the following well-known Yukawa couplings to the Higgs field:

$$\mathcal{L} \sim \lambda_e^{ij} \bar{e}_{R,i} \phi^\dagger L_j + \lambda_u^{ij} \bar{u}_{R,i} \phi q_j + \lambda_d^{ij} \bar{d}_{R,i} \phi^\dagger q_j + \text{h.c.} \tag{7.1}$$

where we have suppressed weak isospin and color indices, while the indices i, j label the fermion generations. At high temperatures, the decay width of quarks and leptons is given essentially by Landau damping terms from the above Yukawa interactions, as well as gauge interactions [165]. The relevant dissipation coefficient is thus of the on-shell form given in Eq. (4.13). Including both Yukawa

and gauge contributions to the fermions' decay width we obtain:

$$\Upsilon^{\rm P}_{\rm SM} \simeq \frac{288\zeta(3)T}{\pi^3}\sum_{i=1}^{3}\left(\frac{(\lambda_e^{ii})^2}{(\lambda_e^{ii})^2+4(g_1^2+3g_2^2)}+\frac{3(\lambda_u^{ii})^2}{(\lambda_u^{ii})^2+4(g_1^2+3g_2^2+8g_3^2)}\right.$$
$$\left.+\frac{3(\lambda_d^{ii})^2}{(\lambda_d^{ii})^2+4(g_1^2+3g_2^2+8g_3^2)}\right), \tag{7.2}$$

where g_i are the SM gauge couplings. We note that dissipation can also occur through the excitation of the $W^{\pm}$ and Z gauge fields, although for simplicity we do not include this in the above expression. As ϕ increases and T decreases eventually the masses of the SM particles will become heavier than the temperature and their on-shell contribution to dissipation becomes Boltzmann suppressed, with low-momentum dissipation of the form in Eq. (4.12) becoming the dominant contribution.

Another example based on the same symmetry group arises within the minimal supersymmetric extension of the SM (MSSM), where two Higgs doublets are required to break the electroweak symmetry and give masses to all quarks and leptons. The MSSM superpotential is given by:

$$W = \mu H_u H_d + y_u H_u Q U^c + y_d H_d Q D^c + y_e H_d L E^c \ . \tag{7.3}$$

As in the SM, in this case one finds dissipative channels for both Higgs scalar components, h_u and h_d, by exciting both fermion and sfermion degrees of freedom in the heat bath. At high temperatures these will have the forms $\Upsilon \propto \phi^2/T$ and $\Upsilon \propto T$ obtained above for sfermions and fermions, respectively, with $\phi = h_u, h_d$ (see also [166]).

The simplest extension of the MSSM, known as the next-to-minimal supersymmetric SM (NMSSM), replaces the μ-term in the superpotential by a trilinear term $g\Phi H_u H_d$, where Φ is a singlet chiral superfield. The effective μ-term is then given by the vev of the scalar component of Φ, a possibility that helps addressing the smallness of the *a priori* unconstrained μ parameter required for successful electroweak symmetry breaking (see e.g. [167]). One can then envisage scenarios where the singlet scalar field, ϕ, is driven towards (or maintained at) a large value during inflation, after which it will roll towards $\langle\phi\rangle = \mu/g$. Its coupling to both

Higgs scalar doublets h_u and h_d is of the form given in Eq. (4.9) and explicitly:

$$\mathcal{L}_{\rm S} = g^2|\phi|^2(|h_d|^2+|h_u|^2) + g\phi^\dagger h_d^\dagger\, y_u^{ij}\tilde{q}_i\tilde{u}_j^c + g\phi^\dagger\, h_u^\dagger(y_d^{ij}\tilde{q}_i\tilde{d}_j^c + y_e^{ij}\,\tilde{l}_i\tilde{e}_j^c) + \text{h.c.}\ , \quad (7.4)$$

so that the singlet field can dissipate its energy through excitation of both scalar doublet components and their fermionic superpartners, which decay into the SM fermions and sfermions. If the initial field value is large, the dominant contribution to the dissipation coefficient is given by off-shell scalar modes as discussed above and the dissipation coefficient is approximately given by:

$$\Upsilon^{\rm LM}_{\rm NMSSM} \simeq C_\phi \frac{T^3}{\phi^2}, \qquad C_\phi \simeq \frac{1}{8\pi}\sum_{ij}\left(3(y_u^{ij})^2 + 3(y_d^{ij})^2 + (y_e^{ij})^2\right)\ , \quad (7.5)$$

where i, j run over family indices.

7.2 Dissipation in Grand Unified Theories: an $SU(5)$ example

There is significant evidence for the unification of the SM gauge couplings at high energy scales, particularly within the context of the MSSM [168, 169, 170, 171], which points towards the existence of a larger gauge symmetry group. Several Grand Unified Theories (GUT) have been proposed where this gauge group is spontaneously broken into the SM gauge group through a Higgs-like mechanism, with $SU(5)$ and $SO(10)$ being the simplest and most studied examples (see e.g. [172]). In GUT models the relevant Higgs fields are coupled to gauge bosons and matter fields, such that fluctuation-dissipation dynamics may play an important role in their cosmological evolution.

If GUT symmetries are restored after inflation, for a sufficiently high reheating temperature, the Higgs fields roll from the symmetric point to the symmetry breaking minimum once the temperature drops below a critical value. This may be preceded by a tunneling event if the transition is first order, depending on the particle content of the GUT model [145], but dissipative rolling will always occur. This scenario may, however, be troublesome for cosmology since symmetry breaking typically leads to the generation of dangerous topological defects such as monopoles, which may overclose the Universe. Although post-inflationary

symmetry restoration is appealing from the point of view of thermal GUT baryogenesis models, there are viable alternative mechanisms for the production of a cosmological baryon asymmetry such as the *dissipative baryo/leptogenesis* mechanism that we describe in Section 7.4.

In the case where GUT symmetries are not restored during reheating, the relevant Higgs fields may nevertheless find themselves displaced from the symmetry breaking minimum after inflation. This occurs if the Higgs fields are light during inflation, being frozen at some initial value or even driven to larger values by random quantum fluctuations. In addition, if the Higgs field couples to the inflaton then it will acquire a Hubble scale mass which can drive it to a minimum during inflation which is distinct from its low energy minimum. Dissipation will then also be relevant in the post-inflationary eras as the fields roll towards the true minimum of their potential.

To illustrate the form of dissipative effects in GUT models, we consider the simplest case of $SU(5)$, bearing in mind that similar processes will generically occur for higher-rank gauge groups where many other dynamical scalars and dissipative channels may be present. In fact, in Section IV we will consider the particular example of a scalar field responsible for the Majorana mass of right-handed neutrinos and which is naturally embedded in $SO(10)$ models.

$SU(5)$ is broken into the SM gauge group by the vev of an adjoint Higgs field, 24_H, which gives masses to the gauge and fundamental Higgs field components that are associated with the broken symmetries. The adjoint scalar potential takes the form:

$$V(24_H) = -\mu^2 \mathrm{Tr}[24_H^2] + a\mathrm{Tr}[24_H^2]^2 + b\mathrm{Tr}[24_H^4] + c\mathrm{Tr}[24_H^3] \ , \tag{7.6}$$

which, in certain parametric regimes, has an absolute minimum in the direction $\phi\,\mathrm{diag}(2,2,2,-3,-3)/\sqrt{30}$ that preserves the SM gauge group. Interactions between the adjoint and fundamental Higgs fields are given by:

$$\begin{aligned} \mathcal{L}_{\rm S} &= -\frac{A^2}{2} 5_H^\dagger 5_H + \frac{B}{4}(5_H^\dagger 5_H)^2 + C\, 5_H^\dagger 5_H \mathrm{Tr}[24_H^2] + D\, 5_H^\dagger 24_H^2 5_H \\ &+ E\, 5_H^\dagger 24_H 5_H \ , \end{aligned} \tag{7.7}$$

while the latter is coupled to the SM matter fermions in the 10 and $\bar{5}$

representations via Yukawa couplings of the form:

$$\mathcal{L}_{\rm Y} = Y_5^{ij}\bar{5}_{Fi}10_{Fj}5_H^* + \frac{1}{8}\epsilon_5 Y_{10}^{ij}10_{Fi}10_{Fj}5_H + \text{h.c.} \tag{7.8}$$

Decomposing these fields in terms of SM representations we find the following interaction Lagrangian involving the symmetry breaking scalar direction ϕ, the doublet and triplet Higgs fields, H and T, and the SM quarks and leptons:

$$\begin{aligned}
\mathcal{L}_{\rm int} &= \left(-\frac{A^2}{2} + \frac{2E}{\sqrt{30}}\phi + \frac{2D}{15}\phi^2 + C\phi^2\right)|T|^2 \\
&+ \left(-\frac{A^2}{2} - \frac{3E}{\sqrt{30}}\phi + \frac{3D}{10}\phi^2 + C\phi^2\right)|H|^2 \\
&- Y_5^{ij}(l_i q_j + d_i^c u_j^c)T^* - Y_{10}^{ij}\left(\frac{1}{2}q_i q_j + u_i^c e_j^c\right)T + Y_5^{ij}(L_i e_j^c + q_i d_j^c)H^* \\
&- Y_{10}^{ij} q_i u_j^c H + \text{h.c.}
\end{aligned} \tag{7.9}$$

As discussed above there are also gauge interactions, but for illustrative purposes we will restrict ourselves to dissipative effects associated with the scalar and Yukawa interactions given above. Let us consider, in particular, the case where ϕ has a large vev after inflation that is displaced from its true minimum. The leading C-terms in Eq. (7.9) give a large mass to the Higgs doublet and triplet, which are initially equal due to the large field vev, while a doublet-triplet mass splitting will only arise close to the minimum. These terms are of the generic form given in Eq. (4.9) for $\chi = H, T$ and we expect the main contribution to dissipation in this regime to correspond to the excitation of virtual Higgs modes which then decay into quarks and leptons. From Eq. (4.12) and the functional form of the dissipative coefficient calculated in [80], we then obtain the following dissipation coefficient:

$$\Upsilon_{SU(5)}^{\rm LM} \simeq \frac{0.44}{C^2}\frac{T^7}{\phi^6}\sum_{i,j}\left[10(Y_5^{ij})^4 + 8(Y_{10}^{ij})^4\right] \ . \tag{7.10}$$

In a supersymmetric realization of $SU(5)$ the SM fermions have scalar superpartners and, due to the holomorphic nature of the superpotential, two distinct Higgs fields in the 5 and $\bar{5}$ representation are required. The relevant part of the

superpotential is given by:

$$W = g\bar{5}_H 24_H 5_H + M\bar{5}_H 5_H + Y_5^{ij}\bar{5}_{F\,i}10_{F\,j}\bar{5}_H + \frac{1}{8}\epsilon_5 Y_{10}^{ij}10_{F\,i}10_{F\,j}5_H \ , \qquad (7.11)$$

where the relevant scalar interactions are:

$$\begin{aligned}\mathcal{L}_{\rm S} &= Y_5^{ij}\left(\frac{2g\phi}{\sqrt{30}}+M\right)\tilde{t_u}^\dagger(\tilde{d}_i^c\tilde{u}_j^c-\tilde{l}_i\tilde{q}_j)+Y_{10}^{ij}\left(\frac{2g\phi}{\sqrt{30}}+M\right)\tilde{t_d}^\dagger\left(\tilde{e}_i^c\tilde{u}_j^c+\frac{1}{2}\tilde{q}_i\tilde{q}_j\right)\\ &+ Y_{10}^{ij}\left(M-\frac{3g\phi}{\sqrt{30}}\right)\tilde{h}_d^\dagger\tilde{q}_i\tilde{u}_j^c+Y_5^{ij}\left(M-\frac{3g\phi}{\sqrt{30}}\right)\tilde{h}_u^\dagger(\tilde{l}_i\tilde{e}_j^c+\tilde{q}_i\tilde{d}_j^c)+\text{h.c.} \qquad (7.12)\end{aligned}$$

As in the non-SUSY model, the low-temperature regime for dissipation will be the relevant one after inflation if ϕ attains a large vev, $g\phi \gg M$, and the GUT symmetry is not restored. Dissipation is in this case dominantly mediated by virtual scalar doublet and triplet Higgs modes that decay mainly into sfermion fields, as shown in [80] for generic SUSY models of this form. The dissipation coefficient is then given by:

$$\Upsilon^{\rm LM}_{SSU(5)} \simeq \frac{1}{16\pi}\frac{T^3}{\phi^2}\sum_{i,j}\left[10(Y_5^{ij})^2+8(Y_{10}^{ij})^2\right] \ . \qquad (7.13)$$

Note that dissipative effects will be more pronounced in this case compared to the non-SUSY model, since the dissipation coefficient is less suppressed by powers of T/m_χ, where χ generically denotes the doublet and triplet Higgs scalars involved.

7.3 Fluctuation - dissipation dynamics in cosmological phase transitions

Despite the numerous studies in the context of condensed matter systems, the dynamics of phase transitions in fundamental particle physics and cosmology remains largely unexplored. The recent discovery of the Higgs boson at the LHC, so far consistent with the SM predictions for the spontaneous breaking of the electroweak gauge symmetry, is the first experimental hint for the occurrence of a fundamental phase transition in the cosmic history and motivates further exploration of this topic. Moreover, the apparent unification of gauge couplings suggests, as discussed above, that one or more phase transitions may have occurred in the early stages of the Universe's history, spontaneously breaking a

higher-ranked gauge group into $SU(3)_c \times SU(2)_L \times U(1)_Y$, in potentially several stages of a progressively lower degree of symmetry.

Cosmological Higgs fields are coupled to matter fields and gauge bosons, and the effects of dissipation and associated fluctuations will necessarily play a role in the evolution of the fields from a symmetric to a spontaneously broken symmetry phase. In this section, we will discuss several potential effects of fluctuation-dissipation dynamics in generic cosmological phase transitions.

7.3.1 Thermal fluctuations and topological defects

The cosmological evolution of a generic Higgs field in the process of spontaneous symmetry breaking follows a Langevin-like equation of the form Eq. (4.6), with both the noise term on the right-hand side and the dissipative friction term on the left-handed side playing an important role at different dynamical stages. Fluctuations will be primarily significant at the onset of the phase transition, just below the critical temperature at which the symmetric Higgs value can no longer be stabilized by thermal effects. In particular, in the absence of random fluctuations the field would remain at the unstable symmetric minimum, since this is nevertheless an extremum of the effective potential. The noise term in the Langevin-like equation is thus crucial in inducing the phase transition and in determining the direction within the vacuum manifold towards which the field's evolution will proceed.

Since the Higgs field is, on average, at rest at the onset of the phase transition, its dynamics will be initially governed by the gaussian and white noise term in the adiabatic regime. As discussed earlier, the stochastic noise term encodes the effective backreaction of the ambient heat bath, also incorporating the inherent quantum nature of the field. On the one hand, the backreaction of the heat bath is directly related to the dissipation coefficient through the fluctuation-dissipation theorem and given by the term proportional to Υ in the noise correlator Eq. (4.7). On the other hand, the remaining quantum noise term, proportional to the Hubble parameter H, can be deduced from a coarse-graining of the quantum Higgs field, with short wavelength modes that are well within the Hubble horizon backreacting on the longer wavelength modes that one is interested in following. This stochastic approach has e.g. been successful in describing field fluctuations in both warm and cold inflation regimes [61].

The phase transition will then initially be driven by the quantum and thermal/dissipative noise terms, which randomly kick the Higgs field away from and towards the symmetric minimum. This will proceed until the amplitude of the noise term becomes sub-dominant compared to the "classical" terms in the equation of motion (see Eq. (4.6) and (4.7)), i.e. roughly when $\sqrt{\Upsilon T} \lesssim V'(\phi)/H^2$ for strong dissipation. Random fluctuations will then effectively cease and the subsequent field dynamics will essentially be classical. However, the field is now spatially inhomogeneous and the classical evolution will drive it to different directions in the vacuum manifold at distinct spacetime points. The classical dynamics can nevertheless homogenize the field within causally connected patches, determined by the field's correlation length, ξ_c, that is at most the size of the cosmological horizon. If the Higgs field is relativistic at this stage, $\xi_c \sim 1/T \ll H^{-1}$, and so the temperature at which the noise term becomes inefficient will set the size and consequently the abundance of any topological defects that may form once the field settles into the lowest energy configuration. Some preliminary studies for the formation of topological defects in phase transitions including the effects of both thermal noise and dissipation have been performed in [173, 174, 175]. It would be interesting to further explore this in the context of the concrete particle physics models discussed above and within realistic cosmological settings. This is, however, beyond the scope of the present work, where we will focus on the dissipative classical evolution.

One other related consequence of the noise term should nevertheless be pointed out. The inhomogeneity of the Higgs field resulting from its initial random motion will also induce a spatial variation of its gauge quantum numbers, generically sourcing magnetic fields [148, 176]. Their strength will then also be determined by the correlation length at the time when the noise term becomes inefficient and, if sufficiently large, this may sow the seeds for galactic magnetic fields.

Although here we will not pursue these issues in further detail, it is worth emphasizing that the Langevin-like equation Eq. (4.6) gives a fundamental framework for these studies. Given a particle physics model, one can compute the dissipation coefficient and associated noise term from first principles, as explicitly done in the previous section for several examples, and use this equation to determine both the quantum and classical dynamics. This allows one to determine the correlation length, the density of topological defects or the strength of generated magnetic fields in a rigorous way. In this way, there is no need

to simply employ statistical arguments to derive these quantities and the field evolution can be completely determined for arbitrary initial conditions.

7.3.2 Dissipative effects: entropy production and additional inflation

Once the effects of the thermal and quantum noises become sub-dominant, the field's evolution becomes classical and is driven by the competition between the scalar potential's slope and the effects of dissipative and Hubble friction. To analyze the concrete effects of dissipation, which have so far been overlooked in the literature and, as we will show, may play an important role, we will consider a generic toy model where a real Higgs field is coupled to fermions through standard Yukawa couplings of the form in Eq. (4.9). This can be easily extended to concrete particle physics models such as the electroweak phase transition or GUT phase transitions by considering the appropriate couplings, particle content and the properties of the vacuum manifold, as illustrated in the previous section.

The fermions induce, as discussed before, both local and non-local corrections to the effective action of the Higgs field. The leading effect of the former are finite temperature corrections to the effective potential, with zero-temperature corrections playing a sub-dominant role that we will for simplicity discard in our analysis. Thermal corrections are significant for relativistic fermions, $m_\psi \ll T$, namely inducing a thermal mass for the Higgs field, while for $m_\psi \gtrsim T$ these corrections are Boltzmann-suppressed and thus irrelevant to the dynamics. The general form of the thermal mass can be obtained by numerical integration, but for our purposes it is sufficiently accurate to explicitly multiply the high-temperature result by a Boltzmann factor (see Appendix A for the full form of the thermal correction), yielding for the effective Higgs potential:

$$V(\phi, T) = \frac{\lambda^2}{4}(\phi^2 - v^2)^2 + \frac{1}{2}\alpha^2 T^2 \phi^2 \exp\left(-\frac{m_{\psi,T}}{T}\right) , \tag{7.14}$$

where $\alpha^2 = g^2 N_{\rm F}/6$, with $N_{\rm F}$ denoting the number of Dirac fermion species. In this expression, the first term corresponds to the simplest symmetry-breaking potential with minima at $\phi = \pm v$ and the second term is the leading thermal correction. In the fermion mass $m^2_{\psi,T} = g^2\phi^2 + h^2T^2$ we also include thermal corrections from coupling to different species in the heat bath, including e.g. gauge

fields, and which we generically parametrize with an effective coupling $h \lesssim 1$. At high temperatures, the second term dominates the effective potential and the Higgs field is thus stabilized at the origin, with $m_{\psi,T} \simeq hT \lesssim T$, while at low temperatures it will roll towards one of the minima at $\phi = \pm v$. The symmetric minimum becomes unstable at a critical temperature:

$$T_{\rm c} = \frac{\lambda v}{\alpha}. \tag{7.15}$$

As soon as the field begins rolling towards the symmetry breaking minimum, it will feel the friction effect of the fermion heat bath. The relevant dissipation coefficient corresponds to the on-shell excitation of light fermions with a thermal decay width and was first computed in [71], yielding:

$$\Upsilon \simeq 11.2 N_{\rm F} T \exp\left(-\frac{m_{\psi,T}}{T}\right) \ . \tag{7.16}$$

Note that, as above, we have multiplied the high-temperature result by a Boltzmann factor which will cut-off on-shell dissipation at low temperatures, $T \lesssim g\phi$, which is sufficiently accurate for our purposes. As we have seen above, virtual modes will also induce dissipation in the latter regime, but since this is a significantly smaller effect we will discard it in our analysis to a first approximation. Also notice that the SM high-temperature dissipation coefficient given in Eq. (7.2) coincides with this expression if one discards gauge interactions. The thermal width of the fermions is roughly given by $\Gamma_\psi \sim m^2_{\psi,T}/T \lesssim T$, and adiabaticity of the dissipative process requires $\Gamma_\psi \gtrsim H$, which is easily satisfied in the radiation-dominated era, where $H \simeq \sqrt{\pi^2/90} g_*^{1/2} T^2/m_{\rm p} \ll T$. For simplicity, we will assume that the radiation bath is made exclusively of fermions, taking $g_* = 7N_{\rm F}/4$, although one can easily include other relativistic degrees of freedom. This will allow us to see the interplay between dissipation and the thermal corrections more clearly as both arise from the coupling to fermions, including gauge fields in g_* will not change our results significantly.

With the form of the effective potential and dissipation coefficient, we may thus describe the dynamics of the phase transition by solving the system of coupled Higgs-radiation equations, given by:

$$\ddot{\phi} + (3H + \Upsilon)\dot{\phi} + V'(\phi) \simeq 0 \ , \qquad \dot{\rho}_{\rm R} + 4H\rho_{\rm R} = \Upsilon \dot{\phi}^2 \ , \tag{7.17}$$

where as discussed above we neglect the effects of the noise term, and $\rho_{\rm R} = (\pi^2/30) g_* T^4$ assuming a nearly-thermal equilibrium state. Dissipation thus plays two distinct roles in the dynamics, on the one hand damping the field's motion and, on the other hand, sourcing the radiation bath through the production of fermion modes.

If the energy density in the scalar field is sufficiently large, it may come to dominate the energy density before the Universe cools down to below the critical temperature. This occurs for $g^2 N_{\rm F} \gtrsim 2\pi\sqrt{g_*}\lambda$, thus inducing a period of *thermal inflation* along the lines proposed in [177] and which may help dilute the abundance of dangerous thermal relics produced e.g. during reheating or earlier cosmological phase transitions. This additional period of inflation can typically last only for a few e-folds until the critical temperature is reached, with the field then rolling towards the symmetry-breaking minimum and oscillating about it.

In the presence of dissipation, the dynamics can be quite different below the critical temperature and an interesting alternative/addition to thermal inflation arises. Firstly, we note that in the radiation era $\Upsilon \gtrsim T \gg H$ and so the main source of friction is dissipation into fermionic modes rather than Hubble expansion. The field's motion will then be overdamped for $\Upsilon \gtrsim |m_\phi|$, where $m_\phi^2 = V''(\phi)$, and underdamped otherwise. For relativistic fermions, close to the origin we have $m_\phi^2 \simeq \alpha^2(T^2 - T_{\rm c}^2)$, while for $\phi = \pm v$ the field mass is $m_\phi^2 = \alpha^2(2T_{\rm c}^2 + T^2)$. This means that the field's trajectory from the symmetric to the symmetry-breaking minimum will be overdamped if during the transition the temperature is above $0.05 g T_{\rm c}/\sqrt{N_{\rm F}}$, which is parametrically below the critical value. This implies that instead of oscillating about $\phi = \pm v$, the field will smoothly evolve towards this value. When the motion is overdamped, the scalar field equation reduces to a slow-roll equation of the form:

$$3H(1+Q)\dot{\phi} \simeq -V'(\phi) \ , \tag{7.18}$$

where $Q \equiv \Upsilon/3H$, such that in the radiation era $Q \sim 8.5\sqrt{N_{\rm F}} m_{\rm p}/T \gg 1$ as argued above and the field's evolution occurs in a strong dissipation regime. Furthermore, the field may remain close to the origin and mimic a cosmological constant if its energy density does not vary significantly within a Hubble time:

$$\frac{1}{H}\frac{\dot{\rho}_\phi}{\rho_\phi} \simeq -3(1+Q)\frac{\dot{\phi}^2}{V} \simeq -2\frac{\Omega_\phi \epsilon_\phi}{1+Q} \ll 1 \ , \tag{7.19}$$

where $\epsilon_\phi = (m_\mathrm{p}^2/2)(V'(\phi)/V(\phi))^2$ is the slow-roll parameter typically considered in slow-roll inflationary models and $\Omega_\phi = \rho_\phi/\rho_\mathrm{total}$ is the Higgs field relative abundance. This condition essentially ensures that the Higgs field does not dissipate a significant fraction of its energy density into the heat bath on cosmological time scales, thus sustaining a cosmological constant-like behavior for small kinetic energy. Note also that the condition above reduces to the slow-roll condition $\epsilon_\phi \ll 1$ in non-dissipative (cold) inflationary models, where the scalar field is the dominant component, and to the slow-roll condition $\epsilon_\phi \ll 1 + Q$ in dissipative (warm) inflation scenarios. It moreover shows that a constant energy density is easier to maintain when the field is subdominant, $\Omega_\phi < 1$.

Close to the origin we find $\epsilon_\phi \simeq 8(m_\mathrm{p}/v)^2(\phi/v)^2$, which can be small if the field is very close to the origin. Inflation is, however, hard to maintain in the absence of dissipation with this type of "hill-top" potential since the curvature parameter $\eta_\phi = m_\mathrm{p}^2 V''/V \simeq -4m_\mathrm{p}^2/v^2$ is too large unless $v \gtrsim m_\mathrm{p}$. Dissipation into the heat bath alleviates this constraint by overdamping the field's motion as shown above. As first shown in [71, 178], it is hard to obtain a very long period of inflation with the dissipation coefficient in Eq. (7.16), in particular the 50-60 e-folds required to solve the horizon and flatness problems, since the fermion mass increases as the field moves towards the minimum and eventually dissipation becomes Boltzmann-suppressed. We note, however, that for supersymmetric models in the low-temperature regime, where dissipation is dominantly mediated by low-momentum scalar field modes, fully successful models of warm inflation have been developed (see e.g. [81, 84, 80, 142]). In such scenarios dissipation can sustain both the slow-roll dynamics of the inflaton field and the temperature of the radiation bath for a sufficiently long period. Nevertheless, the dissipation coefficient in Eq. (7.16) can sufficiently overdamp the field's motion to allow for a few e-folds of inflation which, analogously to thermal inflation, can dilute dangerous relics generated prior to the phase transition. The slow-roll equation Eq. (7.18) can be solved when the field is close to the origin in a radiation-dominated Universe, yielding:

$$\phi \propto \exp\left[\frac{0.1\alpha^2}{N_\mathrm{F}^{3/2}}\frac{m_\mathrm{p}}{T}\left(\left(\frac{T_\mathrm{c}}{T}\right)^2 - 3\right)\right] , \tag{7.20}$$

so that the field increases exponentially below the critical temperature. Since $\epsilon_\phi\Omega_\phi/Q \propto \phi^2/T^3$ in this case, slow-roll can only be maintained for a finite

period of time. The Higgs field may become dominant at a temperature $T_\phi \simeq g_*^{-1/4}\alpha T_c/\sqrt{\lambda}$, so if the scalar self-coupling is sufficiently small the field will overcome the radiation before the end of the slow-roll regime and induce a period of inflation. In Figure 7.1 we show a numerical example of a phase transition close to the GUT scale where a short period of inflationary expansion occurs.

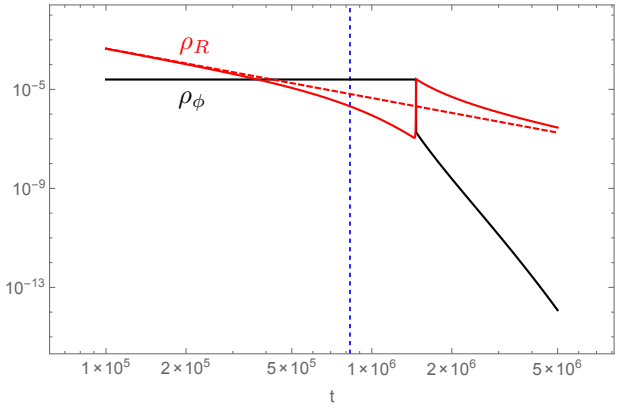

Figure 7.1: Evolution of the field and radiation energy density during a phase transition (solid lines), for a case where the field comes to dominate the energy density. The dashed red line shows the evolution of the radiation energy density in the absence of a phase transition. In this example, $\lambda = 0.01$, $N_{\rm F} = 10$, $v = 10^{15}$GeV, $g^2 = 1/N_{\rm F}$ and $h = 0.1$. Time here is shown in units of the scale 10^{15} GeV. The vertical dashed line indicates the time when the critical temperature is reached.

It is clear in this figure that the field's motion is always overdamped, exhibiting no field oscillation, even though slow-roll is only maintained for a finite period, with inflation lasting in this example for ~ 1.5 e-folds. The field then evolves quickly to the symmetry-breaking minimum, which is actually time-dependent until the field's thermal mass becomes exponentially suppressed. We note that this transition is fast in terms of the cosmological Hubble time, although still adiabatic from the microphysical perspective. We emphasize that dissipation prevents the field from oscillating about the minimum, as opposed to what is commonly considered in phase transitions when this effect is not taken into account. Therefore, in the presence of dissipation, the Higgs field will not behave as pressureless matter after the phase transition.

During the Higgs-dominated phase, the radiation density is diluted exponentially by the accelerated expansion until the end of the slow-roll regime. With

the increase in the field's velocity, the dissipative source term in the radiation evolution equation Eq. (7.17) grows substantially, allowing radiation to once more become the dominant component. We note that in warm inflation models where 50-60 e-folds of inflationary expansion can be sustained, generically in the low-T rather than the high-T regime considered here, $\rho_{\rm R}$ typically reaches a quasi-steady evolution with the dissipative source term balancing the Hubble dilution effect. In the example shown above, inflation does not last sufficiently long for this quasi-equilibrium to be reached, with first dilution and then dissipation playing a dominant role in the radiation evolution.

A crucial point to emphasize is that the expansion history can be significantly modified even if inflation does not occur, i.e. in parametric regimes where slow-roll cannot be sustained until the field can dominate. On the one hand, when the field is slowly rolling, its energy density increases the expansion rate, therefore diluting the ambient radiation more quickly even if it is sub-dominant. On the other hand, once slow-roll is over and the field quickly settles into the symmetry-breaking minimum, it can dissipate a significant part of its energy density into the heat bath. This is illustrated in Figure 7.2, where slow-roll ends just before the scalar field's abundance becomes comparable to the heat bath.

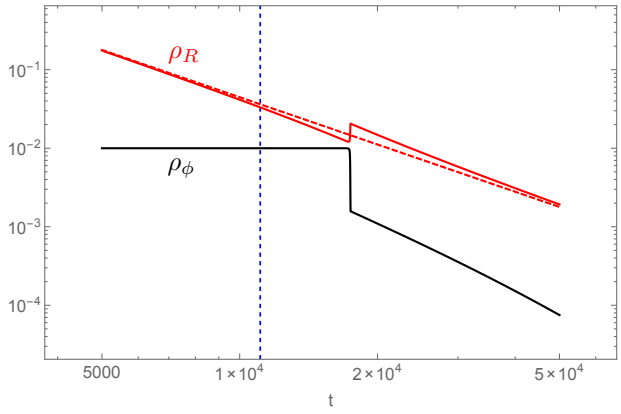

Figure 7.2: Evolution of the field and radiation energy density during a phase transition (solid lines), for a case where the field never dominates the energy density. The dashed red line shows the evolution of the radiation energy density in the absence of a phase transition. In this example, $\lambda = 0.2$, $N_{\rm F} = 1$, $v = 10^{15}$ GeV, $g^2 = 1/N_{\rm F}$ and $h = 0.1$. Time here is shown in units of the scale 10^{15} GeV. The vertical dashed line indicates the time when the critical temperature is reached.

This figure clearly shows that the most significant effects occur at the end

of the slow-roll regime, when the Higgs field's relative abundance is maximal, leading first to a dilution and then to an increase in the radiation energy density. The latter eventually relaxes to the value it would have in the absence of a phase transition, since the relation $\rho_{\rm R}(t)$ is an attractor of the Friedmann equation in a radiation-dominated Universe. One can solve the equation of motion for radiation in the absence of a dissipative source to find:

$$\rho_{\rm R}(t) = \frac{3m_{\rm p}^2}{4t^2}\left[1+\frac{1}{t}\left(\frac{\sqrt{3}m_{\rm p}}{2\rho_{\rm R_0}^{1/2}}-t_0\right)\right]^{-2} . \tag{7.21}$$

At sufficiently large t the radiation becomes insensitive to its initial value and shows an attractor behaviour tending towards $\rho_{\rm R}(t) = 3m_{\rm p}^2/4t^2$. This explains why the radiation approaches the standard evolution given by the dotted red line in Figs. 7.1 and 7.2 at late times after dissipation (particle production) becomes irrelevant. However, the increase in the Hubble parameter during the phase transition makes the Universe expand by a larger factor than in the standard radiation domination scenario. In Figure 7.3 we show the evolution of the Hubble parameter and radiation energy density relative to a standard radiation-dominated Universe, for different numbers of fermion species. As one can easily conclude, increasing $N_{\rm F}$ enhances the effect of dissipation and the relative change of H and $\rho_{\rm R}$.

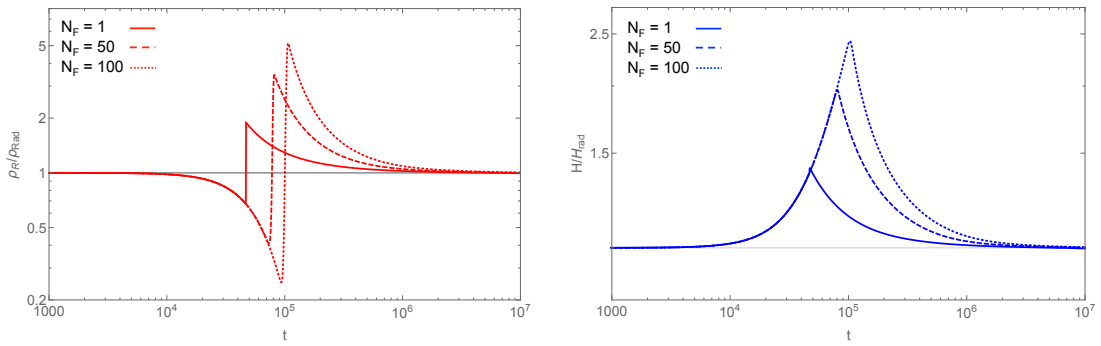

Figure 7.3: In the left (right) hand plot we show the evolution of the radiation energy density (Hubble parameter) compared to that of a standard radiation dominated Universe. In this example, $\lambda = 0.1$, $v = 10^{15}$ GeV, $g^2 = 1/N_{\rm F}$ and $h^2 = 0.1$, Time here is shown in units of the scale, 10^{15} GeV.

The additional expansion will have a diluting effect on any decoupled particle species, for which the number density redshifts as $n \propto a^{-3}$. This includes

e.g. topological relics such as monopoles or thermal relics such as gravitinos generated prior to the phase transition. Considering an initial time t_i before the critical temperature is reached and a final time t_f after the field has settled into the symmetry breaking minimum, we have for a generic decoupled species:

$$n_f = n_i \exp\left[-3\int_{t_i}^{t_f} H dt'\right] . \tag{7.22}$$

Assuming no changes in the number of relativistic degrees of freedom, the entropy density of the heat bath before and after the phase transition are related by $s_f/s_i = (T_f/T_i)^3$. This implies that the number density-to-entropy ratio of the decoupled species is diluted by a factor:

$$\frac{n_f/s_f}{n_i/s_i} = \frac{\exp\left[-3\int_{t_i}^{t_f} H dt'\right]}{(T_f/T_i)^3} . \tag{7.23}$$

In Fig. 7.4 we show numerical results for this dilution factor as a function of the number of fermion species, showing that stronger dissipative effects lead to a more significant dilution of dangerous relics, by enhancing either the maximum value of Ω_ϕ attained or the duration of the late period of warm inflation. For example, observational constraints on the abundance of GUT monopoles require at least $n_{\rm M}/s \lesssim 10^{-11}$ [13, 179], so it is unlikely that a single phase transition subsequent to monopole formation can yield the required dilution factor unless a very large number of dissipative channels is involved. Even if a complete dilution cannot be achieved, this may, for example, alleviate the bounds on the reheating temperature after inflation concerning the overproduction of gravitinos. In particular, since $\Omega_{3/2} \propto T_{\rm R}$ (see e.g. [180]), bounds on $T_{\rm R}$ will increase by the inverse of the dilution factor in Eq. (7.23). Furthermore, the cumulative effect of several different stages of symmetry breaking may potentially result in a significant dilution factor that should be taken into account.

In summary, we have shown that dissipative effects during a cosmological phase transition may have a significant effect on the cosmic history. By overdamping the motion of the associated Higgs field, dissipation not only prevents oscillations about the symmetry-breaking minimum but also leads to a period of slow-roll and potentially late-time warm inflation. The energy density in the field and the entropy produced by dissipative effects will also

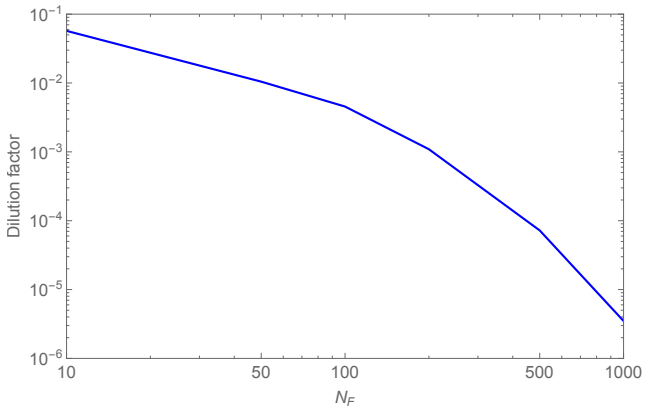

Figure 7.4: Dilution factor for frozen relics during a phase transition as a function of the number of fermions coupled to the Higgs field, for $\lambda = 10^{-2}$, $v = 10^{15}$ GeV, $g^2 = 1/N_{\rm F}$ and $h = 0.1$.

generically increase the amount of Hubble expansion during the phase transition and parametrically dilute the abundance of frozen relics.

One or more short periods of late time warm inflation during phase transitions could have significant observational effects. On the one hand, their existence implies that the main period of inflation can be considerably shorter than the overall 50-60 e-folds of accelerated expansion required by the observed flatness and homogeneity of the Universe. This will therefore change observational predictions for large scales, along the lines suggested in [181] for the case of thermal inflation. On the other hand, small scale perturbations will be generated during these periods, although they should be well within the horizon today and hence potentially too damped to be studied in galaxy surveys or CMB observations. Although this requires further inspection and a detailed study that is outside the scope of this work, we nevertheless emphasize that dissipation will modify the evolution of fluctuations, therefore yielding distinct observational predictions from a period of thermal inflation. Since both thermal and dissipative (warm) inflation may occur within the same phase transition, it would be interesting to explore the combined effects of these two types of inflationary expansion on the spectrum of cosmological perturbations.

7.4 Dissipative baryogenesis and leptogenesis

As we have seen in the previous section, dissipation may have a significant effect in the dynamics of a cosmological scalar field in the process of spontaneous symmetry breaking. Significant effects arose in this case when the field became a non-negligible component of the energy balance in the Universe, either itself increasing the Hubble rate or leading to a significant entropy production. In this section, we will consider an effect of dissipation that may occur even when the dissipating scalar field carries a very small fraction of the energy in the Universe and plays a subdominant role in entropy production.

Dissipation leads to the production of particles within the heat bath to which a dynamical scalar is coupled to, continuously disturbing its equilibrium. The degrees of freedom within the heat bath will *a priori* include the SM particles and their anti-particles, as well as potentially dark matter particles and other beyond the SM species. The rate at which each particle species is produced is related to its fractional contribution to the dissipation coefficient, as explicitly shown in [182]. It is then natural to envisage scenarios where particles and anti-particles are produced at different rates by a dissipating scalar field, necessarily involving interactions that violate baryon/lepton number as well as the C and CP symmetries, according to the conditions first established by Sakharov [27]. This was first explored in the context of warm inflation in a mechanism dubbed *warm baryogenesis* [26] (see earlier chapters for more details), where the same interactions responsible for damping the inflaton's motion and sustaining a radiation bath during inflation were shown to yield a significant baryon asymmetry, parametrically within the observed window.

Here, we will show that *dissipative baryogenesis* is a much more general mechanism that may occur in the dynamics of any cosmological scalar field with non-equilibrium dissipative dynamics and interactions satisfying the Sakharov conditions. We will illustrate this by looking at a concrete example based on the interactions employed in standard thermal leptogenesis scenarios with right-handed neutrinos and which is naturally motivated within GUT models. Although dissipative baryo/leptogenesis will occur in several different dynamical regimes, we will focus on low-temperature dissipative models to explicitly show that the production of a lepton asymmetry does not require temperatures above the right-handed neutrino mass threshold as in the standard thermal scenarios.

Our example further shows that no symmetries need to be restored in the early Universe to generate the observed baryon asymmetry, thus avoiding the several potential cosmological problems that this may cause.

We will first consider the relevant particle physics interactions and describe how they lead to dissipative effects that may produce more particles than their anti-particles, and afterwards describe the dynamics of dissipative baryogenesis in the radiation-dominated era.

7.4.1 Interactions and dissipative particle production rates

Leptogenesis is amongst the most popular models for the generation of a cosmic baryon asymmetry [183, 184, 185, 186, 187, 28]. In the simplest models, it is based on the out-of-equilibrium decays of heavy right-handed Majorana neutrinos, which violate lepton number as well as C and CP. The resulting lepton asymmetry is later on converted into a baryon asymmetry by electroweak sphaleron processes [188], which conserve $B - L$ but not the two global charges independently. Heavy right-handed neutrino singlets are the simplest addition to the SM particle content, yielding light neutrino masses through the seesaw mechanism, thereby providing an interesting connection between cosmology and low-energy particle physics.

Right-handed neutrinos also fit nicely within the **16** fundamental representation of the $SO(10)$ GUT gauge group and their large Majorana mass required by the seesaw mechanism can in this case be generated by the vev of a Higgs field in the **126** representation [189]. It is thus natural to consider the cosmological dynamics of this scalar field, which to our knowledge remains unexplored, including in particular the dissipative effects associated with its couplings to right-handed neutrinos. We will then consider a supersymmetric model where the relevant interactions are encoded in the superpotential:

$$W = \frac{1}{2} g_a \Phi N_a^c N_a^c + y_{ai} N_a^c H_u L_i + f(\Phi) \ , \tag{7.24}$$

which involves the right-handed neutrino superfields, N_a, as well as the SM lepton and Higgs doublet superfields, L_i and H_u, respectively. We consider three neutrino and lepton generations denoted by the indices a and i and note that $SU(2)$ gauge indices are implicit in the superpotential. The chiral superfield Φ can be identified with the scalar direction within the **126** representation of

$SO(10)$ that gives a Majorana mass to the right-handed neutrinos, as discussed above, or more generally as a SM singlet with self-interactions encoded in the analytic function $f(\Phi)$. Without loss of generality, we will take its scalar vev as a real field $\langle\Phi\rangle = \phi/\sqrt{2}$.

Dissipation of the scalar field's energy will in this case proceed through the excitation of the right-handed neutrinos and their scalar superpartners in the cosmic heat bath and their subsequent decay into the MSSM (s)leptons and Higgs(inos). The cosmological evolution of the ϕ field will depend on its potential, given by $|f'(\phi)|^2$, and crucially on its behavior during inflation. As anticipated above, we will be mainly interested in studying the regime where right-handed neutrinos are too heavy to be thermally produced and therefore standard leptogenesis scenarios are inefficient. This is natural in scenarios where the field is light and hence overdamped during inflation, either remaining frozen at some potentially large initial value or driven towards a large vev by de Sitter fluctuations. In the low-temperature regime where the reheat temperature after inflation is below the right-handed neutrino mass threshold, dissipation proceeds through the excitation of virtual modes in the heat bath as discussed earlier in this work. Scalar modes, in this case the right-handed sneutrinos decaying dominantly into sleptons and Higgs bosons, yield the leading contribution to the dissipation coefficient [81], which is given approximately by:

$$\Upsilon = C_\phi \frac{T^3}{\phi^2}, \qquad C_\phi \simeq \frac{1}{16\pi} \sum_{a,i} y_{ai} y_{ai}^* \ . \tag{7.25}$$

This coefficient therefore determines the overall entropy production rate in the form of MSSM particles produced in the thermal bath by the decays of the virtual right-handed sneutrinos. These decays violate lepton number, since the Majorana mass term precludes a consistent assignment of L to N_a^c, and may also violate C and CP if the Yukawa coupling matrix has non-trivial phases, which is possible for at least three matter generations. If this is the case then out-of-equilibrium dissipation will naturally induce an overabundance of sleptons over anti-sleptons in the heat bath (or vice-versa, although we will assume this to be the case).

The rate at which sleptons and anti-leptons are produced can be computed from the imaginary part of their self-energies, following the generic procedure

first described in [182]:

$$\dot{n}(p) = \mathrm{Im}\left[2\int_{-\infty}^{t} dt_2 \frac{e^{-i\omega_p(t-t_2)}}{2\omega_p}\Sigma_{21}(p,t,t_2)\right] . \tag{7.26}$$

Integrating over the 3-momentum p and summing over the energies of all the light particle species yields a source term for the radiation energy density $\Upsilon\dot{\phi}^2$ corresponding to the dissipation coefficient in Eq. (7.25). We are, however, interested in the difference between the slepton and anti-slepton production rates, which as we will show is a sub-leading effect compared to the overall dissipative entropy production. To compute the slepton self-energies we first consider the relevant scalar and Yukawa interactions resulting from the superpotential in Eq. (7.24), which are given by:

$$\mathcal{L}_{\mathrm{S}} = \frac{g_a^2}{2}\phi^2|\tilde{N}_a|^2 + \frac{g_a\phi}{\sqrt{2}}y_{aj}\tilde{N}_a^* h_u \tilde{l}_j + h.c \tag{7.27}$$

$$\begin{aligned}\mathcal{L}_{\mathrm{Y}} &= \frac{1}{2}y_{ai}\Big(\tilde{N}_a^c\bar{\tilde{h}}_u P_L l_i + \tilde{N}_a^c\bar{l}_i P_L\tilde{h} + h_u\bar{l}_i P_L N_a + h_u\bar{N}_a P_L l_i + \tilde{l}_i\bar{\tilde{h}}_u P_L N_a \\ &+ \tilde{l}_i\bar{N}_a P_L\tilde{h}_u + h.c\Big) .\end{aligned} \tag{7.28}$$

In Fig. 7.5 we show the leading 1- and 2-loop diagrams contributing to the slepton self-energies. We note that, even though dissipation is dominated by scalar modes, at 2-loop order fermions and scalars will give comparable contributions to the slepton self energy. It is also interesting to note that even though the final asymmetry is independent of the lepton number assignment chosen for the right-handed neutrinos, this choice determines which diagrams actually exhibit L-violation. For example, the Yukawa sector always violates L, whereas scalar interactions preserve it for $L(N_a^c) = 1$. In scenarios where $B-L$ is a spontaneously broken gauge symmetry, the N_a^c superfield will have lepton number -1 and L is violated by both types of interactions.

Analogously to standard leptogenesis scenarios, CP violation arises only through the interference between the leading and next-to-leading diagrams. The leading diagram corresponds in this case to the top-left diagram in Fig. 7.5, the imaginary part of which yields the (tree-level) decay of the right-handed sneutrinos. The slepton self-energies can be computed using standard thermal field theory techniques and we refer the reader to [182, 26] for more technical details. Slepton and anti-slepton self-energies are related by charge conjugation

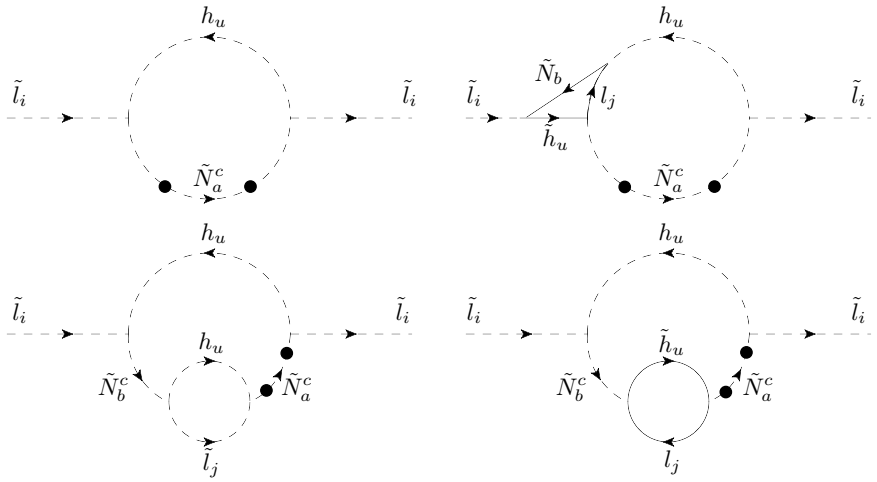

Figure 7.5: The 1-loop and 2-loop diagrams contributing to the slepton self energy. Black circles indicate background field (i.e. right-handed sneutrino mass) insertions.

and we obtain for the difference between the self-energies, to leading order:

$$\Delta\Sigma_{21}^{\tilde{l}_i} = \frac{3}{16\pi}\sum_{a,b}\sum_{j}\int dp\int dk\, C(p,k)\left(\frac{T}{m_b}\right)^4\frac{m_b}{m_a}\mathrm{Im}(y_{bi}y_{aj}^*y_{bj}y_{ai}^*)\ , \qquad (7.29)$$

where $m_a = g_a\phi/\sqrt{2}$ are the right-handed sneutrino masses to leading order, assuming the MSSM Higgs and sleptons have zero or at least negligible expectation values at this stage in the cosmological evolution. We note that once the sum over all heavy sneutrino and light field generations is performed, only the diagrams involving fermionic propagators contribute to the self-energy difference above. The factor $C(p,k)$ encodes the main loop kinematics (i.e. the one loop diagram without the couplings) and is common to the self-energy of all the different particle species and therefore determines the overall dissipation coefficient given above. The temperature and mass dependencies arise from computing the imaginary parts of the second order loops in Fig. 7.5 and taking the loop momenta of the light particles to be $\mathcal{O}(T)$, which is a sufficiently good approximation for our purposes. Adding the self-energies of all particle species we obtain to leading order the following result which will ultimately give the overall radiation production rate:

$$\Sigma_{21}^{\mathrm{R}} = 8\sum_{a}\sum_{j}\int dp\int dk\, C(p,k)y_{aj}y_{aj}^*\ . \qquad (7.30)$$

The relative rate at which a lepton asymmetry is produced by dissipation can then be obtained by taking the quotient of Eqs. (7.29) and (7.30) as the remaining integral factors in Eq. (7.26) cancel, yielding:

$$r_{\rm L} \equiv \frac{\dot{n}_{\rm L}}{\dot{n}^{d}_{\rm R}} \simeq \frac{3}{64\pi}\frac{1}{\sum_a (yy^\dagger)_{aa}} \sum_{a\neq b} \left(\frac{T}{m_b}\right)^4 \frac{m_b}{m_a} {\rm Im}\left[(yy^\dagger)^2_{ba}\right] \ , \tag{7.31}$$

where the sum over light fields running in the loop is implicit. Note that, as in thermal leptogenesis, a non-vanishing asymmetry can only be produced if at least two of the right-handed sneutrinos are non-degenerate, thus requiring distinct g_a couplings in the superpotential Eq. (7.24).

A couple of important properties of the asymmetry production rate should be emphasized. Firstly, the dissipation coefficient in Eq. (7.25) is independent of the g_a couplings to leading order, so that all three right-handed sneutrino species will be virtually excited by the motion of the ϕ field and contribute to the lepton asymmetry. This is in contrast to thermal scenarios, where the out-of-equilibrium decay of the lightest right-handed (s)neutrino will give a dominant contribution. Secondly, the asymmetry production rate is suppressed by $(T/m_a)^4 \ll 1$, which is associated with the fact that the right-handed sneutrinos are only virtually excited, as opposed to thermal leptogenesis scenarios. This means that while in the latter mechanism one must consider small couplings and CP violating phases to yield the observed baryon asymmetry, in dissipative leptogenesis a small baryon-to-entropy ratio can result solely from the low temperature suppression. We note that the leading scalar loop diagrams contributing to the asymmetry are only suppressed by a factor $(T/m_a)^2$, but as mentioned above their overall contribution cancels out when summing over the different generations. This is a specific feature of the interaction structure considered in leptogenesis, with a single type of decay channel for the heavy right-handed sneutrinos, so that in more general models of dissipative baryogenesis, such as the one considered in [26], the asymmetry production rate will be larger.

The light neutrino mass hierarchy inferred from experimental bounds motivates considering a hierarchical structure in the right-handed neutrino sector as well, e.g. $g_1 \ll g_2 \ll g_3$. In this case the asymmetry production rate reduces to:

$$r_{\rm L} \simeq \frac{3}{64\pi}\left(\frac{T}{m_1}\right)^4 \frac{1}{\sum_a (yy^\dagger)_{aa}} \sum_{a\neq 1}^{N_R} \left(\frac{m_1}{m_a}\right) Im[(yy^\dagger)^2_{1a}] \ , \tag{7.32}$$

which is suppressed relative to its thermal leptogenesis counterpart by a factor $(1/8)(T/m_1)^4$, as well as the fact that in the latter case only the lightest right-handed neutrino contributes to the factor $\sum_a (yy^\dagger)_{aa}$ in the denominator which corresponds to the overall entropy production rate. To simplify our dynamical analysis of dissipative leptogenesis, we collect all couplings and mass differences into an effective parameter ϵ, such that:

$$r_{\rm L} \simeq \epsilon y^2 \left(\frac{T}{m_1}\right)^4 \ , \tag{7.33}$$

where we assumed that the Yukawa couplings have roughly the same magnitude y.

7.4.2 Dynamics of the lepton asymmetry generation

Having determined the rate at which lepton number is produced by dissipation, we will now consider the dynamics of the scalar field ϕ, which is coupled to the evolution of the overall entropy and lepton number density via the system of equations:

$$\ddot{\phi} + (3H + \Upsilon)\dot{\phi} + V'(\phi) = 0 \ , \tag{7.34}$$

$$\dot{s} + 3Hs = \frac{\Upsilon \dot{\phi}^2}{T} \ , \qquad \dot{n}_{\rm L} + 3Hn_{\rm L} = \frac{45\zeta(3)}{2\pi^4}\frac{g_L}{g_*}\frac{\Upsilon\dot{\phi}^2}{T} r_{\rm L} \ , \tag{7.35}$$

where $g_{\rm L}$ is the number of relativistic degrees of freedom with non-vanishing lepton number, for which we will take the MSSM value $g_{\rm L} = 33.75$ as a reference, as well as the associated $g_* = 228.75$ for the overall number of relativistic species. The entropy equation can be derived from Eq. (4.16) using the fact that $s = 2\pi^2 g_* T^3/45$. The lepton number density equation can likewise be obtained using $n_{\rm L} = g_{\rm L}\zeta(3)T^3/\pi^2$ and that the fraction of dissipation which sources the lepton number density is $r_{\rm L}\Upsilon\dot{\phi}^2/T$. We will consider the evolution in the low-temperature dissipative regime, where the dissipation coefficient takes the form in Eq. (7.25). We will assume that the Yukawa couplings have roughly the same magnitude for all three generations, such that $C_\phi \simeq 9y^2/16\pi$, although this assumption is not crucial for our subsequent analysis. The lepton number density is sourced, as computed in the previous section, by a fraction $r_{\rm L}\Upsilon$ of the overall dissipation coefficient.

We are interested in the evolution of the field ϕ in a regime where it has a large vev, such that right-handed (s)neutrinos have a large mass and cannot be produced on-shell. This implies that, as opposed to the example considered in the previous section, we assume that there is no symmetry restoration after inflation. As a concrete example, we take the simple symmetry breaking potential of the previous section, given in Eq. (7.14), although thermal mass corrections will always be Boltzmann-suppressed in the regime that we are interested in exploring.

We note that if the field ϕ comes to dominate over the radiation energy density, or at least attains a significant relative abundance, then a sizeable lepton asymmetry can be produced, which is the case of the warm baryogenesis mechanism during inflation [26]. We will show, however, that the observed baryon asymmetry can also be produced when the field is sub-dominant and dissipation does not contribute significantly to the overall entropy of the Universe.

It is convenient to express the lepton number density in terms of the lepton-to-entropy ratio, $Y_{\rm L} \equiv n_{\rm L}/s$, which becomes constant once a lepton asymmetry stops being efficiently produced. We then have:

$$\dot{Y}_{\rm L} \simeq C_{\rm L}\frac{T^3}{\phi^6}\dot{\phi}^2, \qquad C_{\rm L} = \frac{90\zeta(3)}{\pi^4}\frac{g_{\rm L}}{g_*}\frac{C_\phi}{C_s}\epsilon\frac{y^2}{g^4}\ , \tag{7.36}$$

where $C_s = 2\pi^2 g_*/45$. The evolution of $Y_{\rm L}$ will then be determined by the dynamics of the ϕ field. We assume the field's self-coupling λ is sufficiently small for it to be overdamped during inflation, $m_\phi^2 = \lambda^2(3\phi^2 - v^2) \ll H_{\rm inf}^2$, where $H_{\rm inf} \lesssim 10^{14}$ GeV from the recent CMB upper bounds on the tensor-to-scalar ratio obtained by the Planck satellite [90]. De Sitter fluctuations will then lead to a distribution of field values $\phi_i \lesssim m_{\rm p}$ in different patches of the inflationary Universe at the start of the radiation era, and which will typically be displaced from the minimum of the potential at $|\phi| = v$.

As it evolves towards the minimum, the field will feel the effects of both Hubble damping and dissipative friction. The latter will play a significant role for:

$$Q = \frac{\Upsilon}{3H} \simeq \sqrt{\frac{10}{\pi^2}}\frac{C_\phi}{\sqrt{g_*}}\frac{Tm_{\rm p}}{\phi^2} \gtrsim 1\ , \tag{7.37}$$

where we have used the standard relation between the Hubble rate and the ambient temperature in a radiation-dominated Universe. On the one hand, if

the field rolls towards the minimum from $|\phi_i| < v$, Q will necessarily decrease in time and so dissipation can at most have a significant effect during the earlier stages of the evolution. On the other hand, for $|\phi_i| > v$, Q may increase as the field value decreases, in particular if it overshoots the minimum and attains a small value during the first oscillation. In any case dissipation can only have a transient effect, since asymptotically the field will settle at the minimum and Q will decrease with the temperature.

For simplicity, we will focus on scenarios where dissipation plays no significant role in the field dynamics. This is, in particular, the case for a large field vev $v \lesssim m_{\rm p}$ and initial displacements $\Delta\phi_i = |\phi_i - v| \lesssim v$, for which $Q \lesssim T/m_{\rm p} \ll 1$. In the standard seesaw mechanism the right-handed (s)neutrino masses are related to the light neutrino masses via:

$$m_{\tilde{N}} = \frac{gv}{\sqrt{2}} \simeq 10^{15} y^2 \left(\frac{0.1 \text{ eV}}{m_\nu}\right) \text{ GeV} \ , \tag{7.38}$$

so that $v \lesssim m_{\rm p}$ implies $g \gtrsim 10^{-3} y^2 (0.1 \text{ eV}/m_\nu)$. Under these conditions the field oscillations are well described by (for $m_\phi t \gg 1$):

$$\phi \simeq v + \Delta\phi_i \left(\frac{t}{t_i}\right)^{-3/4} \cos\left(m_\phi (t - t_i)\right) \ , \tag{7.39}$$

where $m_\phi = \sqrt{2}\lambda v$ is the field mass at the minimum, $\Delta\phi_i \equiv \phi_i - v$ and $t_i = (2H_i)^{-1} \sim (2m_\phi)^{-1}$ is the time at which the field becomes underdamped and effectively starts oscillating. We may then substitute this into Eq. (7.36) to estimate the lepton-to-entropy ratio produced by dissipation as the field oscillates. We note that since the field velocity is small before the onset of oscillations, no significant lepton number will be produced until the field becomes underdamped. Taking the average field value $\langle\phi\rangle = v$ and the average field velocity $\langle\dot{\phi}^2\rangle \simeq m_\phi^2 \Delta\phi_i^2 (t/t_i)^{-3/2}/2$, we can then integrate Eq. (7.36) from $t = t_i$ to obtain asymptotically:

$$Y_{\rm L} \simeq \frac{C_{\rm L}}{4 g_*^{3/4}} \left(\frac{45}{2\pi^2}\right)^{3/4} (m_{\rm p} t_i)^{3/2} \frac{m_\phi^2 \Delta\phi_i^2}{v^6} \frac{1}{t_i^2} \ . \tag{7.40}$$

For $g_* = 228.75$ and $g_{\rm L} = 33.75$ in the MSSM, and taking into account the relation between the asymptotic baryon and lepton numbers after conversion by

sphaleron processes, $B_f = -(8/23)L_i$ [28], this yields:

$$\eta_s \simeq 0.1 \left(\frac{m_\nu}{0.1\text{ eV}}\right)^2 \left(\frac{m_{\tilde{N}}}{10^{15}\text{ GeV}}\right)^{1/2} \left(\frac{\Delta\phi_i}{v}\right)^2 \left(\frac{m_\phi}{m_{\tilde{N}}}\right)^{5/2} \epsilon\ . \tag{7.41}$$

The baryon asymmetry thus depends parametrically on the ratio of the field and sneutrino masses, $m_\phi/m_{\tilde{N}} = 2\lambda/g$. Adiabaticity of the dissipative process requires the field to move slowly compared to the sneutrino decay rate, $\dot{\phi}/\phi \sim m_\phi \ll \Gamma_{\tilde{N}} \simeq y^2 m_{\tilde{N}}/16\pi$. Additionally, for the asymmetry to be produced below the sneutrino mass threshold, we require $T < m_{\tilde{N}}$ at the onset of field oscillations, $H \sim m_\phi$. This then implies $m_\phi/m_{\tilde{N}} \lesssim m_{\tilde{N}}/m_{\rm p}$, which is typically a stronger constraint than adiabaticity of the dissipative processes. Saturating this bound, we obtain for the final baryon asymmetry:

$$\eta_s \simeq 10^{-10} \left(\frac{m_\nu}{0.1\text{ eV}}\right)^2 \left(\frac{m_{\tilde{N}}}{2\times 10^{15}\text{ GeV}}\right)^3 \left(\frac{\Delta\phi_i}{v}\right)^2 \left(\frac{\epsilon}{0.05}\right)\ . \tag{7.42}$$

We thus see that the observed baryon asymmetry, $\eta_s \sim 10^{-10}$ [190], can be obtained through adiabatic dissipation for sneutrino masses close to the GUT scale, which generate neutrino masses in the range suggested by atmospheric neutrino oscillations for $\mathcal{O}(1)$ Yukawa couplings [136]. As opposed to standard leptogenesis models, the amount of CP-violation, parametrized by ϵ, need not be very small in this case since the produced baryon asymmetry is naturally small. We note that Eq. (7.42) is an estimate that is accurate up to $\mathcal{O}(1)$ factors, since the onset of field oscillations does not occur exactly for $H = m_\phi$, so the above values for the masses should be taken only as reference values.

The exact value of the produced asymmetry can be computed numerically, and in Figures 7.6 and 7.7 we give examples for the numerical evolution of the field ϕ and the asymmetry $n_{\rm B}/s$ in the regime considered above, for different values of the field mass parametrized by the self-coupling λ. In all examples shown, dissipation has a sub-dominant effect on the field evolution, as discussed above, and its main effect is the production of a baryon asymmetry. We have checked in all cases that the adiabatic condition is satisfied and that the temperature is below the sneutrino mass threshold at the onset of field oscillations.

We thus conclude that the produced asymmetry can have a range of values both below and above the observational window. Most of the lepton number is produced in the first few oscillations of the field, where the field velocity, and

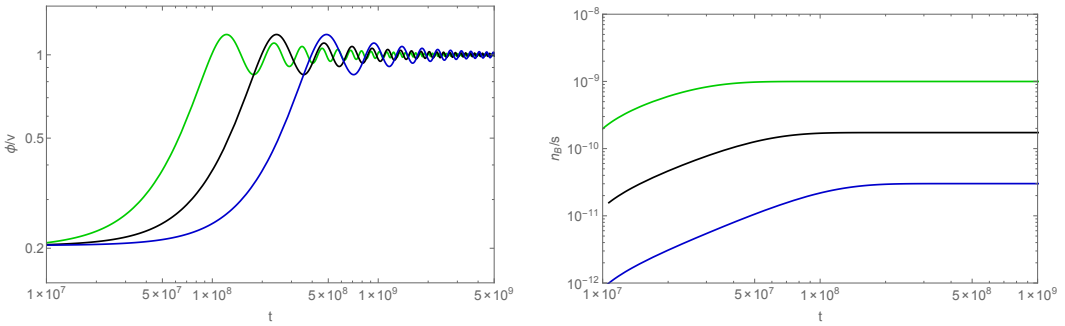

Figure 7.6: Numerical results for the evolution of the field ϕ and the baryon asymmetry $\eta_s = n_{\rm B}/s$, starting from a field value below the minimum at $v = 10^{18}$ GeV. The quartic self-coupling $\lambda = 1 \times 10^{-8}, 2 \times 10^{-8}, 4 \times 10^{-8}$ for the blue, black and green curves, respectively. We have taken $g = 10^{-3}$, $y = 3$ and $\epsilon = 1/64\pi$ in all cases. Time is given in Planck units.

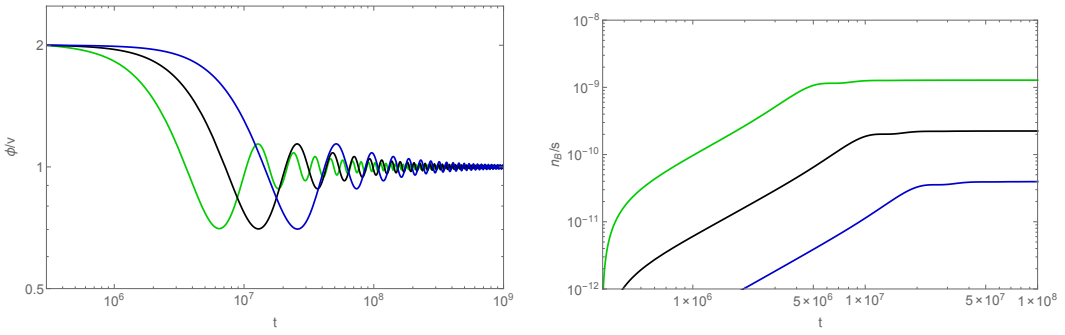

Figure 7.7: Numerical results for the evolution of the field ϕ and the baryon asymmetry $\eta_s = n_{\rm B}/s$, starting from a field value above the minimum at $v = m_{\rm p}$. The quartic self-coupling $\lambda = 1 \times 10^{-7}, 2 \times 10^{-7}, 4 \times 10^{-7}$ for the blue, black and green curves, respectively. We have taken $g = 10^{-3}$, $y = 3$ and $\epsilon = 1/64\pi$ in all cases. Time is given in Planck units.

hence the dissipative lepton source, is larger, with the lepton-to-entropy ratio stabilizing within a few oscillation periods.

We note that, even though the adiabatic dissipation coefficient decreases with the temperature, and hence becomes negligible at late times, the full dissipation coefficient includes a zero-temperature part that corresponds to the standard decay width for an oscillating field [182]. This corresponds in the present scenario to the 4-body decay of the ϕ field into Higgs and slepton pairs mediated by virtual right-handed sneutrinos, since the latter's on-shell production is kinematically forbidden. As shown in [182], this contribution is suppressed by $(m_\phi/T)^3$, as well as numerical factors, with respect to the adiabatic component. We may

thus safely neglect this contribution in computing the lepton asymmetry, which is produced when $m_\phi \sim H \ll T$, bearing nevertheless in mind that this will lead to the decay of the ϕ field after it becomes non-relativistic at late times.

In the particular model of leptogenesis that we have considered, a lepton (and hence baryon) asymmetry is produced by the dynamical evolution of a scalar SM singlet that determines the Majorana mass of right-handed (s)neutrinos. This is, however, a much more general result and dissipative baryogenesis should occur in any scenario where fields whose decay violates the B/L- and C, CP-symmetries are coupled to (and acquire mass from) a dynamical scalar field, including e.g. the $SU(5)$ model considered in Section 7.2. Depending on the field masses and couplings, the observed baryon asymmetry may be entirely produced by off-shell dissipative effects, with no need for temperatures above the B-violating field mass threshold. This may then avoid symmetry restoration in the early Universe and the production of dangerous thermal relics during the associated phase transitions. In addition, dissipative baryogenesis generically yields potentially observable signatures, as we describe below.

7.4.3 Isocurvature perturbations

As obtained above, the baryon asymmetry that results from dissipative processes will depend on the initial field displacement from the true minimum of its potential. If, as we assumed earlier, the field is light during inflation, we then expect super-horizon quantum fluctuations $\langle \delta\phi_i^2 \rangle = (H_{\rm inf}/2\pi)^2$ in the initial field value. These will then result in fluctuations in the final baryon-to-entropy ratio and hence baryon isocurvature modes that can be tested with CMB observations.

This is also a feature of the warm baryogenesis scenario during (warm) inflation [26], where both inflaton and temperature fluctuations generate baryon isocurvature modes. The main difference to the case analyzed in this work resides, firstly, in the fact that the field responsible for producing the baryon asymmetry never dominates the energy balance in the Universe. Consequently, the resulting baryon isocurvature modes will be uncorrelated with the main (adiabatic) curvature perturbations sourced by the inflaton. Secondly, the baryon asymmetry is produced at the onset of field oscillations rather than in a slow-roll regime. Since this occurs when $H \sim m_\phi$, fluctuations in the ambient temperature will only delay or expedite the production of the baryon asymmetry, but they do

not change its final value. From Eq. (7.42), we have that:

$$S_{\rm B} = \frac{\delta\eta_s}{\eta_s} = 2\frac{\delta\phi_i}{\Delta\phi_i} \ , \tag{7.43}$$

such that we can write the relative contribution of uncorrelated baryon isocurvature modes to the CMB spectrum as:

$$B_{\rm B}^2 = \frac{S_{\rm B}^2}{P_\zeta^2} \simeq \frac{r}{2}\left(\frac{m_{\rm p}}{\Delta\phi_i}\right)^2 \ , \tag{7.44}$$

where $P_\zeta^2 \simeq 2\times10^{-9}$ is the amplitude of the adiabatic curvature perturbation spectrum [1] and r is the tensor-to-scalar ratio. This gives a contribution to the total matter isocurvature power spectrum that is suppressed by the relative abundance of baryons $(\Omega_{\rm B}/\Omega_{\rm m})^2 B_{\rm B}^2 \simeq 0.03 B_{\rm B}^2$. From the constraints posed by the Planck satellite on uncorrelated CDM isocurvature modes with a scale invariant spectrum at a comoving wavenumber $k_{\rm low} = 0.002\ {\rm Mpc}^{-1}$ [1], we deduce the bound $B_{\rm B} \lesssim 1.03$. The result above satisfies this bound for initial field displacements:

$$\Delta\phi_i > 0.68\sqrt{r} m_{\rm p} \ . \tag{7.45}$$

If the tensor-to-scalar ratio is close to the current upper bound $r \lesssim 0.1$ [1], this requires field displacements $\Delta\phi_i \gtrsim 0.2 m_{\rm p}$. Although the value of the baryon asymmetry does not depend directly on the actual value of the field displacement, but rather on the ratio $\Delta\phi_i/v$, we have seen above that the observed baryon asymmetry can be entirely produced by off-shell dissipative effects for $\Delta\phi_i \sim v \sim m_{\rm p}$. The bound above is thus consistent with the generation of the observed baryon asymmetry. On the other hand, low-scale inflationary models with $r \ll 0.1$ are consistent with initial field displacements parametrically below the Planck scale.

We note, however, that in supergravity models scalar fields may acquire masses parametrically close to the Hubble scale during inflation, and hence be driven to a local minimum that does not necessarily coincide with the low-energy global minimum [191]. In this case dissipation may also produce a baryon/lepton asymmetry as the field rolls towards the true minimum after inflation, although field masses of the order of the Hubble scale may somewhat change the dynamics. In these scenarios there will be, however, no significant field fluctuations on super-

horizon scales, which makes them less appealing from the observational point of view.

Evidence for baryon isocurvature modes will nevertheless constitute a strong hint for dissipative baryogenesis, which is thus a testable mechanism. In addition, the particular case of dissipative leptogenesis considered above can be related to low-energy neutrino phenomenology, thus yielding two independent potential ways of probing the production of a baryon asymmetry.

7.5 Discussion

Scalar fields are ubiquitous in the best-motivated extensions of the Standard Model of particle physics and their dynamics has in most cases a very significant cosmological impact. Since they generically interact with other matter and gauge degrees of freedom, dissipative effects are a crucial feature determining how scalar fields evolve in the cosmological heat bath. This leads to additional friction, entropy production and scalar field fluctuations. These effects are, in the leading adiabatic approximation, fully encoded in a single dissipation coefficient, which can be computed from the fundamental Lagrangian defining the properties and interactions of a given scalar field.

The study of dissipative effects has so far been mostly restricted to the early period of inflation, where dissipation may, in fact, completely change the inflaton dynamics and the associated generation of primordial curvature perturbations [142, 95, 89, 161, 162, 5, 11, 59, 60, 84, 163, 7] (see Chapter 4). More recently, a few studies have also begun to explore the importance of dissipation in the dynamics of reheating after inflation [192, 193, 97, 194, 80], assuming it proceeds from a supercooled stage where dissipative dynamics plays a negligible role, and also in the dynamics of a curvaton field [195].

It was the purpose of this work to set the stage for a much broader exploration of dissipative dynamics in the evolution of cosmological scalar fields, which in many cases only begins in the radiation-dominated era once the Hubble expansion rate and the ambient temperature have decreased sufficiently. A scalar field will typically find itself displaced from the absolute minimum of its effective potential after inflation and, in evolving towards it, the field will necessarily dissipate part of its energy into the ambient heat bath. Dissipation is thus, in particular, an inherent part of the process of spontaneous symmetry breaking and can modify

the dynamics of the several phase transitions that may have occurred in the early cosmic history. The evaporation of a Bose condensate may also lead to an effective friction term along the lines suggested in [196].

A natural starting point for our study was to compute, for the first time, the dissipation coefficient inherent to different scalar fields in particle physics models of the early Universe, and which we hope will be useful for future studies. We have, in particular, considered the electroweak Higgs field(s) in the SM and its minimal supersymmetric extension, the scalar singlet yielding the μ-term in the NMSSM, the adjoint Higgs direction breaking the GUT $SU(5)$ group to the SM, and a SM singlet giving a Majorana mass to right-handed neutrinos (embedded e.g. in $SO(10)$). For a given dynamical scalar, the dissipation coefficient takes different forms depending on the properties of the fields it is coupled to, namely their mass, spin, multiplicity and coupling constants. Dissipation proceeds generically through the excitation and decay of these fields and the associated coefficient takes different forms depending on whether on-shell or off-shell excitation is dominant. Note, for example, that while on-shell modes resonantly enhance dissipation, their occupation numbers become Boltzmann-suppressed at temperatures below their mass threshold and virtual modes then yield the dominant contribution. Generically, dissipation coefficients depend both on the field value and the ambient temperature, thus constituting dynamical quantities.

We then proceeded to explore the dynamical impact of dissipative effects by solving the Langevin-like equation that determines the evolution of a cosmological scalar field, Eq. (4.6), in different scenarios. In this work we have focused mainly on the effects of dissipation and entropy production, although we have also briefly discussed the importance of the dissipative noise term, which we plan to explore in more detail in a future work. This term will be crucial, for example, in the initial stages of a cosmic phase transition, randomly kicking the associated Higgs field away from the unstable symmetric point. Fluctuation-dissipation will then play an important role in the formation of topological defects and also potentially in sourcing cosmic magnetic fields. There are various works in the literature which make statistical arguments for the distribution of seed magnetic domains. In a related context, statistical arguments are made on the initial distribution of a scalar field, such as in examining the initial condition problem of inflation [91, 197, 198, 199]. The Langevin-like Eq. (4.6) provides a dynamical equation from

which such distributions can be calculated rather than just argued statistically.

The friction effects associated with dissipation will slow down a field's evolution towards the minimum of its potential and damp the amplitude of its oscillations about the minimum. This will prolong a cosmic phase transition, potentially even completely overdamping the associated Higgs field. One interesting outcome of our analysis is the possibility of dissipation keeping the field in a slow-roll regime close to the symmetric value, such that it drives a late period of warm inflation. This may last for a few e-folds, which may be sufficient to dilute dangerous thermal relics such as gravitinos or GUT monopoles formed at earlier stages. In fact, a period of thermal inflation above the critical temperature and a period of (dissipative) warm inflation below the critical temperature can occur within the same phase transition. Although they have a similar dilution effect, these two periods have inherently different field dynamics, as well as fluctuations, and we hope in the future to investigate more closely their potentially distinct observational impact in the CMB and/or matter power spectrum.

We have also observed that a slow-roll period typically ends with a Higgs field falling fast towards the symmetry-breaking minimum, in the process producing a significant amount of entropy. We have thus concluded that, even if the field does not become dominant during the slow-roll phase, a parametric dilution of unwanted relics will still occur as a combined result of this entropy production and enhancement of the expansion rate during the phase transition.

In this work, we have also shown that, even if dissipation does not significantly enhance friction or entropy production, it may nevertheless lead to a small but crucial effect - the generation of a cosmological baryon asymmetry. This occurs due to the out-of-equilibrium nature of dissipative processes when B-/L- and C-/CP-violating interactions are involved. We have explicitly shown that the observed baryon asymmetry can be generated in a scenario of dissipative leptogenesis, where a SM scalar singlet giving a Majorana mass to right-handed (s)neutrinos excites the latter while rolling towards the minimum of its potential. This can occur at temperatures below the right-handed (s)neutrino mass threshold, with dissipation dominantly exciting virtual modes. We expect this to be a generic feature, also found earlier in the context of warm baryogenesis during inflation [26], such that it is possible to produce the observed baryon asymmetry while avoiding symmetry restoration and subsequent production of topological defects. Furthermore, the baryon-to-entropy ratio generated through

dissipation is generically field and temperature dependent, thus leading to baryon isocurvature perturbations that may be probed in the near future with CMB observations. If the observed asymmetry is produced by dissipation, we may thus hope to be able to test the violation of fundamental symmetries at high energies.

Our results show that going beyond the leading approximation of non-interacting adiabatic fluids can have a very significant impact in cosmology. Fluctuation-dissipation dynamics is present in any dynamical interacting system and, in particular, we have explicitly shown that this is the case for the SM Higgs field and for many other dynamical scalars present in its extensions. Significant dissipative effects are already a feature of near-equilibrium and near-adiabatic dynamics and thus should motivate further exploration of this topic, not only within this regime but also for more general non-equilibrium cosmological systems.

Up to now cosmology has been very successful in explaining almost all observations through the simple model of a thermalized Universe that is expanding. Phase transitions have been added to this picture to reconcile it with unified models of particle physics. There is a need to press beyond this simple picture and look with greater detail at the dynamics in the early Universe. The early Universe is a many-body system with limited initial condition information. A theoretical treatment of it requires a statistical dynamical approach, which can extend on the thermal equilibrium hot big bang model. Phase transitions and other regimes of scalar field evolution in the early Universe have, up to now, only been treated classically. This chapter has shown that the extension of this classical treatment leads to fluctuation-dissipation dynamics. In an earlier paper it was shown how fluctuation-dissipation effects would also extend the treatment of the Universe evolution in the general hot big bang regime [76]. Combined with the work in this chapter, this provides an extended dynamical framework to examine key unsolved problems of the early Universe.

The underlying principle behind both the work in this chapter and [76] is the same as in the original warm inflation work - that many of the most fundamental quantities measured in cosmology, those associated with some underlying field dynamics, only provide a coarse-grained information about that dynamics and not necessarily about its microphysical properties. This is the concept that separates the warm and cold paradigms of inflation. In cold inflation, the observables such as the index and bispectrum, are interpreted to probe precise information about

an underlying classical dynamics with quantum fluctuations superposed upon it. The uncertainity in this semiclassical approach is only that associated with the quantum mechanical uncertainty. In contrast warm inflation goes further to a full statistical state where these observables are interpreted to provide only coarse-grained information about the underlying fundamental dynamics. There can be many statistical dynamical realization of the coarse-grained dynamics. One common feature is the presence of energy fluxes amongst the coarse-grained cells, often related through the underlying dynamics. The fluctuation-dissipation relations examined in this paper are one, perhaps most common, example of such relations, and these can provide observable, testable, consequences.

Several problems in cosmology today need to be approached beyond the semiclassical approximation of thermal equilibrium dynamics, such as the generation of curvature and isocurvature perturbations, baryogenesis, leptogenesis, generation of dark matter, origin of cosmic magnetic fields, initial conditions of phase transitions, and dynamics during a phase transition or scalar field evolution. Adhering to just a thermal, semiclassical dynamical viewpoint of the underlying dynamics in the early Universe can restrict the scope of theoretical investigation that is possible, and can lead to misleading directions of interpretation, such as doing elaborate model building where some simple statistical interpretation could actually bring the predictions in line with observation. The work in this chapter has highlighted these points and provided a methodology that can be used for such exploration along with several example applications.

Chapter 8

Conclusions

In this thesis we have shown how the dual effects of fluctuations and dissipation can arise for scalar fields within common particle physics models. This fluctuation-dissipation dynamics can lead to interesting consequences for the cosmological evolution of the numerous scalar fields employed within particle physics and cosmology, which in turn can have important effects for the evolution of the Universe.

Within the context of inflation this dynamics can give rise to a period of warm inflation where dissipation can sustain a radiation bath despite the quasi-exponential expansion. Warm inflation can successfully solve the horizon, flatness and monopole problems as well as generate the primordial density perturbations from classical, thermal fluctuations. This can be done within a renormalisable framework with a simple quartic potential allowing for inflation to be triggered from chaotic initial conditions [142]. All of these features place warm inflation as being a strong contender to describe the early inflationary epoch. In addition there is the possibility of producing the matter -antimatter asymmetry during this period through dissipation, with associated isocuvature perturbations. Together with non gaussianity and the modified consistency relations, these could help to distinguish the warm inflation scenario from the many degenerate inflationary models on the market.

As a slight aside it is often misconstrued that warm inflation has more free parameters and as such is less predictive than the cold inflation scenario. This is not true. Within cold inflation the necessary couplings to other degrees of freedom are largely unconstrained and thus the duration and nature of the reheating period is unknown. This leads to an uncertainty in the number of e-folds before the end of

inflation where cosmological scales leave the horizon and thus each model sweeps out a range of predictions in the $n_{\rm s} - r$ plane. In contrast within warm inflation one specifies the field multiplicities, couplings and initial field value and the inflationary dynamics is fully determined and so to some extent the interactions are constrained from CMB observables. In addition in scenarios where dissipation increases during inflation sufficiently such that radiation smoothly takes over, there is no separate reheating period. This then constrains the number of e-folds of inflation and in a standard post inflation cosmology, predicts a single number and not a range.

It is also worth reiterating that the old criticisms of warm inflation were relevant to dissipation within the high temperature regime, where it is difficult to sustain the required number of e-folds of inflation due to the dominance of the thermal corrections to the potential over the effects of dissipation [71]. In contrast the work in this thesis is focussed on the low temperature regime where the thermal corrections are Boltzmann suppressed, whilst dissipation itself can be large. This occurs in part due to the supersymmetric interaction structure which allows for a cancellation of the inflaton-heavy field coupling, g within the dissipation coefficient. Thus dissipation can be large for $N_X \gg 1$ and thermal corrections are controlled for $g^2 N_X \lesssim 1$. In general for the T^3/ϕ^2 dissipation coefficient it can be shown that $N_X \gtrsim 10^5$ in order to obtain 50 e-folds with $T_*/H_* \gtrsim 1$ [161]. Such a large number of mediator fields may appear at first undesirable, however there are many orders of magnitude, about 15, in energy between the electroweak scale and the Planck scale and thus it would be peculiar if there were no extra degrees of freedom inhabiting this region. In addition the inflaton field is usually taken to be a Standard Model gauge singlet and as such should be free to couple democratically to the multitude of fields which commonly arise with high energy completions of the Standard Model. To be more concrete we note that these models of warm inflation can be realised within string theoretical models [57] where this large number may be naturally accounted for by a moderately large number of D-branes. Despite this, a goal of current and future research is to try and realise warm inflation successfully with fewer numbers of mediator fields and progress in this direction looks promising. One should bear in mind that the addition of a large multiplicities of fields may have the effect of modifying the strength of gravity during inflation leading to a suppressed Planck mass along the lines suggested in [200]. This is something that will require further

investigation in the future.

We also considered the effects of fluctuation-dissipation dynamics on other cosmological scalar fields, focussing in particular on scalar fields inducing phase transitions. The same interactions which lead to symmetry restoration in the early Universe also give rise to fluctuation-dissipation dynamics, resulting in effects that should not a priori be neglected. As we have seen such dynamics can drastically affect the evolution of the Universe, leading in some cases to late time periods of accelerated expansion, which can aid in the dilution of heavy relics, as well as generating cosmic asymmetries with associated isocurvature perturbations. To date relatively little work has been done in this area and it would be interesting to further pursue various avenues within this framework. At least one phase transition, the electroweak phase transition, occurred in the early Universe and it would be interesting to study it in detail building upon the work done in Chapter 7, as well as also studying the effects that fluctuation-dissipation dynamics can have on other light scalar fields present during a period of warm inflation.

The recent Planck results have been incredibly impressive in confirming the standard ΛCDM model as being the most accurate description of the Universe. In addition the simplest early chaotic models of inflation based on monomial potentials (in the absence of dissipation or non-minimal couplings to gravity) are now disfavoured due to the current bounds on the tensor to scalar ratio, with instead lower scale, perhaps more complicated, inflationary models being preferred. The bounds on isocurvature perturbations and non gaussianity have also improved without evidence for either having been found and there is no preference for a running of the spectral index. All this evidence, or lack of, could point to single field models of inflation with low energy scales. However, if this is the case then one must demonstrate how inflation can then be triggered from general chaotic initial conditions. Alternatively the data could be pointing towards the presence of a thermal bath during inflation with the dynamics being driven by fluctuations and dissipation and thermal fluctuations acting as the source of the primordial density perturbations.

The absence of primordial gravitational waves in the CMB data, despite the brief claims by the BICEP2 collaboration, has perhaps halted the progress in inflationary model building. This is the clear next challenge for early Universe observational cosmology which will be taken up by a variety of future experiments

and will require a better understanding of the astrophysical foregrounds that mimic the polarisation effects gravitational waves have on the CMB. The next generation of experiments claim to be able to measure r down to $\sim 10^{-3}$, which should be low enough to test one of the earliest models of inflation, Starobinsky inflation as well as the various classes of models which show attractor behaviour to this point (see e.g [201, 202] and references therein). If r is detected then it is important to be able to measure certain aspects of its spectrum, in particular the spectral index. Standard slow roll models of single field inflation predict $r = 8|n_t|$ and so any deviation from this would allow for this whole class of inflationary models to be ruled out. Indeed if it is found that $r \leq 8|n_t|$ then this would hint at either a radiation bath present during inflation, or that inflation was driven by the dynamics of multiple fields. In addition if n_t is measured and found to be $n_t \geq 0$ then the whole inflationary paradigm is in serious trouble (unless the null energy condition is violated). This however would be good news for the alternative models. For example bouncing Universes, where cosmological scales become larger than the Hubble radius during a contracting phase, or for emergent cosmologies such as string gas cosmology with both generically predicting a blue tensor index [34]. Indeed it is worth emphasising that a detection of primordial gravitational waves on their own does not prove that inflation occurred, just like the detection of the gaussian adiabatic spectrum does not prove that the perturbations have a quantum vacuum origin. The results of the upcoming experiments will be exciting, hopefully announcing the detection of primordial gravitational waves and other deviations from the simplest adiabatic spectrum allowing us to further our understanding of the earliest moments of the Universe.

Appendix A

Thermal field theory

In order to understand how fluctuation-dissipation dynamics arises within a quantum field theory framework it is necessary to introduce thermal field theory. Although the details of these calculations are not strictly relevant for the understanding (on some level) of the work in this thesis, hopefully the following discussion will give a better idea of what is involved. For a more detailed introduction to finite temperature field theory the following references are recommended [203, 204, 156]. In addition to this we will also introduce the concept of symmetry restoration at finite temperature which will be relevant for the chapter of this thesis concerning cosmological phase transitions. It is particularly interesting to note that the same interactions which give rise to symmetry restoration also induce dissipative effects with associated noise and so a complete description of the dynamics of a phase transition requires considering both of these effects.

Real time formalism

We begin by introducing the density matrix operator which contains the probabilities that a system is in a particular quantum state upon which we want to measure an observable. The need for such an operator arises naturally within quantum statistical mechanics where there are mixed states i.e. statistical ensembles of quantum states, all corresponding to the same macrostate. In order to follow the system's evolution it is thus necessary to study how this operator

evolves in time. This is given by the von Neumann equation:

$$i\frac{\partial\hat{\rho}(t)}{\partial t} = \left[\hat{H}(t), \hat{\rho}(t)\right] \ . \tag{A.1}$$

For a system in thermal equilibrium $\dot{\rho} = 0$ and so non-equilibrium scenarios arise whenever the density operator does not commute with the Hamiltonian. The solution to this in the Schrödinger picture is given by:

$$\hat{\rho}(t) = \hat{U}(t, t_0)\hat{\rho}(t_0)\hat{U}^{-1}(t, t_0) \ , \tag{A.2}$$

where $\hat{U}(t, t_0) = \mathbb{T}\exp(-i\int_{t_0}^{t}\hat{H}(t')dt')$ is the usual time ordered evolution operator. Expectation values of operators are obtained by averaging over the statistical ensemble:

$$\langle\hat{\mathcal{O}}(t)\rangle = \frac{\mathrm{Tr}\left[\hat{\mathcal{O}(t)}\hat{\rho(t)}\right]}{\mathrm{Tr}\left[\hat{\rho}(t)\right]} \ . \tag{A.3}$$

Inserting time evolution operators and specifying the density matrix at some time in the infinite past we can write:

$$\langle\hat{\mathcal{O}}(t)\rangle = \frac{\mathrm{Tr}\left[\hat{U}(-\infty,\infty)\hat{U}(\infty,t)\hat{\mathcal{O}(t)}\hat{U}(t,-\infty)\hat{\rho}(-\infty)\right]}{\mathrm{Tr}\left[\hat{\rho}(-\infty)\right]} \ . \tag{A.4}$$

This is the Keldysh contour where one defines $\hat{\rho}(-\infty)$ then evolves the system to $+\infty$ before evolving back to $-\infty$ evaluating an operator at a time t either on the forward or backwards branch creating a closed time path (CTP). This is the so called in-in formalism where as opposed to introducing well defined initial (in) and final (out) states as in standard QFT, one just defines an initial "in" state, which is usually a state of thermal equilibrium. This choice arises from the desire to not specify some future asymptotic state which in out of equilibrium scenarios will not be simply related to the initial state. This requires the presence of a two branch contour with the time ordering of operators replaced by contour ordering.

In QFT we wish to compute correlation functions of field operators and so in order to do this it is convenient to define field operators on the forwards and backwards branches e.g. ϕ_1, ϕ_2. In this formalism there are thus four propagators corresponding to whether the field operators are both inserted on the same forward/backward path or on opposite paths. One can define a generating

functional for such a configuration:

$$Z[J_1, J_2] = \int \mathcal{D}[\phi_1]\mathcal{D}[\phi_2]\rho[\phi_1(-\infty), \phi_2(-\infty)]e^{iS[\phi_1]+i\int d^4x J_1\phi_1 - iS[\phi_2]-i\int d^4x J_2\phi_2} \ . \tag{A.5}$$

One can then compute correlation functions by taking derivatives with respect to the external sources, J_1, J_2 in the usual way.

The effective action

To obtain the equation of motion of a given field one uses the principle of least action, that the path taken by the field will extremise the action. In the presence of quantum corrections one would like an analogous method to this classical picture to find the equations of motion, this requires modifying the standard action and introducing the *effective action*. This effective action is defined by the Legendre transformation of the energy functional, $W[J] = -i\log Z[J]$, where $W[J]$ is the generating function of n-point connected correlation functions. For example the one point function is given by $\langle\phi(x)\rangle_J = \delta W[J]/\delta J(x)$.

$$\Gamma[\phi_{\rm cl}] = W[J] - \int d^4x J(x)\phi_{\rm cl}(x) \ . \tag{A.6}$$

This effective action is then the generating functional of all the 1 particle irreducible diagrams (1PI) with the special property that:

$$\left.\frac{\delta\Gamma}{\delta\phi_{\rm cl}}\right|_{\phi_{\rm cl}=\langle\phi\rangle} = 0 \ . \tag{A.7}$$

In other words the one point function in the absence of a source can be identified with the classical field which extremises the action. The leading contribution to the action will come from field configurations which extremise it and so we let $\phi(x) = \phi_{\rm cl}(x) + \eta(x)$, where $\phi_{\rm cl}(x)$ extremises the action. One can then expand in powers of $\eta(x)$, compute the gaussian path integrals and to second order in the fluctuations this has the form:

$$\Gamma[\phi_{\rm cl}] = S[\phi_{\rm cl}] + \frac{i}{2}{\rm Tr}\log\left(\Box + V''(\phi_{\rm cl})\right) \ . \tag{A.8}$$

One can then expand the trace of the logarithm, which gives the one loop correction, as:

$$\begin{aligned}\mathrm{Tr}\log\left[\Box + V''(\phi_{\rm cl})\right] &= \mathrm{Tr}\log\left[\left(\Box + m^2\right)\left(1 + DV''(\phi_{\rm cl})\right)\right] \\ &= \mathrm{Tr}\log\left[\Box + m^2\right] + \sum_{n=1}^{\infty}\frac{(-1)^{n+1}}{n}\mathrm{Tr}\left(DV''(\phi_{\rm cl})\right)^n \ , \end{aligned} \tag{A.9}$$

where $D = (\Box + m^2)^{-1}$ is the propagator and the first term is field independent. This can then be viewed as a diagrammatic expansion of one loop diagrams with increasing number of vertices.

In general the effective potential may contain higher order derivative terms but, for a constant field configuration $\phi_{\rm c}(x,t) = \phi_{\rm c}$, the quantum effective action becomes proportional to the effective potential, or in other words the effect of the quantum interactions is just to modify the potential. As we will see for the case of a time varying field these higher order terms may lead to additional friction in the scalar field's equation of motion.

The finite temperature effective action

We now wish to consider the finite temperature analogue. One can thus define an equivalent effective action in the Schwinger-Keldysh CTP formalism:

$$e^{i\Gamma[\phi_1,\phi_2]} = \int_{\rm 1PI}\mathcal{D}[\phi_1']\mathcal{D}[\phi_2']\rho[\phi_1'(-\infty),\phi_2'(-\infty)]e^{iS[\phi_1+\phi_1']-iS[\phi_2+\phi_2']} \ , \tag{A.10}$$

where the $'$ superscripts indicate the fluctuations about the classical field value and only the 1PI diagrams contribute. In the Keldysh representation we define $\phi_{\rm c} = (\phi_1 + \phi_2)/2$ and $\phi_\triangle = \phi_1 - \phi_2$ and the equation of motion is determined from $\delta\Gamma/\delta\phi_\triangle|_{\phi_\triangle=0} = 0$. Due to the special properties of this representation, the effective action can be expanded generically in the following form:

$$\begin{aligned}\Gamma[\phi_{\rm c},\phi_\triangle] = &-\int d^4x\phi_\triangle\left[(\partial^2 + m^2)\phi_{\rm c} + \frac{\partial V(\phi_{\rm c})}{\partial\phi_{\rm c}}\right] \\ &-\int d^4x\int d^4y\phi_\triangle(x)\Sigma_{\rm R}(x,y)\phi_{\rm c}(y) \\ &+\frac{i}{2}\int d^4x\int d^4y\phi_\triangle(x)\Sigma_{\rm F}(x,y)\phi_\triangle(y) + \mathcal{O}(\phi_\triangle^3) \ . \end{aligned} \tag{A.11}$$

This is analogous to the zero temperature result shown previously where the first term is the classical action and the second two terms arise as the lowest order terms in the expansion of the logarithm. $\Sigma_{\rm R}$ and $\Sigma_{\rm F}$ are components of the 2×2 self energy matrix.

As we mentioned previously, in the Keldysh representation the equation of motion seems to only care about terms linear in $\phi_\triangle$. However, the third quadratic term in the expansion can be written as a functional integral over an auxiliary field, $\xi(x)$ as follows:

$$\exp\left(-\frac{1}{2}\int d^4x \int d^4y \phi_\triangle(x)\Sigma_{\rm F}(x,y)\phi_\triangle(y)\right) = |{\rm det}\Sigma_{\rm F}|^{1/2}$$
$$\times \int \mathcal{D}\xi \exp\left(-\frac{1}{2}\int d^4x d^4y \xi(x)\Sigma_{\rm F}^{-1}(x,y)\xi(y) + i\int d^4x \xi(x)\phi_\triangle(x)\right) \ . \quad \text{(A.12)}$$

Thus a linear term in $\phi_\triangle$ has been generated. The equations of motion are then:

$$(\partial^2 + m^2)\phi_{\rm c} + V'(\phi_{\rm c}) + \int d^4y \Sigma_{\rm R}(x,y)\phi_{\rm c}(y) = \xi(x) \ . \quad \text{(A.13)}$$

This is an effective Langevin equation with the ξ term on the right hand side behaving as a stochastic noise with a gaussian distribution:

$$\langle \xi(x) \rangle = 0 \ , \qquad \langle \xi(x)\xi(y) \rangle = \Sigma_{\rm F}(x,y) \ . \quad \text{(A.14)}$$

This can be thought of as a coarse graining procedure, where degrees of freedom operating on very short time scales (relative to the ϕ fields motion) have been integrated out to give an effective stochastic noise term. If the scalar field is stationary then the integral term in the equation of motion just acts as a correction to the effective potential. However if ϕ is evolving then we can introduce a dissipative kernel, $\Sigma_{\rm R}(x,y) = -\partial\mathcal{D}(x,y)/\partial t$ and by integrating by parts we find:

$$(\partial^2 + m^2)\phi_{\rm c} + V'(\phi_{\rm c}) + \int d^4y \mathcal{D}(x,y)\dot{\phi}_{\rm c}(y) = \xi(x) \ . \quad \text{(A.15)}$$

A particularly interesting scenario occurs when the background field is evolving slowly on the timescales of the particle physics interactions. This *adiabatic regime* can occur naturally within a period of inflation where the scalar field is overdamped or indeed in other cosmological scenarios. If this is the case then

we can write (for a homogeneous field):

$$\int d^4y \Sigma_{\rm R}(x,y)\phi_{\rm c}(y) \simeq \int d^4y \Sigma_{\rm R}(x,y)\left(\phi_{\rm c}(t) + \dot{\phi}_c(t)(t-t') + ..\right) \ , \qquad \text{(A.16)}$$

and so in this case the equation of motion takes a local form:

$$(\partial^2 + m^2)\phi_{\rm c} + V'(\phi_{\rm c}) + \Upsilon\dot{\phi}_c = \xi \ , \qquad \text{(A.17)}$$

where we have absorbed the linear term into the effective potential and defined the dissipative coefficient $\Upsilon = -\int d^4x' \Sigma_{\rm R}(x')t'$. In this adiabatic regime the fluid is able to respond quickly to changes in the background field and as such remains close to thermal equilibrium throughout the evolution.

A very important and powerful result of this approach is that the power spectrum of the noise if related to the strength of dissipation through a fluctuation-dissipation relation. In thermal equilibrium the self energies corresponding to the different correlators become related and one can show that (in the regime $\omega \ll T$):

$$\langle \xi(\mathbf{p},t)\xi(\mathbf{p}',t')\rangle = 2T\int \frac{d\omega}{2\pi}\mathcal{D}(\mathbf{p},\omega)e^{i\omega(t-t')} \ . \qquad \text{(A.18)}$$

and in particular in the adiabatic limit this expression simplifies and we find:

$$\langle \xi(\mathbf{p},t)\xi(\mathbf{p}',t')\rangle = 2\Upsilon T(2\pi)^3\delta(\mathbf{p}-\mathbf{p}')\delta(t-t') \ . \qquad \text{(A.19)}$$

The noise term is now markovian and gaussian. For a more detailed discussion of the noise and its relation to dissipation within this QFT framework see [74].

Symmetry restoration at finite temperature

In an attempt to keep the thesis more self contained we will briefly introduce the concept of symmetry restoration at finite temperature. In the case where $\phi_{\rm cl} =$ constant, the effective action becomes proportional to the effective potential. This zero temperature effective potential takes the form at one loop:

$$\begin{aligned} V_{\rm eff} &= V_{\rm cl}(\phi_{\rm cl}) + \frac{i}{2}{\rm Tr}\log\left(\Box + M^2(\phi_{\rm cl})\right) \\ &= V_{\rm cl}(\phi_{\rm cl}) + \frac{i}{2}\int \frac{d^4p}{(2\pi)^4}\log\left(p^2 + M^2(\phi_{\rm cl})\right) \ . \end{aligned} \qquad \text{(A.20)}$$

Using the imaginary time formalism of finite temperature field theory one can find the thermal effective potential by making the replacement (again see [203, 204, 156] for more background details):

$$\int \frac{d^4k_E}{(2\pi)^4} \to T \sum_{n=-\infty}^{n=+\infty} \int \frac{d^3k}{(2\pi)^3} \ , \qquad k_0 \to \omega_n = \frac{2n\pi}{\beta} \ . \tag{A.21}$$

Note that the imaginary time formalism is not generally suitable for out of equilibrium scenarios where the real time formalism is better suited. In the imaginary time formalism the time component becomes compactified with (anti-) periodic boundary conditions arising for the fields. The fields thus have a discrete spectrum of modes in this dimension, justifying the replacement rules given above. Thus the one loop correction takes the form:

$$V_{1-\text{loop}} = \frac{T}{2} \sum_{n=-\infty}^{n=+\infty} \int \frac{d^3k}{(2\pi)^3} \log\left(\omega_n^2 + \omega^2\right) \ . \tag{A.22}$$

where $\omega^2 = \mathbf{k}^2 + M^2(\phi_{\text{cl}})$. Summing over the Matsubara frequencies, ω_n one obtains:

$$V_{1-\text{loop}} = \int \frac{d^3k}{(2\pi)^3} \log\left(\frac{\omega}{2} + T \log\left(1 - e^{-\omega/T}\right)\right) \ . \tag{A.23}$$

The expression has split itself into a zero and finite temperature part. The finite temperature correction to the effective potential thus takes the form:

$$V^T_{1-\text{loop}} = \frac{T^4}{2\pi^2} \int_0^\infty dx\, x^2 \log\left(1 - e^{-\sqrt{x^2+y^2}}\right) \ , \qquad y^2 \equiv M^2(\phi_{\text{cl}})/T^2 \ . \tag{A.24}$$

At high temperatures, $y \ll 1$, this integral admits a useful expansion (see e.g. [203, 204, 156]) and ignoring the constant zero-temperature part, the effective potential becomes:

$$V = V + \frac{M^2(\phi_{\text{cl}})T^2}{24} - \frac{M^3(\phi_{\text{cl}})T}{12\pi} + ... \tag{A.25}$$

An analogous computation can be done for the contribution from fermionic degrees of freedom, with the only real difference arising from the now anti-periodic

boundary conditions and for (Dirac) fermions we find:

$$V = V + \frac{M^2(\phi_{\rm cl})T^2}{12} + ... \tag{A.26}$$

The interesting thing to note is the absence of a cubic term in the high temperature expansion of the fermionic effective potential, which will have important consequences for symmetry breaking. In addition, unlike at zero temperature, the contributions to the effective potential from bosons and fermions do not cancel, this is a consequence of finite temperature effects breaking SUSY albeit in a different way to the standard SUSY breaking scenarios.

Let us consider a scalar field with the following Lagrangian with a simple "Higgs-like" potential:

$$\mathcal{L} = \frac{1}{2}\partial_\mu\phi\partial^\mu\phi + \frac{\lambda}{4}(\phi^2 - v^2)^2 + \frac{g^2}{2}\phi^2\chi^2 + f\phi\psi\bar{\psi} \ . \tag{A.27}$$

If the bosonic and fermionic degrees of freedom are in thermal equilibrium then they induce a thermal correction to the scalar fields effective potential, which at high temperatures has the form:

$$V_{\rm eff} = \frac{\lambda}{4}\left(\phi^2 - v^2\right)^2 + \frac{g^2 + 2f^2}{24}\phi^2T^2 - \frac{g^3}{12\pi}\phi^3T + ... \tag{A.28}$$

At zero temperature this potential has a minimum at $\phi = \pm v$, however at sufficiently large temperatures the origin becomes the minimum. As the temperature cools the thermal corrections decrease and the origin becomes unstable. This occurs at temperatures parametrically close to v:

$$T_{\rm C} = \sqrt{\frac{12\lambda}{g^2 + 2f^2}}v \ . \tag{A.29}$$

In the absence of the cubic term, at temperatures $T < T_{\rm C}$ the field can move towards the new minimum which continues to evolve until $T = 0$. As the field value increases, so too do the masses of the particles it couples to and thus at some point the thermal corrections will effectively switch off as they become non relativistic.

With the addition of the cubic term the phase transition may become first

order. The cubic term can keep the field stabilised at the origin despite the temperature being $T < T_{\mathrm{C}}$. The transition to the true minimum then occurs through quantum tunnelling with regions of the true vacuum nucleating at different points in space. Thus the particle content of the theory decides on the order of the phase transition. For example in GUT groups the symmetry breaking field couples almost exclusively to bosons making it likely that the phase transition is strongly first order [205]. If the theory is supersymmetric however the additional fermionic content can ameliorate this and effectively make the phase transition second order.

Bibliography

[1] P.A.R. Ade et al. Planck 2015. XX. Constraints on inflation. 2015.

[2] P.A.R. Ade et al. A Joint Analysis of BICEP2/Keck Array and Planck Data. *Phys.Rev.Lett.*, 2015.

[3] Arjun Berera and Li-Zhi Fang. Thermally induced density perturbations in the inflation era. *Phys.Rev.Lett.*, 74:1912–1915, 1995.

[4] Arjun Berera. Warm inflation. *Phys.Rev.Lett.*, 75:3218–3221, 1995.

[5] Arjun Berera. Thermal properties of an inflationary universe. *Phys.Rev.*, D54:2519–2534, 1996.

[6] Arjun Berera and Li-Zhi Fang. Thermally induced density perturbations in the inflation era. *Phys.Rev.Lett.*, 74:1912–1915, 1995.

[7] Arjun Berera, Ian G. Moss, and Rudnei O. Ramos. Warm Inflation and its Microphysical Basis. *Rept.Prog.Phys.*, 72:026901, 2009.

[8] L.Z. Fang. Entropy generation in the early Universe by dissipative processes near the Higgs phase transitions. *Phys.Lett.*, B95:154–156, 1980.

[9] I.G. Moss. Primordial inflation with spontaneous symmetry breaking. *Phys.Lett.*, B154:120, 1985.

[10] Junichi Yokoyama and Kei-ichi Maeda. On the Dynamics of the Power Law Inflation Due to an Exponential Potential. *Phys.Lett.*, B207:31, 1988.

[11] Arjun Berera. Warm inflation at arbitrary adiabaticity: A Model, an existence proof for inflationary dynamics in quantum field theory. *Nucl.Phys.*, B585:666–714, 2000.

[12] Arjun Berera. Interpolating the stage of exponential expansion in the early universe: A Possible alternative with no reheating. *Phys.Rev.*, D55:3346–3357, 1997.

[13] Edward W. Kolb and Michael S. Turner. The Early Universe. *Front.Phys.*, 69:1–547, 1990.

[14] David H. Lyth and Andrew R. Liddle. The primordial density perturbation: Cosmology, inflation and the origin of structure. 2009.

[15] Joao G. Rosa. Introduction to cosmology, 2014.

[16] J. A. Wheeler and K. W. Ford. Geons, Black Holes, and Quantum Foam: A Life in Physics, 1998.

[17] P.A.R. Ade et al. Planck 2015 results. XVI. Isotropy and statistics of the CMB. 2015.

[18] I. Horvath, J. Hakkila, and Z. Bagoly. The largest structure of the Universe, defined by Gamma-Ray Bursts. 2013.

[19] III Gott, J. Richard, Mario Juric, David Schlegel, Fiona Hoyle, Michael Vogeley, et al. A map of the universe. *Astrophys.J.*, 624:463, 2005.

[20] T.W.B. Kibble. Topology of Cosmic Domains and Strings. *J.Phys.*, A9:1387–1398, 1976.

[21] Edmund J. Copeland, M. Sami, and Shinji Tsujikawa. Dynamics of dark energy. *Int.J.Mod.Phys.*, D15:1753–1936, 2006.

[22] Jerome Martin. Everything You Always Wanted To Know About The Cosmological Constant Problem (But Were Afraid To Ask). *Comptes Rendus Physique*, 13:566–665, 2012.

[23] Steven Weinberg. The Cosmological Constant Problem. *Rev.Mod.Phys.*, 61:1–23, 1989.

[24] P.A.R. Ade et al. Planck 2015 results. XIV. Dark energy and modified gravity. 2015.

[25] F. Zwicky. Die Rotverschiebung von extragalaktischen Nebeln. *Helvetica Physica Acta*, 6:110–127, 1933.

[26] Mar Bastero-Gil, Arjun Berera, Rudnei O. Ramos, and Joao G. Rosa. Warm baryogenesis. *Phys.Lett.*, B712:425–429, 2012.

[27] A.D. Sakharov. Violation of CP Invariance, c Asymmetry, and Baryon Asymmetry of the Universe. *Pisma Zh.Eksp.Teor.Fiz.*, 5:32–35, 1967.

[28] James M. Cline. Baryogenesis. 2006.

[29] Alan H. Guth. The Inflationary Universe: A Possible Solution to the Horizon and Flatness Problems. *Phys.Rev.*, D23:347–356, 1981.

[30] Andrei D. Linde. A New Inflationary Universe Scenario: A Possible Solution of the Horizon, Flatness, Homogeneity, Isotropy and Primordial Monopole Problems. *Phys.Lett.*, B108:389–393, 1982.

[31] Andreas Albrecht and Paul J. Steinhardt. Cosmology for Grand Unified Theories with Radiatively Induced Symmetry Breaking. *Phys.Rev.Lett.*, 48:1220–1223, 1982.

[32] Andrei D. Linde. Chaotic Inflation. *Phys.Lett.*, B129:177–181, 1983.

[33] Andrei D. Linde. Eternally Existing Selfreproducing Chaotic Inflationary Universe. *Phys. Lett.*, B175:395–400, 1986.

[34] Robert H. Brandenberger. Alternatives to the inflationary paradigm of structure formation. *Int.J.Mod.Phys.Conf.Ser.*, 01:67–79, 2011.

[35] Paul J. Steinhardt and Neil Turok. Cosmic evolution in a cyclic universe. *Phys.Rev.*, D65:126003, 2002.

[36] Fedor L. Bezrukov and Mikhail Shaposhnikov. The Standard Model Higgs boson as the inflaton. *Phys.Lett.*, B659:703–706, 2008.

[37] Andrew R. Liddle and David H. Lyth. COBE, gravitational waves, inflation and extended inflation. *Phys. Lett.*, B291:391–398, 1992.

[38] Daniel Baumann. TASI Lectures on Inflation. pages 523–686, 2011.

[39] Viatcheslav F. Mukhanov, H. A. Feldman, and Robert H. Brandenberger. Theory of cosmological perturbations. Part 1. Classical perturbations. Part 2. Quantum theory of perturbations. Part 3. Extensions. *Phys. Rept.*, 215:203–333, 1992.

[40] Julien Lesgourgues. TASI Lectures on Cosmological Perturbations. pages 29–97, 2013.

[41] P.A.R. Ade et al. Planck 2015 results. XIII. Cosmological parameters. 2015.

[42] Andrew R. Liddle and David H. Lyth. The Cold dark matter density perturbation. *Phys. Rept.*, 231:1–105, 1993.

[43] David H. Lyth. What would we learn by detecting a gravitational wave signal in the cosmic microwave background anisotropy? *Phys.Rev.Lett.*, 78:1861–1863, 1997.

[44] Andrew R Liddle and Samuel M Leach. How long before the end of inflation were observable perturbations produced? *Phys.Rev.*, D68:103503, 2003.

[45] Masahiro Kawasaki, Toyokazu Sekiguchi, and Tomo Takahashi. Differentiating CDM and Baryon Isocurvature Models with 21 cm Fluctuations. *JCAP*, 1110:028, 2011.

[46] Juan Martin Maldacena. Non-Gaussian features of primordial fluctuations in single field inflationary models. *JHEP*, 0305:013, 2003.

[47] Andrei D. Linde. Particle physics and inflationary cosmology. *Contemp.Concepts Phys.*, 5:1–362, 1990.

[48] Lev Kofman, Andrei D. Linde, and Alexei A. Starobinsky. Reheating after inflation. *Phys. Rev. Lett.*, 73:3195–3198, 1994.

[49] Lev Kofman, Andrei D. Linde, and Alexei A. Starobinsky. Towards the theory of reheating after inflation. *Phys.Rev.*, D56:3258–3295, 1997.

[50] Rouzbeh Allahverdi, Robert Brandenberger, Francis-Yan Cyr-Racine, and Anupam Mazumdar. Reheating in Inflationary Cosmology: Theory and Applications. *Ann.Rev.Nucl.Part.Sci.*, 60:27–51, 2010.

[51] Lev A. Kofman. The Origin of matter in the universe: Reheating after inflation. 1996.

[52] Alan H. Guth. The Inflationary Universe: A Possible Solution to the Horizon and Flatness Problems. *Phys.Rev.*, D23:347–356, 1981.

[53] Arjun Berera and Thomas W. Kephart. The Ubiquitous Inflaton in String-Inspired Models. *Phys.Rev.Lett.*, 83:1084–1087, 1999.

[54] Arjun Berera. Warm inflation solution to the eta problem. page AHEP2003/069, 2004.

[55] Mar Bastero-Gil, Arjun Berera, James B. Dent, and Thomas W. Kephart. Towards Realizing Warm Inflation in String Theory. 2009.

[56] Yi-Fu Cai, James B. Dent, and Damien A. Easson. Warm DBI Inflation. *Phys.Rev.*, D83:101301, 2011.

[57] Mar Bastero-Gil, Arjun Berera, and Joao G. Rosa. Warming up brane-antibrane inflation. *Phys.Rev.*, D84:103503, 2011.

[58] A.N. Taylor and A. Berera. Perturbation spectra in the warm inflationary scenario. *Phys.Rev.*, D62:083517, 2000.

[59] Lisa M H Hall, Ian G Moss, and Arjun Berera. Scalar perturbation spectra from warm inflation. *Phys.Rev.*, D69:083525, 2004.

[60] Ian G. Moss and Chun Xiong. On the consistency of warm inflation. *JCAP*, 0811:023, 2008.

[61] Rudnei O. Ramos and L.A. da Silva. Power spectrum for inflation models with quantum and thermal noises. *JCAP*, 1303:032, 2013.

[62] Sujata Gupta, A. Berera, A.F. Heavens, and S. Matarrese. Non-Gaussian signatures in the cosmic background radiation from warm inflation. *Phys.Rev.*, D66:043510, 2002.

[63] Ian G Moss and Chun Xiong. Non-Gaussianity in fluctuations from warm inflation. *JCAP*, 0704:007, 2007.

[64] Bin Chen, Yi Wang, and Wei Xue. Inflationary nonGaussianity from thermal fluctuations. *JCAP*, 0805:014, 2008.

[65] Ian G. Moss and Timothy Yeomans. Non-gaussianity in the strong regime of warm inflation. *JCAP*, 1108:009, 2011.

[66] Mar Bastero-Gil, Arjun Berera, Ian G. Moss, and Rudnei O. Ramos. Theory of non-Gaussianity in warm inflation. *JCAP*, 1412(12):008, 2014.

[67] Sam Bartrum, Arjun Berera, and Joao G. Rosa. Fluctuation-dissipation dynamics of cosmological scalar fields. *Phys.Rev.*, D91(8):083540, 2015.

[68] Sidney R. Coleman and Erick J. Weinberg. Radiative Corrections as the Origin of Spontaneous Symmetry Breaking. *Phys.Rev.*, D7:1888–1910, 1973.

[69] R Kubo. The fluctuation-dissipation theorem. *Reports on Progress in Physics*, 29(1):255, 1966.

[70] Akio Hosoya and Masa-aki Sakagami. Time Development of Higgs Field at Finite Temperature. *Phys.Rev.*, D29:2228, 1984.

[71] Junichi Yokoyama and Andrei D. Linde. Is warm inflation possible? *Phys.Rev.*, D60:083509, 1999.

[72] Masahiro Morikawa. Classical Fluctuations in Dissipative Quantum Systems. *Phys.Rev.*, D33:3607, 1986.

[73] Marcelo Gleiser and Rudnei O. Ramos. Microphysical approach to nonequilibrium dynamics of quantum fields. *Phys.Rev.*, D50:2441–2455, 1994.

[74] Arjun Berera, Ian G. Moss, and Rudnei O. Ramos. Local Approximations for Effective Scalar Field Equations of Motion. *Phys.Rev.*, D76:083520, 2007.

[75] Yuhei Miyamoto, Hayato Motohashi, Teruaki Suyama, and Jun'ichi Yokoyama. Langevin description of gauged scalar fields in a thermal bath. *Phys.Rev.*, D89:085037, 2014.

[76] Mar Bastero-Gil, Arjun Berera, Ian G. Moss, and Rudnei O. Ramos. Cosmological fluctuations of a random field and radiation fluid. *JCAP*, 1405:004, 2014.

[77] Alexei A. Starobinsky. Stochastic de Sitter (Inflationary) stage in the early Universe. *Lect.Notes Phys.*, 246:107–126, 1986.

[78] S. Winitzki and A. Vilenkin. Effective noise in stochastic description of inflation. *Phys.Rev.*, D61:084008, 2000.

[79] Ian G Moss and Chun Xiong. Dissipation coefficients for supersymmetric inflatonary models. 2006.

[80] Mar Bastero-Gil, Arjun Berera, and Rudnei O. Ramos. Dissipation coefficients from scalar and fermion quantum field interactions. *JCAP*, 1109:033, 2011.

[81] Mar Bastero-Gil, Arjun Berera, Rudnei O. Ramos, and Joao G. Rosa. General dissipation coefficient in low-temperature warm inflation. *JCAP*, 1301:016, 2013.

[82] Arjun Berera, Marcelo Gleiser, and Rudnei O. Ramos. Strong dissipative behavior in quantum field theory. *Phys.Rev.*, D58:123508, 1998.

[83] Ian G Moss and Chun Xiong. Dissipation coefficients for supersymmetric inflatonary models. 2006.

[84] Mar Bastero-Gil and Arjun Berera. Warm inflation model building. *Int.J.Mod.Phys.*, A24:2207–2240, 2009.

[85] Mar Bastero-Gil, Arjun Berera, Rudnei O. Ramos, and Joao G. Rosa. General dissipation coefficient in low-temperature warm inflation. 2012.

[86] Masahide Yamaguchi and Junichi Yokoyama. Numerical approach to the onset of the electroweak phase transition. *Phys.Rev.*, D56:4544–4561, 1997.

[87] Chris Graham and Ian G. Moss. Density fluctuations from warm inflation. *JCAP*, 0907:013, 2009.

[88] Shaun Hotchkiss, Anupam Mazumdar, and Seshadri Nadathur. Observable gravitational waves from inflation with small field excursions. *JCAP*, 1202:008, 2012.

[89] Sam Bartrum, Arjun Berera, and Joao G. Rosa. Gravitino cosmology in supersymmetric warm inflation. *Phys.Rev.*, D86:123525, 2012.

[90] P.A.R. Ade et al. Planck 2013 results. XXII. Constraints on inflation. 2013.

[91] Anna Ijjas, Paul J. Steinhardt, and Abraham Loeb. Inflationary paradigm in trouble after Planck2013. 2013.

[92] Renata Kallosh and Andrei Linde. Superconformal generalization of the chaotic inflation model $\frac{\lambda}{4}\phi^4 - \frac{\xi}{2}\phi^2 R$. *JCAP*, 1306:027, 2013.

[93] Rafael Cerezo and Joao G. Rosa. Warm Inflection. *JHEP*, 1301:024, 2013.

[94] Tomohiro Matsuda. Particle production and dissipation caused by the Kaluza-Klein tower. *Phys.Rev.*, D87:026001, 2013.

[95] Sam Bartrum, Arjun Berera, and Joo G. Rosa. Warming up for Planck. *JCAP*, 1306:025, 2013.

[96] Juan C. Bueno Sanchez, Mar Bastero-Gil, Arjun Berera, Konstantinos Dimopoulos, and Kazunori Kohri. The gravitino problem in supersymmetric warm inflation. *JCAP*, 1103:020, 2011.

[97] Marco Drewes and Jin U. Kang. The Kinematics of Cosmic Reheating. *Nucl.Phys.*, B875:315–350, 2013.

[98] Kaushik Bhattacharya, Subhendra Mohanty, and Raghavan Rangarajan. Temperature of the inflaton and duration of inflation from WMAP data. *Phys.Rev.Lett.*, 96:121302, 2006.

[99] G.R. Dvali, Q. Shafi, and Robert K. Schaefer. Large scale structure and supersymmetric inflation without fine tuning. *Phys.Rev.Lett.*, 73:1886–1889, 1994.

[100] Juan Carlos Bueno Sanchez, Mar Bastero-Gil, Arjun Berera, and Konstantinos Dimopoulos. Warm hilltop inflation. *Phys.Rev.*, D77:123527, 2008.

[101] P.A.R. Ade et al. Planck 2013 Results. XXIV. Constraints on primordial non-Gaussianity. *Astron.Astrophys.*, 571:A24, 2014.

[102] M. Bastero-Gil, A. Berera, and R.O. Ramos. Shear viscous effects on the primordial power spectrum from warm inflation. *JCAP*, 1107:030, 2011.

[103] Susana J. Landau, Claudia G. Scoccola, and Daniel Sudarsky. Cosmological constraints on non-standard inflationary quantum collapse models. *Phys.Rev.*, D85:123001, 2012.

[104] Amjad Ashoorioon, Konstantinos Dimopoulos, M.M. Sheikh-Jabbari, and Gary Shiu. Reconciliation of High Energy Scale Models of Inflation with Planck. *JCAP*, 1402:025, 2014.

[105] Mar Bastero-Gil, Arjun Berera, Rudnei O. Ramos, and Joao G. Rosa. Warm baryogenesis. *Phys.Lett.*, B712:425–429, 2012.

[106] Savas Dimopoulos and Lawrence J. Hall. Baryogenesis at the MeV Era. *Phys.Lett.*, B196:135, 1987.

[107] A.N. Taylor and Andrew R. Liddle. Gravitino production in the warm inflationary scenario. *Phys.Rev.*, D64:023513, 2001.

[108] Juan C. Bueno Sanchez, Mar Bastero-Gil, Arjun Berera, Konstantinos Dimopoulos, and Kazunori Kohri. The gravitino problem in supersymmetric warm inflation. *JCAP*, 1103:020, 2011.

[109] Heinz Pagels and Joel R. Primack. Supersymmetry, Cosmology and New TeV Physics. *Phys.Rev.Lett.*, 48:223, 1982.

[110] Steven Weinberg. Cosmological Constraints on the Scale of Supersymmetry Breaking. *Phys.Rev.Lett.*, 48:1303, 1982.

[111] M. Yu. Khlopov and Andrei D. Linde. Is It Easy to Save the Gravitino? *Phys.Lett.*, B138:265–268, 1984.

[112] M. Bolz, A. Brandenburg, and W. Buchmuller. Thermal production of gravitinos. *Nucl.Phys.*, B606:518–544, 2001.

[113] Josef Pradler and Frank Daniel Steffen. Thermal gravitino production and collider tests of leptogenesis. *Phys.Rev.*, D75:023509, 2007.

[114] Masahiro Kawasaki, Fuminobu Takahashi, and T.T. Yanagida. Gravitino overproduction in inflaton decay. *Phys.Lett.*, B638:8–12, 2006.

[115] M. Hashimoto, K.I. Izawa, Masahiro Yamaguchi, and T. Yanagida. Gravitino overproduction through moduli decay. *Prog.Theor.Phys.*, 100:395–398, 1998.

[116] Motoi Endo, Koichi Hamaguchi, and Fuminobu Takahashi. Moduli-induced gravitino problem. *Phys.Rev.Lett.*, 96:211301, 2006.

[117] Kazunori Kohri, Masahiro Yamaguchi, and Jun'ichi Yokoyama. Production and dilution of gravitinos by modulus decay. *Phys.Rev.*, D70:043522, 2004.

[118] Motoi Endo, Fuminobu Takahashi, and T.T. Yanagida. Inflaton Decay in Supergravity. *Phys.Rev.*, D76:083509, 2007.

[119] H. Fujisaki, K. Kumekawa, Masahiro Yamaguchi, and M. Yoshimura. Particle production and gravitino abundance after inflation. *Phys.Rev.*, D54:2494–2503, 1996.

[120] Hans Peter Nilles, M. Peloso, and L. Sorbo. Nonthermal production of gravitinos and inflatinos. *Phys.Rev.Lett.*, 87:051302, 2001.

[121] W.M. Yao et al. Review of Particle Physics. *J.Phys.G*, G33:1–1232, 2006.

[122] Masahiro Kawasaki, Kazunori Kohri, Takeo Moroi, and Akira Yotsuyanagi. Big-Bang Nucleosynthesis and Gravitino. *Phys.Rev.*, D78:065011, 2008.

[123] I.V. Falomkin, G.B. Pontecorvo, M.G. Sapozhnikov, M. Yu. Khlopov, F. Balestra, et al. Low-energy anti-P He-4 annihilation and problems of the modern cosmology, GUT and SUSY models. *Nuovo Cim.*, A79:193–204, 1984.

[124] Jonathan L. Feng, Shufang Su, and Fumihiro Takayama. Supergravity with a gravitino LSP. *Phys.Rev.*, D70:075019, 2004.

[125] Jonathan L. Feng, Shu-fang Su, and Fumihiro Takayama. SuperWIMP gravitino dark matter from slepton and sneutrino decays. *Phys.Rev.*, D70:063514, 2004.

[126] M. Kawasaki and T. Moroi. Gravitino production in the inflationary universe and the effects on big bang nucleosynthesis. *Prog.Theor.Phys.*, 93:879–900, 1995.

[127] Masahiro Kawasaki, Kazunori Kohri, and Takeo Moroi. Hadronic decay of late - decaying particles and Big-Bang Nucleosynthesis. *Phys.Lett.*, B625:7–12, 2005.

[128] Kazunori Kohri, Takeo Moroi, and Akira Yotsuyanagi. Big-bang nucleosynthesis with unstable gravitino and upper bound on the reheating temperature. *Phys.Rev.*, D73:123511, 2006.

[129] Masahiro Kawasaki, Kazunori Kohri, and Takeo Moroi. Big-Bang nucleosynthesis and hadronic decay of long-lived massive particles. *Phys.Rev.*, D71:083502, 2005.

[130] Josef Pradler and Frank Daniel Steffen. Constraints on the Reheating Temperature in Gravitino Dark Matter Scenarios. *Phys.Lett.*, B648:224–235, 2007.

[131] E. Komatsu et al. Five-Year Wilkinson Microwave Anisotropy Probe (WMAP) Observations: Cosmological Interpretation. *Astrophys.J.Suppl.*, 180:330–376, 2009.

[132] D.G. Cerdeno and C. Munoz. An introduction to supergravity. *PoS*, CORFU98:011, 1998.

[133] Hans Peter Nilles. Supersymmetry, Supergravity and Particle Physics. *Phys.Rept.*, 110:1–162, 1984.

[134] J. Wess and J. Bagger. Supersymmetry and supergravity. 1992.

[135] Luis E. Ibanez and Angel M. Uranga. String theory and particle physics: An introduction to string phenomenology. 2012.

[136] K.A. Olive et al. Review of Particle Physics. *Chin.Phys.*, C38:090001, 2014.

[137] David Wands. Multiple field inflation. *Lect.Notes Phys.*, 738:275–304, 2008.

[138] Christopher Gordon and Antony Lewis. Observational constraints on the curvaton model of inflation. *Phys.Rev.*, D67:123513, 2003.

[139] Maria Beltran, Juan Garcia-Bellido, and Julien Lesgourgues. Isocurvature bounds on axions revisited. *Phys.Rev.*, D75:103507, 2007.

[140] G. Hinshaw, D. Larson, E. Komatsu, D.N. Spergel, C.L. Bennett, et al. Nine-Year Wilkinson Microwave Anisotropy Probe (WMAP) Observations: Cosmological Parameter Results. 2012.

[141] P.A.R. Ade et al. Planck 2013 results. XXII. Constraints on inflation. 2013.

[142] Sam Bartrum, Mar Bastero-Gil, Arjun Berera, Rafael Cerezo, Rudnei O. Ramos, et al. The importance of being warm (during inflation). *Phys.Lett.*, B732:116–121, 2014.

[143] Yi Wang and YinZhe Ma. Precision of future experiments measuring primordial tensor fluctuation. *Sci.China Phys.Mech.Astron.*, 57:1466–1470, 2014.

[144] D.A. Kirzhnits and Andrei D. Linde. Symmetry Behavior in Gauge Theories. *Annals Phys.*, 101:195–238, 1976.

[145] Andrei D. Linde. Phase Transitions in Gauge Theories and Cosmology. *Rept.Prog.Phys.*, 42:389, 1979.

[146] Andrei D. Linde. Decay of the False Vacuum at Finite Temperature. *Nucl.Phys.*, B216:421, 1983.

[147] Michael Dine, Robert G. Leigh, Patrick Y. Huet, Andrei D. Linde, and Dmitri A. Linde. Towards the theory of the electroweak phase transition. *Phys.Rev.*, D46:550–571, 1992.

[148] T. Vachaspati. Magnetic fields from cosmological phase transitions. *Phys.Lett.*, B265:258–261, 1991.

[149] Herbert B. Callen and Theodore A. Welton. Irreversibility and generalized noise. *Phys.Rev.*, 83:34–40, 1951.

[150] John W. Negele and H. Orland. *Quantum Many Particle Systems*. Perseus, 1988.

[151] Ulrich Weiss. *Quantum Dissipative Systems (Series in Modern Condensed Matter Physics)*. World Scientific Publishing Company, 3 edition, March 2008.

[152] A.O. Caldeira and A.J. Leggett. Quantum tunneling in a dissipative system. *Annals Phys.*, 149:374–456, 1983.

[153] N. Goldenfeld. *Lectures on phase transitions and the renormalization group*. Westview Press, 1992.

[154] D. Boyanovsky, D. Cormier, H.J. de Vega, and R. Holman. Out-of-equilibrium dynamics of an inflationary phase transition. *Phys.Rev.*, D55:3373–3388, 1997.

[155] D. Boyanovsky, D. Cormier, H.J. de Vega, R. Holman, and S. Prem Kumar. Nonperturbative quantum dynamics of a new inflation model. *Phys.Rev.*, D57:2166–2185, 1998.

[156] E.A. Calzetta and B.L.B. Hu. *Nonequilibrium Quantum Field Theory*. Cambridge Monographs on Mathematical Physics. Cambridge University Press, 2008.

[157] Ian Lawrie. Dissipation in equations of motion of scalar fields. *Phys. Rev. D*, 67:045006, Feb 2003.

[158] Ian Lawrie. Perturbative nonequilibrium dynamics of phase transitions in an expanding universe. *Phys. Rev. D*, 60:063510, Aug 1999.

[159] Esteban Calzetta and B. Hu. Stochastic dynamics of correlations in quantum field theory: From the schwinger-dyson to boltzmann-langevin equation. *Phys. Rev. D*, 61:025012, Dec 1999.

[160] A. Ringwald. Evolution Equation for the Expectation Value of a Scalar Field in Spatially Flat Rw Universes. *Annals Phys.*, 177:129, 1987.

[161] Mar Bastero-Gil, Arjun Berera, Rudnei O. Ramos, and Joao G. Rosa. Observational implications of mattergenesis during inflation. 2014.

[162] Arjun Berera. Warm inflation. *Phys.Rev.Lett.*, 75:3218–3221, 1995.

[163] Arjun Berera and Rudnei O. Ramos. Construction of a robust warm inflation mechanism. *Phys.Lett.*, B567:294–304, 2003.

[164] Xavier Calmet and Matthias Keller. Cosmological Evolution of Fundamental Constants: From Theory to Experiment. 2014.

[165] Daisuke Satow, Yoshimasa Hidaka, and Teiji Kunihiro. Spectral Function of Fermion Coupled with Massive Vector Boson at Finite Temperature in Gauge Invariant Formalism. *Phys.Rev.*, D83:045017, 2011.

[166] Kohei Kamada and J. Yokoyama. On the realization of the MSSM inflation. *Prog.Theor.Phys.*, 122:969–986, 2010.

[167] Ulrich Ellwanger, Cyril Hugonie, and Ana M. Teixeira. The Next-to-Minimal Supersymmetric Standard Model. *Phys.Rept.*, 496:1–77, 2010.

[168] John R. Ellis, S. Kelley, and Dimitri V. Nanopoulos. Probing the desert using gauge coupling unification. *Phys.Lett.*, B260:131–137, 1991.

[169] C. Giunti, C.W. Kim, and U.W. Lee. Running coupling constants and grand unification models. *Mod.Phys.Lett.*, A6:1745–1755, 1991.

[170] Ugo Amaldi, Wim de Boer, and Hermann Furstenau. Comparison of grand unified theories with electroweak and strong coupling constants measured at LEP. *Phys.Lett.*, B260:447–455, 1991.

[171] Paul Langacker and Ming-xing Luo. Implications of precision electroweak experiments for M_t, ρ_0, $\sin^2\theta_W$ and grand unification. *Phys.Rev.*, D44:817–822, 1991.

[172] Graham G. Ross. *Grand Unified Theories*. 1985.

[173] Pablo Laguna and Wojciech Hubert Zurek. Critical dynamics of symmetry breaking: Quenches, dissipation and cosmology. *Phys.Rev.*, D58:085021, 1998.

[174] G.J. Stephens, E.A. Calzetta, B.L. Hu, and S.A. Ramsey. Defect formation and critical dynamics in the early universe. *Phys.Rev.*, D59:045009, 1999.

[175] Adrian Martin and Anne-Christine Davis. Evolution of fields in a second order phase transition. *Phys. Rev. D*, 52:3298–3313, Sep 1995.

[176] Dario Grasso and Hector R. Rubinstein. Magnetic fields in the early universe. *Phys.Rept.*, 348:163–266, 2001.

[177] David H. Lyth and Ewan D. Stewart. Cosmology with a TeV mass GUT Higgs. *Phys.Rev.Lett.*, 75:201–204, 1995.

[178] Arjun Berera, Marcelo Gleiser, and Rudnei O. Ramos. A First principles warm inflation model that solves the cosmological horizon / flatness problems. *Phys.Rev.Lett.*, 83:264–267, 1999.

[179] John Preskill. Magnetic Monopoles. *Ann.Rev.Nucl.Part.Sci.*, 34:461–530, 1984.

[180] Josef Pradler and Frank Daniel Steffen. Thermal gravitino production and collider tests of leptogenesis. *Phys.Rev.*, D75:023509, 2007.

[181] Masahiro Kawasaki, Tomo Takahashi, and Shuichiro Yokoyama. Density Fluctuations in Thermal Inflation and Non-Gaussianity. *JCAP*, 0912:012, 2009.

[182] Ian G. Moss and Chris M. Graham. Particle production and reheating in the inflationary universe. *Phys.Rev.*, D78:123526, 2008.

[183] M. Fukugita and T. Yanagida. Baryogenesis Without Grand Unification. *Phys.Lett.*, B174:45, 1986.

[184] Alexander Kusenko, Kai Schmitz, and Tsutomu T. Yanagida. Leptogenesis via axion oscillations after inflation. 2014.

[185] Sacha Davidson, Enrico Nardi, and Yosef Nir. Leptogenesis. *Phys.Rept.*, 466:105–177, 2008.

[186] Alexander Kusenko, Lauren Pearce, and Louis Yang. Postinflationary Higgs relaxation and the origin of matter-antimatter asymmetry. 2014.

[187] M.A. Luty. Baryogenesis via leptogenesis. *Phys.Rev.*, D45:455–465, 1992.

[188] Gerard 't Hooft. Symmetry Breaking Through Bell-Jackiw Anomalies. *Phys.Rev.Lett.*, 37:8–11, 1976.

[189] K.S. Babu and R.N. Mohapatra. Predictive neutrino spectrum in minimal SO(10) grand unification. *Phys.Rev.Lett.*, 70:2845–2848, 1993.

[190] Brian Fields and Subir Sarkar. Big-Bang nucleosynthesis (2006 Particle Data Group mini-review). 2006.

[191] Michael Dine, Lisa Randall, and Scott D. Thomas. Baryogenesis from flat directions of the supersymmetric standard model. *Nucl.Phys.*, B458:291–326, 1996.

[192] Kyohei Mukaida and Kazunori Nakayama. Dynamics of oscillating scalar field in thermal environment. *JCAP*, 1301:017, 2013.

[193] Kyohei Mukaida and Kazunori Nakayama. Dissipative Effects on Reheating after Inflation. *JCAP*, 1303:002, 2013.

[194] Keisuke Harigaya and Kyohei Mukaida. Thermalization after/during Reheating. *JHEP*, 1405:006, 2014.

[195] Kyohei Mukaida, Kazunori Nakayama, and Masahiro Takimoto. Curvaton Dynamics Revisited. *JCAP*, 1406:013, 2014.

[196] Irina Dymnikova and Maxim Khlopov. Decay of cosmological constant as Bose condensate evaporation. *Mod.Phys.Lett.*, A15:2305–2314, 2000.

[197] G.F. Mazenko, Robert M. Wald, and W.G. Unruh. Does a Phase Transition in the Early Universe Produce the Conditions Needed for Inflation? *Phys.Rev.*, D31:273–282, 1985.

[198] Andreas Albrecht, Robert H. Brandenberger, and R. Matzner. Numerical Analysis of Inflation. *Phys.Rev.*, D32:1280, 1985.

[199] Andreas Albrecht, Robert H. Brandenberger, and Richard Matzner. Inflation With Generalized Initial Conditions. *Phys.Rev.*, D35:429, 1987.

[200] Ignatios Antoniadis and Subodh P. Patil. The Effective Planck Mass and the Scale of Inflation. *Eur.Phys.J.*, C75:182, 2015.

[201] David C. Edwards and Andrew R. Liddle. The observational position of simple non-minimally coupled inflationary scenarios. *JCAP*, 1409(09):052, 2014.

[202] Renata Kallosh, Andrei Linde, and Diederik Roest. Universal Attractor for Inflation at Strong Coupling. *Phys.Rev.Lett.*, 112(1):011303, 2014.

[203] J.I. Kapusta and Charles Gale. Finite-temperature field theory: Principles and applications. 2006.

[204] M.L. Bellac. *Thermal Field Theory*. Cambridge Monographs on Mathematical Physics. Cambridge University Press, 2000.

[205] Andrei D. Linde. Grand Bang. *Phys.Lett.*, B99:391, 1981.